NUMERICAL AND EXPERIMENTAL INVESTIGATIONS OF OPTIMAL FATTY ACID METHYL ESTER HYBRID FOR ENHANCED ENGINE PERFORMANCE AND EMISSION MITIGATION IN THE CONVENTIONAL COMPRESSION IGNITION STRATEGY

By

Awogbemi, Omojola (HND, PGDip., M. Eng.)

217080448

Supervisor: Prof. Freddie L. Inambao

Co-Supervisor: Dr Emmanuel I. Onuh

Thesis submitted in fulfilment of the requirements for the degree of
DOCTOR OF PHILOSOPHY IN ENGINEERING (PhD)
(MECHANICAL ENGINEERING)
College of Agriculture, Engineering and Science, University of KwaZulu-Natal,
Durban, South Africa

2020

As the candidate's supervisors, we have approved this thesis for submission.

Signed:

Name: Prof. Freddie L. Inambao   Date: 21st August, 2020

Name: Dr Emmanuel I. Onuh   Date: 21st August, 2020

Declaration 1 – Plagiarism

I, Awogbemi, Omojola, declare that:

1. The research reported in this thesis, except where otherwise indicated is my original research.

2. This thesis has not been submitted for any degree or examination at any other university.

3. This thesis does not contain other persons' data, pictures, graphs or other information, unless specifically acknowledged as being sourced from other persons.

4. This thesis does not contain other persons' writing unless specifically acknowledged as being sourced from other researchers. Where other written sources have been quoted, then:

   a) Their words have been re-written but the general information attributed to them has been referenced.
   b) Where their exact words have been used, then their writing has been placed in italics and inside quotation marks, and reference.

5. This thesis does not contain text, graphics or tables copied and pasted from the internet, unless specifically acknowledged, and the source being detailed in the thesis and in the References sections.

Signed   Date: 21 August, 2020.

Declaration 2 - Publications

This section presents the articles that form part and/or include the research presented in this thesis. The following papers have been published, accepted or are under review:

ISI/SCOPUS/DoHET Accredited Journals

1. **Awogbemi, O.,** Inambao F., Onuh E. I. (2018). "Performance and Emissions of Compression Ignition Engines Fuelled with Waste Cooking Oil Methyl Ester – A Critical Review," International Journal of Applied Engineering Research (IJAER), Volume 13, Number 11, pp. 9706-9723, Research India Publications. https://www.ripublication.com/ijaer18/ijaerv13n11_135.pdf

2. **Awogbemi, O.,** Inambao F., Onuh E. I. (2019). "Prediction of Properties, Engine Performance, and Emissions of Compression Ignition Engines Fuelled with Waste Cooking Oil Methyl Ester – A Review of Numerical Approaches," International Review of Mechanical Engineering (IREME), Volume 13, Number 2, pp 97-110, Praise Worthy Prize Publishers. https://www.praiseworthyprize.org/jsm/index.php?journal=ireme&page=article&op=view&path%5B%5D=23191. DOI: https://doi.org/10.15866/ireme.v13i2.16496

3. **Awogbemi, O.,** Inambao F., Onuh E. I. (2019). "Development and Characterization of Chicken Eggshell Waste as Potential Catalyst for Biodiesel Production," International Journal of Mechanical Engineering and Technology, Volume 9, Number 12, pp. 1329-1346, IAEME Publications. http://www.iaeme.com/MasterAdmin/UploadFolder/IJMET_09_12_134/IJMET_09_12_134.pdf

4. **Awogbemi, O,** Onuh E. I., Inambao F. (2019). "Comparative Study of Properties and Fatty Acid Composition of some Neat Vegetable Oils and Waste Cooking Oils," International Journal of Low-Carbon Technologies, Volume 14, Number 3 pp 417-425. Published by Oxford University Press. https://academic.oup.com/ijlct/advance-article/doi/10.1093/ijlct/ctz038/5527146. DOI: https://doi.org/10.1093/ijlct/ctz038 .

5. **Awogbemi, O.,** Inambao F., Onuh E. I. (2020). "Effect of Usage on the Fatty Acid Composition and Properties of Neat Palm Oil, Waste Palm Oil, and Waste Palm Oil Methyl Ester," International Journal of Engineering & Technology (IJET), 9 (1) pp. 110-117. Science Publishing Corporation. https://www.sciencepubco.com/index.php/ijet/article/view/29557. DOI: 10.14419/ijet.v9i1.29557

6. **Awogbemi, O.,** Inambao F., Onuh E. I. (2020). "Application of Multiple Linear Regression for the Prediction of some Properties of Biodiesel using Fatty Acid Compositions," Journal of Engineering and Applied Sciences (JEAS), Volume: 15, Issue 8, page No.: 1951-1961. Medwell Publications. https://medwelljournals.com/abstract/?doi=jeasci.2020.1951.1961. DOI: 10.36478/jeasci.2020.1951.1961

7. **Awogbemi, O.,** Inambao F., Onuh E. I. (2019). "Modelling and Optimization of Transesterification of Waste Sunflower Oil to Fatty Acid Methyl Ester: A Case of Response Surface Methodology vs Taguchi Orthogonal Approach," International Journal of Engineering Research and Technology (IJERT), Volume 12, Number 12, pp. 2346-2361. International Research Publication House. http://www.irphouse.com/ijert19/ijertv12n12_40.pdf

8. Onuh E. I., Inambao F., **Awogbemi, O.** (2019). "Performance and Emission Evaluation of Biodiesel Derived from Waste Restaurant Oil and Moringa oleifera: A Comparative Study," International Journal of Ambient Energy. Taylor & Francis. https://www.tandfonline.com/doi/full/10.1080/01430750.2019.1594377. DOI: https://doi.org/10.1080/01430750.2019.1594377.

9. **Awogbemi, O.,** Inambao F., Onuh E. I. (2020). "Optimization of FAME Composition for Improved Engine Performance and Emissions Reduction," International Journal of Low-Carbon Technologies. Published by Oxford University Press.

https://academic.oup.com/ijlct/advance-article/doi/10.1093/ijlct/ctaa027/5836492

DOI: https://doi.org/10.1093/ijlct/ctaa027

10. **Awogbemi, O.,** Inambao F., Onuh E. I. (2019). "Development and Application of Artificial Neural Network for the Prediction of Engine Performance and Emission Characteristics of Diesel Engine using Fatty Acid Compositions," International Journal of Engineering Research and Technology (IJERT), Volume 12, Number 12, pp. 2362-2377. International Research Publication House. http://www.irphouse.com/ijert19/ijertv12n12_41.pdf

International and DHET accredited conferences

1. **Awogbemi, O.,** Inambao F., Onuh E. I. (2018). "A Review of the Performance and Emissions of Compression Ignition Engine fuelled with Waste Cooking Oil Methyl Ester," presented at the 2018 International Conference on the Domestic Use of Energy (DUE) held at Cape Peninsula University of Technology, Cape Town, South Africa, 3 - 5 April 2018. Published by IEEE Xplore, https://ieeexplore.ieee.org/stamp/stamp.jsp?tp=&arnumber=8384399&tag=1 DOI:10.23919/due.2018.8384399 .

2. **Awogbemi, O**, Inambao F., and Onuh E. I. (2019) "Modelling and Optimization of Synthesis of Waste Sunflower Methyl Ester by Taguchi Approach," Proceedings of The World Congress on Engineering 2019, 3-5 July 2019, London, U.K., pp137-143. Available on http://www.iaeng.org/publication/WCE2019/WCE2019_pp137-143.pdf

3. **Omojola Awogbemi**, Josiah Pelemo, Freddie Inambao, and Emmanuel I. Onuh (2020). "Physico-Chemical Properties, Thermal degradation, and Spectroscopic studies of Hybridized Waste Palm Oil". Presented at the International conference on energy and sustainable environment (ICESE 2020), Covenant University, Ota, Nigeria. 28 – 30 July, 2020.

The candidate is the main and corresponding author for all the publications and conference presentations while Prof. Freddie L. Inambao is the supervisor and Dr Emmanuel I. Onuh is the co-supervisor.

Dedication

This work is dedicated to the Most High God, the sustenance of my existence. And to my family for their love, understanding, and for standing by me through thick and thin.

Acknowledgements

Abstract

The utilization of petroleum-based diesel fuel to power compression ignition (CI) engines has been hampered by inefficient combustion process resulting in unsatisfactory engine performance and emission of hazardous gases. Fatty acid methyl ester (FAME), due to its renewability, biodegradability, and environmentally friendly emissions, has been acknowledged as a viable alternative fuel for CI engines. The application of waste cooking oil (WCO) as feedstock for FAME production did not conflict with food chain, guarantees appropriate disposal of used vegetable oil, and prevents contamination of aquatic and terrestrial habitats.

The FAME was produced by transesterification of WCO samples collected from restaurants, catalyzed by calcium oxide derived from chicken eggshell waste powder subjected to high-temperature calcination. Properties and fatty acid (FA) composition of the FAME were determined, the fuel used to power an unmodified CI engine, and measure the performance and emission characteristics experimentally. Numerical techniques, including, matrix laboratory, response surface methodology, Taguchi orthogonal, artificial neural network, and multiple linear regression were utilized to unearth the optimal FAME candidate, determine the properties, FA composition, performance and emission characteristics of the newly generated FAME and were found to agree with experimental results. It was discovered that FAME candidate with a concentration of palmitic acid of 36.4 % and oleic acid of 59.8 % produced improved brake thermal efficiency and brake mean effective pressure as well as reduced fuel consumption, and other regulated emissions.

Table of Contents[1]

---

[1] Only chapters that were written for this thesis and not as journal articles show subheadings.

List of Figures[2]

---

[2] Only the figures that appear in chapters that were written for this thesis appear in this List.

List of Tables[3]

---

[3] Only the tables that appear in chapters that were written for this thesis appear in this List.

List of Plates

List of Appendices

Nomenclature

B100	Unblended biodiesel
C16:1	Palmitoleic acid
C18:1	Oleic acid
C16:0	Palmitic acid
C18:2	Linoleic acid
C18:3	Linolenic acid
C14:0	Myristic acid
C20:0	Arachidic acid
C12:0	Lauric acid
C18:0	Stearic acid
C20:1	Eicosenic acid
R	Regression coefficient
R^2	Coefficient of determination
R^2_{adj}	Adjusted R^2
rc	Compression ratio
S	Entropy
S	Stroke
HHV	High heating value
LHV	Low heating value
N	Number of moles
Sfc	Specific fuel consumption

Acronyms/Abbreviations

AOAC	Association of Official Agricultural Chemists
ANFIS	Adaptive network-based fuzzy inference system
ANN	Artificial neural network
AV	Acid value
ASTM	American Society for Testing and Materials
BSFC	Brake specific fuel consumption
BTE	Brake thermal efficiency
CCD	Central composite design
CFD	Computational fluid dynamics
CFPP	Cold filter plugging point
CH_4	Methane
CI	Compression ignition
CN	Cetane number
CO	Carbon monoxide
CO_2	Carbon dioxide
DOE	Design of experiment
DTA	Differential thermal analysis
DTG	Differential thermogravimetry
EGR	Exhaust gas recirculation

EGT	Exhaust gas temperature
EPA	Environmental Protecting Agency
FA	Fatty acid
FAEE	fatty acid ethyl ester
FAME	Fatty acid methyl ester
FFA	Free fatty acid
FP	Flash point
FTIR	Fourier transform infrared
GCMS	Gas chromatography-mass spectrometry
ICE	Internal combustion engine
KV	Kinematic viscosity
LII	Laser-induced incandescence
LTC	Low-temperature combustion
M	Molecular weight
MAPE	Mean absolute percentage error
MATLAB	Matrix laboratory
MLR	Multiple linear regression
MOME	Moringa oil methyl ester
MSE	Mean squared error
NA	Natural aspirated

NMR	Nuclear magnetic resonance
HNMR	Hydrogen nuclear magnetic resonance
HSDI	High speed direct injection
NOx	Oxides of nitrogen
NRDE	Non-road diesel engines and equipment
OVAT	One-variable-at-a-time
PBD	Petroleum-based diesel
PDI	Phase Doppler interferometry
RSM	Response surface methodology
SEM	Scanning electron microscopy
SI	Spark ignition
SO_2	Sulphur dioxide
SV	Saponification value
SVM	Support vector machines
SVO	Straight vegetable oil
TEM	Thermal electron microscopy
TGA	Thermogravimetric analysis
UHC	Unburnt Hydrocarbon
ULSD	Ultra-low sulfur diesel
USEPA	United state environmental protection agency

WCO	Waste cooking oil
WCOME	Waste cooking oil methyl ester
WSFO	Waste sunflower oil
WSME	Waste sunflower methyl ester
XRD	X-ray diffractometer

CHAPTER 1: INTRODUCTION

1.1   Introduction

At no other period since 1892 when a German Engineer, Rudolph Diesel, designed the diesel engine has the need to discover sustainable alternatives replacement for fossil-based diesel fuel been more compelling. Compression ignition (CI) engines have been observed to be more efficient, rugged, safer, reliable, and requires less maintenance compared to spark ignition (SI) engines. Though more expensive than SI engines, CI engines have found applications in construction, industrial, agricultural, and transportation industries despite the obvious shortcomings associated with the engine. The quest for the development and deployment of affordable, renewable, biodegradable, and environmentally benign fuel to power CI engines has been on the increase in recent years. The upsurge in the global population, urbanization, and industrial revolution has exerted immense pressure on the available existing energy sources [1]. The contemporary world population reached 7.7 billion in June 2019 with about 55 % residing in urban areas, the global population has been predicted to attain 9.8 billion in 2050 with an estimated 68 % living in the cities [2, 3]. With the larger percentage of the populace living in the cities, the competition for the limited available facilities in the cities, including energy sources, will become more intense. This huge population has brought with it the need for effective and timely movement of goods and services for economic and commercial purposes. Thus, the observed challenging operation of petroleum-based diesel (PBD) fuel, the damaging effect of the emission of hazardous gases from the tailpipe of CI engines, and the inevitable depletion of fossil fuel reserves based on present consumption rate has precipitated a more focused search for viable alternatives for the PBD fuel [4].

The transportation sector consumes over 90 % of total fossil fuel products and over 25 % of global energy as shown in Figure 1 [5]. The percentage of the total energy used for on-road transport is estimated to increase from the present 28 % to 50 % by 2030 and further to 80 % by 2050 [6].

The total energy consumption in the transport sector was 110 million TJ in 2015 comprising cars and bikes, bus, air, passenger rail, and air freight. Heavy trucks, light trucks, and marine engines jointly consume 35 % of the transportation sector energy as shown in Figure 2 [7, 8]. This does not include the increasing number of CI engines used in irrigation, industrial, and earthmoving equipment in the construction sector and other non-road diesel engines and equipment (NRDE).

Non energy = 9 %

Transport = 28 %

Residential and
Others = 33 %

Industry = 30 %
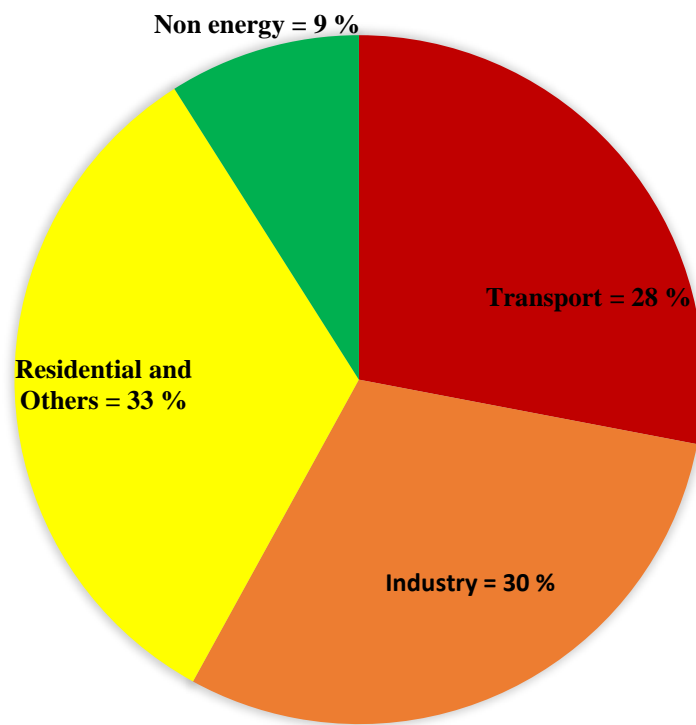
Figure 1.Global final energy consumption by sector
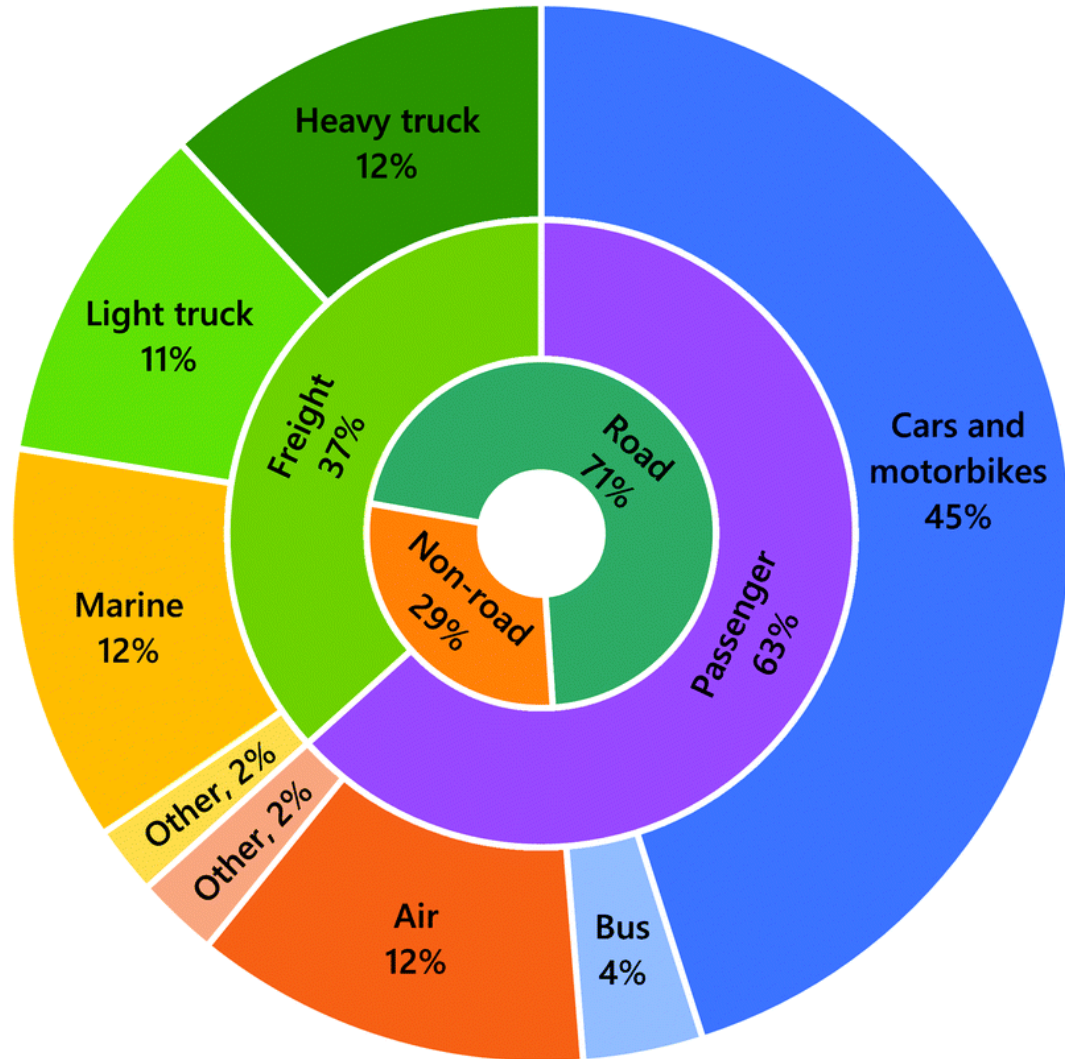
Figure 2. Summary of global energy utilization in the transport sector 2015

The desire to overcome the twin problems of inefficient engine performance and emission of environmentally unpleasant gases that has accompanied the utilization of PBD fuel in CI engines has resulted in experimentation involving various alternatives, including straight vegetable oil (SVO) and its blends [9, 10]. The many complications associated with the use of SVO has limited its adaptation and continued usage thereby turning attention to biofuels [11, 12]. Biofuels are produced from the conversion of biomass, vegetable or animal resources into fuel. Biofuels are categorized as biogas, bioethanol, and biodiesel [13]. The use of biodiesel has gained more prominence and attracted researchers' interest in recent years due to its ease of production, renewability, biodegradability, among other reasons, and is projected to account for 20 % of all on-road CI engine fuel by the year 2020 [14, 15].

3

Biodiesel, commonly known as fatty acid methyl ester (FAME), is synthesized from various feedstock, including vegetable oils, non-edible oils, animal (chicken, beef, pig) fats, waste cooking oil (WCO), waste/recovered fats, etc., and contain long-chain methyl or ethyl esters. The introduction, utilization, and commercialization of biodiesel globally has resulted in the development of standard properties and test methods by the American Society for Testing and Materials ASTM D6751[16] and by the European Committee for Standardization EN 14214 [16]. Based on geographical differences, other countries have developed their own standards, drawing from the two major standards, and are now well-documented standards [17]. FAME can be tested, categorized, and characterized based on the method prescribed by these protocols. FAME properties have been found to impact greatly on a fuel's behavior, storage, performance, transportation, combustion, and emissions in CI engines. Figure 3 displays the impact of some of the properties of FAME [18].
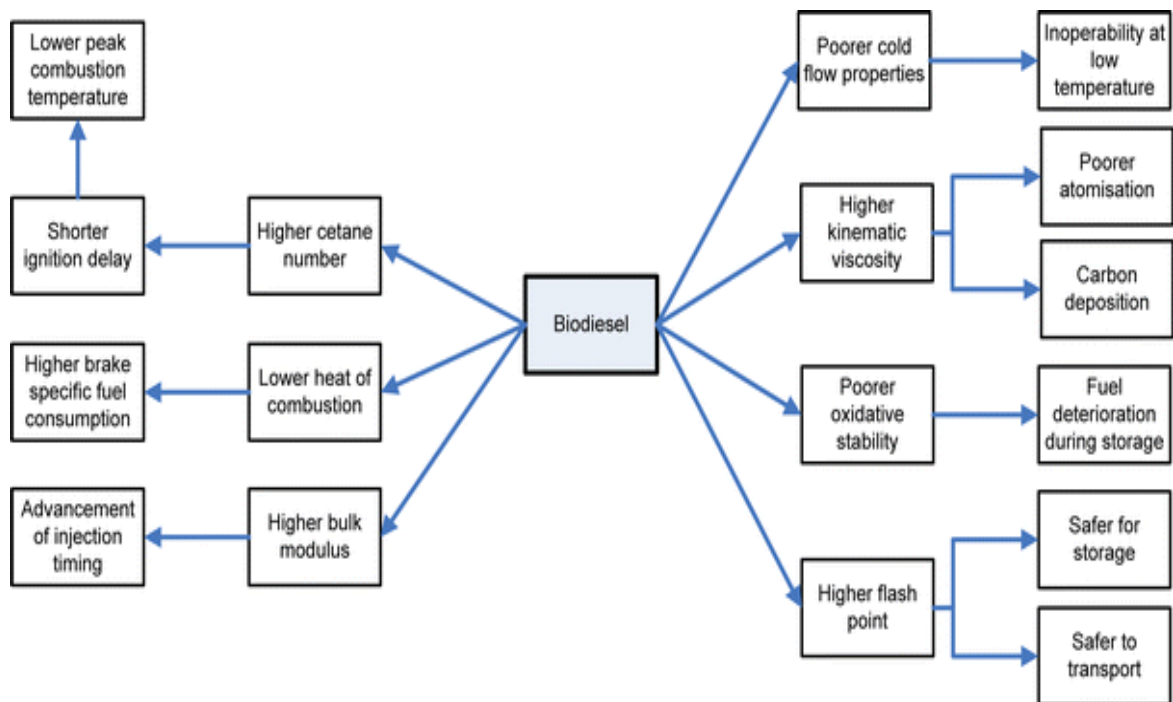
Figure 3. Biodiesel properties compared with PBD fuel and their impact

1.2   Research motivation

Biodiesel has become a favorite alternative fuel for CI engines owing to the practicability of the conversion technology, compatibility with the existing handling infrastructure for traditional PBD fuel, and miscibility with other fuels. Due to the combination of these factors, the use of biodiesel has gained a foothold among fuel consumers and captured a substantial market share. This has led to sustained interest among fuel refiners, engine manufacturers, and automobile producers in the need to improve the properties, engine performance parameters, and tailpipe exhaust gas characteristics of CI engines powered with FAME. The promulgation and enforcement of performance standards and strict emission benchmarks by the United States Environmental Protection Agency (USEPA) has continued to put enormous pressure on engine manufacturers to halt the degradation of the environment by respecting the relevant performance and emission benchmarks. Also, despite the benefits from the adaptation and application of FAME in CI engines, widespread adoption and utilization has been hampered by affordability and accompanied by operational challenges. The cost of biodiesel has remained high with the cost of feedstock believed to make up 70 % to 95 % of the total production expenses [19, 20]. Used vegetable oil sourced from restaurants, canteens, and takeaway joints, waste animal (beef, pig, chicken, etc.) fats from slaughterhouses, rendered fats and recovered grease from wastewater treatment plants offer advantages and have replaced edible and non-edible feedstocks. The edible feedstocks, like vegetable oils, are not only expensive (therefore producing an unimpressive return on investment), but are not readily available, and, more importantly, conflict with food security and land-use change [21, 22].

Efforts to produce FAME at least cost possible using unsophisticated production infrastructure has dominated discourse and experimentation among researchers. The use of catalysts derived from materials hitherto termed as waste to replace synthetic catalysts are not only cost-effective but also contribute to sanitation and reduce the quantity of waste at dumpsites. Adopting optimal refining technology for FAME production is heavily dependent on the type and composition of feedstocks, catalyst selection, process parameters, and purification techniques. Also, although

FAME has been produced and tested either in blended and unblended forms using various engine modification techniques to achieve better engine performance and reduced emission, the relevant question to ask, which forms the motivation for this study, is whether an optimal FAME candidate capable of guaranteeing acceptable engine performance and mitigated regulated emissions in a conventional CI engine has been unearthed. Can numerical and experimental techniques be deployed to produce FAME with requisite properties and specifications for better engine performance and reduced tailpipe emissions?

1.3   Problem statement

The need to upgrade engine performance and reduce the tailpipe emissions of regulated gases of CI engine fueled by FAME has continued to engage researchers' attention. This is not only to maximize the benefits of combustion efficiency and power output of the oxygenated fuel but also to meet the ever-increasingly stringent emission standards and requirements. The utilization of numerical methods to model and predict fuel properties, engine performance parameters, and emission characteristics using a limited number of FA compositions has not been sufficiently frequently explored despite its strong theoretical base and connections. This is believed to offer great opportunities and can be seen as a panacea compared to the rigorous, laborious, costly, high laboratory infrastructure requirement for real-time tests. There is an urgent need to unravel an optimal FAME candidate derived from WCO with the capability for better engine performance and mitigated emissions when used in a conventional CI engine. Hence this work employed numerical and experimental techniques to determine an optimal candidate in terms of FA composition.

1.4   Background to the study

This work lies within the renewable energy field of study. It seeks to develop a sustainable and alternative fuel for CI engines to replace PBD fuel. Such an alternative fuel must offer cost, performance and environmental advantages, and be produced in line with international best practices and protocols. The utilization of PBD fuel in CI on-road and off-road engines has been plagued with challenges notably economic, performance, environmental, and emissions. In order

to qualitatively and quantitatively meet the perpetually soaring energy and fuel requirements, researchers have been developing and testing various brands of biofuel to meet performance and emission requirements [23, 24]. The application of biodiesel as a transportation fuel in agricultural, construction, marine, and rail equipment has continued to increase, necessitating increased research. Transport vehicles continue to consume the largest percentage of biodiesel [25-27].

1.4.1   Production of biodiesel

Various techniques have been adopted to convert vegetable oils, waste cooking oil, algae, biomass, and other waste materials into fuel. Vegetable oils contain long and viscous triglycerides which have to be transformed into low viscosity oil suitable for a CI engine. Various feedstocks have been identified as having the capacity of being converted to biodiesel, though availability, cost, and ease of conversion varies considerably. Compared with other biodiesel production techniques, transesterification is believed to be the simplest technique of converting feedstock to biodiesel. Pyrolysis involves exposing the feedstock to thermal degradation to remove the oxygen. Products of pyrolysis of vegetable oil include alkanes, alkenes, aromatics, and carboxylic acids in varying forms and concentrations. However, the prohibitive cost of production and distillation infrastructure has restricted the widespread application of this method. The micro-emulsification process involves adding alcohol (methanol, ethanol) to vegetable oil to reduce its viscosity and so make it more suitable as a CI engine fuel. Additives like surfactants and cetane improvers are added to the products of micro-emulsification to further improve its performance. CI engines fueled with the products of micro-emulsification over a prolonged time are prone to defects such as carbon deposition, injector malfunctioning, and incomplete combustion [28-30]. Over the years, four generations of biodiesel have been identified. Table 1 compares the benefits and drawbacks of various biofuel production techniques while Table 2 depicts the processing technology, merits, and challenges of the four generations of biodiesel.

Table 1. Comparison of some biodiesel production techniques

Production techniques	Advantages	Disadvantages
Pyrolysis	• Easy process • Free from Pollution	• Involves elevated temperature • Costly apparatus required • Impure product
Micro-emulsion	• Uncomplicated	• Reduced volatility and stability
Dilution	• Easy process	• Inchoate combustion • Carbon deposition in engines
Transesterification	• Simple process • Industrial-scale production • Properties of biodiesel produced comparable to PBD fuel	• Multiple separation processes • High moisture and impurity levels • Costly catalysts • Generation of wastewater
Superfluid method	• Short reaction time • No need for a catalyst • High conversion	• High energy consumption • High cost of apparatus

The choice of focus for this research study is the second generation of biodiesel, due to the advantages highlighted in Table 2. Some of the challenges militating against the adoption of the second generation biodiesel are being tackled by the use of used vegetable oil, recovered fat from beef and chicken, as against other non-edible oils like *Nicotiana tabacum* (tobacco), *Pongamia pinnata* (karanja), *Salvadora oleoides* (pilu), *Sapindus mukorossi* (soapnut), tomato seed, tung, *Terminala catappa*, etc. [31]. The adoption of used vegetable oil is cost-effective, eliminates the cost of disposal of used vegetable oil, prevents consumption of unhealthy WCO, and reduces the time and land required to cultivate biodiesel-producing crops. Inappropriate disposal of WCO has been found to block pipes and sewerage plants and contaminate aquatic and terrestrial habitats [32, 33].

Table 2. Processing technology, benefits, and challenges of generations of biodiesel [34, 35]

Generation of Biodiesel	Feedstock	Processing technique	Benefits	Problems
First	Palm oil, sunflower oil, soybean oil, corn oil, canola oil	Esterification and transesterification of oils. Purification	• Environmentally friendly • Commercially produced • Production parameters are attainable • Fairly cost-effective	• Limited feedstock • Food vs fuel debate • Requires arable land for cultivation • Contributes to deforestation • Unsustainable • Use of pesticides and fertilizers pose a concern
Second	Non-edible oil, waste cooking oil, waste and recovered animal fats.	Pre-treatment of feedstock Esterification and transesterification of feedstock. Purification	• No food-fuel conflict • Environmentally friendly • Cost-effective • Pesticides and fertilizers not needed	• Requires pretreatment • High cost of conversion • Land arable land or forests to grow • Deforestation concerns

Third	Microalgae, Macroalgae	Algae cultivation, harvesting, oil extraction, transesterification	• No food-fuel conflict • High yield • Arable land not needed • Easy conversion • Environmentally friendly	• Underdeveloped advanced technology • Large initial cost of cultivation • Complicated and expensive harvesting
Fourth	Microalgae Microbes	Metabolic engineering of algae, cultivation, harvesting, transesterification	• No food-fuel conflict • High yield • More CO_2 capture ability • High production rate • Non-arable land needed for cultivation • Prohibitive cost for large scale cultivation • Easy conversion	• Prohibitive preliminary investment • Research still at the preliminary stage • High initial cost for large cultivation • Harvesting of microalgae and microbes are expensive

Transesterification involves the reaction of low molecular weight alcohol and the triglycerides contained in the feedstock in the presence of various types of catalyst. Figure 4 presents a representation of the three steps involved in the transesterification reaction for the synthesis of FAME while Figure 5 depicts a combination of the three steps' processes. The choice of alcohol determines the nomenclature of the resulting ester. Frequently used alcohols include methanol, ethanol, propanol, isopropanol, and butanol. Though ethanol is less expensive than methanol, methanol is commonly used. When bioethanol is used as methanol, completely bio-based biodiesel is produced. If methanol is utilized as the alcohol, the product of the reaction is called FAME while fatty acid ethyl ester (FAEE) results from the application of ethanol as alcohol [36, 37]. Subject to the value of free fatty acids (FFAs), the number of steps involved in the transesterification process can be determined. If the FFA value of the feedstock is above 1 mgKOH/g, transesterification is preceded by the esterification process. Esterification is a single-step process with tetra oxo-sulphate IV acid as a homogenous catalyst to bring the FFA to less than 1 mgKOH/g. If the FFA is lower than 1 mgKOH/g, a single step transesterification process is adopted. Due to the low quality of some of the feedstock, especially WCO, waste animal fats, and recovered fats and grease, pretreatment processes are required prior to transesterification [38, 39]. FAME from WCO are believed to exhibit better properties and enhanced engine performance compared to biodiesel from other sources [40, 41].
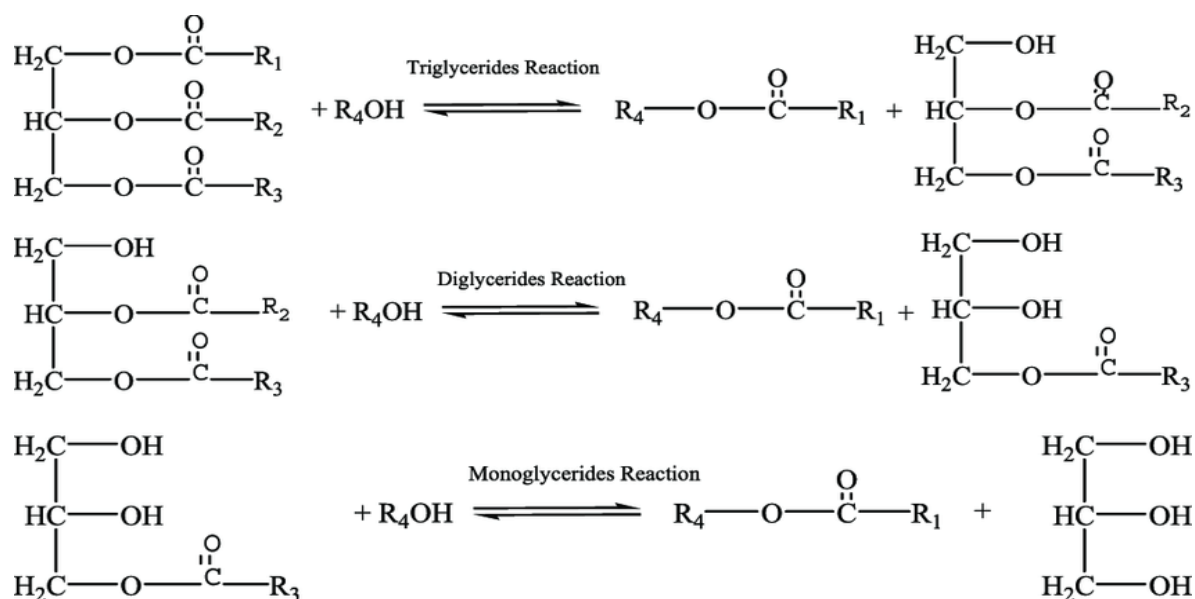
Figure 4. Three steps equation for transesterification reaction [42, 43]
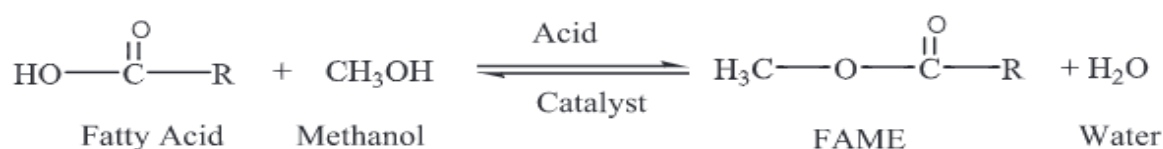
Figure 5. General transesterification reaction [43]

The transesterification reaction can take place with or without a catalyst. The non-catalytic transesterification process is believed to occur at a pressure range of 45 bar to 65 bar, temperature of 200 ºC to 400 ºC and in the presence of alcohol [44]. Compared with the catalytic transesterification process, the supercritical transesterification process has been found to take place in a shorter time and requiring a simpler purification process as removal of a catalyst is not needed. However, the non-catalytic transesterification process is limited to batch process, requires high temperatures, pressurized reaction vessels, and high energy costs. The catalyst for transesterification process can either be homogeneous, heterogeneous, or biocatalyst (enzyme) [45]. Figure 6 shows the types of catalysts for transesterification [46, 47]. Table 3 compares the advantages and disadvantages of homogeneous, heterogeneous, and biocatalysts.

Table 3. Pros and cons of various catalysts [45, 48-50]

Types of catalyst	Example	Pros	Cons
Homogeneous	NaOH, KOH, CH$_3$ONa, H$_2$SO$_4$	• Faster reaction • The reaction occurs at mild temperature conditions • Unaffected by FFA and moisture content • Application to esterification and transesterification processes • Favors superior kinetics	• Formation of soap • Low yield • Large wastewater generated • Slow reaction • Leads to corrosiveness
Heterogeneous	CaO, Mg/Zr, Mg-Al hydrotalcite, ZnO/KF, ZnO/Ba, Na/BaO, K$_2$CO$_3$ supported MgO, Al$_2$O$_3$/ZrO$_2$/WO$_3$, Al$_2$O$_3$/KNO$_3$ vanadium phosphate solid, Fe-Zn double metal cyanide complex	• Easy separation • Reusability and regeneration • Longer lifetime of the catalyst • Reduces waste disposal problem • Noncorrosive • Alkaline catalyst has higher selectivity • Environmentally friendly and recyclable • Comparatively cheap	• High temperature is required • Leaching of catalyst • Limited diffusion • High oil to methanol ratio • Not as effective as homogeneous base catalysts • Higher cost of acid catalysts compared to alkaline catalyst
Biobased (Enzyme)	Lipase, Candida antaractia	• Requires less purification • Occurs at low temperature • Product completely bio-based	• Expensive • Reduced reaction rate • Enzyme inactivated when exposed to alcohol
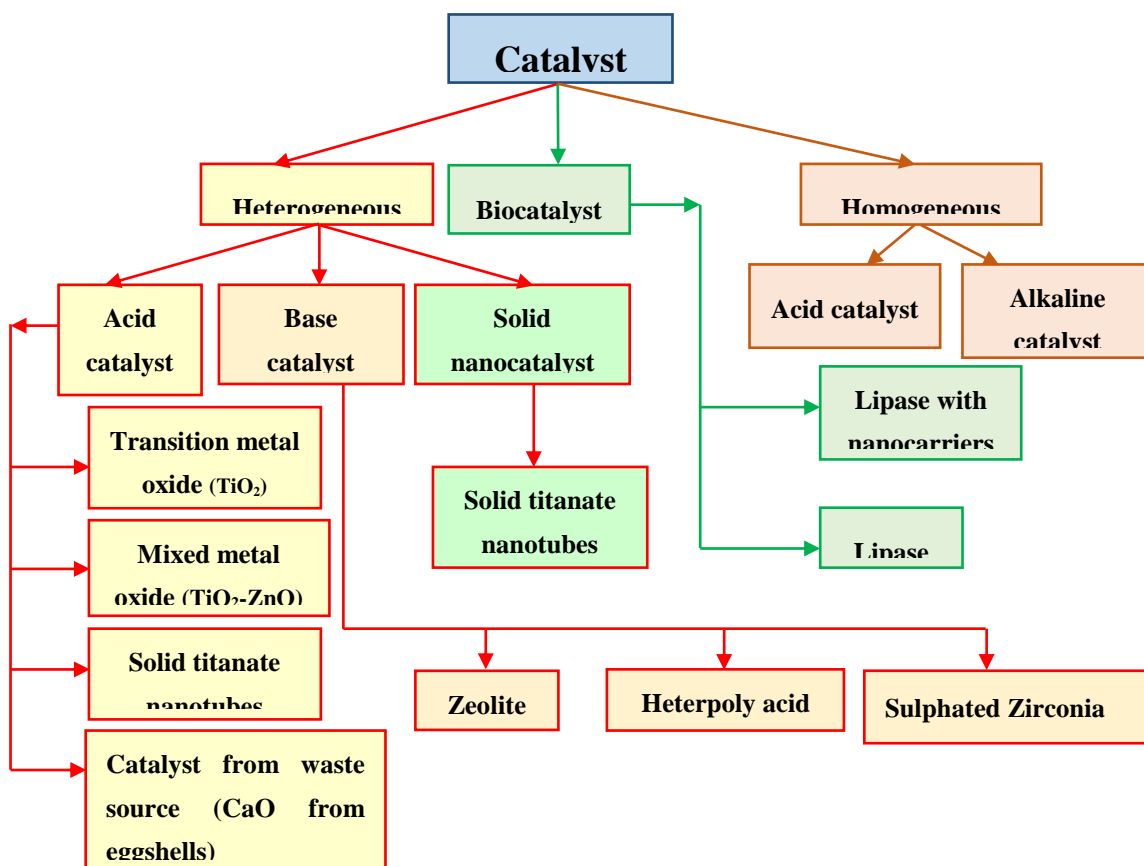
Figure 6. Categories of catalysts for biodiesel generation

11

1.4.2 Process parameters for transesterification reaction and optimization

The transition from feedstock to biodiesel is measured by certain parameters including conversion efficiency, yield, and ester content. Equations 1, 2, and 3 are used to estimate oil conversion [51], yield [52], and ester content [53].

$$Conversion\ (\%) = \frac{Weight\ of\ glycerol\ obtained}{Weight\ of\ biodiesel} \times 100 \tag{1}$$

$$Yield\ (\%) = \frac{Weight\ of\ biodiesel}{Weight\ of\ oil} \times 100 \tag{2}$$

$$Ester\ content\ (\%) = \left(\frac{\sum A - A_{IS}}{A_{IS}}\right)\left(\frac{C_{IS}V_{IS}}{m}\right) \times 100 \tag{3}$$

Where:

$\sum A$ = addition of the areas under all peaks from $C_{14:0}$ to $C_{24:1}$

A_{IS} = area under the peak of methyl heptadecanoate ($C_{17:0}$) used as the internal standard

C_{IS} = concentration of the $C_{17:0}$ solution (gmL^{-1})

V_{IS} = volume of the $C_{17:0}$ solution (mL) and

m = sample weight (mg)

Biodiesel yield and oil conversion are influenced by certain process parameters. Some of these parametric conditions include FFA value, reaction temperature, reaction time, alcohol:oil ratio, catalyst:oil ratio, catalyst type, catalyst concentration, catalyst particle size, and mixing or agitation rate [44]. The choice of a particular parameter influences the choice of another parameter. For example, the choice of methanol as alcohol will mean the reaction temperature should be less than 60 °C. Also, if the FFA value of feedstock is greater the 1 mgKOH/g, a two-step process comprising acid-catalyzed esterification and alkaline catalyzed transesterification reactions is adopted. Various optimization techniques can be employed for the determination of the effect of the diverse operating and parametric process factors in oil conversion and biodiesel production thereby determining the optimal operating parameters [54-56]. Generally, under varying catalysts and feedstocks, the process parameters for the optimal generation of biodiesel are those that agree with the established standards, particularly the ASTM D6751 and EN 14214

standards. Some of the established parametric conditions and the effects of the choice of catalyst on the production process are presented in Table 4 while Table 5 depicts the outcomes of optimization of the catalytic transesterification reaction.

Table 4. Parametric process for biodiesel production and performance of different catalyst [57-60]

Parameter	Homogeneous catalyst		Heterogeneous catalyst		Supercritical catalyst	Bio-based catalyst
	Base	Acid	Base	Acid		
Reaction temperature (°C)	40 - 75	50 - 100	60 - 65	30 - 460	230 - 350	35 - 60
Reaction pressure	Atmospheric pressure		0.05 - 20 Mpa		19 - 35 Mpa	N/A
Alcohol:oil ratio	3:1 - 9:1	30:1 - 50:1	6:1 - 18:1	6:1 - 70:1	40:1 - 45:1	3:1 - 18:1
Reaction time	1 - 4 h	> 4 h	0.5 - 2 h	3 - 20 h	3 min - 1 h	> 24 h
Glycerol recovery	Hard	Modest	Modest	Simple	Simple	Simple
Product purification	Hard	Modest	Simple	Simple	Simple	Simple
Catalyst cost	Cheap		Moderate		Expensive	
Effect of water	Inhibit reaction	Tolerant to low water content	Inhibit reaction	Tolerant to low water content	Increase reaction rate	Negative effect if excessive
Effect of FFA	Form Soap	No influence	No influence		No influence	
Reusability	No	Yes	Yes		Yes	

Table 5. Some results of optimization of catalytic transesterification reaction [18, 61]

Variable	Effects
Moisture and FFA	• Increases moisture • FFA lowers ester yield • Acid value < 1 mgKOH/g, for the alkali-catalyzed process • Reactants reasonably anhydrous • High moisture content reduces catalyst effectiveness • Increased moisture leads to a reduction in ester yield
Catalyst type and concentration	• Base-catalyst precipitates quicker ester conversion • Acidic-catalyst is slower, works with high FFA and feedstock moisture content • High catalyst concentration causes high conversion yield
Reaction temperature	• Higher reaction temperature increases conversion efficiency and reaction rate
Molar ratio	• Improved ester conversion rate due to greater molar ratio
Reaction time	• Longer reaction time improves conversion yield

1.4.3   Purification of biodiesel

For biodiesel to meet the internationally established ASTM D6751 and EN 14214 standards, the product of the FAME production techniques must be purified. Crude and unpurified biodiesel will compromise engine performance, cause unwanted emissions, as well as complicate handling,

storage, and transportation of the fuel [62]. During purification, impurities such as soap, water, unreacted alcohol, glycerol, metals, etc. are washed away from the crude biodiesel. Table 6 shows the major impurities in crude biodiesel and their effects on the engine. Biodiesel can be purified either through wet washing or dry washing. In water or wet washing, acidified water, ionized water, and other organic solvents, or ionic liquids are used to clean the crude biodiesel. Dry washing, on the other hand, utilizes adsorption and ion-exchange, and membrane separation techniques for purifying crude biodiesel. However, it is generally believed that a single method of purification might be insufficient to achieve clean and pure biodiesel which meets the relevant standards, therefore a combination of wet and dry washing techniques may be needed to achieve a robust biodiesel purification or refinement technology [63, 64].

Despite the extra cost, space for additional purification infrastructure, problems of disposal of spent ion-exchange resin, and treatment of the attendant wastewater generated during purification, the wet purification technique has been widely used. The extra cost and efforts expended during purification pale into insignificance though when compared with the alternative cost of the use of crude biodiesel. Crude biodiesel is deficient in meeting the standards as specified by ASTM D6751 and EN 14214, deteriorate engine performance, and therefore has the capacity to reduce the lifespan of engine parts.

The spent ion-exchange resin can be utilized as compost and additives for animal feed, and the wastewater can be recycled and used for irrigation purposes [65]. Glycerol obtained from the purification of crude biodiesel has found extensive applications as a raw material in chemical industries, personal care products, textile, food, and therapeutic industries. Glycerol is useful in treating renal diseases and disorders of carbohydrate metabolism as well as food supplements for animals, osmoregulatory, cryoprotectant, and thermoregulatory agents [66, 67]. This shows the usefulness of all the products along the biodiesel production value chain.

Table 6. Biodiesel impurities and their effects [50, 59, 68]

Impurity	Effects
FFA	• Rusting of engine parts • Reduced oxidation stability

Water	• Hydrolysis
	• Corrosion of fuel lines, injector pumps, and engine parts
	• Failure of fuel pump and piston corrosion
	• Filter blockage due to bacteriological growth
	• Reduced heat of combustion
	• Ice formation leading to congealing of fuels
Methanol	• Reduced kinematic viscosity, density, and flash point values
	• Rusting of parts made of aluminum and zinc
	• Weakening of natural rubber seals, hoses, and gaskets
Glycerides	• High value of kinematic viscosity
	• Deposition of carbon residue in the injectors
	• Crystallization
Metals (Soap, catalyst)	• Deposition of carbon residue and damage to injectors
	• Obstruction of filter plugging and fuel lines
	• Deterioration of the engine
Glycerol	• Settling and storage problems
	• Fuel tank base deposits and injector damage
	• Increased aldehydes and acrolein emissions
	• Compromised engine durability

1.4.4 Characterization of catalyst, feedstock, and FAME

Catalysts have the capability of lowering the activation energy thereby accelerating the rate of a chemical reaction therefore saving time and cost of energy. However, catalysts can also inhibit the rate of a chemical reaction if an appropriate one is not chosen. A wide range of treatment can be performed on catalysts to enhance their performance. Over the years, different techniques have been advanced to prepare and enhance the capability of heterogeneous catalysts including impregnation, sol-gel, co-precipitation, sulfonation, co-mixing, physical mixing, and calcination. These techniques require extra infrastructure, technicalities, and, sometimes, additional costs to ensure improvement in the performance capability of the catalysts [43]. Solid catalysts can be characterized by thermogravimetric analysis (TGA), Fourier transform infrared (FTIR), differential thermal analysis (DTA), differential thermogravimetry (DTG), X-Ray diffraction (XRD), flame photometric analysis, scanning electron microscopy (SEM), hydrogen nuclear magnetic resonance (HNMR) spectroscopy, thermal electron microscopy (TEM), etc., among other characterization techniques [69-71].

WCO has been considered as a prominent and inexpensive feedstock for FAME due to its advantages over other feedstocks. WCO, being a low-grade feedstock, needs to be treated before conversion to FAME by transesterification process [72, 73]. The pre-treatment procedures arise

as an outcome of the chemical modifications that will have occurred during the persistent high-temperature degradation and contamination by the food that was fried in the oil. The pre-treatment processes involve ridding the WCO of food debris, moisture, and other impurities. The treated WCO can be subjected to determination of acid value (AV), saponification value (SV), iodine value, and molecular weight of the WCO (MW_{oil}). The FFA must be reduced to < 1 mgKOH/g for it to be suitable for the one-step transesterification process [74]. The AV, SV, FFA, and MW_{oil} can be estimated by Equations 4 to 7.

$$A.V = \frac{A \times MM_{KOH} \times 56.1}{W} (mg\ KOH/g) \tag{4}$$

$$FFA = \frac{A.V}{2} \tag{5}$$

$$S.V = \frac{MM_{KOH}(B-S) \times M_{HCl}}{W} \tag{6}$$

$$MW_{oil} = \frac{(56.1 \times 1000 \times 3)}{S.V} \tag{7}$$

Where:

A = volume of potassium hydroxide (KOH) used

W = Feedstock weight

B = volume of hydrochloric acid (HCl) in (ml) required

S = volume of HCl in (ml) required by the sample

MM_{KOH} = molar concentration of KOH

M = molar concentration of HCl

W = weight of the feedstock oil in (g)

Techniques for determining these properties are expressed in the Association of Official Agricultural Chemists (AOAC), ASTM, and EN methods. WCO can also be characterized by gas chromatography-mass spectrometry (GCMS), TGA, FTIR, etc. with a view to determining their composition and behavior. The FA composition of the feedstock has been discovered to influence properties like cetane number (CN), cloud point, flash point (FP), oxidation stability, cold filter plugging point (CFPP), kinematic viscosity (KV), etc.

After purification, FAME is subjected to physical and chemical properties determination and characterization in accordance with methods and procedures specified by their respective AOAC, ASTM, and EN standard procedures. The standard specifications and test methods for FAME B100 are specified by ASTM D 6751 [75], EN 14214 [76, 77], Worldwide Fuel Charter [78], South African National Standard (SANS 1935:2011) [79], among other standards for various countries. The FA compositions are determined by GCMS analysis and have been discovered to impact the performance, handling, storage, transportation, emission characteristics, and behavior of the fuel. Some of the essential properties of FAME linked to its FA composition profile include density, CN, calorific value, KV, iodine number, FP, pour point, cloud point, and CFPP. These properties can be predicted by linear regression models based on the fuel FA compositional profile [80].

1.4.5 Engine performance and emission characteristics of FAME

Apart from availability and economic factors, engine performance and the quality of the exhaust gases are major determining factors in the selection of FAME as an alternative fuel for CI engines. Engine tests are carried out based on established engine test protocols which require that the basic descriptions of the test engine such as manufacturer name, model, model year, power rating, fuel type, number of stroke per cycle, etc. should be clearly stated. Notable performance criteria include torque, power output, brake thermal efficiency (BTE), brake specific fuel consumption (BSFC), and exhaust gas temperature (EGT) are measured at varying engine speeds and loads. Waste cooking oil methyl ester (WCOME) has been found to be a sustainable replacement for PBD fuel in a conventional CI engine owing to its better performance which is attributable to its composition [81]. Due to the oxygenated nature and other fingerprints of FAME, WCOME has been found to present better combustion efficiency and thermal efficiency compared to PBD fuel [82].

The United States Environmental Protection Agency (USEPA) identified carbon monoxide (CO), unburnt hydrocarbon (UHC), particulate matter (PM), nitrogen oxide (NOx), and smoke opacity as major regulated emissions emanating from CI engines. The higher oxygen content of WCOME,

more than any other inherent property, has been identified as a determining factor for the quantity of emission of unmodified CI engine fueled by WCOME [81, 83]. This further justifies the adoption of WCOME as an alternative fuel PBD fuel in order to meet the emission requirements that is becoming increasingly stringent.

1.4.6 Numerical interventions

Due to the escalated intensity of activities in the engine research space, it has become imperative to adopt prediction, modeling, and simulation to speed up and improve the quality of research and their outcomes. Real-time laboratory investigations have increasingly become not only cumbersome, expensive, time-wasting but also involve highly technical person and infrastructure outlay. Numerical techniques, on the other hand, have been found to be fast, cost-effective, flexible, easy to understand and able to predict various scenarios, thereby accelerating the pace, quality, and accuracy of engine research. Researchers, fuel engineers, operators of refineries, engine designers and manufacturers, performance and emission experts have explored innovations in high-speed soft computing to exploit mathematical relations and models to predict, evaluate, optimize, simulate, and authenticate the fingerprints, engine performance parameters, and emission attributes of CI engines [84, 85].

The use of optimization techniques has been found to reduce cost, materials, time of the experiment, and to eradicate 'trial by error' thereby increasing the conversion efficiency during transesterification. Diverse optimization techniques including response surface methodology (RSM), Taguchi orthogonal array (Taguchi OA) [86], artificial neural networks (ANN) [87], matrix laboratory (MATLAB), adaptive neuro-fuzzy inference systems (ANFIS) [88], Box-Behnken design [89], and genetic algorithm (GA) [90], among others have been utilized to optimize the transesterification of feedstocks to FAME. These techniques can be used individually, in combination or in comparison with other techniques using soft computing methods with a view to determining the optimal combination of process parameters for FAME production. Process parameters like catalyst to oil ratio (%w/w), catalyst particle size (µm), reaction temperature (°C), reaction time (min) and methanol to oil ratio can be optimized while

the interrelationship among these identified process parameters can be depicted using three dimensional (3D) surface plots of RSM, ramps and other plots. The Taguchi OA and RSM methods available on the design of experiment (DoE) are among of the most effective and easy to use optimization techniques and the outcomes are usually appraised using statistical parameters including standard error, sum of squares, correlation coefficient (R), F- and p-values, standard deviation, coefficient of determination (R^2), and adjusted R^2 (R^2_{adj}).

Multiple linear regression, ANN, and computational fluid dynamics (CFD), among other numerical approaches, have been used to predict and model FAME fingerprints, performance parameters, and emission characteristics of unmodified CI engine with acceptable outcomes [91-94]. The application of these numerical techniques has gained traction in recent years and has simplified the otherwise cumbersome real-time engine testing process. The holistic utilization of these numerical techniques is the future of fuel and engine research.

The application of mathematical and numerical techniques for the determination of an optimal FAME candidate capable of stimulating enhanced performance and reduced emission can be achieved using parameters with strong theoretical pedestal and verifiable correlations. Attempts to use thermodynamic, temperature, and other correlative models to deliver acceptable models for optimal mix has not been successful owing largely to their deficiency in theoretical footings, despite their appealing and unsophisticated outlook. These models have been unable to generate an optimal candidate partly due to the fact that they do not derive their correlations from the composition of FAME [95, 96]. Composition-based models are computed based on FA compositions and are straightforward and take into consideration the distinctive fingerprints of the individual FAMEs. FAME composition has great influence and produces a more acceptable outcome that can predict the candidate with the optimal mix to enhance engine performance in addition to lowering the emission characteristics of CI engines. The accuracy of this technique can be traced to its stronger theoretical base when compared with other models [97, 98]. Linear mathematical correlations are developed using FA compositions for some important FAME

fingerprints and a trained ANN is used to predict engine performance and emission characteristics.

1.5   Research questions

Arising from the background for this study and the quest to advance biodiesel research, the relevant questions to ask whose answers could address some of the challenges identified in the application of FAME as a renewable, biodegradable, and sustainable fuel for an unmodified CI engine, include the following:

i.   Bearing in mind the current challenges and inadequacies associated with the blending of FAME and retrofitting of CI engines, can an optimal FAME candidate be unearthed in terms of FA composition with the capability of producing enhanced engine performance and mitigated emission in a conventional CI engine?

ii. How well will the developed optimal FAME candidate behave in terms of engine performance parameters and emission characteristics when used to run an unmodified CI engine?

iii. Can the cost of biodiesel production be made more affordable from the standpoint of feedstock and catalysts selection, production techniques, and in line with the principle of conversion of waste to fuel application strategies?

iv. How can the FA composition of FAME be explored to accurately predict the properties, engine performance, and emission characteristics in an unmodified CI engine using linear and nonlinear models?

v.   What is the appropriateness of optimization techniques in simplifying and improving the interrelationship among biodiesel production process parameters with a view to reduced production cost and time while escalating the conversion efficiency?

vi. To what extent can the advantages derivable from the application of WCO as biodiesel feedstock be further explored?

1.6 Aim and objectives of the study

The aim of this research was to engage numerical and experimental techniques to develop an optimal FAME candidate for improved engine performance and mitigated emission characteristics in an unmodified CI engine.

The objectives of the study are summarized as follows:

1. Carry out an extensive literature survey of feedstock and catalyst selection, production of unblended biodiesel, numerical and experimental investigations of engine performance and emission characteristics.

2. Explore mathematical, numerical, and experimental techniques to determine an optimal FAME candidate based on a strong theoretical base with capability for generating improved engine performance and mitigated emission of regulated gases.

3. Develop and train an ANN model with the capacity to accurately predict engine performance and emission characteristics of a conventional CI engine fueled with the newly developed optimal FAME candidate.

4. Synthesize, develop, and characterize a suitable catalyst from existing waste with a view to reducing production cost and improving sanitation.

5. Use appropriate optimization techniques to engender cheaper and more effective process parameters towards affordable biodiesel production process.

6. Model a suitable tool and technique for predicting the thermo-physical properties of the newly developed FAME.

1.7 Significance of the study

The search for an affordable and sustainable alternative fuel to PDB fuel has been intensified over the years due to the reasons advanced above. Various techniques and strategies such as blending, low-temperature combustion, exhaust gas recirculation, etc. have offered little optimism in

meeting engine performance requirements and strict emission standards in spite of the efforts and resources expended in this regard [99, 100]. Also, most countries, particularly in sub-Sahara Africa, have not been able to meet their share of renewable fuel and therefore face a serious energy scarcity threat bearing in mind the volatility in the global fossil fuel market and environmental degradation [101]. The adoption of biodiesel to bridge this gap has been plagued with challenges. Though considerable research has been conducted with much still ongoing in this regard, some gaps still exist and need to be addressed.

One of the major significances of this work is that by determining the optimal FAME mix there is an opportunity to engineer a biofuel to a precise chemical mix that guarantees desirable performance and mitigated emissions. This is an advancement from the existing situation where FAMEs are not produced based on the need for improved performance. This research has shown how FAME can be produced to specifications based on the selection and management of production parameters and processes.

Targeted investigations are needed to evaluate the factors militating against the adequate production of biodiesel to meet the ever-increasing on-road and off-road applications. Global biodiesel need can be met with the adoption of feedstocks that do not conflict with food security, do not contend with land or require irrigation infrastructure for growing food crops, and which are affordable, readily available, and environmentally amenable. Challenges associated with production, characterization, storage and transportation infrastructure of biodiesel must be met in such a way that global standards and regulations are not compromised. Emissions arising from the utilization of pure biodiesel must be eco-friendly and meet international standards [102]. The right policy, tools, techniques, and strategies to conduct cutting edge researches in biodiesel studies and utilization to optimize the potential benefits must be created, adopted and implemented.

1.8   Research scope and delineation

The scope of this research is restricted to the numerical and experimental investigation into the determination and use of an optimal FAME candidate for improved engine performance and

mitigated emissions in a conventional CI engine strategy. The techniques and tools used were limited by the availability, cost, and time constraints.

1.9   Main contributions to the field of study

The application of biodiesel as an alternative fuel for CI engine has not been without its attendant challenges, particularly in terms of its performance and emissions characteristics. This research explored numerical and experimental techniques to develop an optimal FAME candidate with the capability to engender enhanced engine performance and mitigated emissions in an unmodified CI engine. Optimization techniques were applied to determine cheaper and better production process parameters using WCO as a feedstock and a catalyst derived from chicken eggshell waste. The optimal FAME candidate was defined by two FA compositions, namely, palmitic acid (C16:0) and oleic acid (C18:1) which were used as inputs to predict the properties, engine performance parameters, and emission characteristics of the new fuel. The possibility of producing FAME to meet certain standards, performance, and emissions requirements was established.

1.10   Thesis layout

The thesis is arranged to respond to the research questions identified in this study in the sequence laid out above. The thesis is a compilation of research outcomes published in peer-reviewed journals and conferences as stipulated by the University of KwaZulu-Natal for the award of a doctoral degree. A total of twelve publications comprising journal and conference papers are arranged in nine chapters.

Chapter 1 contains the introduction, research motivation, problem statement, and background of the research. The research questions, aim and objectives of the study, as well as the significance of the study and major contributions to the field of study as well as the research scope and delineation were presented.

Chapter 2 provides critical reviews of the properties, engine performance, and emissions characteristics of CI engines fueled with WCOME. This is divided into two parts.

Part 1 reviews the experimental standards, text cycles, benchmarks, and protocols involved in measuring engine performance parameters and emission characteristics of a conventional CI engine. Performance parameters like BSFC, BTE, and EGT, and emission characteristic like CO, CO_2, NOx, UHC, PM, and smoke intensity of CI engine fueled with WCOME are compared with a CI engine fueled with PBD fuel. International standard specifications of FAME by ASTM and EN 14214, ASTM D6751, Worldwide Fuel Charter, and other countries were discussed.

Part 2 presents various numerical approaches in assessing engine performance parameters and emission characteristics in line with international benchmarks and protocols. In this paper, the correlation between properties, engine performance and emission characteristics of FAME, various mathematical, numerical, ANN, CFD, and other techniques for the prediction of properties, engine performance, and emission characteristics are presented

Chapter 3 focuses on the application of modelling, optimization and linear regression tools in biodiesel research. It consists of three parts.

Part 1 explores the application of the Taguchi orthogonal approach (Taguchi OA) for the modelling and optimization of production of biodiesel. To overcome the challenges associated with the conventional one-variable-at-a-time experimental technique, the paper utilized the Taguchi OA to determine the optimized parametric parameters for the conversion of waste sunflower oil (WSFO) to waste sunflower methyl ester. The interconnection and interrelationship between production parameters like a catalyst:WSFO ratio (%w/w), reaction time (min), reaction temperature (ºC), particle size of catalyst (µm), and methanol:WSFO ratio were examined. The influence of each parameter on conversion efficiency was determined using analysis of variance (ANOVA) and other statistical tools.

Part 2 compares the use of response surface methodology (RSM) and Taguchi OA for the modelling and optimization of biodiesel production. The optimum conditions for the transesterification process were determined by the application of RSM and Taguchi OA for the purpose of achieving timely and cost-effective FAME production. It was discovered that RSM presents a more reliable route especially in handling more parameters with nonlinear relations,

and predicted a higher yield, while Taguchi OA offers a cheaper route and linear relations among the parameters.

Part 3 examines the application of linear regression for the prediction of the fingerprints of biodiesel employing FA composition as inputs. Multiple linear regression (MLR) was applied to model linear relations for the prediction of the density, cetane number, calorific value, and kinematic viscosity of biodiesel using palmitic, stearic, oleic, linoleic and linolenic acids as input. The predictive capabilities of the models were verified using statistical analysis.

Chapter 4 reports the outcome of the numerical approach for the determination of optimal FAME mix for enhanced engine performance and mitigated emission. Mathematical and numerical techniques (MATLAB) were employed to solve linear equations generated for the properties of biodiesel, based on their FA compositions and in accordance with acceptable standards, for the determination of an optimal FAME candidate capable of producing better engine performance and mitigated emissions. The numerically generated FAME candidate was produced by the transesterification of waste sunfoil and waste palm oil to FAME.

Chapter 5 presents the comparative study of engine performance and emission evaluation of biodiesel derived from waste oil and *Moringa oleifera* oil. Waste oil methyl ester and moringa oil methyl ester were tested on a 3.5 kW rated, direct injection, single cylinder CI engine. The BTE, BSFC, brake specific unburnt hydrocarbon, brake specific carbon monoxide, and brake specific nitrogen oxide of the engine when running on the two FAME samples were compared.

Chapter 6 describes the development, training, and application of ANN for the prediction of engine performance and emission characteristics of a diesel engine using fatty acid compositions. The trained ANN utilized NNTool on the MATLAB platform to develop the model using a back-propagation algorithm with a Levenberg-Marquardt (LM) learning algorithm to predict BSFC, BMEP, BTE, EGT, CO, smoke intensity, UHC, and NOx. Palmitic acid (C16:0) and oleic acid (C18:1) were used as inputs and a total of 125 sample data were mined from literature to train the model. The regression coefficient and other statistical indicators of the training, validation, and

test data gave satisfactory value, an indication of high predictive proficiency of the model, and demonstrated an improvement on previous efforts.

Chapter 7 presents strategies for the development and characterization of chicken eggshell waste as a potential catalyst for the synthesis of FAME. Boiled, calcined, and uncalcined chicken eggshell powder of different particle sizes were developed into a CaO catalyst and characterized by SEM, TEM, XRD, TGA, and FTIR. The outcome of the investigation showed that high-temperature calcination has the capacity to convert waste chicken eggshell powder to a reusable, cost-effective, and environmentally friendly catalyst for transesterification reaction.

Chapter 8 depicts the properties, and fatty acid compositions of the feedstock and FAME. It consists of two parts.

Part 1 compares the properties and FA compositions of neat vegetable oils and used vegetable oils. This paper compares the FA compositions, iodine value, pH, density, congealing temperature, acid value, kinematic viscosity, cetane index and acid number of neat vegetable oil and samples of waste vegetable oil (WVO) used to fry different food items. The effects of consumption of WVO on human health and aquatic habitat were highlighted.

Part 2 illustrates the effect of usage on the FA composition and properties of neat palm oil (NPO), waste palm oil (WPO), and waste palm oil methyl ester (WPOME). This paper is an extension of the previous research listed in this chapter. In the present scenario, the WPO samples were converted to WPOME. The effect of usage properties, FA compositions, and degree of saturation of the WPOME samples were analyzed and compared with NPO and WPO samples.

Chapter 9 draws the conclusions of the research and offers recommendations for future work.

References

[1]   P. Sadorsky, "Shifts in energy consumption driven by urbanization." In: Davidson, *The Oxford Handbook of Energy and Society,* p. 179, 2018.
[2]   UN. World Urbanization Prospects: The 2018 revision. Available: https://esa.un.org/unpd/wup/Publications/Files/WUP2018-KeyFacts.pdf.

[3]   Worldometers.   Current   World   Population.   Available: https://www.worldometers.info/world-population/.

[4]   BP. Statistical review of world energy, 67th edition, June 2018. Available: https://www.bp.com/content/dam/bp/business-sites/en/global/corporate/pdfs/energy-economics/statistical-review/bp-stats-review-2018-full-report.pdf.

[5]   IEA. Key world energy statistics 2018. Available: https://webstore.iea.org/key-world-energy-statistics-2018.

[6]   TERM, "Transport indicators tracking progress towards environmental targets in Europe; No 7/2015; European Environment Agency: Copenhagen, Denmark," 2015.

[7]   EIA. Energy Information Administration, International Energy Outlook. Available: https://www.eia.gov/outlooks/ieo/ 2017.

[8]   I. Staffell *et al.*, "The role of hydrogen and fuel cells in the global energy system," *Energy & Environmental Science,* vol. 12, no. 2, pp. 463-491, 2019.

[9]   G. Dwivedi and M. Sharma, "Potential and limitation of straight vegetable oils as engine fuel–An Indian perspective," *Renewable and Sustainable Energy Reviews,* vol. 33, pp. 316-322, 2014.

[10]   Q. Li, F. Backes, and G. Wachtmeister, "Application of canola oil operation in a diesel engine with common rail system," *Fuel,* vol. 159, pp. 141-149, 2015.

[11]   S. Sidibé *et al.*, "Use of crude filtered vegetable oil as a fuel in diesel engines state of the art: Literature review," *Renewable and Sustainable Energy Reviews,* vol. 14, no. 9, pp. 2748-2759, 2010.

[12]   S. Che Mat *et al.*, "Performance and emissions of straight vegetable oils and its blends as a fuel in diesel engine: A review," *Renewable and Sustainable Energy Reviews,* vol. 82, pp. 808-823, 2018.

[13]   F. Aydın and H. Öğüt, "Effects of using ethanol-biodiesel-diesel fuel in single-cylinder diesel engine to engine performance and emissions," *Renewable Energy,* vol. 103, pp. 688-694, 2017.

[14]   S. Jain, "The current and future perspectives of biofuels," in *Biomass, Biopolymer-Based Materials, and Bioenergy*: Elsevier, pp. 495-517, 2019.

[15]   D. Dias, A. P. Antunes, and O. Tchepel, "Modelling of emissions and energy use from biofuel fuelled vehicles at urban scale," *Sustainability,* vol. 11, no. 10, p. 2902, 2019.

[16]   H.   Jääskeläinen.   Biodiesel   standards   &   properties.   Available: https://www.dieselnet.com/tech/fuel_biodiesel_std.php.

[17]   R. Goosen, K. Vora, and C. Vona, "Establishment of the guidelines for the development of biodiesel standards in the APEC region," ed: April, 2009.

[18]   J.-H. Ng, H. K. Ng, and S. Gan, "Advances in biodiesel fuel for application in compression ignition engines," *Clean Technologies and Environmental Policy,* vol. 12, no. 5, pp. 459-493, 2010.

[19]   R. R. Shahruzzaman *et al.*, "Modified local carbonate mineral as deoxygenated catalyst for biofuel production via catalytic pyrolysis of waste cooking oil," in *AIP Conference Proceedings*, vol. 2030, no. 1, p. 020006: AIP Publishing, 2018.

[20] K. Dhanasekaran and M. Dharmendirakumar, "Biodiesel characterization and optimization study of used frying palm oil," *International Journal of Current Research and Academic Review,* vol. 2, pp. 105-120, 2014.

[21] D. F. Correa *et al.*, "Towards the implementation of sustainable biofuel production systems," *Renewable and Sustainable Energy Reviews,* vol. 107, pp. 250-263, 2019.

[22] L. P. Chrysikou, *et al.*, "Waste cooking oils exploitation targeting EU 2020 diesel fuel production: Environmental and economic benefits," *Journal of Cleaner Production,* vol. 219, pp. 566-575, 2019.

[23] J. Hill *et al.*, "Environmental, economic, and energetic costs and benefits of biodiesel and ethanol biofuels," *Proceedings of the National Academy of sciences,* vol. 103, no. 30, pp. 11206-11210, 2006.

[24] G. Knothe, "Biodiesel and renewable diesel: a comparison," *Progress in Energy and Combustion Science,* vol. 36, no. 3, pp. 364-373, 2010.

[25] C. M. Noor, M. Noor, and R. Mamat, "Biodiesel as alternative fuel for marine diesel engine applications: A review," *Renewable and Sustainable Energy Reviews,* vol. 94, pp. 127-142, 2018.

[26] S. Zailani *et al.*, "Barriers of biodiesel adoption by transportation companies: A case of Malaysian transportation industry," *Sustainability,* vol. 11, no. 3, p. 931, 2019.

[27] C. Stead *et al.*, "Introduction of biodiesel to rail transport: lessons from the road sector," *Sustainability,* vol. 11, no. 3, p. 904, 2019.

[28] S. Raj and M. Bhandari, "Comparison of Methods of production of biodiesel from Jatropha curcas," *Journal of Biofuels,* vol. 8, no. 2, pp. 58-80, 2017.

[29] H. Ibifubara, N. I. Obot, and M. A. Chendo, "Comparative studies on some edible oils for biodiesel production in Nigeria," *Energy,* vol. 9, no. 10, p. 11, 2014.

[30] A. Atabani *et al.*, "Edible and nonedible biodiesel feedstocks: Microalgae and future of biodiesel," in *Clean Energy for Sustainable Development*: Elsevier, pp. 507-556 2017.

[31] K. Dutta, A. Daverey, and J.-G. Lin, "Evolution retrospective for alternative fuels: First to fourth generation," *Renewable Energy,* vol. 69, pp. 114-122, 2014.

[32] B. Abdullah *et al.*, "Fourth generation biofuel: A review on risks and mitigation strategies," *Renewable and Sustainable Energy Reviews,* vol. 107, pp. 37-50, 2019.

[33] A. E. Atabani *et al.*, "Non-edible vegetable oils: A critical evaluation of oil extraction, fatty acid compositions, biodiesel production, characteristics, engine performance and emissions production," *Renewable and Sustainable Energy Reviews,* vol. 18, pp. 211-245, 2013.

[34] W. A. Kawentar and A. Budiman, "Synthesis of Biodiesel from second-used cooking oil," *Energy Procedia,* vol. 32, pp. 190-199, 2013.

[35] K.-C. Ho,et al., "Biodiesel production from waste cooking oil by two-step catalytic conversion," *Energy Procedia,* vol. 61, pp. 1302-1305, 2014.

[36] A. Martínez *et al.*, "In-situ transesterification of Jatropha curcas L. seeds using homogeneous and heterogeneous basic catalysts," *Fuel,* vol. 235, pp. 277-287, 2019.

[37]   M. B. Navas *et al*., "Transesterification of soybean and castor oil with methanol and butanol using heterogeneous basic catalysts to obtain biodiesel," *Chemical Engineering Science,* vol. 187, pp. 444-454, 2018.

[38]   A. B. Avagyan and B. Singh, "Biodiesel from plant oil and waste cooking oil," in *Biodiesel: Feedstocks, Technologies, Economics and Barriers*: Springer, pp. 15-75, 2019.

[39]   J. Borton *et al*., "Conversion of high free fatty acid lipid feedstocks to biofuel using triazabicyclodecene catalyst (homogeneous and heterogeneous)," *Energy & Fuels,* vol. 33, no. 4, pp. 3322-3330, 2019.

[40]   O. S. Valente *et al*., "Physical–chemical properties of waste cooking oil biodiesel and castor oil biodiesel blends," *Fuel,* vol. 90, no. 4, pp. 1700-1702, 2011.

[41]   E. Zahir *et al.*, "Study of physicochemical properties of edible oil and evaluation of frying oil quality by Fourier Transform-Infrared (FT-IR) spectroscopy," *Arabian Journal of Chemistry,* vol. 10, pp. S3870-S3876, 2017.

[42]   X. Yin *et al*., "Comparison of four different enhancing methods for preparing biodiesel through transesterification of sunflower oil," *Applied Energy,* vol. 91, no. 1, pp. 320-325, 2012.

[43]   N. Mansir *et al.*, "Modified waste egg shell derived bifunctional catalyst for biodiesel production from high FFA waste cooking oil. A review," *Renewable and Sustainable Energy Reviews,* vol. 82, pp. 3645-3655, 2018.

[44]   P. Verma and M. P. Sharma, "Review of process parameters for biodiesel production from different feedstocks," *Renewable and Sustainable Energy Reviews,* vol. 62, pp. 1063-1071, 2016.

[45]   G. Baskar and R. Aiswarya, "Trends in catalytic production of biodiesel from various feedstocks," *Renewable and Sustainable Energy Reviews,* vol. 57, pp. 496-504, 2016.

[46]   I. Ambat, V. Srivastava, and M. Sillanpää, "Recent advancement in biodiesel production methodologies using various feedstock: A review," *Renewable and Sustainable Energy Reviews,* vol. 90, pp. 356-369, 2018.

[47]   S. H. Shuit *et al*., "Evolution towards the utilisation of functionalised carbon nanotubes as a new generation catalyst support in biodiesel production: an overview," *RSC Advances,* vol. 3, no. 24, pp. 9070-9094, 2013.

[48]   M. K. Lam, K. T. Lee, and A. R. Mohamed, "Homogeneous, heterogeneous and enzymatic catalysis for transesterification of high free fatty acid oil (waste cooking oil) to biodiesel: a review," *Biotechnology Advances,* vol. 28, no. 4, pp. 500-518, 2010.

[49]   V. G. Tacias-Pascacio *et al.*, "Comparison of acid, basic and enzymatic catalysis on the production of biodiesel after RSM optimization," *Renewable Energy,* vol. 135, pp. 1-9, 2019.

[50]   V. B. Veljković, I. B. Banković-Ilić, and O. S. Stamenković, "Purification of crude biodiesel obtained by heterogeneously-catalyzed transesterification," *Renewable and Sustainable Energy Reviews,* vol. 49, pp. 500-516, 2015.

[51]   D. Vujicic *et al*., "Kinetics of biodiesel synthesis from sunflower oil over CaO heterogeneous catalyst," *Fuel,* vol. 89, no. 8, pp. 2054-2061, 2010.

[52] T. Maneerung, S. Kawi, and C. Wang, "Gasification bottom ash as a CaO catalyst source for biodiesel production from transesterification of palm oil," *Energy Conversion and Management,* vol. 112, pp. 199-207, 2016.

[53] W. W. S. Ho *et al.*, "Evaluation of palm oil mill fly ash supported calcium oxide as a heterogeneous base catalyst in biodiesel synthesis from crude palm oil," *Energy Conversion and Management,* vol. 88, pp. 1167-1178, 2014.

[54] A. Inayat *et al.*, "Fuzzy modeling and parameters optimization for the enhancement of biodiesel production from waste frying oil over montmorillonite clay K-30," *Science of The Total Environment,* vol. 666, pp. 821-827, 2019.

[55] M. Ayoub *et al.*, "Process optimization for biodiesel production from waste frying oil over Montmorillonite clay K-30," *Procedia Engineering,* vol. 148, pp. 742-749, 2016.

[56] N. Banerjee *et al.*, "Optimization of process parameters of biodiesel production from different kinds of feedstock," *Materials Today: Proceedings,* vol. 5, no. 11, Part 2, pp. 23043-23050, 2018.

[57] R. E. Gumba *et al.*, "Green biodiesel production: a review on feedstock, catalyst, monolithic reactor, and supercritical fluid technology," *Biofuel Research Journal,* vol. 3, no. 3, pp. 431-447, 2016.

[58] Y. M. Sani et al., "Solid acid-catalyzed biodiesel production from microalgal oil—The dual advantage," *Journal of Environmental Chemical Engineering,* vol. 1, no. 3, pp. 113-121, 2013.

[59] I. J. Stojković *et al.*, "Purification technologies for crude biodiesel obtained by alkali-catalyzed transesterification," *Renewable and Sustainable Energy Reviews,* vol. 32, pp. 1-15, 2014.

[60] H. Taher *et al.*, "A review of enzymatic transesterification of microalgal oil-based biodiesel using supercritical technology," *Enzyme Research,* vol. 2011, 2011.

[61] A. K. Agarwal, "Biofuels (alcohols and biodiesel) applications as fuels for internal combustion engines," *Progress in Energy and CombustionSscience,* vol. 33, no. 3, pp. 233-271, 2007.

[62] I. Atadashi *et al.*, "Refining technologies for the purification of crude biodiesel," *Applied Energy,* vol. 88, no. 12, pp. 4239-4251, 2011.

[63] H. Bateni, A. Saraeian, and C. Able, "A comprehensive review on biodiesel purification and upgrading," *Biofuel Research Journal,* vol. 4, no. 3, pp. 668-690, 2017.

[64] J. M. Fonseca, et al., "Biodiesel from waste frying oils: Methods of production and purification," *Energy Conversion and Management,* vol. 184, pp. 205-218, 2019.

[65] S. Živković and M. Veljković, "Environmental impacts the of production and use of biodiesel," *Environmental Science and Pollution Research,* vol. 25, no. 1, pp. 191-199, 2018.

[66] C. J. Mota, B. P. Pinto, and A. L. De Lima, *Glycerol: A versatile renewable feedstock for the chemical industry*. Springer, 2017.

[67] M. R. Monteiro, *et al.*, "Glycerol from biodiesel production: Technological paths for sustainability," *Renewable and Sustainable Energy Reviews,* vol. 88, pp. 109-122, 2018.

[68]   M. Berrios and R. L. Skelton, "Comparison of purification methods for biodiesel," *Chemical Engineering Journal,* vol. 144, no. 3, pp. 459-465, 2008.

[69]   R. S. Malani, *et al.*, "Ultrasound–assisted biodiesel production using heterogeneous base catalyst and mixed non–edible oils," *Ultrasonics Sonochemistry,* vol. 52, pp. 232-243, 2019.

[70]   J. Gardy *et al.*, "A magnetically separable SO4/Fe-Al-TiO2 solid acid catalyst for biodiesel production from waste cooking oil," *Applied Catalysis B: Environmental,* vol. 234, pp. 268-278, 2018.

[71]   Z. Ma and F. Zaera, "Characterization of heterogeneous catalysts," *Surface and Nanomolecular Catalysis,* pp. 1-37, 2006.

[72]   T. T. V. Tran *et al.*, "Green biodiesel production from waste cooking oil using an environmentally benign acid catalyst," *Waste Management,* vol. 52, pp. 367-374, 2016.

[73]   M. Farooq, A. Ramli, and D. Subbarao, "Biodiesel production from waste cooking oil using bifunctional heterogeneous solid catalysts," *Journal of Cleaner Production,* vol. 59, pp. 131-140, 2013.

[74]   M. Chai *et al.*, "Esterification pretreatment of free fatty acid in biodiesel production, from laboratory to industry," *Fuel Processing Technology,* vol. 125, pp. 106-113, 2014.

[75]   Standard specification for biodiesel fuel blend stock (B100) for middle distillate fuels. Report no. D6751-08. ASTM; 2008.

[76]   G. Knothe, "The biodiesel handbook. 1-302. Knothe, G., Van Gerpen, J., and Krahl, J," ed: AOCS Press, Urbana, IL, 2005.

[77]   European Committee for Standardization. EN 14214: automotive fuels – fatty acid methyl esters (FAME) for diesel engines – requirements and test methods. Report no. EN 14214:2008. Management Centre; 2008.

[78]   Worldwide Fuel Charter. Available on http://www.oica.net/wp-content/uploads//WWFC5-2013-Final-single-page-correction2.pdf, 2013.

[79]   South African National Standard (SANS 1935:2011) for automotive biodiesel — Fatty Acid Methyl Esters (FAME) for diesel engines — Requirements and test methods. available on www.sabs.co.za.

[80]   L. F. Ramírez-Verduzco, J. E. Rodríguez-Rodríguez, and A. del Rayo Jaramillo-Jacob, "Predicting cetane number, kinematic viscosity, density and higher heating value of biodiesel from its fatty acid methyl ester composition," *Fuel,* vol. 91, no. 1, pp. 102-111, 2012.

[81]   C. Patel *et al.*, "Comparative compression ignition engine performance, combustion, and emission characteristics, and trace metals in particulates from waste cooking oil, Jatropha and Karanja oil derived biodiesels," *Fuel,* vol. 236, pp. 1366-1376, 2019.

[82]   O. Özener *et al.*, "Effects of soybean biodiesel on a DI diesel engine performance, emission and combustion characteristics," *Fuel,* vol. 115, pp. 875-883, 2014.

[83]   M. Suresh, C. P. Jawahar, and A. Richard, "A review on biodiesel production, combustion, performance, and emission characteristics of non-edible oils in variable compression ratio diesel engine using biodiesel and its blends," *Renewable and Sustainable Energy Reviews,* vol. 92, pp. 38-49, 2018.

[84]   U. Rajak *et al.*, "Numerical investigation of performance, combustion and emission characteristics of various biofuels," *Energy Conversion and Management,* vol. 156, pp. 235-252, 2018.

[85]   S. Salam and T. N. Verma, "Appending empirical modelling to numerical solution for behaviour characterisation of microalgae biodiesel," *Energy Conversion and Management,* vol. 180, pp. 496-510, 2019.

[86]   Y. H. Ta, *et al.*, "Application of RSM and Taguchi methods for optimizing the transesterification of waste cooking oil catalyzed by solid ostrich and chicken-eggshell derived CaO," *Renewable Energy,* vol. 114, pp. 437-447, 2017.

[87]   A. Sarve, S. S. Sonawane, and M. N. Varma, "Ultrasound assisted biodiesel production from sesame (Sesamum indicum L.) oil using barium hydroxide as a heterogeneous catalyst: comparative assessment of prediction abilities between response surface methodology (RSM) and artificial neural network (ANN)," *Ultrasonics Sonochemistry,* vol. 26, pp. 218-228, 2015.

[88]   M. Mostafaei, H. Javadikia, and L. Naderloo, "Modeling the effects of ultrasound power and reactor dimension on the biodiesel production yield: Comparison of prediction abilities between response surface methodology (RSM) and adaptive neuro-fuzzy inference system (ANFIS)," *Energy,* vol. 115, pp. 626-636, 2016.

[89]   V. B. Veljković *et al.*, "Modeling of biodiesel production: Performance comparison of Box–Behnken, face central composite and full factorial design," *Chinese Journal of Chemical Engineering,* 2018.

[90]   M. Corral Bobadilla *et al.*, "Optimizing biodiesel production from waste cooking oil using genetic algorithm-based support vector machines," *Energies,* vol. 11, no. 11, p. 2995, 2018.

[91]   A. P. Tchameni *et al.*, "Predicting the rheological properties of waste vegetable oil biodiesel-modified water-based mud using artificial neural network," *Geosystem Engineering,* vol. 22, no. 2, pp. 101-111, 2019.

[92]   E. G. Giakoumis and C. K. Sarakatsanis, "Estimation of biodiesel cetane number, density, kinematic viscosity and heating values from its fatty acid weight composition," *Fuel,* vol. 222, pp. 574-585, 2018.

[93]   O. D. Samuel and M. O. Okwu, "Comparison of Response Surface Methodology (RSM) and Artificial Neural Network (ANN) in modelling of waste coconut oil ethyl esters production," *Energy Sources, Part A: Recovery, Utilization, and Environmental Effects,* vol. 41, no. 9, pp. 1049-1061, 2019.

[94]   A. Datta and B. K. Mandal, "Numerical prediction of the performance, combustion and emission characteristics of a CI engine using different biodiesels," *Clean Technologies and Environmental Policy,* vol. 20, no. 8, pp. 1773-1790, 2018.

[95]   G. R. Stansell, V. M. Gray, and S. D. Sym, "Microalgal fatty acid composition: implications for biodiesel quality," *Journal of Applied Phycology,* journal article vol. 24, no. 4, pp. 791-801, 2012.

[96] N. Cotabarren, P. Hegel, and S. Pereda, "Thermodynamic model for process design, simulation and optimization in the production of biodiesel," *Fluid Phase Equilibria,* vol. 362, pp. 108-112, 2014.

[97] S. Pinzi, *et al*. "The effect of biodiesel fatty acid composition on combustion and diesel engine exhaust emissions," *Fuel,* vol. 104, pp. 170-182, 2013.

[98] P. R. Menon and A. Krishnasamy, "A composition-based model to predict and optimize biodiesel-fuelled engine characteristics using artificial neural networks and genetic algorithms," *Energy & Fuels,* vol. 32, no. 11, pp. 11607-11618, 2018.

[99] S. M. Krishna *et al.*, "Performance and emission assessment of optimally blended biodiesel-diesel-ethanol in diesel engine generator," *Applied Thermal Engineering,* vol. 155, pp. 525-533, 2019.

[100] R. Piloto-Rodríguez *et al.*, "Conversion of fatty acid distillates into biodiesel: engine performance and environmental effects," *Energy Sources, Part A: Recovery, Utilization, and Environmental Effects,* pp. 1-12, 2019.

[101] H. Hosseinzadeh-Bandbafha *et al.*, "A comprehensive review on the environmental impacts of diesel/biodiesel additives," *Energy Conversion and Management,* vol. 174, pp. 579-614, 2018.

[102] B. Ashok and K. Nanthagopal, "Eco friendly biofuels for CI engine applications," in *Advances in Eco-Fuels for a Sustainable Environment*: Elsevier, pp. 407-440, 2019.

[103] G. Dwivedi and M. P. Sharma, "Impact of cold flow properties of biodiesel on engine performance," *Renewable and Sustainable Energy Reviews,* vol. 31, pp. 650-656, 2014.

[104] L. Wood. (2017) Global Biodiesel Market Forecasts to 2025. Available on https://www.researchandmarkets.com/research/cc7mbw/global_biodiesel. *Research and Markets*.

[105] Statista. Biofuels: global consumption 1990-2035. Available on https://www.statista.com/statistics/243942/worldwide-consumption-of-biofuels/ .

[106] E. Onuh, F. Inambao, and O. Awogbemi, "Performance and emission evaluation of biodiesel derived from waste restaurant oil and Moringa oleifera: A comparative study," *International Journal of Ambient Energy,* pp. 1-8, 2019.

[107] E. Onuh and F. L. Inambao, "A comparative evaluation of biodiesel derived from waste restaurant oil and Moringa," in *2017 International Conference on Domestic Use of Energy (DUE)*, 2017, pp. 210-218: IEEE.

[108] P. Pranav, T. Patel, and K. P. Singh, "Development of database and mathematical models for predicting engine performance parameters using biodiesel," *International Journal of Agricultural and Biological Engineering,* vol. 10, no. 3, p. 121, 2017.

[109] H. Jääskeläinen. Research Engines for Optical Diagnostics. Available on https://www.dieselnet.com/tech/diesel_comb_res.php#tech.

[110] B. Sajjadi, A. A. A. Raman, and H. Arandiyan, "A comprehensive review on properties of edible and non-edible vegetable oil-based biodiesel: Composition, specifications and prediction models," *Renewable and Sustainable Energy Reviews,* vol. 63, pp. 62-92, 2016.

[111] S. M. Miraboutalebi, P. Kazemi, and P. Bahrami, "Fatty Acid Methyl Ester (FAME) composition used for estimation of biodiesel cetane number employing random forest and artificial neural networks: a new approach," *Fuel,* vol. 166, pp. 143-151, 2016.

[112] M. Balat and H. Balat, "Progress in biodiesel processing," *Applied Energy,* vol. 87, no. 6, pp. 1815-1835, 2010.

[113] G. Knothe, J. Krahl, and J. Van Gerpen, *The biodiesel handbook*. Elsevier, 2015.

[114] A. Atabani *et al.*, "Non-edible vegetable oils: a critical evaluation of oil extraction, fatty acid compositions, biodiesel production, characteristics, engine performance and emissions production," *Renewable and Sustainable Energy Reviews,* vol. 18, pp. 211-245, 2013.

[115] R. Piloto-Rodríguez *et al.*, "Prediction of the cetane number of biodiesel using artificial neural networks and multiple linear regression," *Energy Conversion and Management,* vol. 65, pp. 255-261, 2013.

[116] M. J. Pratas *et al.*, "Biodiesel density: Experimental measurements and prediction models," *Energy & Fuels,* vol. 25, no. 5, pp. 2333-2340, 2011.

[117] R. Sakthivel *et al.*, "A review on the properties, performance and emission aspects of the third generation biodiesels," *Renewable and Sustainable Energy Reviews,* vol. 82, pp. 2970-2992, 2017.

[118] E. Alptekin, M. Canakci, and H. Sanli, "Biodiesel production from vegetable oil and waste animal fats in a pilot plant," *Waste Management,* vol. 34, no. 11, pp. 2146-2154, 2014.

[119] P. Saxena, S. Jawale, and M. H. Joshipura, "A review on prediction of properties of biodiesel and blends of biodiesel," *Procedia Engineering,* vol. 51, pp. 395-402, 2013.

[120] H. Sanli, M. Canakci, and E. Alptekin, "Predicting the higher heating values of waste frying oils as potential biodiesel feedstock," *Fuel,* vol. 115, pp. 850-854, 2014.

[121] A. E. Atabani, "A comprehensive review on biodiesel as an alternative energy resource and its characteristics," *Renewable and Sustainable Energy Reviews,* vol. 16, no. 4, pp. 2070-2093, 2012.

[122] K. Muralidharan, D. Vasudevana, and K. N. Sheeba, "Performance, emission and combustion characteristics of biodiesel fuelled variable compression ratio engine," *Energy,* vol. 36, no. 8, pp. 5385-5393, 2011.

[123] U. Rashid, F. Anwar, and G. Knothe, "Evaluation of biodiesel obtained from cottonseed oil," *Fuel Processing Technology,* vol. 90, no. 9, pp. 1157-1163, 2009.

[124] F. Al-Shanableh, E. Ali, and M. A. Savaş, "Fuzzy logic model for prediction of cold filter plugging point of biodiesel from various feedstock," *Procedia Computer Science,* vol. 120, pp. 245-252, 2017.

[125] P. A. Leggieri, M. Senra, and L. Soh, "Cloud point and crystallization in fatty acid ethyl ester biodiesel mixtures with and without additives," *Fuel,* vol. 222, pp. 243-249, 2018.

[126] M. A. Wakil *et al.*,, "Influence of biodiesel blending on physicochemical properties and importance of mathematical model for predicting the properties of biodiesel blend," *Energy Conversion and Management,* vol. 94, pp. 51-67, 2015.

[127] G. Knothe and L. F. Razon, "Biodiesel fuels," *Progress in Energy and Combustion Science,* vol. 58, pp. 36-59, 2017.

[128] G. Knothe and K. R. Steidley, "Kinematic viscosity of biodiesel fuel components and related compounds. Influence of compound structure and comparison to petrodiesel fuel components," *Fuel,* vol. 84, no. 9, pp. 1059-1065, 2005.

[129] P. S. Mehta and K. Anand, "Estimation of a lower heating value of vegetable oil and biodiesel fuel," *Energy & Fuels,* vol. 23, no. 8, pp. 3893-3898, 2009.

[130] S. Pinzi *et al*., "Multiple response optimization of vegetable oils fatty acid composition to improve biodiesel physical properties," *Bioresource Technology,* vol. 102, no. 15, pp. 7280-7288, 2011.

[131] M. Mostafaei, "Prediction of biodiesel fuel properties from its fatty acids composition using ANFIS approach," *Fuel,* vol. 229, pp. 227-234, 2018.

[132] M. Agarwal, K. Singh, and S. Chaurasia, "Prediction of biodiesel properties from fatty acid composition using linear regression and ANN techniques," *Indian Chemical Engineer,* vol. 52, no. 4, pp. 347-361, 2010.

[133] M. J. Ramos *et al*., "Influence of fatty acid composition of raw materials on biodiesel properties," *Bioresource Technology,* vol. 100, no. 1, pp. 261-268, 2009.

[134] L. F. Ramírez-Verduzco, J. E. Rodríguez-Rodríguez, and A. d. R. Jaramillo-Jacob, "Predicting cetane number, kinematic viscosity, density and higher heating value of biodiesel from its fatty acid methyl ester composition," *Fuel,* vol. 91, no. 1, pp. 102-111, 2012.

[135] M. Gülüm and A. Bilgin, "Measurements and empirical correlations in predicting biodiesel-diesel blends' viscosity and density," *Fuel,* vol. 199, pp. 567-577, 2017.

[136] R. Razavi *et al*., "An insight into the estimation of fatty acid methyl ester based biodiesel properties using a LSSVM model," *Fuel,* vol. 243, pp. 133-141, 2019.

[137] F. Al-Shanableh, A. Evcil, and M. A. Savaş, "Prediction of cold flow properties of biodiesel fuel using artificial neural network," *Procedia Computer Science,* vol. 102, pp. 273-280, 2016.

[138] J. Li, W. Yang, and D. Zhou, "Modeling study on the effect of piston bowl geometries in a gasoline/biodiesel fueled RCCI engine at high speed," *Energy Conversion and Management,* vol. 112, pp. 359-368, 2016.

[139] K. Ryu, "Effects of pilot injection pressure on the combustion and emissions characteristics in a diesel engine using biodiesel–CNG dual fuel," *Energy Conversion and Management,* vol. 76, pp. 506-516, 2013.

[140] W. Tutak *et al*., "A comparative study of co-combustion process of diesel-ethanol and biodiesel-ethanol blends in the direct injection diesel engine," *Applied Thermal Engineering,* vol. 117, pp. 155-163, 2017.

[141] T. Selvan and G. Nagarajan, "Combustion and emission characteristics of a diesel engine fuelled with biodiesel having varying saturated fatty acid composition," *International Journal of Green Energy,* vol. 10, no. 9, pp. 952-965, 2013.

[142] P. Tamilselvan and G. Nagarajan, "Combustion and emission characteristics of a diesel engine fuelled with biodiesel having varying palmitic acid, stearic acid and oleic acid in

their fuel composition," *International Journal of Oil, Gas and Coal Technology,* vol. 8, no. 3, pp. 353-368, 2014.

[143] E. Jiaqiang *et al.*, "Effects of fatty acid methyl esters proportion on combustion and emission characteristics of a biodiesel fueled diesel engine," *Energy Conversion and Management,* vol. 117, pp. 410-419, 2016.

[144] Z. Zhang *et al.*, "Effects of fatty acid methyl esters proportion on combustion and emission characteristics of a biodiesel fueled marine diesel engine," *Energy Conversion and Management,* vol. 159, pp. 244-253, 2018.

[145] A. O. Barradas Filho *et al.*, "Application of artificial neural networks to predict viscosity, iodine value and induction period of biodiesel focused on the study of oxidative stability," *Fuel,* vol. 145, pp. 127-135, 2015.

[146] S. K. Hoekman *et al.*, "Review of biodiesel composition, properties, and specifications," *Renewable and Sustainable Energy Reviews,* vol. 16, no. 1, pp. 143-169, 2012.

[147] X. Meng, M. Jia, and T. Wang, "Neural network prediction of biodiesel kinematic viscosity at 313K," *Fuel,* vol. 121, pp. 133-140, 2014.

[148] N. Moradi-kheibari *et al.*, "Chapter 13 - Fatty acid profiling of biofuels produced from microalgae, vegetable oil, and waste vegetable oil," in *Advances in feedstock conversion technologies for alternative fuels and bioproducts*, M. Hosseini, Ed.: Woodhead Publishing, 2019, pp. 239-254.

[149] S. Mitra, P. Bose, and S. Choudhury, "Mathematical modeling for the prediction of fuel properties of biodiesel from their FAME composition," in *Key Engineering Materials*, vol. 450, pp. 157-160: Trans Tech Publ, 2011.

[150] O. Awogbemi, F. L. Inambao, and E. I. Onuh, "Development and Characterization of Chicken Eggshell waste as Potential Catalyst For Biodiesel Production," *International Journal of Mechanical Engineering and Technology,,* vol. 9, no. 12, pp. 1329 - 1346, 2018.

[151] I. M. Monirul *et al.*, "Assessment of performance, emission and combustion characteristics of palm, jatropha and Calophyllum inophyllum biodiesel blends," *Fuel,* vol. 181, pp. 985-995, 2016.

[152] A. N. Ozsezen *et al.*, "Performance and combustion characteristics of a DI diesel engine fueled with waste palm oil and canola oil methyl esters," *Fuel,* vol. 88, no. 4, pp. 629-636, 2009.

[153] M. Serrano *et al.*,, "Oxidation stability of biodiesel from different feedstocks: influence of commercial additives and purification step," *Fuel,* vol. 113, pp. 50-58, 2013.

[154] I. M. Rizwanul Fattah *et al.*, "Effect of antioxidant on the performance and emission characteristics of a diesel engine fueled with palm biodiesel blends," *Energy Conversion and Management,* vol. 79, pp. 265-272, 2014.

[155] D. Kumar and A. Ali, "Nanocrystalline K–CaO for the transesterification of a variety of feedstocks: Structure, kinetics and catalytic properties," *Biomass and Bioenergy,* vol. 46, pp. 459-468, 2012.

CHAPTER 2: REVIEW OF PROPERTIES, ENGINE PERFORMANCE, AND EMISSION CHARACTERISTICS OF COMPRESSION IGNITION ENGINES FUELLED WITH WASTE COOKING OIL METHYL ESTER

This chapter provides critical reviews of the properties, engine performances, and emissions characteristics of CI Engines fuelled with waste cooking oil methyl ester. This consists of two articles.

Article 1 gives a critical review of engine performance and emission characteristics of unmodified CI engines fuelled with unblended FAME. The various engine test protocols, emission standards, performance criteria, and emission characteristics are highlighted. The article has been published in *International Journal of Applied Engineering Research*.

Awogbemi, O., Inambao F., Onuh E. I. (2018). "Performance and Emissions of Compression Ignition Engines Fuelled with Waste Cooking Oil Methyl Ester – A Critical Review," International Journal of Applied Engineering Research (IJAER), ISSN 0973-4562, Volume 13, Number 11, pp. 9706-9723, Research India Publications. https://www.ripublication.com/ijaer18/ijaerv13n11_135.pdf.   (Published)

Article 2 presented a critical review of the various numerical approaches employed in estimating the properties, engine performance parameters, and emission characteristics of an unmodified CI engine fuelled with FAME. Among other subtopics, the article establishes the nexus between FAME properties, engine performance and emission characteristics of CI engines fuelled by B100 WCOME, numerical and optical interventions in engine research, and discussed the outcomes of numerical approaches to predictions in engine performance and emission characteristics before drawing conclusions. The article was published in *International Review of Mechanical Engineering.*

Awogbemi, O., Inambao F., Onuh E. I. (2019). "Prediction of Properties, Engine Performance, and Emissions of Compression Ignition Engines Fuelled with Waste Cooking Oil Methyl Ester – A Review of Numerical Approaches," International Review of Mechanical Engineering (IREME), Volume 13, Number 2, ISSN 1970 – 8734, pp 97-110, Praise Worthy Prize Publishers. https://www.praiseworthyprize.org/jsm/index.php?journal=ireme&page=article&op=view&path%5B%5D=23191.   (Published)

CHAPTER 2 ARTICLE 1: Performance and Emissions of Compression Ignition Engines Fuelled with Waste Cooking Oil Methyl Ester – A Critical Review

Performance and Emissions of Compression Ignition Engines Fuelled with Waste Cooking Oil Methyl Ester – A Critical Review

[1]Awogbemi, O, Inambao, F. and Onuh E.I

Green Energy Solution Research Group, Discipline of Mechanical Engineering,
University of KwaZulu-Natal, Howard College campus, Durban 4041, South Africa.

Abstract

The high cost of edible feedstocks, the food vs fuel debate, the threat of deforestation, environmental pollution, damage to wildlife habitats, etc., has shifted the attention of researchers to the production of biodiesel from waste cooking oil (WCO). This paper reviews recent research on the performance and emission characteristics of waste cooking oil methyl ester (WCOME) in unmodified conventional compression ignition (CI) engines. The general consensus among most authors is that the use of WCOME was found to result in increased brake specific fuel consumption (BSFC), brake thermal efficiency (BTE) and higher exhaust gas temperature (EGT) when compared with petroleum-based diesel fuel. Most authors reported that CI engines fuelled with pure WCOME emitted less carbon monoxide (CO), carbon dioxide (CO_2), and particulate matter (PM), but higher nitrogen oxide (NOx) compared with diesel fuel. The oxygenated nature and other fingerprints of the biodiesel were responsible for the outcomes of the tests. However most of the research was not carried out in substantial compliance with established performance regulations and emission protocols. A niche for a formulated hybrid fatty acid methyl ester (FAME) from WCOME to enhance engine performance and mitigate emissions in line with international best practices and established emission benchmarks exists. This can be investigated through computational means using MATLAB, artificial neural networks (ANN), and computational fluid dynamics (CFD) The paper highlights these possibilities.

Keywords: Biodiesel, emission, hybrid FAME, performance, waste cooking oil

INTRODUCTION AND BACKGROUND

The performance and emission characteristics of unmodified diesel engines fueled with neat petroleum-based diesel (PD) fuel has been revealed to have many inadequacies in recent years. The application of biodiesel, as a renewable alternative, is also not without shortcomings. The high cost of feedstock, interference of edible feedstocks with the food chain, the large expanse of land needed for cultivation, the threat of deforestation and damage to wildlife habitats have necessitated the search for other cheap and readily available feedstocks. The use of waste cooking oil (WCO) as feedstock will not only mitigate the high cost of production by up to 45%, but also eliminate the shortcoming highlighted above [1, 2]. The USA,

Brazil and Germany have continued to dominate the global production of biodiesel (Figure 1). Table I shows the annual volume of used vegetable oil collection in some countries. An estimated 200 000 tons of waste cooking oil are generated but uncollected annually in South Africa. The uncollected WCO contributes to soil and water contamination, sewage blockages, and damage to aquatic life [3, 4]. Generally, biodiesel has been found to be disadvantageous due to its distribution and transportation difficulties, degradation under storage, blocking of fuel filters, injectors, and hoses, emission of higher nitrogen oxide, corrosive nature against copper and brass, extreme engine wear, and unsuitability for use at low temperature [5, 6]. However, its application offers enormous and far reaching benefits.
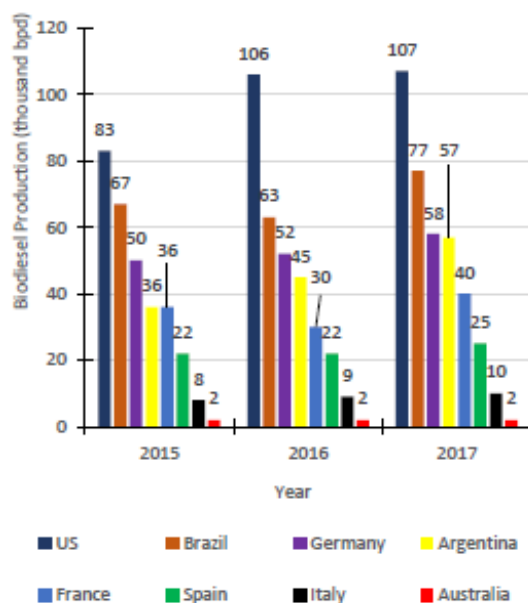
Figure 1. World best producer of biodiesel (thousand bpd) 2015-2017 [7]

40

Table 1. Annual collection of WCO (Million tons)

Country	WCO collection (Million tons)
South Africa	0.06
Malaysia	0.06
Canada	0.135
UK	0.2
Japan	0.6
China	4.5

In recent years, a lot of research has been conducted on the performance and emission characteristics of waste cooking oil methyl esters (WCOME) with varying outcomes. The relevant questions to ask, however, are whether these tests have been performed in line with the test protocols and if the results of the emission tests are in line with the locally or globally recognized standards and benchmarks. Also have these researches been able to come up with the optimal fatty acid methyl ester (FAME) hybrids that will enhance the performance and mitigate emissions of conventional unmodified compression ignition (CI) engines? FAME is a mixture of free fatty acids (FFA), the properties, performance, and behaviours of which are dependent on the fatty acid composition and its degree of saturation. There is a need to continue to investigate the optimal mix of fatty acids to ensure the best performance outcome and emissions mitigation.

This research is a review of various recent works on the use of WCOME in conventional CI engines, with a view to revealing the research gaps for further works. This will be conducted with emphasis on the procedures and criteria adopted by various researchers. The necessity for the use of numerical and computational tools to predict the properties, optimal performance and emission characteristics of hybrid FAME will also be highlighted.

PERFORMANCE REGULATIONS AND EMISSION BENCHMARKS

Engine performance is a measure of degree of effectiveness in the conversion of fuel into useful work by internal combustion engines. This is measured on the basis of known performance parameters, namely: load, speed, torque, brake power, brake specific fuel consumption, brake thermal efficiency, exhaust gas temperature and the emission of regulated gases. As part of the engine test protocols, specifications of the engine must be disclosed, namely: manufacturer, model, model year, displacement, power rating (hp), configuration, bore (m) x stroke (m), induction, fuel type, engine stroke per cycle, and injection. The United States Environmental Protection Agency (EPA) promulgated the new source performance standards (NSPS) for stationary compression ignition engines as a benchmark on emissions of PM, NOx, CO and non-methane hydrocarbons (NMHC) all measured in g/kWh. Depending on the net power (kW) and model year of the engine and other parameters, the USA, EU, Japan, etc., have different standards for measuring regulated emissions for diesel engines [8].

The EU 13 mode cycle for performance and emission measurements for all CI engines are shown in Table 2. The USEPA emission benchmarks for various categories of diesel engines are presented in Table 3, while Table 4 shows the EU emission standards [8, 9].

Table 2. EU 13 mode of emission measurement [8]

Mode	Speed	Load (%)	Duration (Min)
1	Idle	-	4
2		10	2
3	Max Torque Speed	25	2
4		50	2
5		75	2
6		100	2
7	Idle	-	2
8		100	2
9	Rated Power Speed	75	2
10		50	2
11		25	2
12		10	2
13	Idle	-	2

The Department of Minerals and Energy of the Republic of South Africa, in 2007, came up with the Biofuels Industrial Strategy with the aim of stimulating biofuel (bioethanol and biodiesel) as a renewable energy component of the country's energy mix. The document aims to ensure energy security, reduce the emission of greenhouse gas, and make biofuel a major contributor to the socioeconomic development of South Africa. The strategy adopted a 5-year pilot programme for 2% biofuel or 400 million litres per year in the energy mix [10]. However, South Africa has no performance and emission standards for reciprocating internal combustion engines. The legal instrument for the carbon tax and offsets to encourage the utilization of less greenhouse gas (GHG) emission gasses is yet to be promulgated [11].

Table 3: EPA Tier 1-4 Non-road Diesel Engine Emission Standards, g/kWh [9].

Engine Power	Tier	Year	CO	HC	NMHC+NOx	NOx	PM
kW < 8	Tier 1	2000	8.0	-	10.5	-	1.0
	Tier 2	2005	8.0	-	7.5	-	0.8
	Tier 4	2008	8.0	-	7.5	-	0.4[a]
8 ≤ kW < 19	Tier 1	2000	6.6	-	9.5	-	0.8
	Tier 2	2005	6.6	-	7.5	-	0.8
	Tier 4	2008	6.6	-	7.5	-	0.4
19 ≤ kW < 37	Tier 1	1999	5.5	-	9.5	-	0.8
	Tier 2	2004	5.5	-	7.5	-	0.6
	Tier 4	2008	5.5	-	7.5	-	0.3
	Tier 4	2013	5.5	-	7.5	-	0.03
37 ≤ kW < 75	Tier 1	1998	-	-	-	9.2	-
	Tier 2	2004	5.0	-	7.5	-	0.4
	Tier 3	2008	5.0	-	4.7	-	-†
	Tier 4	2008	5.0	-	4.7	-	0.3[b]
	Tier 4	2013	5.0	-	4.7	-	0.03
56 ≤ kW < 130	Tier 4	2012-1014[c]	5.0	0.19	-	0.40	0.02
75 ≤ kW < 130	Tier 1	1997	-	-	-	9.2	-
	Tier 2	2003	5.0	-	6.6	-	0.3
	Tier 3	2007	5.0	-	4.0	-	-†
130 ≤ kW < 225	Tier 1	1996	11.4	1.3	-	9.2	0.54
	Tier 2	2003	3.5	-	6.6	-	0.2
	Tier 3	2006	3.5	-	4.0	-	-†
130 ≤ kW < 560	Tier 4	2011-2014[d]	3.5	0.19	-	0.40	0.02
225 ≤ kW < 450	Tier 1	1996	11.4	1.3	-	9.2	0.54
	Tier 2	2001	3.5	-	6.4	-	0.2
	Tier 3	2006	3.5	-	4.0	-	-†
450 ≤ kW < 560	Tier 1	1996	11.4	1.3	-	9.2	0.54
	Tier 2	2002	3.5	-	6.4	-	0.2
	Tier 3	2006	3.5	-	4.0	-	-†
kW ≥ 560	Tier 1	2000	11.4	1.3	-	9.2	0.54
	Tier 2	2006	3.5	-	6.4	-	0.2

Category	Tier	Year	CO	HC	NMHC	NOx	PM
Generator sets > 900kW	Tier 4	2011	3.5	-	0.40	0.67	0.10
All engines except gensets > 900 kW	Tier 4	2011	3.5	-	0.40	3.5	0.10
Generator sets	Tier 4	2015	3.5	-	0.19	0.67	0.03
All engines except gensets	Tier 4	2015	3.5	-	0.19	3.5	0.04

† Not adopted, engines must meet Tier 2 PM standard.
a - Hand-startable, air-cooled, DI engines may be certified to Tier 2 standards through 2009 and to an optional PM standard of 0.6 g/kWh starting in 2010
b - 0.4 g/kWh (Tier 2) if manufacturer complies with the 0.03 g/kWh standard from 2012
c - PM/CO: full compliance from 2012; NOx/HC: Option 1 (if banked Tier 2 credits used)—50% engines must comply in 2012-2013; Option 2 (if no Tier 2 credits claimed)—25% engines must comply in 2012-2014, with full compliance from 2014.12.31
d - PM/CO: full compliance from 2011; NOx/HC: 50% engines must comply in 2011-2013

Table 4. EU emission standards for CI engines [8]

Category	Date	CO (g/kWh)	HC (g/kWh)	NOx (g/kWh)	PM (g/kWh)	Smoke (m⁻¹)
EURO I	1992-1993	4.5	1.1	8.0	0.612 (0.36)¹	-
EURO II	Oct. 1995-Oct. 1996	4.0	1.1	7.0	0.15	-
EURO III	Oct. 2000-Oct. 2001	2.1	0.56	5.0	0.1	0.8
EURO IV	Oct. 2005-Oct. 2006	1.5	0.46	3.5	0.02	0.5
EURO V	Oct. 2008-Oct.2009	1.5	0.46	2.0	0.02	0.5

FAME COMPOSITION, BIODIESEL PROPERTIES AND HYBRIDIZATION OUTCOMES

The production of biodiesel by the transesterification of vegetable oils or animal fats using triglycerides and alcohol in the presence of an alkalis catalyst, results in the formation of FAME. The fatty acid fingerprint of the biodiesel is dependent on the feedstock and can be determined by a gas chromatography mass spectrometry (GC-MS) analysis. Of the fatty acid constituents of FAME (Table 5), palmitic acid, stearic acid, oleic acid, and linolenic acid have been found to be dominant [12, 13].

Factors such as chain length and branching, degree of saturation, number and position of double bonds, etc., determine the quality, behaviour, physical and chemical properties of FAME. Apart from the inherent properties of FAME itself, production, handling, storage process and procedures also affect its properties. Countries, including Argentina, Brazil, China, EU, Japan, Kenya, New Zealand, South Africa, USA, etc., in line with international protocols and benchmarks, have set standard specifications for FAME in their respective countries. Table 6 shows the specifications of FAME in the USA, EU and some countries including South Africa.

As part of efforts to improve the characteristics, properties and performance of biodiesel feedstock, hybridization of feedstock has been proposed. Hybridization involves blending two or more different feedstocks or B100 biodiesels in varying proportions to produce an entirely new product with a different fingerprint and improved properties compared to the parent stocks. Hybridization, whether in-situ, ex-situ, bi or poly, is not only cost effective but also leads to better yield and quality, and enhanced physico-chemical and thermal properties of FAME when compared with biodiesel from the parent feedstock [13, 14]. However, the FAME derived from hybridization has not been tested on CI engines to verify its performance and emission characteristics, and hence no optimal FAME hybrid has been discovered.

Table 5: Fatty acid composition of FAME [15-17]

Common name	Scientific nomenclature	Chemical formula	Abbreviation	Molecular weight (g/mol)
Saturated fatty acid series				
Palmitic acid	Hexadecanoic acid	$C_{16}H_{32}O_2$ ($C_{15}H_{31}COOH$)	16:0	256.42
Stearic acid	Octadecanoic acid	$C_{18}H_{36}O_2$ ($C_{17}H_{35}COOH$)	18:0	284.47
Lauric acid	Dodecanoic acid	$C_{12}H_{24}O_2$ ($C_{11}H_{23}COOH$)	12:0	200.31
Myristic acid	Tetradecanoic acid	$C_{14}H_{28}O_2$ ($C_{13}H_{27}COOH$)	14:0	228.37
Acetic acid	Ethanoic acid	$C_2H_4O_2$ (CH_3COOH)	2.0	60.05
Butyric acid	Butanoic acid	$C_4H_8O_2$ (C_3H_7COOH)	4.0	88.10
Caproic acid	Hexanoic acid	$C_6H_{12}O_2$ ($C_5H_{11}COOH$)	6.0	116.16
Caprylic acid	Octanoic acid	$C_8H_{16}O_2$ ($C_7H_{15}COOH$)	8.0	144.21
Capric	n-decanoic	$C_{10}H_{20}O_2$ ($C_9H_{19}COOH$)	10.0	172.26
Behenic acid	Docosanoic acid	$C_{22}H_{44}O_2$ ($C_{21}H_{43}COOH$)	22:0	340.58
Lignoceric acid	Tetracosanoic acid	$C_{24}H_{48}O_2$ ($C_{23}H_{47}COOH$)	24.0	368.63
Arachidic acid	Eicosanoic acid	$C_{20}H_{40}O_2$ ($C_{19}H_{39}COOH$)	20:0	312.52
Unsaturated fatty acid series. One double bond				
Oleic acid	cis-9-Octadecenoic acid	$C_{18}H_{34}O_2(CH_3(CH_2)_7 CH=CH(CH_2)_7COOH)$	18:1	282.45
Eladic acid	trans-9-octadecenoic acid	$CH_3(CH_2)_7 CH=CH(CH_2)_7COOH$	3.1	282.45
Myristoleic acid	cis-9-Tetradecenoic acid	$C_{14}H_{26}O_2 (CH_3(CH_2)_3CH=CH(CH_2)_7COOH$	14:1	226.35
Palmitoleic acid	cis-9-Hexadecenoic acid	$C_{16}H_{30}O_2 (CH_3(CH_2)_5 CH=CH(CH_2)_7 COOH)$	16:1	254.40
Two double bonds				
Linoleic acid	cis-9,12-Octadecadienoic acid	$C_{18}H_{32}O_2 (CH_3(CH_2)_4CH=CHCH_2CH=CH(CH_2)_7COOH$	18:2	280.44
Three double bonds				
Linolenic acid	cis-9,12,15-Octadecatrienoic acid	$C_{18}H_{30}O_2 (CH_3CH_2CH=CHCH_2CH=CHCH_2CH=CH(CH_2)_7COOH$	18:3	278.42
Elaeostearic acid	cis 9,11,13-octadecatrienoic acid	$CH_3(CH_2)_3CH=CHCH=CHCH=CH(CH_2)_7COOH$	18:3	278.42

9709

PERFORMANCE OF WCOME

The performance of any fuel is determined by the thermochemical composition and properties of the fuel. The major performance criteria of a diesel engine are brake specific fuel consumption, brake thermal efficiency and exhaust gas temperature. Table 7 presents the summary of outcomes of various researches on the use of pure WCOME as fuel for diesel engines as reported by various authors. The oxygen content, heating value, density, and viscosity of pure biodiesel have been found to influence its behaviour and performance in a conventional compression ignition engine.

Effect on brake specific fuel consumption

Measured in gram per kilowatt hour (g/kWh), the brake specific fuel consumption (BSFC) is a measure of how much fuel is consumed in one hour to produce one kilowatt of brake power. It portrays the combustion efficiency of an IC engine that burns fuel to yield rotational power at the crankshaft.

In their study, Mahesh et al. [29] attributed higher BSFC in a diesel engine to the effects of density, viscosity and heating value (HV) of B100 WCOME. On their part, Zhu et al. [30] and An et al. [31] cited higher oxygen content, decreased low heating value (LHV) and high viscosity of biodiesel as responsible for increased BSFC.

Though they used engines with different configurations Hirkude and Padalkar [32], Sharon et al. [33] and Ozsezen and Canakci [34] reported a 24%, 14.55% and 10% increment in BSFC with used cooking oils compared with neat diesel fuel. They attributed the results to the lower energy content, higher density, increased LHV, higher viscosity, and lower calorific value (CV) of the pure biodiesel. Gopal et al. [35], Hwang et al. [36] and Nedayali and Shirneshan [37] blamed viscosity, density, and reduced lower heating value of B100 WCOME for the higher value of BSFC recorded when biodiesel was experimented with on an unmodified diesel engine.

Man et al. [38], Geng at al. [39], Sanli et al. [40] and Attia and Hassaneen [41] tested pure WCOME on various configurations of unmodified CI engine and reported an increase of 11.03%, 11.53%, 14.17% and 30% respectively of the BSFC when compared with neat PD fuel. Higher oxygen content, reduced heating value, higher density, higher viscosity and low calorific value were cited as responsible for the outcomes.

However, the authors disregarded the recommended test cycle for such tests as specified by regulatory bodies while carrying out the fuel consumption test on an unmodified compression ignition engine under varying engine loads.

Key conclusions on brake specific fuel consumption:

- All the authors agreed that the application of B100 WCOME led to higher brake specific fuel consumption in a diesel engine.

- Higher oxygen content, reduced lower heating value, calorific value, higher viscosity, and density of the B100 WCOME triggered increased fuel consumption.

- Most of the works reviewed jettisoned international performance protocols including disclosure of test engine specifications, observance of test cycles, etc.

Effect on brake thermal efficiency

Brake thermal efficiency (BTE) is the ratio of brake power to fuel power. It is a performance index used to evaluate how well an engine converts the heat from a fuel to useful mechanical energy.

The BTE of pure biodiesel was found to be lower than that of neat diesel fuel. This was as a result of high viscosity, density, increased lower heating value and poor volatility of the oxygenated B100 which led to poor atomization and combustion [32, 33, 35]. In the same vein Nedayali and Shirneshan [37], Attia and Hassaneen [41] and Prabu et al. [42] blamed the higher BTE of B100 on lower calorific value, increased BSFC, and low air-fuel mixing of pure biodiesel. Mahesh et al. [29] found that the BTE of pure WCOME was not significantly different from that of diesel fuel.

On the other hand, some authors reported that the brake thermal efficiency of B100 WCOME was higher than that of neat diesel fuel. They attributed these outcomes to higher oxygen content that ensured a more complete combustion, increased combustion temperature of B100 particularly at higher engine load [31, 38, 40, 43]. Though the 13-mode test cycle was adopted by two of the authors, the authors failed to disclose the model, year, and other important specifications of the test engine in line with established test protocols for engine performance.

Key conclusions on brake thermal efficiency:

- 58.33% of the authors reported lower BTE, 33.33% reported higher BTE while 8.33% reported no significant difference in BTE in CI engine fuelled with B100 WCOME.

- Viscosity, calorific value, lower heating value, density, higher oxygen content and fuel consumption influenced the brake thermal efficiency of diesel engine fuelled with B100 WCOME.

- Partial compliance with performance test protocols as regards to test cycles, disclosure of engine specifications and parameters was observed.

9710

44

Table 6: Standard specification of FAME of various countries

Property (Unit)	Argentina [15]	Australia [18]	Austria [15]	Brazil [19]	China [20]	Chinese Taipei[20]	Colombia [15]	European Union [21]	Test Methods	Germany [22]	Indonesia [23]
	Resolution 1283/2006		ON C1191	ANP Act No. 42 / 2004	GB/T 20828-2007	CNS 15072 K5155	Resolution 180782; Feb 2007	EN 14214	Test Methods	DIN V 51606	SNI 04-7182-2006
Acid no (mg KOH/g, max)	0.5	0.8	0.8	0.8	0.8	0.5	0.8	0.5	EN 14104	0.5	0.8
Carbon residue (wt. %, max)		0.05	0.05	0.05	0.3		0.3	0.3		0.05	0.05
Cetane index (min)							49				
Cetane no. (min)	45	51	49	45	49	51	47	51	EN ISO 5165	49	51
CFPP (°C, max)		Report	≤ 0		Report	0	Report	-5 to -44	EN 116		18
Cloud point (°C, max)				Report			Report	Variable	EN 23015		
Copper strip corrosion (3 hr, at 50 °C, max)	Class 1	Class 1		No. 1	1	1	No 1	No 1	EN ISO 2160	No 1	No. 3
Density (Kg/m^3)	875-900	860-890	850-890	Report	820-900	860-900	860-900	860-900	EN ISO 3675 / EN ISO 12185	875-900	850-890
Distillation (T90, °C, max)		360		360			360				360
Ester content (wt. %, min)	96.5	96.5				96.5	96.5	96.5	EN 14103		96.5
Flash point (°C, max)	100	120	100	100	130	120	120	101	EN ISO 2719	110	100
Monoglycerides (wt. %, max)				1.0	0.8	0.8		0.8	EN 14105	0.8	
Diglycerides (wt. %, max)				0.25	0.2	0.2		0.2	EN 14105	0.4	
Triglycerides (wt. %, max)				0.25	0.2	0.2		0.2	EN 14105	0.4	
Free glycerol (wt. %, max)	0.02	0.02	0.02	0.02	0.02	0.02	0.02	0.02	EN 14105 / EN 14106	0.02	0.02
Total glycerol (wt. %, max)	0.24	0.25	0.24	0.38	0.24	0.25	0.25	0.25	EN 14105	0.25	0.24
Iodine number ($g I_2/100g$, max)	135		120	120		120	120	120	EN 14111 / EN 16300	115	115
Kinematic Viscosity @ 40°C (mm^2/s)	3.5-5.0	3.5-5.0	3.5-5.0	3.5-5.0	1.9-6.0	3.5-5.0	1.9-5.0	3.5-5.0	EN ISO 3104	3.5-5.0	2.3-6.0
Linolenic acid methyl esters (wt. %, max)						12.0		12.0	EN 14103		
Metal (Ca+Mg), ppm, max		5.0				5.0		5.0	EN 14538		

Property (Unit)	Japan [24]	Kenya [25]	Korea [26]	New Zealand [26]	South Africa [27]	Taiwan [23]	Thailand [23]	The Philippines [26]	United States of America [21]	Test Methods	Worldwide fuel charter [28]
	JIS K2390	KS 2227:2010		NZS 7500:2005	SANS 1935:2011	CNS 15072K5155		PNS 2020:2003	ASTM D6751	ASTM Test Methods	Biodiesel guidelines
Metal (Na+K), ppm, max			5.0	10		5.0	5.0	5.0		EN 14108 EN 14109 EN 14538	18
Methanol (wt. %, max)		0.2	0.2	0.5		0.2	0.2	0.2	0.3	EN14110	
Oxidation stability (hrs @ 110°C, min)	6	6		6	6	6	6	6		EN 14112	
Phosphorus (ppm, max)	10	10	20	10		10	10	4.0 mg/kg	10	EN 14107 PrEN 16294	10
Polyunsaturated acid methyl esters (wt. %, max)						1.0		1.0		EN 15779	
Sulfated ash (wt. % max)		0.02	0.02	0.02	0.02	0.02	0.02	0.02	0.03	ISO 3987	0.02
Total contamination (mg/kg, max)			100	10		24	500	24	20	EN 12662	
Total sulphur (ppm, max)	10	10		10	50	10	10	10 mg/kg	10	EN ISO 20846 EN ISO 20884 EN ISO 13032	100
Water and sediment (% vol., max)	0.05	0.05	0.05	0.02			0.05	0.05	0.03	EN ISO 12937	0.05
Water (ppm, max)					500	500					
Acid no (mg KOH/g, max)	0.5	0.5	0.5	0.5	0.8	0.5	0.5	0.5	0.5	D664	0.5
Carbon residue (wt. %, max)	0.3	0.3		0.05	0.05	0.3		0.05	0.05	D4530	0.05
Cetane index (min)	51										
Cetane no. (min)	51	51		51	45	51	51	51	47	D613	51
Cloud point(°C, max)								Report	Report	D2500	
Copper strip corrosion (3 hr, at 50°C, max)	No 1	Class 1	Class 1	No. 1	No. 1	No. 1	Class 1	No. 1	No. 3	D130	Light rusting
Density (Kg/m³)	860-900	860-900	860-900	860-900	860-900	860-900	860-900	860-900			860-900
Distillation (T90, °C, max)	360				360(T-95)			360	360	D1160	

Property									Test Method	
Ester content (wt. %, min)	96.5	96.5	96.5	96.5	96.5	96.5	96.5	96.5		96.5
Flash point (°C, max)	120	120	120	120	100	100	120	100	93	D93	100
Monoglycerides (wt. %, max)	0.8	0.8	0.8	0.8	1.0	0.8	0.8	0.8	0.40	D6584	0.8
Diglycerides (wt. %, max)	0.2	0.2	0.2	0.2	0.25	0.2	0.2	0.2			0.2
Triglycerides (wt. %, max)	0.2	0.2	0.2	0.2	0.2	0.2	0.2	0.2			0.2
Free glycerol (wt. %, max)	0.02	0.02	0.02	0.02	0.02	0.02	0.02	0.02	0.02	D6584	0.02
Total glycerol (wt. %, max)	0.25	0.25	0.24	0.25	0.38	0.25	0.25	0.24	0.24	D6584	0.24
Iodine number (gI_2/100g, max)	120	140	140	140	140	120	120	120			130
Kinematic Viscosity @ 40°C (mm²/s)	3.5-5.0	3.5-5.0	1.9-5.0	2.0-5.0	3.5-5.0	3.5-5.0	3.5-5.0	2.0-4.5	1.9-6.0	D445	2.0-5.0
Linolenic acid methyl esters (wt. %, max)	12.0	12.0		12.0	12.0	12.0	12		12.0		12.0
Metal (Ca+Mg), ppm, max	5.0		5.0	5.0	5.0	5.0	5	5.0	5.0	EN 14538	5.0
Metal (Na+K), ppm, max	5.0	5.0	5.0	5.0	10	5.0	5	5.0	5.0	EN 14538	5.0
Methanol (wt. %, max)	0.2	0.2	0.2	0.2	0.2	0.2	0.2	0.2	0.20	EN14110	0.2
Oxidation stability (hrs @ 110°C, min)	2	6	6	6	6	6	6	6	3	EN 14112	10
Phosphorus (ppm, max)	10	10	10	10	10	10	10	10	10	D4951	4
Polyunsaturated acid methyl esters (wt. %, max)	1.0	1.0	1.0	1.0	1.0	1.0	1.0				1.0
Sulfated ash (wt. %, max)	0.02	0.02	0.01	0.02	0.02	0.02	0.02	0.02	0.02	D874	0.005
Total contamination (mg/kg, max)	24	24	24	24	24	24	24				24
Total sulphur (ppm, max)	10	10	10	10	10	10	10		15	D5453	10
Water and sediment (% vol., max)	0.05	0.05	0.05	0.05	0.02	0.05	0.05	0.05	0.05	D2709	0.05
Water (ppm, max)	500		500	500		500					

47

Effect on exhaust gas temperature

The temperature of the exhaust gas of an IC engine is an indicator of the rate of heat released during fuel combustion. High temperature of the exhaust gas is one of the drawbacks of the diesel engine; engine designers and manufacturers are devising means of mitigating excessive EGT. Manesh el al. [29], Hirkude and Padalkar [32], and Sharon et al. [33] reported that the EGT was higher when an unmodified CI engine was fuelled by pure WCOME. The saturated and oxygenated nature of B100 allowed a better and more complete combustion and hence increased temperature of the exhaust gas.

On the other hand, some authors recorded a lower EGT when a CI engine was fuelled with B100. This was attributed to the latent heat of evaporation, high viscosity, and poor atomization of B100 caused by its high viscosity [39, 41, 42]. The authors did not adopt any test mode/cycles and as such no values were taken at 0% load, 100% load, idle and maximum speed, etc as specified by performance test protocols.

Key conclusions on exhaust gas temperature:

- 50% of the authors reported higher EGT with B100 WCOME while 50% reported otherwise.

- High density, high viscosity, poor volatility, lower heating value, lower calorific value, higher oxygen content, high latent heat of evaporation of WCOME influenced the EGT of a diesel engine.

- The 13-mode test cycle and other test cycles were not carried out as stipulated by performance test protocols.

EMISSION CHARACTERISTICS OF WASTE COOKING OIL METHYL ESTER

One of the motivations for the deployment of B100 WCOME as alternative fuel for diesel engines is to mitigate the release of toxic exhaust gas to the environment. The regulated emissions to be considered are CO, CO_2, UHC, smoke opacity, and PM/Soot. The summary of effects of application of B100 WCOME ester on emissions from various researches is presented in Table 7.

Carbon monoxide emission

The presence of carbon monoxide (CO) in exhaust gas is an indication of incomplete combustion of fuel in an IC engine. Fuelling of diesel engines with biodiesel brings CO emission within the acceptable limits recommended by regulatory bodies. The higher oxygen content which allows for more complete and improved combustion, low carbon content, higher cetane number, and increased air-fuel mixing of B100 were reported to be responsible for the reduced CO emission of CI engine fuelled with B100 WCOME.

While Man et al. [38], Sanli et al. [40], and Hirkude and Padalkar [32] reported 7% to 25%, 15% to 25%, and 21% to 45% reduction respectively Gopal et al. [35], Sharon et al. [33], and Ozsezen and Canakci [34] gave 31%, 52.5% and 67% as their percentage reduction respectively. In addition, other

researchers cited high viscosity, inadequate time for combustion and for oxidation of carbon monoxide to carbon dioxide, insufficient oxygen particularly at higher engine speed, as being responsible for low carbon monoxide emission with B100 compared with neat PD fuel [29-31, 36, 41, 42].

However, Kumar and Jaikumar [44] reported that pure WCOME generated more CO emissions compared to PD fuel. Unfortunately, most of these authors did not measure the CO emission in g/kWh, and the full specifications of the engine were not disclosed, particularly the model, model year, and power rating. These make comparison with CO emission benchmarks cumbersome. Some of the results did not fall within the internationally accepted benchmark for CO emission.

Key conclusions on CO emission:

- Pure WCOME produced less CO emission than neat PD fuel by up to 67%.

- 92.3% of the authors reviewed reported that pure WCOME produced less CO emission.

- Higher oxygen content, air-fuel mixing, increased fuel consumption, higher cetane number, etc., precipitated reduced CO emission.

- Lack of requisite information like the engine specifications and model year did not give room for comparing the result of most authors with the standard emission benchmarks.

Carbon dioxide emission

The release of carbon dioxide (CO_2) is an important parameter for measuring the combustion efficiency of a CI engine. Increased CO_2 emission is an indication of complete combustion of the fuel. The oxygenated fingerprint of B100 WCOME ensured a more complete combustion and oxidation of more carbon monoxide to carbon dioxide hence increased CO_2 emission [29, 33]. On the contrary, some authors reported about 8% reduction in CO_2 emission when they tested B100 WCOME on a CI engine. They ascribed the outcomes to the reduction in BSFC and total combustion duration (TCD) of pure biodiesel [31, 34, 40]. However, these outcomes could not be compared with emission benchmarks since neither US EPA nor EU has benchmarks for carbon dioxide emission.

Key conclusions on CO_2 emission:

- Few researchers investigated the effect of B100 WCOME on carbon dioxide emission compared to carbon monoxide.

- 60% of the authors reviewed agreed that WCOME emitted less carbon dioxide than neat PD fuel while 40% reported otherwise. The higher oxygen content of biodiesel resulted in the emission of more CO_2.

Table 7: Summary of the performance and emissions of diesel engine fuelled with waste cooking oil methyl ester

Fuel Tested	Engine type	Test conditions	Test outcomes		Ref
			Performance	Emissions	
B100 WCOME and diesel	• 1C, 4S, water cooled diesel engine	• Constant engine speed • BMEP of 0N/m² to 25N/m² at 5N/m² step	• BSFC of WCOME > diesel fuel • No significant difference in BTE • EGT of WCOME > diesel fuel • Partial compliance with protocol	• CO emission of WCOME < diesel fuel • CO₂ emission of WCOME > diesel fuel • NOx emission of WCOME > diesel fuel • UHC emission of WCOME < diesel fuel • Smoke opacity of WCOME < diesel fuel • No complete engine specifications	[29]
B100 WCOME and EuroV diesel fuel	• 4C, NA, DI, water-cooled 88 kW diesel engine	• Varying BMEP at constant engine speed of 1800 rpm • Maximum engine torque of 240 Nm	• BSFC of WCOME < Euro V diesel fuel by 10.8% • Partial compliance with protocol	• BSCO of WCOME < Euro V diesel fuel > benchmark • BSNOx of WCOME > Euro V diesel fuel by 11% > benchmark • BSHC of WCOME < Euro V diesel fuel > benchmark • BSPM of WCOME < Euro V diesel fuel < benchmark	[30]
B100 WCOME and diesel fuel	• In-line 4C, 4S • Turbocharged, DI, 75 kW diesel engine	• Engine speed of 800 rpm to 3 600 rpm at intervals of 400 rpm • 25%, 50%, and 100% load	• BSFC of WCOME > diesel fuel • BTE of WFOME > diesel fuel • Partial compliance with protocol	• CO emission of WCOME < diesel fuel < benchmark • CO₂ emission of WCOME < diesel fuel • NOx emission for WCOME < diesel fuel < benchmark • UHC emission for WCOME < diesel fuel < benchmark	[31]
B100 WFOME and diesel fuel	• 1C, 4S. • DI, 3.78 kW diesel engine	• Constant engine speed of 1 500 rpm • Brake load from 0.5 kW to 4 kW in steps of 0.5 kW	• BSFC of WFOME > diesel by 24% • BTE of WFOME < diesel fuel • EGT of WFOME < diesel fuel • Partial compliance	• CO emission of WFOME < diesel fuel by 21% to 45% • NOx emission of WFOME > diesel fuel • PM of WFOME was 23% to 47% < diesel fuel • Lack of data on benchmark and wrong unit	[32]
B100 WPOME and diesel fuel	• 1C, 4S, water cooled NA, DI, 5.2kW diesel engine	• Constant speed of 1 500 rpm. • Brake power 1 kW to 6 kW in intervals of 1 kW	• BFSC of WPOME > diesel fuel by 14.55% • BTE of WPOME < diesel fuel • EGT of WPOME > diesel fuel • Partial compliance	• CO emission of WPOME < diesel fuel by 52.9% • CO₂ emission of WPOME > diesel fuel • NOx emission of WPOME > diesel fuel • UHC emission of WPOME < diesel fuel by 9.53% to 38.09% • Smoke density of WPOME < diesel fuel by 10% to19% • No data for engine category	[33]
B100 WPOME and diesel fuel	• 6C, 4S • Water-cooled, NA, DI, 81 kW diesel engine	• Varying engine speeds of 1 000 rpm to 2 000 rpm in steps of 250 rpm • Injector opening pressure of 197 bar	• BSFC of WPOME > PBDF by 10% • Partial compliance with test protocols	• CO emission of WPOME < PBDF by 67% < benchmark • CO₂ emission of WPOME < PBDF by 8% • NOx emission for WPOME > PBDF by 11% > benchmark • UHC emission of WPOME < PBDF by 26% < benchmark • Smoke opacity of WPOME was 63% to 74% > PBDF	[34]
B100 WCOME and diesel fuel	• 1C, 4S, air cooled • DI, 4.4 kW diesel engine	• Brake power from 1 kW to 5 kW at intervals of 1kW • Constant speed of 1 500 rpm	• BSFC of B100 WCOME > diesel fuel • BTE of WCOME < diesel fuel • Partial compliance with test protocols	• CO emission of WCOME 31% < diesel fuel • NOx emission of WCOME 18.33% > diesel fuel • UHC emission of WCOME 57% < diesel fuel • No data for engine category	[35]
B100 WCOME and diesel fuel	• 1C • Common-rail DI diesel engine	• Engine speed of 1 400 rpm • Injection pressures of 80 MPa and 160 MPa	• BSFC of B100 WCOME > diesel fuel due to reduced LHV of WCOME • Partial compliance with test protocols	• CO emission of WCOME < diesel fuel • NOx emission for WCOME > diesel fuel • UHC emission from WCOME < diesel fuel	[36]

49

Fuel	Engine	Operating conditions	Performance findings	Emission findings	Ref
B100 WCOME and diesel fuel	12C, 4S, water cooled, 486kW supercharged diesel engine generator	• Constant engine speed of 1 530 rpm • Engine loads of 25%, 50%, 75%, & 100%	• BSFC of B100 WCOME > diesel fuel • BTE of B100 was < No. 2 diesel fuel • Partial compliance	• Smoke emissions from WCOME < diesel fuel • No disclosure of requisite engine specifications NA	[37]
B100 WCOME and diesel fuel	4C, naturally aspirated, DI, 88kW diesel engine	• Engine speeds of 0 rpm, 1 280 rpm, 1 920 rpm, and 2 560 rpm • Maximum power of 88kW/3200rpm	• BSFC of B100 WCOME > diesel fuel by 11.03% • BTE of B100 WCOME > diesel fuel • Full compliance with test protocols	• CO emission of WCOME was 7% to 25% < diesel fuel < benchmark • NOx emission of WCOME > diesel fuel by 2% to 20% > benchmark • UHC emission of WCOME < diesel fuel by 2% to 23%	[38]
B100 WCOME and diesel fuel	6C, in-line, water-cooled, DI, 178.2 kW diesel engine	• 125 Nm, 250 Nm, and 375 Nm @ 1 050 rpm • 273 Nm, 546 Nm, and 819 Nm @ 1 500 rpm	• BSFC of B100 WCOME > diesel fuel by 11.53% • EGT of WCOME < diesel fuel • Partial compliance with test protocols	• NOx emission of WCOME < diesel fuel > benchmark	[39]
B100 WFOME and PBDF	6C, 4S, water cooled, DI, turbocharged, intercooled 136kW diesel engine	• Engine torque of 600 Nm. • Engine speeds of 1 100 rpm, 1 400 rpm and 1 700 rpm	• BSFC of B100 WFOME > PBDF by 14.17 • BTE of WFOME > diesel fuel • Partial compliance	• CO emission of WCOME < PBDF > benchmark • CO_2 emission from WCOME < PBDF • NOx emission from WCOME > PBDF > benchmark • UHC emission of WCOME was 23.74% to 36.19% < PBDF < benchmark	[40]
B100 WCOME and PBDF	1C, 4S, air cooled, DI, naturally aspirated diesel engine	• Fuel injection at 24° Crank angle bTDC • Rated power of 5.775 kW at 1 500 rpm	• BSFC of B100 WCOME > diesel fuel by 30% • BTE of WCOME < neat diesel fuel by 6% • EGT of WCOME was 2% < diesel fuel • Partial compliance	• CO emission of WCOME 15% to 25% < diesel fuel < benchmark • NOx emission from WCOME < diesel fuel by 6% • UHC emission of WCOME < diesel fuel by 20% • Smoke opacity of WCOME > neat diesel fuel 20%	[41]
B100 WCOME and diesel fuel	1C, 4S, air cooled, DI, stationary diesel engine	• Engine speeds of 1 800 rpm, 2 500 rpm, and 3 600 rpm	• BSFC of B100 WCOME > diesel fuel • BTE of B100 WCOME < diesel fuel • EGT of WCOME < diesel fuel • Partial compliance	• CO emission < diesel fuel • NOx emission for WCOME > diesel fuel by 17% • The smoke emission of WCOME < diesel fuel by 51% • Wrong unit and inadequate data for engine category	[42]
B100 WCOME and diesel fuel	4C, naturally aspirated DI diesel engine	• Engine loads of 0.16 MPa, 0.33 MPa, 0.49 MPa, 0.65 MPa, and 0.73 MPa	• BSFC of B100 WCOME > diesel fuel • BTE of B100 WCOME > diesel fuel • Partial compliance		[43]
B100 WCOME and diesel	1C, 4S, water cooled, naturally aspirated DI, CI engine	• Power output of 3.7 kW at 1 500 rpm • Injection timing 27%TDC	• BTE of B100 WCOME < diesel fuel • Partial compliance	• CO emission of neat WCO > neat diesel fuel • UHC emission > neat diesel fuel by 20% • No complete data for engine category	[44]

WCOME = Waste cooking oil methyl ester. WFOME = Waste frying oil methyl ester. WPOME = Waste palm oil methyl ester C = Cylinder. S = Stroke. NA = Naturally aspirated. DI = Direct injection. bTDC = before Top Dead Centre. B100 = Pure unblended biodiesel.

50

Nitrogen oxide emission

Nitrogen oxide (NOx) is a product of oxidation of nitrogen which forms more than 70% of the air intake for engine combustion. Nitrogen oxide can be formed by Zeldovich (thermal) mechanism and Fenimore (prompt) mechanism. While Zeldovich is influenced by increased temperature, Fenimore is influenced by free radicals such as CH and CH2 formed from the fuel react with nitrogen to form NOx [43].

Fuelling a compression ignition engine with pure WCOME was reported to result in 1% to 20% more nitrogen oxide when compared with neat diesel fuel. The increased NOx emission was blamed on higher oxygen and nitrogen content, delay of ignition, and higher combustion temperature, increased injection pressure, and high bulk modulus of pure biodiesel [28, 30, 32, 33]. The increased combustion temperature, higher heat of combustion of B100 and high temperature of the combustion chamber occasioned by complete combustion of the oxygenated biodiesel triggered the Zeldoivch mechanism that eventually led to increased NOx emission [27, 31, 34, 38]. On the other hand, An et al. [14], Geng et al. [37] and Attia and Hassaneen [39] reported that NOx emissions from B100 WCOME were lower compared to neat diesel fuel. They attributed their outcome to low heating value and low viscosity of B100.

Key conclusions on NOx emission:

- 80% of the works reviewed reported higher nitrogen oxide emission from pure biodiesel while about 20% reported otherwise.

- High oxygen content, high in-cylinder, prolonged residence time, high nitrogen content, delayed ignition, and high bulk modulus accounted for higher NOx from biodiesel.

- Lack of full disclosure of specifications of test engines prevented comparison with standard benchmarks.

Unburned hydrocarbon emission

Unburned hydrocarbon (UHC) is a gaseous form of hydrocarbon. The presence of UHC in the exhaust of diesel engines indicates incomplete combustion of the fuel as a result of quenching of flame at the cylinder wall, particularly at the crevice regions.

Mahesh et al. [27], Zhu et al. [28] and An et al. [29] observed that higher oxygen content of pure WCOME allowed for more complete and cleaner combustion which resulted in lesser UHC emission compared with neat PD fuel. Also, a reduction of 9.53% to 38.09%, 20%, 23.74% to 36.19%, 26%, and 57% in UHC emissions were reported by Sharon et al. [31], Attia and Hassaneen [39], Sanli et al. [38], Ozsezen and Canakci [32], and Gopal et al. [33] respectively when an unmodified CI engine was fuelled by biodiesel compared with neat diesel fuel. This was attributed to the oxygenated fingerprint of B100 WCOMEl.

Hwang et al. [34] attributed the increased hydrocarbon emission from pure WCOME to higher viscosity of B100 WCOME which caused poor atomization. This was further confirmed by Man et al. [36] and Kumar and Jaikumar [42] who observed a reduction 2% to 23%, and 20% respectively in UHC emission.

Key conclusions on UHC emission:

- About 90.9% of the literature reviewed reported a reduction on UHC emission from pure biodiesel.

- Higher oxygen content of B100 WCOME caused lower unburnt hydrocarbon emissions.

- Most of the results could not be compared with recognized emission standards due to non-disclosure of the model year of the test engine and other details.

Smoke opacity emission

Formation of smoke emission is as a result of shortage of oxygen in the combustion chamber, partial combustion of fuels, the cooling effect of fuel and the complications of combustion delay.

Sharon et al. [33], Prabu et al. [42], and Ozsezen et al. [34] recorded a decrease of 10% to 19%, 51%, and 63% to 74% respectively in smoke opacity of a diesel engine fuelled with B100 compared with when fuelled with neat diesel fuel. They attributed the reduction to higher oxygen content and less aromaticity of B100. Manesh et al. [29] and Hwang et al. [36] cited higher oxygen content and lower carbon content of WCOME as being responsible for reduced smoke emission compared with diesel fuel. On the other hand, Attia and Hassaneen [41] reported that the use of B100 WCOME led to a 20% increase in smoke opacity compared with neat diesel fuel. The high viscosity of B100 WCOME was blamed for this outcome.

Key conclusions on smoke opacity emission:

- 83% of the literature surveyed reported a decrease in smoke opacity emission while 17% dissented.

- The use of pure biodiesel triggered a decrease of between 10% and 74% in smoke opacity emission due to higher oxygen content and lower carbon content of pure biodiesel.

- Inadequate disclosure of specifications of test engine prevented comparison with emission standards and benchmarks.

Particulate Matter emission

Particulate matter (PM) emitted from diesel engines consists of volatile organic compounds (VOC), carbonaceous soot particles, and solid phase materials found in the air.

In their research to investigate the PM emission in an unmodified diesel engine fuelled by pure WCOME, Zhu et al. [30] reported a lower particulate matter as a result of higher oxygen content and less aromaticity of B100 which led to more complete oxidation and dilution of aromatics respectively. PM emission was found to decrease by 23% to 47% with the use of biodiesel fuel due to the higher oxygen content of WCOME compared with PD fuel [32].

Key conclusions on particulate matter emission:

- The application of pure WCOME led to reduction of PM

emission.

- Higher oxygen content and less aromatic nature of WCOME was generally cited as a major cause of the reduction of particulate matter.

- Lack of full disclosure of specifications of test engine prevented comparison with emission standards and benchmarks.

NUMERICAL APPROACH TO PREDICTION AND VALIDATION OF DIESEL ENGINE PERFORMANCE AND EMISSION CHARACTERISTICS

High financial outlay, time, and the technicalities involved in conducting performance and emission experiments have continued to pose challenges to the analysis of the behaviour of fuels in real life internal combustion engines. Researchers, fuel engineers, fuel refiners, engine manufacturers, combustion analysts, etc., have continued to explore the advancement in the high-speed digital computing to develop mathematical models to accurately predict, analyze, and validate engine performance and emissions. The utilization of mathematical models and computer simulations are cost effective, save time, are less laborious, innovative, flexible, and have the capability to forecast and predict "what-if" scenarios [45]. The various models developed by researchers can be broadly divided into either single zone, two zone, or multi zone models.

Single zone models use ordinary differential equations to obtain the cylinder temperature, pressure, and mass. This model enjoys wide usage due to its easy deployment. Two zone combustion models guarantee more accurate and far-reaching results than single zone models. Multi zone models allow comprehensive evaluation of fuel-air distribution in the combustion chamber which allows accurate computation of exhaust gas composition. The multi zone model also considers the calculation of conservation of mass, momentum and energy as well as stochastic and computational fluid dynamics (CFD), but disregards the effects of droplets on turbulence [46]. Characteristically, necessary assumptions concerning constant pressure, constant volume and limited pressure are made for each process of an ideal diesel engine cycle, namely isentropic compression, adiabatic combustion, isentropic expansion, and adiabatic exhaust [47]. This forms the basis for the combustion and emission models.

The rate of combustion, heat transfer, fuel consumption, etc., are governed by the combustion model. The liquid fuel injected into the cylinder is heated then mixed with an adequate amount of air in the air zone to prepare the fuel for combustion in accordance with the chemical kinetic equation. In predicting the engine performance, the fuel spray, heat release, ignition delay submodels, etc., are employed while pollutant formation including the emission of hydrocarbons, oxides of nitrogen, smoke and particulate matter are governed by the emission submodels [46, 48]. Table 8 shows the outcomes of the application of numerical tools to predict and validate performance and emissions of B100 in conventional unmodified compression ignition engines within the last decade.

Datta and Mandal [49] used DIESEL-RK simulation software to predict the brake specific fuel consumption, brake thermal efficiency, and nitrogen oxide emission of a single cylinder, four stroke naturally aspirated direct injection diesel engine. The predicted parameters only deviated from the experimental value by a maximum of 0.8% which was attributed to various assumptions made in the modelling. Awad et al. [50] used a single zone combustion model to predict the performance and combustion characteristics of a diesel engine fuelled with B100 and reported that the predicted result agreed with the experimental results with 2.2% to 2.5% variation. Amba Prasad Rao et al. [51] developed a wide-ranging computational phenomenological model to predict and validate the performance and emissions of a single cylinder CI engine fuelled with pure rapeseed methyl esters. They concluded that the model did not only effectively predict the indicated power, indicated specific fuel consumption (ISFC), indicated thermal efficiency (ITE), nitric oxide (NOx), and soot density, but also the variation, with experimental results being within 10%.

Lesnik et al. [52] used an AVL BOOST simulation program to predict the performance and emissions of a six cylinder, four stroke naturally aspirated CI engine fuelled with B100. The predicted results were found to be between 0.794% and 8.554% of the experimental results. Paul et al. [53] carried out a numerical study of the performance and emission characteristics of a diesel engine using a DIESEL-RK model. The model accurately predicted the BSFC, BTE, NOx, PM, CO_2 and smoke emissions and validated the experimental results.

9718

52

Table 8: Outcomes of different numerical tools for engine performance and emissions of CI engines fuelled with FAME

Fuel tested	Engine type	Test conditions	Models	Submodels	Parameters predicted	Outcomes	Ref
B100	1C, 4S, DI	Brake power: 0 kW to 4 kW	Diesel RK	• Engine friction • Heat release model • NOx formation model • Soot and PM formation model	• BSFC, BTE, EGT • NOx, CO₂, PM, and smoke	Maximum ARD of 0.8% deviation between the predicted and experimental results	[49]
B100	1C, 4S, NA	Power output of 7.5 kW at 2 500 rpm	Single zone combustion model	• Flow through orifice model • Modified Arrhenius law • Triple Wiebe law • Woschnis semi empirical model	• Performance characteristics • Heat release rate • Injection pressure • Fuel burning rate	ARD between 2.2% and 2.5%	[50]
B100	1C	Equivalence ratio 0 Phi to 0.8 Phi, -40°C to 120°C Crank angle	Zero-dimensional Thermodynamics based model	Phenomenological model	Indicated power, ISFC, ITE, NOx and soot density	Successful prediction and validation with ARD of 10% of experimental results	[51]
B100	6C, 4S, NA water cooled	Engine speed: 1 300 rpm to 2 000 rpm / Crank angle: 3 500 CA to 4 000°CA	AVL BOOST simulation model	• Combustion model • Emission formation models for NOx and CO	Torque, power, BSFC, NOx, CO	The predicted parameters within 0.794% to 8.554% of experimental results	[52]
B100	2C, 4S DI diesel engine	Brake power: 1 kW to 5 kW	Diesel RK	• Combustion model • NOx formation model • Soot formation model • PM model	• BSFC, BTE • NOx, CO₂, PM, and smoke emissions	Accurate prediction and validation of performance and emission characteristics within acceptable ADR	[53]
B100	1C, 4S, DI diesel engine	Constant speed of 1 500 rpm / Brake power of 0 kW to 4.4 kW steps of 1.1 kW	Diesel RK	Multizone combustion and emission models	• BSFC • CO, UHC, NOx, smoke opacity	Maximum deviation between predicted and experimental results was 4.64%	[54]
B100	1C, 4S, DI diesel engine	BMEP: 0 MPa to 1.0 MPa steps of 0.2 MPa	ANFIS model	Performance and emission sub-models	• Power, BSFC, BTE, EGT • CO, HC, and NO emissions	Mean relative errors between predicted and experimental results was 1.40% to 27.40%.	[55]
B100	1C, 4S, DI diesel engine		MATLAB ANN model		• BTE, BSFC, EGT • CO, CO₂, HC, NOx	Overall mean absolute percentage error is 4.863001%	[56]
B100	1C, 4S, diesel engine		MATLAB ANN model		• BTE, BSFC, EGT • CO, CO2, HC, NOx and smoke	Percentage error of between 0.10 and 0.03%	[57]
B100	1C, 4S DI diesel engine		Taguchi-Fuzzy model		• BTE, EGT • CO, CO₂, HC, NOx, and smoke	Correlation coefficient of 0.897-0.998	[58]

C = Cylinder, S = stroke, NA = Naturally Aspirated, DI = Direct Ignition. CA = Crank angle. ARD = average relative deviation

Dawody and Bhatti [54] also employed DIESEL-RK software to predict the BSFC, CO, UHC, NOx, and smoke opacity of a single cylinder direct injection CI engine fuelled with B100. They reported that the software accurately predicted the parameters and the outcomes were in good agreement with the experimental results. The utilization of an adaptive neuro-fuzzy inference system (ANFIS) by Hosoz et al. [53] to predict the performance and emissions of one cylinder four stroke diesel engine fuelled with B100 WCOME showed that the ANFIS approach effectively predicted the power, BSFC, BTE, EGT, UHC, NOx, and CO. The results were in line with the experimental outcomes with mean relative errors of 1.40% to 27.40%.

The use of Taguchi-Fuzzy model for the prediction of engine performance and emission characteristics was also reported to be effective in predicting the performance and emission characteristics of a diesel engine with reasonable agreement with experimental results [55]. Various researchers have used artificial neural networks (ANN) to predict and validate the performance and emission characteristics of conventional diesel engine fuelled with B100. Javed et al. [56] corroborated that ANN gave a good prediction and validation of with an average of 4.863% deviation from experimental results while Rao et al. [57] established an average correlation coefficient of 0.999 for the prediction of brake thermal efficiency, brake specific fuel consumption, exhaust gas temperature, HC, NOx, CO_2, CO and smoke.

Key conclusions on numerical approaches to predict engine performance and emission characteristics:

- Numerical models and simulations are an effective and innovative way to predict and validate engine performance and emission characteristics of CI engines.

- The outcomes of these models validated the experimental results with the percentage deviations being within the acceptable average relative deviation (ARD).

- Gaps still exist in the numerical prediction and optimization properties of WCOME for optimum performance and mitigated emissions particularly for optimal hybrid FAME.

CONCLUSIONS

Waste cooking oil offers obvious advantages over other feedstocks for affordable biodiesel production to meet the ever-growing demand for biodiesel. The application of B100 WCOME results in increased BSFC, BTE and higher EGT as well as less CO, CO_2, PM, UHC, but higher NOx emissions when compared with diesel fuel. The peculiar fingerprint of B100 WCOME, particularly the high oxygen content and the degree of saturation, have been found to greatly influence the behaviour, performance and emission characteristics of the fuel.

However, the literature review revealed that the recommended engine test cycle modes were not followed in carrying out the tests. Also, some of the results could not be compared with the standard emission benchmarks set by USEPA, EU and other local bodies due to lack of full disclosure of the specification of test engine like the power (kW), the model, and the model year.

Furthermore, a hybrid FAME for optimal performance and emissions within the acceptable standards and benchmarks has not yet been achieved. The outcomes of various hybridizations of feedstocks have not been tested for performance and emission characteristics in line with USEPA and EU standards. South Africa should expedite actions in setting up its emission standards in the same way that Japan, South Korea, Brazil, Argentina, etc., have.

Though numerical models have been employed to predict the performance and emissions of diesel engines, research gaps still exist in the numerical prediction and optimization properties of WCOME for optimum engine performance and mitigated emissions. The application of numerical and computational tools including MATLAB, Artificial Neural Network (ANN) and Computational Fluid Dynamics (CFD) to formulate hybrid FAME for optimal performance will no doubt be a worthwhile effort.

ACKNOWLEDGEMENT

REFERENCES

[1] Datta, A. and Mandal, B. K., 2016, "A Comprehensive Review of Biodiesel as an Alternative Fuel for Compression Ignition Engine," Renewable and Sustainable Energy Rev., 57, pp. 799-821.

[2] Roy, A. S., Chingkheihunba, A. and Pakshirajan, K., 2016, "An Overview of Production, Properties, and Uses of Biodiesel from Vegetable Oil," in Green Fuels Technology: Biofuels, C. R. Soccol, S. K. Brar, C. Faulds, and L. P. Ramos, Eds., eds, Springer International Publishing, Cham, Switzerland, pp. 83-105.

[3] Hamze, H., Akia, M. and Yazdani, F., 2015, "Optimization of Biodiesel Production from the Waste Cooking Oil Using Response Surface Methodology," Process Saf. Environ. Prot., 94, pp. 1-10.

[4] ETA-Florence Renewable Energies, 2013, "Guidelines for UCO Collection, Transport and Promotion Campaigns Based on Previous Experiences," Available: https://ec.europa.eu/energy/intelligent/projects/sites/iee-projects/files/projects/documents/deliverable_d2.3-guidelines_for_uco_collection.pdf

[5] Mahmudul, H. M., Hagos, F. Y., Mamat, R., Adam, A. A., Ishak, W. F. W. and Alenezi, R., 2017, "Production, Characterization and Performance of Biodiesel as an Alternative Fuel in Diesel Engines – A Review," Renewable Sustainable Energy Rev., 72, pp. 497-509.

[6] Yang, Z., Kumar, A. and Huhnke, R. L., 2015, "Review of Recent Developments to Improve Storage and Transportation Stability of Bio-Oil," Renewable Sustainable Energy Rev., 50, pp. 859-870.

[7] International Energy Agency, 2016, Oil market report, Available:

https://www.iea.org/media/omrreports/tables/2016-08-11.pdf

[8] DieselNet, 2014 "Worldwide emission standards. Heavy duty and off-highway vehicles, 2015-2016, Delphi" Available: http://pdf.directindustry.com/pdf/delphi-power-train/worldwide-emission-standard-heavy-duty-off-highway-vehicle/54988-634887.html

[9] DieselNet, 2017 "Emission Standards. United States: Nonroad Diesel Engines," Available: https://www.dieselnet.com/standards/us/nonroad.php#cycles

[10] Department of Minerals and Energy, 2007, "Biofuels Industrial Strategy of the Republic of South Africa," Available http://www.energy.gov.za/files/esources/renewables/biofuels_indus_strat.pdf(2).pdf

[11] Department of National Treasury, 2016, "Draft Regulations: Carbon Offsets," Available: http://www.treasury.gov.za

[12] Miraboutalebi, S. M., Kazemi, P. and Bahrami, P., 2016, "Fatty Acid Methyl Ester (FAME) Composition Used for Estimation of Biodiesel Cetane Number Employing Random Forest and Artificial Neural Networks: A New Approach," Fuel, 166, pp. 143-151.

[13] Eloka-Eboka A. C. and Inambao, F. L., 2016, "Hybridization of Feedstocks—A New Approach in Biodiesel Development: A Case of Moringa and Jatropha Seed Oils," Energy Sources Part A: Recovery Utilization Environ. Effects, 38, pp. 1495-1502.

[14] Giwa, S., Adekomaya, O., and Nwaokocha, C., 2016, "Potential Hybrid Feedstock for Biodiesel Production in the Tropics," Front. Energy, 10, pp. 329-336.

[15] Hoekman, S. K., Broch, A., Robbins, C., Ceniceros, E. and Natarajan, M., 2012, "Review of Biodiesel Composition, Properties, and Specifications," Renewable Sustainable Energy Rev., 16, pp. 143-169.

[16] Borges, M., Díaz, L., Gavín, J. and Brito, A., 2011, "Estimation of the Content of Fatty Acid Methyl Esters (FAME) in Biodiesel Samples from Dynamic Viscosity Measurements," Fuel Process. Technol., vl. 92, pp. 597-599.

[17] Gopinath, A., Sairam, K., Velraj, R. and Kumaresan, G., 2015, "Effects of the Properties and the Structural Configurations of Fatty Acid Methyl Esters on the Properties of Biodiesel Fuel: A Review," Proc. Inst. Mech. Eng. Part D: J. Automobile Eng., 229, pp. 357-390.

[18] Attorney-General's Department, Canberra, Australia, 2009, "Fuel Standard (Biodiesel) Determination 2003 as Amended," Prepared by the Office of Legislative Drafting and Publishing, Available https://www.legislation.gov.au/Details/F2009C00146/Download

[19] DieselNet, 2017 "Brazil, Diesel Fuel, Biodiesel Fuel," Available:

https://www.dieselnet.com/standards/br/fuel_biodiesel.php

[20] Goosen, R., Vora, K. and Vona, C., 2009, "Establishment of the Guidelines for the Development of Biodiesel Standards in the APEC Region," Available: https://www.apec.org/-/media/APEC/Publications/2009/4/Guidelines-for-the-Development-of-Biodiesel-Standards-in-the-APEC-Region-April-2009-APEC-21st-Centur/09_ewg_biodiesel_THA.pdf.

[21] Jääskeläinen, H., 2009, "Biodiesel Standards & Properties," Available: https://www.dieselnet.com/tech/fuel_biodiesel_std.php

[22] Biofuels Systems Group, 2018, "Biodiesel Standards," Available: https://www.biofuelsystems.com/specification.htm

[23] Sarin, A. ed., 2012, Biodiesel Production and Properties. Royal Society of Chemistry Publishing, Cambridge, UK.

[24] DieslNet, 2006 "Quality Assurance Law Specifications for Japanese Industrial Standard (JIS)," Available: https://www.dieselnet.com/standards/jp/fuel_biodiesel.php

[25] Ndegwa, G., Moraa, V., Jamnadass, R., Mowo, J., Nyabenge, M. and Iiyama, M., 2011, "Potential for Biofuel Feedstock in Kenya," ICRAF Working Paper No. 139, World Agroforestry Centre, Nairobi, Kenya.

[26] J. Hamilton, J. Jones, J. Stepan, G. Dierkers, J. Finnell, H. Friedman, et al., 1997, "Biodiesel Research Progress 1992-1997," Prepared for: National Renewable Energy Laboratory, Golden, Colorado, USA.

[27] South African Bureau of Standards, 2011, "South African National Standard (SANS 1935:2011) for Automotive biodiesel — Fatty Acid Methyl Esters (FAME) for diesel engines — Requirements and test methods," Available: www.sabs.co.za

[28] European Automobile Manufacturers Association, 2013, "Worldwide Fuel Charter," Available: http://www.oica.net/wp-content/uploads//WWFC5-2013-Final-single-page-correction2.pdf

[29] Mahesh, S. E., Ramanathan, A., Begum, K. M. S. and Narayanan, A., 2015, "Biodiesel Production from Waste Cooking Oil using KBr Impregnated CaO as Catalyst," Energy Convers. Manage., 91, pp. 442-450.

[30] Zhu, L., Cheung, C., Zhang, W. and Huang, Z., 2011, "Combustion, Performance and Emission Characteristics of a DI Diesel Engine Fueled with Ethanol–Biodiesel Blends," Fuel, 90, pp. 1743-1750.

[31] An, H., Yang, W., Maghbouli, A., Li, J., Chou, S. and Chua, K., 2013, "Performance, Combustion and Emission Characteristics of Biodiesel Derived from Waste Cooking Oils," Appl. Energy, 112, pp. 493-499.

[32] Hirkude, J. B. and Padalkar, A. S., 2012, "Performance and Emission Analysis of a Compression Ignition Engine

Operated on Waste Fried Oil Methyl Esters," Appl. Energy,. 90, pp. 68-72.

[33] Sharon, H., Karuppasamy, K., Kumar, D. S. and Sundaresan, A., 2012, "A test on DI diesel engine fueled with methyl esters of used palm oil," Renewable Energy, 47, pp. 160-166.

[34] Ozsezen A. N. and Canakci, M., 2011, "Determination of Performance and Combustion Characteristics of a Diesel Engine Fueled with Canola and Waste Palm Oil Methyl Esters," Energy Convers. Manage., 52, pp. 108-116.

[35] Gopal, K. N., Pal, A., Sharma, S., Samanchi, C., Sathyanarayanan, K. and Elango, T., 2014, "Investigation of Emissions and Combustion Characteristics of a CI Engine Fueled with Waste Cooking Oil Methyl Ester and Diesel Blends," Alexandria Eng. J., 53, pp. 281-287.

[36] Hwang, J., Qi, D., Jung, Y. and Bae, C., 2014, "Effect of Injection Parameters on the Combustion and Emission Characteristics in a Common-Rail Direct Injection Diesel Engine Fueled with Waste Cooking Oil Biodiesel," Renewable Energy, 63, pp. 9-17.

[37] Nedayali A. and Shirneshan, A., 2016, "Experimental Study of the Effects of Biodiesel on the Performance of a Diesel Power Generator," Energy Environ., 27, pp. 553-565.

[38] Man, X., Cheung, C., Ning, Z., Wei, L. and Huang, Z., 2016, "Influence of Engine Load and Speed on Regulated and Unregulated Emissions of a Diesel Engine Fueled with Diesel Fuel Blended with Waste Cooking Oil Biodiesel," Fuel, 180, pp. 41-49.

[39] Geng, P., Mao, H., Zhang, Y., Wei, L., You, K., Ju, J., et al., 2017, "Combustion Characteristics and NOx Emissions of a Waste Cooking Oil Biodiesel Blend in a Marine Auxiliary Diesel Engine," Appl. Therm. Eng., 115, pp. 947-954.

[40] Sanli, H., Canakci, M. ,Alptekin, E., Turkcan, A. and Ozsezen, A., 2015, "Effects of Waste Frying Oil Based Methyl and Ethyl Ester Biodiesel Fuels on the Performance, Combustion and Emission Characteristics of a DI Diesel Engine," Fuel, 159, pp. 179-187.

[41] Attia A. M. and Hassaneen, A. E., 2016, "Influence of Diesel Fuel Blended with Biodiesel Produced from Waste Cooking Oil on Diesel Engine Performance," Fuel, 167, pp. 316-328.

[42] Prabu, S. S., Asokan, M., Roy, R., Francis, S. and Sreelekh, M., 2017, "Performance, Combustion and Emission Characteristics of Diesel Engine Fuelled with Waste Cooking Oil Bio-Diesel/Diesel Blends with Additives," Energy, 122, pp. 638-648.

[43] Wei, L., Cheung, C. and Ning, Z. 2017, "Influence of Waste Cooking Oil Biodiesel on Combustion, Unregulated Gaseous Emissions and Particulate Emissions of a Direct-Injection Diesel Engine," Energy, 127, pp. 175-185.

[44] Kumar M. S. and Jaikumar, M., 2014, "A Comprehensive Study on Performance, Emission and Combustion Behavior of a Compression Ignition Engine Fuelled with WCO (Waste Cooking Oil) Emulsion as Fuel," J. Energy Inst., 87, pp. 263-271.

[45] Gogoi T. and Baruah, D., 2010, "A Cycle Simulation Model for Predicting the Performance of a Diesel Engine Fuelled by Diesel and Biodiesel Blends," Energy, 35, pp. 1317-1323.

[46] Kumar S. and Chauhan, M. K. 2013, "Numerical Modeling of Compression Ignition Engine: A Review," Renewable Sustainable Energy Rev., 19, pp. 517-530.

[47] Heywood, J. B., 1988, Internal Combustion Engine Fundamentals, McGraw-Hill, New Your, USA.

[48] Lakshminarayanan P. A. and Aghav, Y. V., 2010, Modelling Diesel Combustion, Springer, New York, USA.

[49] Datta A. and Mandal, B. K., 2017, "Engine Performance, Combustion and Emission Characteristics of a Compression Ignition Engine Operating on Different Biodiesel-Alcohol Blends," Energy, 125, pp. 470-483.

[50] Awad, S., Varuvel, E. G., Loubar, K. and Tazerout, M., 2013, "Single Zone Combustion Modeling of Biodiesel from Wastes in Diesel Engine," Fuel, 106, pp. 558-568.

[51] Rao, G. A. P., Shashank, M., Babu, M. V. and Murthy, K. M., 2017, "Simulation of CI Engine Flow Processes for Prediction of Performance and Emissions with Different Fuels," Int. J. Ambient Energy, pp. 1-9,.

[52] Lešnik, L., Iljaž, J., Hribernik, A. and Kegl, B., 2014, "Numerical and Experimental Study of Combustion, Performance and Emission Characteristics of a Heavy-Duty DI Diesel Engine Running on Diesel, Biodiesel and their Blends," Energy Convers. Manage., 81, pp. 534-546.

[53] Paul, G., Datta, A. and Mandal, B. K., 2014, "An Experimental and Numerical Investigation of the Performance, Combustion and Emission Characteristics of a Diesel Engine Fueled with Jatropha Biodiesel," Energy Procedia, 54, pp. 455-467.

[54] Al Dawody M. F. and Bhatti, S. K., 2014, "Experimental and Computational Investigations for Combustion, Performance and Emission Parameters of a Diesel Engine Fueled with Soybean Biodiesel-Diesel Blends," Energy Procedia, vol. 52, pp. 421-430.

[55] Hosoz, M., Ertunc, H. M. Karabektas, M. and Ergen, G., 2013, "ANFIS Modelling of the Performance and Emissions of a Diesel Engine Using Diesel Fuel and Biodiesel Blends," Appl. Therm. Eng., 60, pp. 24-32.

[56] Javed, S,. Satyanarayana Murthy, Y. V. V., Baig, R. U. and Prasada Rao, D., 2015, "Development of ANN Model for Prediction of Performance and Emission Characteristics of Hydrogen Dual Fueled Diesel Engine with Jatropha Methyl Ester Biodiesel Blends," J. Nat. Gas Sci. Eng., 26, pp. 549-557.

[57] Prasada Rao, K., Victor Babu, T., Anuradha, G. and Appa

Rao, B. V. 2017, "IDI Diesel Engine Performance and Exhaust Emission Analysis using Biodiesel with an Artificial Neural Network (ANN)," Egypt. J. Pet., 26, pp. 593-600.

[58] Sakthivel G. and Ilangkumaran, M., 2017, "Optimisation of Compression Ignition Engine Performance with Fishoil Biodiesel using Taguchi-Fuzzy Approach," Int. J. Ambient Energy, 38, pp. 146-160.

CHAPTER 2 ARTICLE 2: Prediction of Properties, Engine Performance and Emissions of Compression Ignition Engines Fuelled with Waste Cooking Oil Methyl Ester - A Review of Numerical Approaches

Prediction of Properties, Engine Performance and Emissions of Compression Ignition Engines Fuelled with Waste Cooking Oil Methyl Ester - A Review of Numerical Approaches

O. Awogbemi, F. Inambao, E. I. Onuh

Abstract – *Given the challenges of renewability, affordability, and sustainability that ultra-low sulfur diesel (ULSD) fuel and first-generation biodiesel currently face, a niche clearly exists for biodiesel sourced from waste cooking oil. Exploring these potentials requires insights into a range of properties as well as performance and emission characteristics. Real-time experimental determination of fatty acid methyl ester (FAME) properties, engine performance and emissions of compression ignition (CI) engines fuelled with unblended FAME is technical, time-consuming, expensive, and requires sophisticated laboratory infrastructure, unlike numerical prediction techniques. Emerging trends and consensus indicate that utilization of numerical simulation and prediction techniques are cost-effective, less laborious, innovative, and flexible. Although FAME properties, engine performance, and emissions have been accurately predicted via various numerical techniques in the recent past, important gaps such as using numerical approaches to determine the optimal FAME mix still exist. The objective of this study was to review the numerical techniques employed in predicting FAME properties, engine performance and emissions of CI engine and investigate whether an optimal FAME candidate can be unearthed through these numerical prediction techniques. This review reports that the outcomes of these numerical predictions agree with experimental data and fall within acceptable average relative deviation but a precise approach to determining an optimal FAME candidate was not achieved. The use of numerical tools like MATLAB and computational fluid dynamics (CFD) in amalgamation with some new measurement techniques including high-speed cameras to accurately predict FAME properties, engine performance, emission characteristics and gain access to the activities in the combustion chambers, were highlighted. These high capacity modeling tools, high-speed cameras, and techniques can be used to accurately forecast an optimal FAME mix to improve engine performance, meet emission benchmarks and advanced engine research, if well harmonized. Copyright © 2019 Praise Worthy Prize S.r.l. - All rights reserved.*

Keywords: *Compression Ignition Engines, CFD, Engine Performance, Numerical Prediction, MATLAB, Optimal Mix*

I. Introduction

The quest for cost-effective, environmentally friendly and readily available alternative fuels to power compression ignition (CI) engines has increased the tempo of research in biodiesel over the last decades. The adoption of used vegetable oil, a cheap and readily available biodiesel feedstock, for the generation of fatty acid methyl ester (FAME) to replace the ultra-low sulfur diesel (ULSD) fuel is as a result of its comparable performance and emissions levels when used in its unblended form to power CI engines. Over the years, CI engines have continued to find applications for on-road and off-road purposes in construction equipment, electricity generating plants, ships, trucks, passenger and personal vehicles, trains and locomotives. According to a report by the Freedonia Group, sales of diesel engines will continue to increase by not less than 7.7% per annum because of their reliability, dependability, high power output and diverse usefulness [1]. The Organization for Economic Cooperation and Development and the Food and Agriculture Organization have projected a minimum of 14% increment in the production and consumption of biodiesel from 2016 to 2025, as shown in Fig. 1, with the bulk of the data emanating from the United States of America, Brazil, Germany, Argentina, France, Spain, etc. [2]. As shown in Fig. 2, waste cooking oil (WCO) features prominently as one of the globally recognized biodiesel feedstocks. The advantages of WCO as a FAME feedstock include low cost, non-interference with the food chain, enhanced waste disposal and a cleaner environment, preservation of aquatic and terrestrial habitats, prevention of drainage blockage as well as serving as an avenue for additional income for households and small-scale businesses. That FAME has been acknowledged as a sustainable

alternative to ULSD fuel is not unconnected with its green nature, low cost, low emissions as well as its inherent properties including lubricity, zero sulfur content and improved biodegradability. Biodiesel retards engine wear and deterioration and contains no poly-aromatic or nitrous poly-aromatic hydrocarbons.

However, its low oxidative stability and depreciation in quality during storage constitute significant challenges that need to be tackled [3], [4].
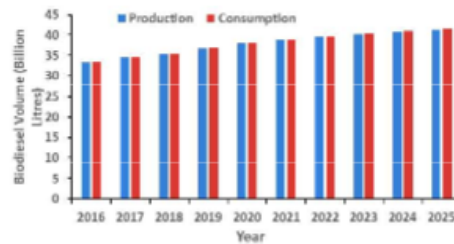
Fig. 1. Global production and consumption of biodiesel (billion liters)

Fig. 2. Global distribution of biodiesel feedstock [5]

Research aimed at improving the properties, behaviours, performance and emission characteristics of unblended FAME has increased substantially in recent years. Real-time experiments and use of engine test beds are the hallmarks of these investigations. However, high levels of technicalities, equipment requirements, the time and cost of conducting real-time experiments and engine tests pose a lot of challenges to researchers in all the aspects of FAME development and engine testing. High-speed digital computers are being employed by fuel refiners and engineers, emission specialists, engine designers, and manufacturers to develop numerical tools and mathematical models to accurately predict and validate FAME properties, engine performance, and emissions. The utilization of mathematical models and computer simulations are cost-effective, time-saving, less laborious, more innovative, more flexible, and have the capability to forecast and predict "what-if" scenarios [6].

Despite the historical and widespread use of numerical tools and techniques in engine research, especially in property predictions, engine performance criteria and emission characteristics, gaps regarding the determination of an optimal FAME mix still exist. The

relevant questions to ask are (i) have these numerical and mathematical approaches been able to effectively predict FAME properties, engine performance and emissions characteristics within acceptable accuracy? (ii) has the engagement of these numerical tools and models been able to unearth an optimal FAME candidate that will improve engine performance and mitigate emissions of pollutants in line with established standards and benchmarks in an unmodified CI engine? The motivation for this study is to critically review the numerical tools and approaches employed by various researchers and come up with applicable formulations for the determination of an optimal FAME mix that would result in peak engine performance and mitigated emissions in line with globally accepted standards and emission benchmarks. This study aims to review numerical tools and techniques applied by various researchers to predict the properties of B100 FAME, and engine performance and emissions of conventional CI engines energized with B100 FAME. This present effort will stress the application of mathematical and numerical predictions targeted at achieving more accurate outcomes of property, engine performance and emissions estimates.

The use of soft computers, numerical and mathematical prediction techniques will not only be cost-effective, innovative, less cumbersome, allows for the consideration of diverse countless scenarios but also shrink the rigidities associated with experimentations.

Also, the use of numerical and optical approaches including high-speed cameras, particularly Phase Doppler Interferometry, Engine Endoscopy, and Laser beam measurements, in engine research in providing access to combustion chambers will be underscored. The objective is to suggest numerical techniques to predict a FAME mix for optimal performance and mitigated emissions. The scope of this work is limited to reviewing the use of numerical tools and techniques to predict FAME properties, engine performance and emissions of the application of B100 FAME in unmodified CI engines and suggest new measurement techniques to advance the course of biofuel combustion engine research.

II. Correlation between Properties, Engine Performance and Emission Characteristics of FAME

There has been a well-established nexus between FAME properties, engine performance and emission characteristics of CI engines fuelled by B100 WCOME.

Fatty acid (FA) composition, the degree of saturation, length of the carbon chain, number and location of double bonds, among other considerations, determine the properties of FAME and by extension, its behavior, performance and emission characteristics. Common fatty acid constituents of FAME include palmitoleic acid (C16:1) oleic acid (C18:1), palmitic acid (C16:0), linoleic (C18:2), linolenic (C18:3), myristic acid (C14:0), arachidic acid (C20:0), lauric acid (C12:0), stearic acid

(C18:0) and eicosenic acid (C20:1) [7]-[9]. The fatty acid compositions are a vital fingerprint of FAME which is contingent on the feedstock source and ascertained by Gas Chromatography Mass Spectrometry (GCMS) analysis. ASTM D6751 and EN 14214 stipulate the standard of FAME properties for the United States of America and Europe respectively and all other countries derive their respective standards from these two sources [10]. The standards, determining factors and effects of some major properties of FAME are shown in Table I.

These properties also affect the behavior, performance, usage, and emissions of FAME. The European Union (EU) and United States Environmental Protection Agency (USEPA) identified brake specific fuel consumption (BSFC), brake thermal efficiency (BTE) and exhaust gas temperature (EGT) as performance criteria while benchmarks have been set for emission of regulated gases, including carbon monoxide (CO), nitric oxide (NOx), carbon dioxide (CO_2), particulate matter (PM) measured in g/kWh, unburnt hydrocarbon (UHC) and smoke [11], [12]. Essential information that must be disclosed for an engine test, in line with acceptable engine test protocols and guidelines for testing engine performance and emission characteristics, include manufacturer's name, model and model year, engine bore and stroke, cycle of operation of the engine, fuel type and mode of fuel injection, as well as power rating. More than any other properties, the oxygenated nature and the degree of saturation can influence the behaviour, the performance, and the emissions of CI engines fuelled by FAME. The application of B100 WCOME has been discovered to enhance BSFC, BTE, EGT and result in less discharge of CO, CO_2, PM, and UHC but the higher discharge of NOx emissions when compared with ULSD [13]-[15].

III. Numerical and Optical Approaches in Engine Research

Internal combustion (IC) engines and the transportation sector, in particular, are in need of systems and technologies that permit improved engine performance, and reduced emission of poisonous and greenhouse gases. The twin challenges for the IC engine is to improve fuel economy and reduce the discharge of toxic gases from the exhaust to ensure judicious use of the scarce energy resources, including tested alternative fuels, and to meet stringent emission regulations. To this end, researchers are making efforts to comply with ever-increasingly strict global emission and fuel economy norms, which are the prime forces driving the global IC engine industry [19]. The major stakeholders in the IC engine chain including the engine designers, engine manufacturers, fuel refiners, and emission specialists who all have different and sometimes overlapping demands and expectations. Engine and fuel customers and consumers demand good engine performance, fuel economy, low fuel and engine cost, reliability, fuel availability, less fuel odour, and convenience. Engine manufacturers demand competitive and profitable costs, fuel economy standards, customer satisfaction, and meeting of emissions criteria while renewable fuel producers demand feedstock availability, product stability and distribution continuity [20].

TABLE I
SOME FAME PROPERTIES, STANDARDS, AND EFFECTS [10], [16]-[18]

Property	Standards ASTM D6751	EN 14214	Test method	Determining factor	Effects on engine
Density (kg/m³)	880	860-900	EN ISO 3675 EN ISO 12185	• Carbon chain length • Degree of saturation	Higher density precipitates • Increased BSFC, BTE, EGT, PM, and CO
Cetane number	47	51	EN ISO 5165	• Carbon chain length • Branching • Degree of unsaturation	High cetane number results in: • Better engine performance • Good auto-ignition • Low CO, HC and PM but high NOx • Increased NOx emission • Reduced vibration and noise • Knocking Too high cetane number triggers: • Overheating • Damage of the injector nozzle.
Kinematic Viscosity @ 40°C (mm²/s)	1.9-6.0	3.5-5.0	EN ISO 3104 EN ISO 20884	• Chemical structure • Carbon chain length • Degree of saturation • Number and position of double bonds • Branching • Amount of unreacted glycerides	High kinematic viscosity leads to: • Increased BSFC, BTE, EGT, CO, UHC and PM
Cold Filter Plugging Point (CFPP)	Max +5	-5 to -44	EN 116	• Number of carbon atoms • Degree of unsaturation	CFPP precipitates: • formation of crystals that can plug the fuel lines and filters
Flash point (°C)	93	101	EN ISO 3679	• Number of carbon atoms and double bonds • Residual alcohol content	Flash point affects: • fuel storage, handling and transportation.

Over the years, there have been increasing discrepancies and gaps between the outcome of laboratory tests and the real-life behavior of engines.

This has necessitated the search for and application of more advanced technologies to remedy the situation, particularly strategies to improve engine performance and reduce the emission of pollutants. The use of catalyst technologies has been employed to improve FAME properties, enhance engine performance and lessen the emission of HC, CO, and NOx in real-life conditions.

These technologies not only prolong the life of engines and ensure value for money, but also lessen the negative effects of these harmful emissions on humans, animals, and the environment. For example, NOx and HC contribute to the formation of ozone and acid rain. CO_2 causes heat-trapping greenhouse gas and accelerates global warming [21]. Some of these technologies include substrate and coating technologies, three-way catalysts, and oxidization catalysts. Technologies that are capable of reducing PM emissions include wall-flow filters, partial-flow filters, and open-filters [22], [23]. Some of the techniques for the optimization of combustion and emission reduction, including turbocharging, exhaust gas recirculation (EGR), low temperature combustion (LTC), high speed direct injection (HSDI) etc., have not been able to meet stringent regulations as a result of their obvious limitations [24]-[26]. In the last decade, researchers have employed various techniques on high performance computers to gain insight and find solutions to some of the difficult in-cylinder processes and hone their skills in harnessing modeling tools to solve real-life engine challenges using experimental data from reliable engine geometry. Various numerical diagnostic measures including optical diagnostic techniques and laser-based measurements have surfaced as indispensable tools in the prediction, measurement, control, and improvement of fuel economy, engine performance, and emission control.

These strategies include numerical and optical tools that allow researchers to have optical access into engine combustion chambers and alter fuel mixing and combustion conditions towards achieving better engine performance and emissions within acceptable limits [27], [28].

III.1.   Regression Analysis

Regression analysis, a predictive machine learning algorithm, defines quantitative relationships between a response variable and explanatory variables. It is a technique to determine a functional relationship between dependent variables (response) and independent variables (predictor). Linear and nonlinear relationships between response and predictor can be expressed as shown in equations (1) and (2) [29], [30]:

$$Y = \beta_0 + \beta_1 X_1 + \beta_2 X_2 + \beta_3 X_3 + \cdots + \beta_n X_n \quad (1)$$

where Y is the dependent variable, β_0 to β_n are equation parameters for linear relations, and X_1 to X_n are independent variables:

$$Y = a_0 (X_1^{a_1})(X_2^{a_2})(X_3^{a_3}) \ldots . (X_n^{a_n}) \quad (2)$$

where a_0 is the dependent variable, $X_1^{a_1}$ to $X_n^{a_n}$ are equation parameters for nonlinear relationships and a_0 to a_n are independent variables.

III.2.   Artificial Neural Networks

Artificial Neural Networks (ANNs) are computational models inspired by the human brain and explore the processing of the brain as a basis to cultivate algorithms that can be used to model multifaceted patterns and prediction problems. Learning algorithms are developed to train ANN models to perform the intended functions.

A neural network learns by adjusting its weights and biases (thresholds) iteratively to generate the desired output called free parameters. For learning to take place, an ANN is trained first using a defined set of rules, also known as the learning algorithm, which can either be gradient descent algorithms or back-propagation algorithms. Characteristically, ANN comprises a large number of artificial neurons arranged as input layers, hidden layers and output layers and connected by hidden neurons as shown in Fig. 3. The input layer receives input that the network will learn, recognizes and processes it, while the hidden layer transforms the input signal into a form the output layer can recognize and use.

One major benefit of the application of ANN for prediction is its ability to learn from examples only and then readily transfer the knowledge to resolve hidden and strongly nonlinear dependencies, in spite of disturbances existing in the training set [29]-[31]. Researchers in the field of IC engines have acknowledged and accepted the competence of ANNs to simulate engine behaviour, capture nonlinear tendencies in complex data, and accurately predict with some measure of acceptable approximates real-time engine behaviour [32].
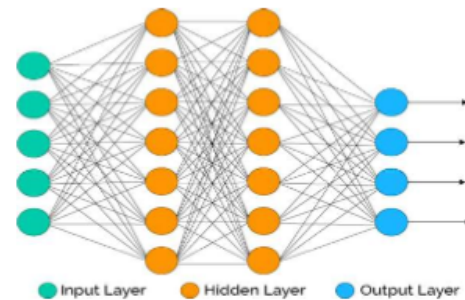
Fig. 3. Arrangements of ANN layers [29]

Developed in the late 1990s, an adaptive neuro-fuzzy inference system or adaptive network-based fuzzy inference system (ANFIS) is a kind of ANN based on Takagi-Sugeno fuzzy inference system. In fuzzy logic,

nonlinearity and complexity of modeling can be handled by rules, membership functions, and inference processes [33]. ANFIS has been used for property and engine performance predictions with acceptable accuracy. The predicted data are compared with the experimental data to determine their accuracy, closeness to standard and conformity. The accuracy of the prediction models is measured by performance metrics namely: the regression coefficient (*R*), the mean squared error (*MSE*) and mean absolute percentage error (*MAPE*), which are expressed as shown in equations (3) to (5):

$$R = \sqrt{1 - \frac{\sum_{i=1}^{n}(T_i - O_i)^2}{\sum_{i=1}^{n} O_i^2}} \qquad (3)$$

$$MSE = \frac{1}{n}\left\{\sum_{i=1}^{n}(T_i - O_i^2)\right\} \qquad (4)$$

$$MAPE = \left(\frac{1}{n}\sum \frac{|Actual - Forecast|}{|Actual|}\right) \times 100 \qquad (5)$$

where T_i = Targeted value of '*i*' samples and O_i = input value of '*i*' samples. Much more than prediction of FAME properties, engine performance and emission characteristics, numerical techniques and approaches should, considering all important parameters, have the capacity to recognize, compile, and analyze all conditions based on realistic and provable assumptions and yield a set of solvable expressions or equations.

Equations and expressions generated to predict FAME properties like density, cetane number, kinematic viscosity, cold flow properties, etc. can be compiled and solved using any of the numerical techniques when analytical methods prove insufficient. Application of linear correlations, optimization techniques and numerical tools to solve the resulting equations can yield values of these parameters that can ensure optimal engine performance and reduced emission of mitigated gases.

These techniques are not only easy to use but can also generate sets of possible solutions.

III.3. Computational Fluid Dynamics

Computational fluid dynamics (CFD) has been verified and validated in recent years as being an invaluable tool in situations where real-time experimental work has been found to be costly, dangerous and/or time-consuming. In recent years, with an increased need for numerical intervention in engine research, major advancements have been made in the application of the CFD model in the quest for fuel efficient and low emission engines, with wide applications and acceptance.

Knowledge of adequate information about the combustion chamber flow field and its effect on fuel spray characteristics has been found to play an important role in improving engine performance and pollutant emission reduction in the CI engine. With increased usage and acceptance of CFD in IC engines and related disciplines, there has been a development process from zero-dimensional models to quasi-dimensional models to multi-dimensional models. While a zero-dimensional model can predict some parameters that influence engine performance, it ignores the chemical reaction process involved in combustion and therefore cannot predict pollutant formation. The quasi-dimensional model, though it can predict engine performance, combustion reactions and emissions formation, has been unable to reveal workable combustion strategy. Multi-dimensional simulation, apart from its capability for flame propagation, pollutant generation analysis, and turbulent kinetic energy, can also predict combustion and emissions generation [34], [35]. In achieving these outcomes, notable commercial CFD models and sub-models, namely Diesel RK, KIVA, FLUENT, VECTIS, FIRE, STAR-CD and AVL BOOST simulation, single zone combustion, and zero dimension thermodynamics based models, have been developed to model, simulate and optimize engine performance and emissions of CI engine fueled with FAME with varying outcomes.

Necessary assumptions are made in the application of appropriate sub-models and equations to predict the required parameters in fuel mixing, fuel combustion and pollutants formation [36]-[39]. These codes are used to simulate engine performance, combustion and emission models with a high degree of efficiency and reliability [40]. The use of CFD will continue to gain acceptance in improving the understanding and workings of CI engines by researchers and industry practitioners and can be explored to not only predict optimal FAME candidates but also simulate various scenarios that can reduce fuel economy, improve engine performance and mitigate emission of regulated pollutants. In addition, high-speed cameras and other optical tools have been used to gain access to the combustion chamber to improve the knowledge of the activities in the combustion chamber during pre-combustion, combustion and post-combustion periods. High-speed cameras are used in conjunction with CFD simulation software for better understanding of the injection, combustion, and pollutant formation processes as well as to verify outcomes of these simulation tools. While the cameras provide a visual image of the fuel mixing and fuel spray processes during the different stages of fuel injection, the CFD AVL BOOST software numerically measures engine operating parameters and emission formation processes [41]. The amalgamation of numerical tools and high-speed cameras have been explored in various forms but largely as phase Doppler interferometry (PDI), engine endoscopy, and laser-based technology, to improve access and gain insight into the happenings in the combustion chamber to deepen knowledge and verify the predicted parameters.

III.4. Phase Doppler Interferometry

Formerly referred to as phase Doppler particle analysis, phase DPI was developed towards the mid-

1980s by the duo of Dr. William Bachalo and Mike Houser as a technique based on the principle of light scattering interferometry. A typical PDI arrangement is shown in Fig. 4. PDI expands the understanding of fuel spray behavior and characterization, particularly in CI engines. Fuel is introduced by an injector nozzle due to the pressure differential between the ambient and the fuel injector, by means of a spray. The quality of spray of biodiesel fuel in a simulated CI engine has been studied over the years and found to affect combustion greatly. A good fuel spray is one that guarantees the penetration of the injected fuel into the combustion chamber at a satisfactory velocity to provoke fuel atomization for swift vaporization, mixing and formation of combustible mixture. The application of biodiesel as CI engine fuel demands the optimization of the entire fuel injection system including the spray characteristics. The study of the feedstock, fingerprint, FA composition, production techniques and parameters of FAME will reveal invaluable information about its spray penetration, spray cone angle, spray-wall interaction and spray area. The use of PDI makes the study of these exceptionally challenging parameters less burdensome and more realistic [27], [42] and can verify the parameters predicted by numerical tools including CFD.
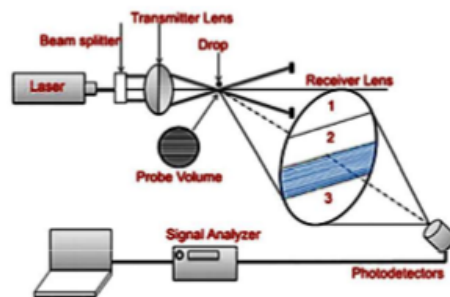
Fig. 4. A schematic diagram of PDI system [34]

Outcomes of several studies [44]-[48] have confirmed the application of PDI numerical techniques to validate experimental data and produce images of the happenings within the combustion chamber. These have increased the knowledge and understanding of numerical and optical techniques for simulating, verifying and validating engine performance and emissions.

III.5. Engine Endoscopy

The limitations of optical engines including the inability to use high loads and speeds, short time usage, high cost of the optical engines, low heat transfer rates of the optical components, and lack of cooling medium of the optical liner have created a niche for engine endoscopy. First used by doctors for medical surgery in 1806, endoscopy as an optical visualization technique has found applications in automotive research particularly in

engines, cylinder heads and intake manifolds of the engine. Endoscopy has now found wide applications in CI engines for combustion diagnostics, spray formation, mixture formation as well as performance and emissions measurements [27], [42], [49]. An engine endoscope is a large, thin tube, which consists of lens for transferring images from the combustion chamber to the endoscope (Fig. 5). The use of endoscopic technique with camera for engine research has been applied to modify combustion, optimize fuel utilization, improve engine performance and reduce emission formation, and has been used by various researchers to advance the course of engine research [50]-[52], including the use of biodiesel fuels on CI engines [53]-[55].
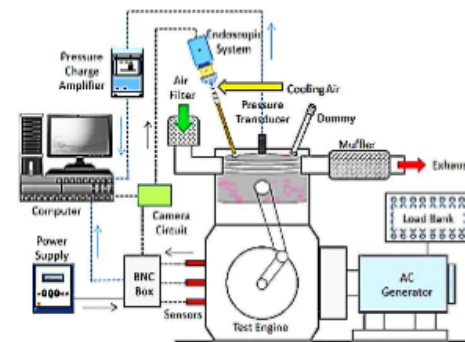
Fig. 5. Schematic of the experimental setup for endoscopic technique [35]

The use of optical techniques like PDI and endoscopy, though novel, have certain challenges including high technical personnel and infrastructure requirements, high cost of manufacturing optical research engines, specialized test environment and inability to predict and measure engine performance and emission situations at high speeds and loads. Further, optical techniques have not been able to determine the optimal FAME candidate that could produce better engine performance and reduced emission in CI engines at all engine speeds and loads.

III.6. Laser-Based Measurements

Laser technologies have been employed to generate better insights into in-cylinder processes governing engine performance and emissions in modern IC engines.

Due to the application of laser technologies, particularly in emission measurements, PM and soot concentration in exhaust gases have been measured more accurately resulting in better understanding of their formation and effects. Of all the techniques, the laser-induced incandescence (LII) technique is seen as very efficient and accurate. The LII is reliable and sensitive in measuring PM and other emissions over a wide range of IC engine conditions to meet the U.S. Environmental

64

Protection Agency (EPA) and other international regulations [56], [57]. Despite the usefulness of laser-based measurements, this method has not been able to unearth a FAME candidate with optimum features and capability to produce better engine performance and bring emissions within established benchmarks.

IV. Outcomes of Numerical Approaches to Predictions in Engine Research

Numerical methods are a range of mathematical tools developed to provide solutions to problems that are difficult or cannot be solved analytically. The Dictionary of Computing defines numerical methods of solution as being routines, processes, approaches, and techniques of using computers to achieve a constructive solution to mathematics-related problems requiring specific numerical outcomes. It is a comprehensive, wide-ranging and explicit set of procedures and techniques aimed at resolving intricate problems, as well as estimating errors [36]. This is achieved through the development of algorithms and other programs for problem formulation and analysis in engineering, pure and applied sciences.

Two necessary conditions for numerical solutions are consistency and convergence. These conditions are mandatory in various numerical tools and approaches employed for the prediction of properties of FAME, as well as performance and emissions of CI engines fueled by FAME in recent years. Key areas of application of MATLAB includes development of algorithms and applications, solving mathematical problems, modeling, simulation and prototyping, computation, graphics, and data analysis [37]. Of all the numerical tools, MATLAB is the most applied for property prediction, engine performance and emission characteristics. The common uses of MATLAB are in the field of teaching and research, control systems, image and signal processing, fingerprints, fuzzy logic, voice recognition, etc. Among the models universally used by researchers for prediction in MATLAB are ANN, thermodynamic models, Simulink, etc. Other numerical approaches include linear regression, analytical correlation, and multiple linear regression which are used for property prediction while ANN and CFD are used for prediction of engine performance and emission characteristics.

IV.1. Property Prediction

Numerical prediction of FAME properties has helped to simplify research in fuel mixing, fuel combustion, engine performance and pollutants formation. Ramírez-Verduzco et al. [60] used analytical correlations to predict the cetane number, kinematic viscosity, density and higher heating value of FAME and reported that the outcomes of the prediction were in agreement with the experimental results. Multiple linear regressions were explored by Piloto-Rodríguez et al. [61] to predict the density of FAME with an acceptable outcome when compared with experimental data. In the same vein,

Mitra et al. [62] used regression analysis to predict the viscosity, density and high heat value (HHV) of FAMEs using their FA compositions. They reported that the linear regression models generated results that are similar to those available in literature. Saldana et al. [63] predicted the density and kinematic viscosity of FAME using machine learning methods including ANN and support vector machines (SVM). The difference between the predicted value and experimental results were within acceptable limits. Aminian and ZareNezha [64] used soft computing models including SVM, an adaptive neuro-fuzzy inference system (ANFIS), and feedforward ANN model trained by genetic algorithm (GA) to predict the viscosity of B100 FAME and reported a correlation of determination and ARD of 0.9964 % and 2.51 % respectively. In the same vein, Eryilmaz et al. [65] harnessed an ANN model to predict the kinematic viscosity of pure hazelnut oil methyl ester (HOME) and reported an R of 0.999986 and RMSE of 0.00149 confirming the applicability of ANN as an effective method for property prediction for FAME. Saldana et al. [63] and Ceyla Özgür and Erdi Tosun [66] applied ANN to predict the density and kinematic viscosity of biodiesel and recorded a reliable outcome which was in good conformity with experimental results. However, the predicted properties were neither compared with ASTM or EU FAME standards nor were attempts made to determine the optimal mix. Al-Shanableh et al. [67] explored 9-6-3 back-propagation ANN to predict the cold flow properties (CFP), namely, cloud point (CP), pour point (PP), and cold filter plugging point (CFPP) of FAME with 98 %, 94 % and 96 % accuracy, respectively, and the predicted values were in agreement with experimental data. The model further revealed that the CFP of biodiesel were influenced primarily by saturation or unsaturation of FA components. The applicability of the MATLAB model, particularly ANFIS, to predict kinematic viscosity (KV), iodine value (IV), CP, and PP, were confirmed by Mostafa Mostafaei [68], and the outcome showed that correlation coefficient (Rs) of 0.989, 0.996, 0.938, and 0.981 for KV, IV, CP, and PP respectively. However, the predicted properties were not compared to existing standards and no optimal candidate was discovered. Giwa et al. [69] predicted the cetane number (CN), kinematic viscosity, flash point (FP), and density and used experimental data collected from some samples of FAME to validate the efficacy of the property prediction model. The outcomes revealed that the ANN prediction accuracy was 96.69 %, 95.80 %, 99.07 %, and 99.40 %, and average absolute deviation of 1.637 %, 1.638 %, 0.997 %, and 0.101 % for cetane number, kinematic viscosity, FP, and density, respectively, confirming the prediction accuracy. In the same vein, Rocabruno-Valdés et al. [70] reported Rs of 0.91946 to 0.99401 and a confidence level of 99 % compared with experimental values when ANN was utilized to predict the density, dynamic viscosity, and cetane number of B100 FAME. This is a further confirmation of ANN as an accurate property prediction

model for FAME thereby reducing experimental time and costs. The prediction was not extended to predicting the optimal FAME candidate that could produce the best possible engine performance and reduced emissions.

From the foregoing, it is possible to say that well-trained ANNs have been employed on numerous occasions to predict FAME properties. The outcomes of the predictions were in conformity with established global standards for FAME and fall within acceptable accuracy and correlation coefficient. However, CFD has not been used to predict FAME properties. One obvious gap in the literature is the inability of researchers to use the various numerical approaches available to unearth an optimal FAME candidate.

IV.2. Engine Performance and Emission Characteristics Prediction

Sharon et al. [71] engaged a MATLAB SIMULINK model to train an ANN to predict the brake power, BSFC, BTE, NOx, HC, CO and smoke density of a CI engine fueled with esters from WCO. The trained ANN made a good prediction of the parameters within acceptable correlation coefficients. However, the authors did not predict the FAME candidate that could produce optimum engine performance and emission characteristics reported that the trained ANN gave a better prediction of the parameters within the acceptable correlation coefficient. In a similar vein, Sharma et al. [72] developed an ANN model for the prediction of the performance and emission characteristics of a CI engine fueled by FAME. The predicted data agreed with the experimental data with Rs of 0.99946, 0.99968, 0.99967, 0.99899, 0.99941 and 0.99991 for the BSFC, BTE, EGT, NOx, smoke and UHC emissions, respectively. Acharya et al. [73] used ANN to predict the values of some engine performance and emission parameters and reported Rs of 0.982, 0.9851, 0.9979, 0.9859, and 0.9781 for BTE, BSFC, CO, smoke, and NOx respectively. Silitonga et al. [74] explored ANN based on a back-propagation algorithm to predict the performance and emissions of a common-rail turbocharged CI engine using MATLAB.

The researchers reported that ANN is a reliable prediction model whose outcome was validated by experimental results. They further reported Rs ranging between 0.9798 and 0.9999 for the ANN model and experimental data set. With a regression coefficient of 0.99360, ANN was reported to be a reliable model for predicting the performance and emissions characteristics of FAME when a Kirloskar AV1, four-stroke direct injection (DI), CI test rig was fueled with FAME [75].

An ANN model was applied by Kshirsagar and Anand [76] to predict the BTE, BSEC, EGT, CO, CO_2, UBHC, NO, and soot of a single cylinder, four stroke, DI, 3.7 kW, CI engine. The model signposted striking conformity as Rs were in the range of 0.99879 to 0.99993 and mean absolute percentage error (MAPE) of 0.87 % to 4.62 %. In their research, Roy et al. [77] reported Rs of between 0.987 and 0.999, and MAPE in

the range of 1.1 % to 4.57 % when they trained ANN to predict the BSFC, BTE, CO2, NOx and PM of an unmodified single cylinder four-stroke common-rail direct injection CI engine. The trained ANN model was reported to predict the investigated parameters with excellent agreement with experimental results. Karthickeyan et al. [78] developed an ANN model to predict the performance and emissions characteristics of orange oil methyl ester (OME). They reported an overall regression coefficient of 0.99129 and MSE of 0.00006189. In experimental and ANN studies of the effects of safflower oil biodiesel on engine performance and exhaust emissions in a CI engine, it was reported that ANN accurately predicted the performance and emission characteristics of the parameters within acceptable correlation coefficients. This confirmed the usefulness of ANN as an effective prediction model, when properly and sufficiently trained [79]. Kuma et al. [80] employed random selection and clustering algorithms to demonstrate the applicability of ANN to predict the performance and emissions of a CI engine fueled with WCOME. The outcome of the ANN prediction models was reported to be in accord with the experimental results of the parameters. In the same vein, the result of a trained AAN model to forecast the BTE, specific fuel consumption, EGT, CO_2, CO, hydrocarbons and NOx confirmed the efficacy of ANN models. The models accurately predicted these parameters within acceptable correlation between the experimental and predicted data with reduced time, costs and effort expended in conducting multiple experiments [81]. The model, however, failed to predict prime engine performance and reduced emissions in line with global benchmarks. Hosoz et al. [82] used a MATLAB fuzzy logic toolbox to develop an ANFIS model to predict the performance and emission characteristics of B100 FAME. The developed and trained ANFIS model yielded good Rs of 0.940 to 1.000, MRE of 1.40 % to 27.40 %, and absolute fractions of variance of 0.9863 to 0.9998 on the outcome of the model in relation to BSFC, BTE, HC and NOx when compared with experimental data. A single zone combustion model was employed to predict engine performance of a CI engine fueled with unblended FAME with reports showing that the outcomes were validated experimentally and found to be within acceptable ARD limits [83]. Al Dawody et al. [84] and Paul et al. [85] used a diesel RK model and combustion and pollutants formation sub-models to predict BSFC, BTE, CO, UHC, and PM of a FAME fueled CI engine.

The outcomes were within acceptable ADR limits [86]. Both ANN and CFD have been successfully utilized to predict CI engine performance criteria and emission characteristics and the outcomes of these predictions agree substantially with experimental results and fall within acceptable accuracy and correlation coefficients.

However, the predicted engine performance was below established standard requirements for CI engines and the emission characteristics higher than emission benchmarks set by USEPA and EU. In addition, optimal

engine performance criteria and mitigated emission characteristics were not predicted by the numerical approaches. Sadly, there has not been any effort to determine the optimal FAME mix that will produce optimal engine performance and reduced emissions that meet emission regulations.

TABLE II
SOME FAME PROPERTIES, STANDARDS, AND EFFECTS [10], [16]-[18]

	Tools	Fuel	Parameters predicted		Result	Ref
Properties	Analytical correlation	FAME	CN, KV, HHV, and density	•	Predicted results agree with data	[38]
	Multiple linear regression	FAME	Density	• •	Predicted data agrees with experimental data Predicted parameters conform to recognized standards	[39]
	Linear regression	FAME	KV, HHV, and density	•	The outcome of the prediction agrees with experimental data	[40]
	ANN	FAME	KV and density	•	The difference between the predicted outcome and experimental data were within acceptable limits	[41]
	ANN	B100 WCO	Viscosity	• •	Correlation of determination of 0.9964 and ADR of 2.51% Predicted value conforms with standard	[42]
	ANN	B100 HOME	KV	• •	R-value of 0.999986 and RMSE of 0.00149 Predicted value agrees with the standard value	[43]
	ANN	B100 WCO	Density and KV	• •	Predicted data agrees with experimental data Predicted parameters conform with recognized standards	[41]
	ANN	B100	Density and KV	• •	MAPE of 16.89% and 0.02% for viscosity and density Predicted parameters conform with recognized standards	[44]
	ANN	FAME	Cold point, pour point, and cold filter plugging point	• •	Predicted data agree with experimental data with prediction accuracy between 94 % and 98 %. Predicted parameters do not conform with recognized standards	[45]
	ANFIS	B100 WCOME	KV, IV, CP, and PP	• •	R-value of 0.989, 0.996, 0.938, and 0.981 for KV, IV, CP, and PP respectively Predicted properties conform to global standards	[46]
	ANN	FAME	CN, FP, KV, and density	• •	High prediction accuracy and acceptable average absolute deviation Predicted parameters conform with recognized standards	[47]
	ANN	B100 FAME	Density, dynamic viscosity, and cetane number	• •	R varies from 0.91946 to 0.99401 Predicted parameters do not fall within prescribed recognized standards	[48]
Engine performance and emission	ANN	B100 WCO	BSFC, BTE, NOx, HC, CO, and smoke	• • •	Correlation coefficients of between 0.9989 and 0.999 Predicted NOx emission higher than global benchmark Optimum performance criteria and mitigated emission were bot predicted	[49]
	ANN	FAME	BSFC, BTE, EGT, NOx, smoke, and UHC	• • •	Predicted data agree with experimental data NOx emission higher than global benchmarks for CI engine Optimal engine performance and emission characteristics were not predicted	[50]
	ANN	B100 WCO	BTE, BSFC, CO, smoke, and NOx	• •	Minimum disparity between the predicted and the experimental values Optimal engine performance and emission characteristics were not predicted	[51]
	ANN	JCME	BSFC, BTE, EGT, NOx, CO, CO₂ and smoke opacity	• •	ANN gave a reliable prediction which was in agreement with experimental data Optimal engine performance and emission characteristics were not predicted	[52]
	ANN	FAME	BTE, BSFC, CO, CO₂, NOx, HC and EGT	• •	ANN gave a reliable prediction of the parameters which were in agreement with experimental result Optimal engine performance and emission characteristics were not predicted	[53]
	ANN	FAME	BTE, BSEC, EGT, CO, CO₂, UBHC, NO, and soot	• •	Predicted data in conformity with experimental data Optimal engine performance and emission characteristics were not predicted	[54]
	ANN	FAME	BSFC, BTE, CO₂, NOx, and PM	• •	Predicted data is close to experimental data Optimal engine performance and emission characteristics were not predicted	[55]
	ANN	OME	BTE, BSFC, CO, NOx, and HC	• •	Lower engine performance and higher emission were predicted by the model Optimal engine performance and emission characteristics were not predicted	[56]
	ANN	SOME	BTE, BSFC, CO₂, CO, HC, and NOx	• •	Acceptable prediction accuracy and variations within acceptable limits Optimal engine performance and emission characteristics were not predicted	[57]
	ANN	WCOME	BTE, BSFC, EGT, NOx, CO,	•	60 % to 100 % prediction efficiency were achieved	[58]

Tools	Fuel	Parameters predicted	Result	Ref
ANN	B100	UBHC, and smoke BTE, BSFC, EGT, NOx, CO, CO₂ and HC	• Higher BSDC and NOx emissions were predicted • Optimal engine performance and emission characteristics were not predicted • Acceptable prediction accuracy and variations within acceptable limits • Optimal engine performance and emission characteristics were not predicted • Predicted results agree with experimental data and within acceptable limits.	[59]
ANFIS	B100 FAME	BSFC, BTE, HC, and NO	• Engine performance lower than global requirements • Optimal engine performance and emission characteristics were not predicted	[60]
CFD	FAME	BTE, BSFC, EGT	• ARD of engine performance characteristics between 2.2 % and 2.5 % • Optimal engine performance and emission characteristics not predicted	[61]
CFD	B100	BSFC, CO, UHC, and NOx	• Outcomes of prediction were validated experimentally • FAME properties were not predicted • The optimal candidate was not predicted	[62]
CFD	B100	BSFC, BTE, CO, UHC, and NOx	• Outcomes of prediction were validated experimentally • FAME properties were not predicted • The optimal candidate was not predicted	[63]

V.   Conclusion

The need to explore numerical approaches to predict the properties, engine performance and emissions of IC engines are advancing rapidly owing to its obvious advantages over real-time engine testing. Numerical prediction approaches are faster, accurate, novel, cheaper, flexible, can be adapted to forecast and predict "what-if" situations, and eliminate all the challenges associated with laboratory engine testing. ANN, MATLAB and CFD simulation software have been extensively used by various researchers to predict FAME properties, engine performance and emission characteristics with acceptable ADR. This has advanced the course of engine research with the aim of improving the FAME fingerprint, improve engine performance and mitigate regulated emissions in CI engines. High capacity modeling tools including high-speed cameras and techniques have been used in advanced engine research laboratories to predict, measure and control fuel economy, engine performance and emission characteristics of IC engines. Specifically, phase PDI, endoscopy and laser-based measurements have found wide acceptance in utilization and accuracy in engine research by allowing researchers optical access to the combustion chambers so as to be able to accurately predict the outputs of combustion processes. High-speed cameras combined with appropriate numerical tools are highly effective and efficient and have provided an improved understanding of the activities in the combustion chamber. However, they are expensive and highly technical. Bearing in mind the above, the use of numerical tools and optical techniques have still not been able to predict a FAME candidate with the requisite fingerprint and characteristics to produce improved engine performance and reduced emissions of regulated gases in an unmodified CI engine. Any effort at unraveling the FAME optimal mix will be valuable and advance the course of engine research and fuel efficiency. One such effort is the generation of sets of linear correlations based on the FA compositions of the FAME for property prediction in line with established standards. The selected properties are such that they influence combustion and performance criteria. A solution which can maximize the objective function, and the constraints, is expected to yield a FAME candidate with the requisite properties capable of producing improved engine performance and reduced emissions. Simulation of engine performance and emission characteristics can be carried out by a viable numerical tool and can be expected to yield acceptable parameters which can then be verified by the necessary experimental measurements and engine tests. Going forward, efforts will be geared towards the use of numerical and optical approaches not only to predict but also to obtain an optimal mix candidate for improved performance and at acceptable emission standards. A niche to fill research gaps in the emerging alternative fuels and high-speed ICEs to numerically unearth the right biofuel in terms of cost, applicability, efficiency and availability cannot be snubbed. The use of linear regression, MATLAB, machine learning, CFD, modeling and optimization approaches, finite element analysis and other soft computing techniques will be explored.

References

[1] World Diesel engine. Available at: https://www.freedoniagroup.com/industry-study/world-diesel-engines-3134.htm 2012

[2] OECD/FAO. Biofuels, In *OECD-FAO Agricultural Outlook 2016-2025*, (OECD Publishing, Paris, 2016). http://dx.doi.org/10.1787/agr_outlook-2016-13-en

[3] B. R. Møser, Influence of Extended Storage on Fuel Properties of

Methyl Esters Prepared from Canola, Palm, Soybean and Sunflower Oils, *Renewable Energy*, Vol. 36, n. 4, pp. 1221-1226, 2011.
https://doi.org/10.1016/j.renene.2010.10.009

[4] W. W. Focke, I. Van der Westhuizen, A. L. Grobler, K. T. Nshoane, J. K. Reddy, and A. S. Luyt, The Effect of Synthetic Antioxidants on the Oxidative Stability of Biodiesel, *Fuel*, Vol. 94, pp. 227-233, 2012.
https://doi.org/10.1016/j.fuel.2011.11.061

[5] M. I. Jahirul, R. J. Brown, W. Senadeera, I. M. O'Hara, and Z. D. Ristovski, The Use of Artificial Neural Networks for Identifying Sustainable Biodiesel Feedstocks, *Energies*, Vol. 6, n. 8, pp. 3764-3806, 2013.
https://doi.org/10.3390/en6083764

[6] T. Gogoi and D. Baruah, A Cycle Simulation Model for Predicting the Performance of a Diesel Engine Fuelled by Diesel and Biodiesel Blends, *Energy*, Vol. 35, n. 3, pp. 1317-1323, 2010.
https://doi.org/10.1016/j.energy.2009.11.014

[7] A. Gopinath, K. Sairam, R. Velraj, and G. Kumaresan, Effects of the Properties and the Structural Configurations of Fatty Acid Methyl Esters on the Properties of Biodiesel Fuel: A Review, *Proceedings of the Institution of Mechanical Engineers, Part D: Journal of Automobile Engineering*, Vol. 229, n. 3, pp. 357-390, 2015.
https://doi.org/10.1177/0954407014541103

[8] S. M. Miraboutalebi, P. Kazemi, and P. Bahrami, Fatty Acid Methyl Ester (FAME) Composition Used for Estimation of Biodiesel Cetane Number Employing Random Forest and Artificial Neural Networks: A New Approach, *Fuel*, Vol. 166, pp. 143-151, 2016.
https://doi.org/10.1016/j.fuel.2015.10.118

[9] E. Onuh and F. L. Inambao, A comparative evaluation of biodiesel derived from waste restaurant oil and Moringa, *in 2017 International Conference on Domestic Use of Energy (DUE)*, 2017, pp. 210-218: IEEE.
https://doi.org/10.23919/DUE.2017.7931846

[10] H. Jääskeläinen. *Biodiesel Standards & Properties*. Available: https://www.dieselnet.com/tech/fuel_biodiesel_std.php

[11] Worldwide emission standards. *Heavy Duty and Off-Highway Vehicles*. Delphi, 2015–2016.
Available: http://delphi.com/docs/default-source/worldwide-emissions-standards/delphi-worldwide-emissions-standards-heavy-duty-off-highway-15-16.pdf

[12] E. Onuh and F. L. Inambao, A property prediction scheme for biodiesel derived from non-edible feedstock, *in 2016 International Conference on the Domestic Use of Energy (DUE)*, 2016, pp. 1-9: IEEE.
https://doi.org/10.1109/DUE.2016.7466718

[13] J. B. Hirkude, and A. S. Padalkar, Performance and Emission Analysis of a Compression Ignition: Engine Operated on Waste Fried Oil Methyl Esters, *Applied Energy*, Vol. 90, n. 1, pp. 68-72, 2012.
https://doi.org/10.1016/j.apenergy.2010.11.028

[14] H. Sharon, K. Karuppasamy, D. S. Kumar, and A. Sundaresan, A Test on DI Diesel Engine Fueled with Methyl Esters of Used Palm Oil, *Renewable Energy*, Vol. 47, pp. 160-166, 2012.
https://doi.org/10.1016/j.renene.2012.04.032

[15] G. Chiatti, O. Chiavola, and E. Recco, Effect of Waste Cooking Oil Biodiesel Blends on Performance and Emissions from a CRDI Diesel Engine, In B. A. Ceper, M. Yildez, (Eds), *Improvement trends for internal combustion engines* (InTech, 2018).
https://doi.org/10.5772/intechopen.69740

[16] G. Knothe, Dependence of Biodiesel Fuel Properties on the Structure of Fatty Acid Alkyl Esters, *Fuel Processing Technology*, Vol. 86, n. 10, pp. 1059-1070, 2005.
https://doi.org/10.1016/j.fuproc.2004.11.002

[17] J. Thangaraja, K. Anand, and P. S. Mehta, Biodiesel NOx Penalty and Control Measures-A Review, *Renewable and Sustainable Energy Reviews*, Vol. 61, pp. 1-24, 2016.
https://doi.org/10.1016/j.rser.2016.03.017

[18] M. S. M. Zaharin, N. R. Abdullah, G. Najafi, H. Sharudin, and T. Yusaf, Effects of Physicochemical Properties of Biodiesel Fuel Blends with Alcohol on Diesel Engine Performance and Exhaust Emissions: A Review, *Renewable and Sustainable Energy*

Reviews, Vol. 79, pp. 475-493, 2017.
https://doi.org/10.1016/j.rser.2017.05.035

[19] A. K. Agarwal, A. P. Singh, and R. K. Maurya, Evolution, Challenges and Path Forward for Low Temperature Combustion Engines, *Progress in Energy and Combustion Science*, Vol. 61, pp. 1-56, 2017.
https://doi.org/10.1016/j.pecs.2017.02.001

[20] Sandia National Laboratories, Next Generation Biofuels and Advanced Engines for Tomorrow's Transportation Needs. DOE Combustion Research Facility, and DOE Joint BioEnergy Institute. *US Department of Energy Publications*. 82, 2009. Available: http://digitalcommons.unl.edu/usdoepub/82

[21] A. A. Desai, A review on Assessment of Air Pollution due to Vehicular Emission in Traffic Area, *International Journal of Current Engineering and Technology*, Vol. 8, n. 2, pp. 356-360, 2018.
https://doi.org/10.14741/ijcet/v.8.2.27

[22] A. Bharadwaj, Where Do Brazil, India, and China Stand? In A. Bharadwaj (Ed), *Environmental regulations and innovation in advanced automobile technologies*, (Springer Singapore, 2018), pp. 51-68.

[23] P.-M. Yang, C.-C. Wang, Y.-C. Lin, S.-R. Jhang, L.-J. Lin, and Y.-C. Lin, Development of Novel Alternative Biodiesel Fuels for Reducing PM Emissions and PM-Related Genotoxicity, *Environmental Research*, Vol. 156, pp. 512-518, 2017.
https://doi.org/10.1016/j.envres.2017.03.045

[24] E. Jiaqiang et al., Effect of Different Technologies on Combustion and Emissions of The Diesel Engine Fueled with Biodiesel: A Review, *Renewable and Sustainable Energy Reviews*, Vol. 80, pp. 620-647, 2017.
https://doi.org/10.1016/j.rser.2017.05.250

[25] P. Bedar and G. Kumar, Experimental Investigation of CRDI Engine Fuelled with Jatropha Curcas Biodiesel for Various EGR Rates, *International Journal of Applied Engineering Research*, Vol. 13, n. 1, pp. 68-71, 2018.

[26] R. K. Maurya, *Characteristics and control of low temperature combustion engines*, (Springer, 2018).
https://doi.org/10.1007/978-3-319-68508-3

[27] A. K. Agarwal and A. P. Singh, Lasers and Optical Diagnostics for Next Generation IC Engine Development: Ushering New Era of Engine Development, In A. K. Agarwal, S. De, A. Pandey, A. P. Singh, *Combustion for power generation and transportation: Technology, challenges and prospects*, (Springer Singapore, 2017), pp. 211-259.

[28] J. Benajes, J. V. Pastor, A. García, and J. Monsalve-Serrano, Redesign and Characterization of a Single-Cylinder Optical Research Engine to Allow Full Optical Access and Fast Cleaning during Combustion Studies, *Experimental Techniques*, Vol. 42, n. 1, pp. 55-68, 2018.
https://doi.org/10.1007/s40799-017-0219-9

[29] E. Tosun, K. Aydin, and M. Bilgili, Comparison of Linear Regression and Artificial Neural Network Model of a Diesel Engine Fueled with Biodiesel-Alcohol Mixtures, *Alexandria Engineering Journal*, Vol. 55, n. 4, pp. 3081-3089, 2016.
https://doi.org/10.1016/j.aej.2016.08.011

[30] E. Tosun, T. Ozgur, C. Ozgur, M. Ozcanli, H. Serin, and K. Aydin, Comparative Analysis of Various Modelling Techniques for Emission Prediction of Diesel Engine Fueled by Diesel Fuel with Nanoparticle Additives, *European Mechanical Science*, Vol. 1, n. 1, pp. 15-23, 2017.
https://doi.org/10.26701/ems.320490

[31] N. S. Gill, *Artificial Neural Networks, Neural Networks Applications and Algorithms*. Available: https://www.xenonstack.com/blog/data-science/artificial-neural-networks-applications-algorithms/

[32] J. Mahanta, *Introduction to Neural Networks, Advantages and Applications*. Available: https://towardsdatascience.com/introduction-to-neural-networks-advantages-and-applications-96851bd1a207

[33] M. Obitko, *Prediction using neural networks*, Available: http://www.obitko.com/tutorials/neural-network-prediction/

[34] Y. Cay, A. Cicek, F. Kara, and S. Sağiroğlu, Prediction of Engine Performance for an Alternative Fuel Using Artificial Neural Network, *Applied Thermal Engineering*, Vol. 37, pp. 217-225,

2012.
https://doi.org/10.1016/j.applthermaleng.2011.11.019

[35] Q. Luo, X. Si, and H. Yin, Application of CFD Technology in the Development and Research of Internal Combustion Engine, *International Conference on Computer and Information Technology Application*, 2016.

[36] C. A. Harch, M. Rasul, N. Hassan, and M. Bhuiya, Modelling of engine performance fuelled with second generation biodiesel, *Procedia Engineering*, Vol. 90, pp. 459-465, 2014.
https://doi.org/10.1016/j.proeng.2014.11.757

[37] N. M. S. Hassan, M. G. Rasul, and C. A. Harch, Modelling and Experimental Investigation of Engine Performance and Emissions Fuelled with Biodiesel Produced from Australian Beauty Leaf Tree, *Fuel*, Vol. 150, pp. 625-635, 2015.
https://doi.org/10.1016/j.proeng.2014.11.757

[38] S. Lahane and K. A. Subramanian, Effect of Different Percentages of Biodiesel–Diesel Blends on Injection, Spray, Combustion, Performance, and Emission Characteristics of a Diesel Engine, *Fuel*, Vol. 139, pp. 537-545, 2015.
https://doi.org/10.1016/j.fuel.2014.09.036

[39] I. Uryga-Bugajska, M. Pourkashanian, D. Borman, E. Catalanotti, and C. Wilson, Theoretical Investigation of the Performance of Alternative Aviation Fuels in an Aero-Engine Combustion Chamber, *Proceedings of the Institution of Mechanical Engineers, Part G: Journal of Aerospace Engineering*, Vol. 225, n. 8, pp. 874-885, 2011.
https://doi.org/10.1177/0954410011402277

[40] T. M. Belal, M. M. El Sayed, and M. M. Osman, Investigating Diesel Engine Performance and Emissions Using CFD, *Energy and Power Engineering*, Vol. 5, n. 02, p. 171, 2013.
https://doi.org/10.4236/epe.2013.52017

[41] L. Lešnik, B. Vajda, Z. Žunič, L. Škerget, and B. Kegl, The Influence of Biodiesel Fuel on Injection Characteristics, Diesel Engine Performance, and Emission Formation, *Applied Energy*, Vol. 111, pp. 558-570, 2013.
https://doi.org/10.1016/j.apenergy.2013.05.010

[42] [42] A. K. Agarwal, S. De, A. Pandey, and A. P. Singh, *Combustion for power generation and transportation: Technology, challenges and prospects*, (Springer Singapore, 2017).

[43] Senthilnathan, S., Gunasekaran, J., Investigation of HCCI Combustion in a DI Diesel Engine for Various Injection Timings – A CFD Study, (2014) *International Journal on Advanced Materials and Technologies (IREAMT)*, 2 (3), pp. 67-73.

[44] H. J. Kim, S. H. Park, and C. S. Lee, A Study on the Macroscopic Spray Behavior and Atomization Characteristics of Biodiesel and Dimethyl Ether Sprays Under Increased Ambient Pressure, *Fuel Processing Technology*, Vol. 91, n. 3, pp. 354-363, 2010.
https://doi.org/10.1016/j.fuproc.2009.11.007

[45] Y. Gao et al., Experimental Study of the Spray Characteristics of Biodiesel Based on Inedible Oil, *Biotechnology Advances*, Vol. 27, n. 5, pp. 616-624, 2009.
https://doi.org/10.1016/j.biotechadv.2009.04.022

[46] A. Ghurri, K. Jae-duk, S. Kyu-Keun, J. Jae-Youn, and K. H. Gon, Qualitative and Quantitative Analysis of Spray Characteristics of Diesel and Biodiesel Blend on Common-Rail Injection System, *Journal of Mechanical Science and Technology*, Vol. 25, n. 4, p. 885, 2011.
https://doi.org/10.1007/s12206-011-0142-4

[47] C. Ejim, B. Fleck, and A. Amirfazli, Analytical Study for Atomization of Biodiesels and their Blends in a Typical Injector: Surface Tension and Viscosity Effects, *Fuel*, Vol. 86, n. 10-11, pp. 1534-1544, 2007.
https://doi.org/10.1016/j.fuel.2006.11.006

[48] S. H. Park, S. H. Yoon, and C. S. Lee, Effects of Multiple-Injection Strategies on Overall Spray Behavior, Combustion, and Emissions Reduction Characteristics of Biodiesel Fuel, *Applied Energy*, Vol. 88, n. 1, pp. 88-98, 2011.
https://doi.org/10.1016/j.apenergy.2010.07.024

[49] C. Gessenhardt, C. Schulz, and S. Kaiser, Endoscopic Temperature Imaging in a Four-Cylinder IC Engine via Two-Color Toluene Fluorescence, *Proceedings of the Combustion Institute*, Vol. 35, n. 3, pp. 3697-3705, 2015.
https://doi.org/10.1016/j.proci.2014.06.085

[50] A. K. Agarwal, A. Agarwal, and A. P. Singh, Time Resolved In-Situ Biodiesel Combustion Visualization Using Engine Endoscopy, *Measurement*, Vol. 69, pp. 236-249, 2015.
https://doi.org/10.1016/j.measurement.2015.03.008

[51] D. Nikolic and N. Iida, Effects of Intake CO2 Concentrations on Fuel Spray Flame Temperatures and Soot Formations, *Proceedings of the Institution of Mechanical Engineers, Part D: Journal of Automobile Engineering*, Vol. 221, n. 12, pp. 1567-1573, 2007.
https://doi.org/10.1243/09544070JAUTO266

[52] D. Xu and J. Chen, Accurate Estimate of Turbulent Dissipation Rate Using PIV Data, *Experimental Thermal and Fluid Science*, Vol. 44, pp. 662-672, 2013.
https://doi.org/10.1016/j.expthermflusci.2012.09.006

[53] Y. Jiotode and A. K. Agarwal, Endoscopic Combustion Characterization of Jatropha Biodiesel in a Compression Ignition Engine, *Energy*, Vol. 119, pp. 845-851, 2017.
https://doi.org/10.1016/j.energy.2016.11.056

[54] J. Jeon, S. I. Kwon, Y. H. Park, Y. Oh, and S. Park, Visualizations of Combustion and Fuel/Air Mixture Formation Processes in a Single Cylinder Engine Fueled with DME, *Applied Energy*, Vol. 113, pp. 294-301, 2014.
https://doi.org/10.1016/j.apenergy.2013.07.033

[55] A. K. Agarwal, A. P. Singh, and A. Agarwal, Evolution, Trends and Applications of Endoscopy in Internal Combustion Engines, *Journal of Energy and Environmental Sustainability*, Vol. 1, pp 56-66, 2016.

[56] H. Jääskeläinen. *Research Engines for Optical Diagnostics*. Available:
https://www.dieselnet.com/tech/diesel_comb_res.php#tech

[57] Artium Technologies, Inc. *Laser-Based Technique for Real-Time Measurement of Emissions in Diesel Engine Exhaust*. Available:
http://www.artium.com/

[58] *Numerical Methods. A Dictionary of Computing*. Encyclopedia.com. Available: http://www.encyclopedia.com

[59] *MATLAB*, Available: https://www.mathworks.com.

[60] L. F. Ramirez-Verduzco, J. E. Rodriguez-Rodriguez, and A. del Rayo Jaramillo-Jacob, Predicting Cetane Number, Kinematic Viscosity, Density and Higher Heating Value of Biodiesel from its Fatty Acid Methyl Ester Composition, *Fuel*, Vol. 91, n. 1, pp. 102-111, 2012.
https://doi.org/10.1016/j.fuel.2011.06.070

[61] R. Piloto-Rodríguez, Y. Sánchez-Borroto, M. Lapuerta, L. Goyos-Pérez, and S. Verhelst, Prediction of the Cetane Number of Biodiesel Using Artificial Neural Networks and Multiple Linear Regression, *Energy Conversion and Management*, Vol. 65, pp. 255-261, 2013.
https://doi.org/10.1016/j.enconman.2012.07.023

[62] S. Mitra, P. Bose, and S. Choudhury, Mathematical Modeling for the Prediction of Fuel Properties of Biodiesel from their FAME Composition, *Key Engineering Materials*, 2011, Vol. 450, pp. 157-160.

[63] D. A. Saldana, L. Starck, P. Mougin, B. Rousseau, N. Ferrando, and B. Creton, Prediction of Density and Viscosity of Biofuel Compounds Using Machine Learning Methods, *Energy & Fuels*, Vol. 26, n. 4, pp. 2416-2426, 2012.
https://doi.org/10.1021/ef3001339

[64] A. Aminian and B. ZareNezhad, Accurate Predicting the Viscosity of Biodiesels and Blends Using Soft Computing Models, *Renewable Energy*, Vol. 120, pp. 488-500, 2018.
https://doi.org/10.1016/j.renene.2017.12.038

[65] T. Eryilmaz, M. Arslan, M. K. Yesilyurt, and A. Taner, Comparison of Empirical Equations and Artificial Neural Network Results in terms of Kinematic Viscosity Prediction of Fuels Based on Hazelnut Oil Methyl Ester, *Environmental Progress & Sustainable Energy*, Vol. 35, n. 6, pp. 1827-1841, 2016.
https://doi.org/10.1002/ep.12410

[66] C. Özgür and E. Tosun, Prediction of Density and Kinematic Viscosity of Biodiesel by Artificial Neural Networks, *Energy Sources, Part A: Recovery, Utilization, and Environmental Effects*, Vol. 39, n. 10, pp. 985-991, 2017.
https://doi.org/10.1080/15567036.2017.1280563

[67] F. Al-Shanableh, A. Evcil, and M. A. Savaş, Prediction of Cold

70

Flow Properties of Biodiesel Fuel Using Artificial Neural Network, *Procedia Computer Science*, Vol. 102, pp. 273-280, 2016.
https://doi.org/10.1016/j.procs.2016.09.401

[68] M. Mostafaei, Prediction of Biodiesel Fuel Properties from its Fatty Acids Composition Using ANFIS Approach, *Fuel*, Vol. 229, pp. 227-234, 2018.
https://doi.org/10.1016/j.fuel.2018.04.148

[69] S. O. Giwa, S. O. Adekomaya, K. O. Adama, and M. O. Mukaila, Prediction of Selected Biodiesel Fuel Properties Using Artificial Neural Network, *Frontiers in Energy*, Vol. 9, n. 4, pp. 433-445, 2015.
https://doi.org/10.1007/s11708-015-0383-5

[70] C. I. Rocabruno-Valdés, L. F. Ramírez-Verduzco, and J. A. Hernández, Artificial Neural Network Models to Predict Density, Dynamic Viscosity, and Cetane Number of Biodiesel, *Fuel*, Vol. 147, pp. 9-17, 2015.
https://doi.org/10.1016/j.fuel.2015.01.024

[71] H. Sharon, R. Jayaprakash, M. Karthigai selvan, D. R. Soban kumar, A. Sundaresan, and K. Karuppasamy, Biodiesel Production and Prediction of Engine Performance Using SIMULINK Model of Trained Neural Network, *Fuel*, Vol. 99, pp. 197-203, 2012.
https://doi.org/10.1016/j.fuel.2012.04.019

[72] A. Sharma, P. K. Sahoo, R. Tripathi, and L. C. Meher, Artificial Neural Network-Based Prediction of Performance and Emission Characteristics of CI Engine Using Polanga as a Biodiesel, *International Journal of Ambient Energy*, Vol. 37, n. 6, pp. 559-570, 2016.
https://doi.org/10.1080/01430750.2015.1023466

[73] N. Acharya, S. Acharya, S. Panda, and P. Nanda, An artificial neural network model for a diesel engine fuelled with mahua biodiesel, In: H. Behera H. and D. Mohapatra (Eds), *Computational intelligence in data mining. advances in intelligent systems and computing*, vol 556, (Springer, Singapore 2017, pp. 193-201).
https://doi.org/10.1007/s11661-016-3824-9

[74] A. Silitonga, H. H. Masjuki, Hwai Chyuan Ong, H. G. How, F. Kusumo, Y. H. Teoh, T. M. I. Mahlia, *Engine performance, emission and combustion in common rail turbocharged diesel engine from Jatropha curcas using artificial neural network*, SAE Technical Paper 2015.

[75] S. Javed, Y. V. V. Satyanarayana Murthy, R. U. Baig, and D. Prasada Rao, Development of ANN Model for Prediction of Performance and Emission Characteristics of Hydrogen Dual Fueled Diesel Engine with Jatropha Methyl Ester Biodiesel Blends, *Journal of Natural Gas Science and Engineering*, Vol. 26, pp. 549-557, 2015.
https://doi.org/10.1016/j.jngse.2015.06.041

[76] C. M. Kshirsagar and R. Anand, Artificial Neural Network Applied Forecast on a Parametric Study of Calophyllum Inophyllum Methyl Ester-Diesel Engine Out Responses, *Applied Energy*, Vol. 189, pp. 555-567, 2017/03/01/ 2017.
https://doi.org/10.1016/j.apenergy.2016.12.045

[77] S. Roy, R. Banerjee, and P. K. Bose, Performance and Exhaust Emissions Prediction of a CRDI Assisted Single Cylinder Diesel Engine Coupled with EGR Using Artificial Neural Network, *Applied Energy*, Vol. 119, pp. 330-340, 2014.
https://doi.org/10.1016/j.apenergy.2014.01.044

[78] V. Karthickeyan, P. Balamurugan, G. Rohith, and R. Senthil, Developing of ANN Model for Prediction of Performance and Emission Characteristics of VCR Engine with Orange Oil Biodiesel Blends, *Journal of the Brazilian Society of Mechanical Sciences and Engineering*, Vol. 39, n. 7, pp. 2877-2888, 2017.
https://doi.org/10.1007/s40430-017-0768-y

[79] I. Örs and V. Bakırcıoğlu, An Experimental and ANNs Study of the Effects of Safflower Oil Biodiesel on Engine Performance and Exhaust Emissions in a CI Engine, *International Journal of Automotive Engineering and Technologies*, Vol. 5, n. 3, pp. 125-135, 201.

[80] S. Kumar, P. S. Pai, B. S. Rao, and G. Vijay, Prediction of Performance and Emission Characteristics in a Biodiesel Engine Using WCO Ester: A Comparative Study of Neural Networks, *Soft Computing*, Vol. 20, n. 7, pp. 2665-2676, 2016.

https://doi.org/10.1007/s00500-015-1666-9

[81] K. Muralidharan and D. Vasudevan, Applications of Artificial Neural Networks in Prediction of Performance, Emission and Combustion Characteristics of Variable Compression Ratio Engine Fuelled with Waste Cooking Oil Biodiesel, *Journal of the Brazilian Society of Mechanical Sciences and Engineering*, Vol. 37, n. 3, pp. 915-928, 2015.
https://doi.org/10.1007/s40430-014-0213-4

[82] M. Hosoz, H. M. Ertunc, M. Karabektas, and G. Ergen, ANFIS Modelling of the Performance and Emissions of a Diesel Engine Using Diesel Fuel and Biodiesel Blends, *Applied Thermal Engineering*, Vol. 60, n. 1, pp. 24-32, 2013/10/02/ 2013.
https://doi.org/10.1016/j.applthermaleng.2013.06.040

[83] S. Awad, E. G. Varuvel, K. Loubar, and M. Tazerout, Single Zone Combustion Modeling of Biodiesel from Wastes in Diesel Engine, *Fuel*, Vol. 106, pp. 558-568, 2013.
https://doi.org/10.1016/j.fuel.2012.11.051

[84] M. F. Al_Dawody and S. K. Bhatti, Experimental and Computational Investigations for Combustion, Performance and Emission Parameters of a Diesel Engine Fueled with Soybean Biodiesel-Diesel Blends, *Energy Procedia*, Vol. 52, pp. 421-430, 2014.
https://doi.org/10.1016/j.egypro.2014.07.094

[85] G. Paul, A. Datta, and B. K. Mandal, An Experimental and Numerical Investigation of the Performance, Combustion and Emission Characteristics of a Diesel Engine Fueled with Jatropha Biodiesel, *Energy Procedia*, Vol. 54, pp. 455-467, 2014.
https://doi.org/10.1016/j.egypro.2014.07.288

[86] Tonon, D., Garcia, E., Thermodynamic Analysis of a Spark Ignition Internal Combustion Engines by Computational Simulations, (2018) *International Review of Mechanical Engineering (IREME)*, 12 (8), pp. 705-713.
doi: https://doi.org/10.15866/ireme.v12i8.15082

Authors' information

Green Energy Solutions Research Group. The discipline of Mechanical Engineering, Howard College, University of KwaZulu-Natal, Durban 404. South Africa.

Awogbemi, Omojola received Higher National Diploma in Mechanical Engineering at the Yaba College of Technology, Lagos, Nigeria, a Postgraduate Diploma and MEng degrees in Mechanical Engineering from the Ekiti State University, Ado Ekiti, Nigeria in 2014. He is currently on study leave for his PhD in the Green Energy Research Solutions, the discipline of Mechanical Engineering, Howard College, University of KwaZulu-Natal, Durban, South Africa. His research interests include Thermofluids, and Renewable Energy Technologies (RET). The focus of the author's current research is performance and emission of hybrid Fatty Acid Methyl Ester in compression ignition engines.
E-mail: 217080448@stu.ukzn.ac.za

Prof. **Freddie L. Inambao** holds a Master of Science (M. Sc) and PhD in Mechanical Engineering with specialization in Thermodynamics and Internal Combustion Engines from Volgograd Polytechnic Institute, Russia. He has lectured in several universities in Southern Africa and currently a Professor in the discipline of Mechanical Engineering, University of KwaZulu-Natal, Howard College, Durban, South Africa. He has successfully supervised many undergraduate, Master and PhD students. He is an expert in Thermodynamics, Internal Combustion Engines, Energy Management, Renewable and Alternative Energy.
E-mail: inambaof@ukzn.ac.za

71

Dr. **Onuh, E. I.** is a Research Assistant at the Green Energy Research Solutions, the discipline of Mechanical Engineering, Howard College, University of KwaZulu Natal, Durban, South Africa where he is co-supervising a PhD candidate. He is a researcher in biodiesel combustion studies.
E-mail: onuhe@ukzn.ac.za

72

CHAPTER 3: PROPERTIES PREDICTION AND OPTIMIZATION TECHNIQUES FOR SYNTHESIS OF FATTY ACID METHYL ESTER

This chapter examines the use of property prediction and optimization techniques in biodiesel research as a panacea in relation to cumbersome and costly real-time laboratory experiments. It consists of three articles.

Article 1 explores the application of the Taguchi OA for the modelling and optimization of production of biodiesel. The advantages of Taguchi OA over the conventional one-variable-at-a-time experimental method was explored to determine the optimal parametric conditions for the transesterification of waste sunflower oil. Taguchi OA was found to generate a cost-effective and time-saving trajectory from waste sunflower oil to waste sunflower methyl ester. The article was published in the proceedings of The World Congress on Engineering, 2019, London, U.K.

> **Awogbemi, O.,** Inambao F., and Onuh E. I. (2019) "Modelling and Optimization of Synthesis of Waste Sunflower Methyl Ester by Taguchi Approach," Proceedings of The World Congress on Engineering 2019, 3-5 July 2019, London, U.K., pp137-143. ISBN: 978-988-14048-6-2. ISSN: 2078-0958 (Print); ISSN: 2078-0966 (Online). Available on http://www.iaeng.org/publication/WCE2019/WCE2019_pp137-143.pdf. (Published)

Article 2 compares the use of response surface methodology and Taguchi OA for the modelling and optimization of the biodiesel production process. The process parameters for transesterification were optimized for cost reduction and conversion efficiency. The article has been accepted for publication in the *International Journal of Engineering Research and Technology*.

> **Awogbemi, O.,** Inambao F., Onuh E. I. (2019). "Modelling and Optimization of Transesterification of Waste Sunflower Oil to Fatty Acid Methyl Ester: A Case of Response Surface Methodology vs Taguchi Orthogonal Approach," International Journal of Engineering Research and Technology (IJERT). International Research Publication House. (Accepted for publication)

Article 3 surveys the application of linear regression for the prediction of properties of biodiesel using FA composition as inputs. Linear equations were generated in terms of five commonest FAs (palmitic, stearic, oleic, linoleic and linolenic) to predict the density, cetane number, calorific value, and kinematic viscosity of FAME. The predictive capabilities of the models were verified using experimental data mined from literature. The outcome of the research has been accepted for publication by the *Journal of Engineering and Applied Sciences.*

> **Awogbemi, O.,** Inambao F., Onuh E. I. (2019). "Application of Multiple Linear Regression for the Prediction of some Properties of Biodiesel using Fatty Acid Compositions," Journal of Engineering and Applied Sciences (JEAS). Scientific Research Publication Company (Accepted for publication).

CHAPTER 3 ARTICLE 1: Modelling and Optimization of Synthesis of Waste Sunflower Methyl Ester by Taguchi Approach

To cite this article: Awogbemi, O, Inambao F., and Onuh E. I. (2019) "Modelling and Optimization of Synthesis of Waste Sunflower Methyl Ester by Taguchi Approach" Proceedings of The World Congress on Engineering 2019, 3-5 July 2019, London, U.K., pp137-143. (Published)

The link to this article: http://www.iaeng.org/publication/WCE2019/WCE2019_pp137-143.pdf

Modelling and Optimization of Synthesis of Waste Sunflower Methyl Ester by Taguchi Approach

Awogbemi, O, *Member, IAENG,* Inambao, F. and Onuh, E. I.

Abstract— The application of used vegetable oil as feedstock for the synthesis of biodiesel has been found to be affordable and does not interfere with the food chain. This present study applied L16 Taguchi design to optimize the catalytic transesterification of waste sunflower oil to waste sunflower methyl ester (WSME). The predicted optimized conditions were catalyst: oil ratio of 2.5:1, reaction time of 75 min, reaction temperature of 90 °C, catalyst particle size of 55 μm and methanol:oil ratio of 8:1. The contribution factor of the significant process parameters is found to be 49.04 % for catalyst:oil ratio, 25.32 % for reaction temperature, 18.44 % for catalyst particle size, and 6.65 % for reaction time. The analysis of variance presented a p-value of 0.0047 and a correlation coefficient of 0.9945. The actual fatty acid (FA) conversion is in satisfactory agreement with the predicted value. Thus, the optimization of the percentage FA conversion using Taguchi design generated optimal parametric conditions for the cost-effective and time-saving transesterification of waste sunflower oil to WSME.

Index Terms—ANOVA, fatty acid, optimization, Taguchi design, transesterification.

I. INTRODUCTION

The burning of fossil fuel to generate energy has come with lots of damaging consequences including air pollution which has led to continuous depletion of ozone layer, emission of greenhouse gas and particulate matter, the formation of smog and escalating global temperature. The application of derivatives of fossil fuel, particularly petroleum-based diesel (PBD) fuel in compression ignition (CI) engines are not only costly, requires highly technical refining process and architecture but also result in not-too-impressive engine performance and emission of regulated gases. When compared with spark ignition engines, CI engines have gained acceptance in on-road and off-road applications partly due to its strength, greater torque, better durability, better fuel economy, superior thermal efficiencies and higher power output [1]. However, the combustion of PBD fuel in CI engines heightens the emission of particulate matters (PM), carbon dioxide (CO_2), sulphur dioxide (SO_2), nitric oxide (NOx), polycyclic aromatic hydrocarbons (PAHs), volatile organic compounds (VOCs) as well as other unregulated but dangerous gases which are harmful to the environment [2] which are major precursor of global

O. Awogbemi is a PhD candidate in Green Energy Solutions Group, Discipline of Mechanical Engineering, University of KwaZulu Natal, Howard College, Durban, 4041, South Africa. (Phone: +27 73 852 9855: e-mail: 217080448@stu.ukzn.ac.za).

F. Inambao is a Professor and Head of Green Energy Solutions Group, Discipline of Mechanical Engineering, University of KwaZulu Natal, Howard College, Durban, 4041, South Africa. (e-mail: inambaof@ukzn.ac.za).

E. I Onuh holds a PhD in Mechanical Engineering and a Research Associate with Green Energy Solutions Group, Discipline of Mechanical Engineering, University of KwaZulu Natal, Howard College, Durban, 4041, South Africa. (e-mail: onuhe@ukzn.ac.za).

and utilization of PBD fuel will continue to emit higher carbon and other greenhouse gasses with its attendant effects warming. The exploitation, extraction, refining of fossil fuel on the environment and deterioration of air quality. The remedy to this situation is to invest in oxygenated fuels like biofuel (bioethanol and biodiesel) as viable alternatives [1, 3].

Biodiesel also branded as fatty acid methyl ester (FAME) is generated from straight vegetable oil through various techniques including pyrolysis, catalytic distillation transesterification, microwave technology, microemulsion, supercritical methanol [4-6]. Transesterification is the reaction of feedstock (oil) with alcohol (methanol or ethanol) in the presence of a catalyst (homogeneous, heterogeneous, enzyme) to synthesize biodiesel and glycerol. The advantages of the transesterification method include its low cost, high conversion efficiency, suitability for household and industrial adaptations, and the closeness of the properties of the product to PBD fuel [7, 8]. The choice of used vegetable oil as a biodiesel feedstock is reinforced by its affordable cost, availability, and non-interference with food security. Collection of used vegetable oil from consumers will prevent its unlawful disposal which usually results in blockage of drains and polluting terrestrial and aquatic habitats [9-11].

The application of conventional one-variable-at-a-time (OVAT) experimental technique is expensive, time-consuming, requires huge laboratory architecture and has not been able to unravel the mutual understanding among the parametric variables. OVAT is also deficient in identifying the significant parameters and the contributing factor of each parameter. In order to solve this problem, OVAT is often replaced by the use design of Experiment (DoE) software, which has the capacity to acquire most of the needed information from a minimum exposure of carefully scheduled experiments by concurrently altering all the process factors. DoE slashes the number of experimental runs, saves time, chemicals and feedstocks, and uncover the mutual interaction among the process independent parameters and the response [12, 13].

Taguchi orthogonal approach (OA) is easy to use, fast and suitable optimization tool that has effected desirable outcomes working within smaller interactions of parameters. In research, Buasri et al. [14] applied Taguchi L9 OA to optimize the process parameters in the transesterification of palm oil to FAME using calcined scallop waste shell. the researchers reported the effectiveness of Taguchi design to determine the optimal reaction conditions. Similarly, Singh and Verma [15] used Taguchi's L27 OA for the optimization of the process parameters in the generation of

methyl ester from waste cooking oil and reported that the approach predicted the optimum condition and the interactions between the parameters and the response. The application of Taguchi design to optimize process parameters in the transesterification of various feedstocks to biodiesel has been reported to have favourable outcomes with four to five variables investigated. These attempts have yielded optimum operating conditions, mutual interactions among the independent parameters as well as determining the contributing factors of each variable [16-18].

This study aims at optimizing independent parametric conditions for the transesterification of waste sunflower oil (WSFO) to waste sunflower methyl ester (WSME) using CaO catalyst produced from high-temperature calcination of waste chicken eggshell. The optimization of parametric conditions (reaction time, reaction temperature, catalyst amount, catalyst particle size and methanol to oil ratio) to predict free fatty acid (FFA) conversion using the Taguchi design will interrogate the relationship between the responses and the independent variables. The level of significance, the mutual interactions, and the contribution factor of the variables will be systematically established. The motivation is to unravel a model equation capable of predicting the responses within acceptable limits with the minimum number of experimental runs. To this end, the scope of this present study is limited to the adoption of the Taguchi method to model an equation to predict the responses within the set parametric factors and levels. The analysis of variance (ANOVA) of the resulting model will be carried out to estimate their implication and the parameters of the preferred model are uncovered using non-linear regression technique.

II. MATERIAL AND METHOD

A. Materials collection and preparation

Waste Sunflower (WSFO) sample was collected at the point of disposal from a takeaway outlet beside Howard College, University of KwaZulu-Natal (UKZN), Durban. The oil has been used repeatedly for fourteen (14) days to fry potato chips. The oil was heated to 110 °C and filtration to remove moisture and impurities. The acid value of the waste oil was determined in line with the American Oil Chemists' Society (AOCS) Ca 5a-40 standard [19].

Waste chicken eggshells were collected from restaurants at the Howard college campus' cafeteria, UKZN. The inner white membrane adhering to the shells were removed, washed and rinse severally with deionized water. The clean shells were oven-dried, pulverized and passed through a 75 μm sieve mesh. The resulting powder was subjected to high-temperature calcination of 900 °C for 3 hours as described in our earlier work [20]. The eggshell powder was subjected to x-ray diffraction (XRD) and scanning electron microscope (SEM) characterization. The calcined eggshell powder is later warehoused in an airtight glass vial in a desiccator to prevent contamination and oxidation. Methanol (analytical grade 99.5 %; Merck, South Africa, univAR) was used as alcohol.

B. Transesterification process

Transesterification of WSFO was carried out in a 500 mL flat bottom flask. The acid value of WSFO allows for one stage transesterification process. The filtered WSFO, methanol and calcined CaO derived from waste chicken eggshell powder were mixed in a flat bottom flask and heated to predetermined. A digital thermocouple was utilized to verify the temperature of the reacting mixture throughout the duration of the experiment. Different catalyst concentration, reaction temperature, reaction time, catalyst:oil and methanol:oil ratio were used during each batch of the transesterification process. A magnetic stirrer at 1200 rpm was used to ensure homogeneous mixing of the reacting solution throughout the process. The resulting mixture was thereafter filtered in a vacuum filtration set up to recover the catalyst. The filtered mixture was transferred to a separating funnel and permitted to settle for 12 hours and the glycerol coagulated at the bottom of the separating funnel. The glycerol is drained out and the remaining crude biodiesel is decanted without the glycerol layer and transferred into a glass container for further purification and analysis.

The FAME conversion (%) of WSFO to biodiesel were estimated by;

$$FFA\ conversion\ \% = \frac{Weight_{Triglycerol} - Weight_{Biodiesel}}{Weight_{Biodiesel}} \times 100\%$$ (1)

C. GCMS analysis of WSME

The fatty acid composition of the WSME was determined using a Shimadzu gas chromatography-mass spectrometer (GCMS) using an ultra-alloy-5 capillary column and GCMS-QP2010 Plus software. A 2 μL sample was injected in splitless mode, helium served as the carrier gas and the total time was 39.81 min. The column temperature profile was as follows: 50 °C for 60 s; then increased at 15 °C/min until 180 °C held for 60 s; then increased at 7 °C/min until 230 °C held for 60 s; then increased at 5 °C/min until 350 °C and held at 350 °C for 5 min.

D. Statistical analysis by Taguchi design

In order to effectively use the Taguchi design, pilot experimentation was conducted in triplicates to determine the independent and dependent parameters and their levels for FFA conversion. A suitable optimization technique was thereafter selected and assign parameters accordingly. The optimization tool was applied to generate a model equation and the predicted response. If the model is significant, the influence of the input parameters and the optimum factor of the significant process parameters are estimated appropriately to determine the best value of the response characteristic. The analysis of variance (ANOVA) was performed to unearth the significance of each parameter. The predicted response compared with the experimental data to determine the level of agreement.

III. RESULT AND DISCUSSION

This section comprises the statistical analysis of the outcome of the Taguchi design, characterization of the catalyst and the GCMS analysis of the biodiesel.

TABLE I
EXPERIMENTAL DESIGN MATRIX SHOWING THE ACTUAL, PREDICTED AND RESIDUAL VALUE

Run	Factors					FFA conversion (%)		Residual
	A	B	C	D	E	Actual Value	Predicted Value	
1	2.5	125	60	75	4	85.43	85.74	-0.31
2	1.5	90	45	75	8	86.76	86.37	0.39
3	1	90	60	55	6	78.32	77.78	0.54
4	1	75	45	45	4	69.45	69.76	-0.31
5	2.5	150	45	65	6	82.5	81.96	0.54
6	2.5	90	75	45	10	71.68	72.30	-0.62
7	2	150	60	45	8	73.78	73.39	0.39
8	1.5	150	75	55	4	85.51	85.82	-0.31
9	2	75	75	75	6	70.86	70.32	0.54
10	2	90	90	65	4	75.45	75.76	-0.31
11	1.5	125	90	45	6	87.54	87.00	0.54
12	1.5	75	60	65	10	81.66	82.28	-0.62
13	1	125	75	65	8	70.55	70.16	0.39
14	1	150	90	75	10	84.66	85.28	-0.62
15	2	125	45	55	10	76.58	77.20	-0.62
16	2.5	75	90	55	8	87.54	87.15	0.39

TABLE II
ANALYSIS OF VARIANCE (ANOVA) OF MODEL AND PROCESS PARAMETERS

Source	Sum of Squares	Contribution factor (%)	Degree of freedom	Mean Square	F Value	p-value Prob > F	
Model	664.95	-	12	55.41	45.02	0.0047	Significant
A	327.91	49.04	3	109.30	88.81	0.0020	
B	44.48	6.65	3	14.83	12.05	0.0352	
C	169.28	25.32	3	56.43	45.85	0.0053	
D	123.27	18.44	3	41.09	33.39	0.0083	
Residual	3.69	0.55	3	1.23			
Cor Total	668.64	100	15				

A. Analysis of variance (ANOVA) of the transesterification process

The experimental design matrix of the actual, predicted and the residual values are shown in table I. The L16 Taguchi design brings up 16 runs. The actual FFA conversion data were generated from the actual experiments while the predicted data were generated by the model equation. The residual is the difference between the actual and the predicted values for each run. The actual FFA conversion ranges between 69.45 % and 87.54 % while the predicted FFA conversion ranges between 69.76 % and 87.15 %.

B. Analysis of variance (ANOVA) of the transesterification process

As shown in table II, the analysis of variance of the selected factorial model and the process parameters show that the model is significant. The p-value of 0.0047 indicates there is only a 0.47 % possibility that an F-value of 45.05 could happen due to noise. The value of probability > F less than 0.05 signposts that the model term is significant. From table II, catalyst:oil ratio, reaction time, reaction temperature, and catalyst particle size are the significant factors that influence the response. The effect of the individual process parameters is estimated by the contribution factor (%) using the following equation 2.

$$\% \, Contributing \, factor = \frac{Sum \, of \, squares \, of \, the \, particular \, variable}{Sum \, of \, sqaures \, of \, all \, the \, variables} \times 100$$

(2)

The catalyst:oil ratio has the highest contribution factor of 49.04 % making it the most significant parameter that influences FFA conversion followed by reaction temperature at 25.32 % and the catalyst particle size with contribution factor of 18.44 %. The calculated contribution factor for reaction time was found to be 6.65 %, making it the parameter with the least influence on the response.

The analysis of variance from the model, as shown in table III, of the correlation coefficient (R^2), adjusted correlation coefficient (R^2_{adj}), and the predicted correlation coefficient (R^2_{pred}) are 0.9945, 0.9724 and 0.8429 respectively. The value of R^2_{pred} agrees reasonably with the R^2_{adj} since the difference between them is less than 0.2. The adequate precision measures the signal to noise ratio. The estimated value of 17.393 indicates adequate signal and greater than the 4 which is suitable. This confirms that the model can be utilized to traverse the design space. The standard deviation is 1.11 while the coefficient of variance is 1.4 % which are low enough and a sign that the model can accurately predict the optimum conditions with elevated accuracy [21-23].

TABLE III
STATISTICAL PARAMETERS ESTIMATED FROM ANOVA STUDY

Parameter	Value	Parameter	Value
Standard Deviation	1.11	R-Squared	0.9945
Mean	79.27	Adj R-Squared	0.9724
C.V. %	1.40	Pred R-Squared	0.8429
PRESS	105.02	Adeq Precision	17.393
-2Log Likelihood	21.94	BIC	57.99
		AICc	229.94

C. Regression model equation

The analysis of the predicted regression model and the different process parameter were carried out using ANOVA.

The ANOVA has identified the significant parameters and their contribution factor to the achievement of the response. The analysis of the regression model was done with the significant process parameters while neglecting the insignificant process parameters using the model equation to estimate the coefficient of each significant process parameter. The regression model equation is shown in equation 3.

$$y = 79.27 - 3.52 * A[1] + 6.1 * A[2] - 5.1 * A[3] - 1.89 * B[1] - 1.21 * B[2] + 0.76 * B[3] - 0.44 * C[1] + 0.53 * C[2] - 4.62 * C[3] - 3.65 * D[1] + 2.72 * D[2] - 1.73 * D[3]$$
(3)

where y = FFA conversion (%), A[1], A[2], and A[3] are the catalyst:oil ratio at the first, second and third levels respectively, B[1], B[2], and B[3] are reaction time at the first, second, and third levels respectively, C[1], C[2], and C[3] are reaction temperature at the first, second, and third levels respectively and D[1], D[2], and D[3] are the catalyst particle size at the first, second, and third levels respectively in line with the factors and levels described in table I. The FFA conversion predicted by the model equation (Equation 3) is in agreement with the actual FFA conversion as shown in fig. 1, which confirms the effectiveness of the model to predict the response.
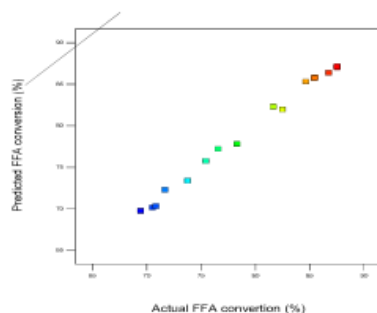
Fig. 1: The actual FFA conversion (%) against predicted FFA conversion (%)

D. Optimum condition

Results achieved from ANOVA indicated that methanol:oil ratio is an insignificant factor in the prediction of FFA conversion using the model established from Taguchi design. In order to achieve the best condition for FFA conversion, catalyst:oil ratio, reaction time, reaction temperature, and catalyst particle size are influential and are termed as significant process parameters. In this study, the optimum conditions are a catalyst:oil ratio of 2.5 %w/w, reaction time of 75 min, a reaction temperature of 90 °C, and catalyst particle size of 55 µm. These conditions, summarized in Table IV, are encapsulated in run 16 which also has the highest actual FFA conversion (table I).

Without a doubt, the model predicted the optimum response in agreement with the actual data.

TABLE IV
OPTIMUM CONDITIONS FOR FFA CONVERSION (%)

Parameter (unit)	Optimum value
A: Catalyst:WSFO ratio (%w/w)	2.5:1
B: Reaction time (min)	75
C: Reaction temperature (°C)	90
D: Particle size of catalyst (µm)	55
E: Methanol:WSFO ratio	8:1

E. Influence of process parameters on FFA conversion

1) Effect of catalyst:oil ratio

Fig. 4(a) shows the effect of catalyst:oil ratio on FFA conversion. Catalyst:oil ratio was varied between 1 %w/w and 2.5 %w/w at a reaction time of 125 min, reaction temperature of 60 °C catalyst particle size of 75 µm and methanol:oil ratio of 4:1. The maximum FFA conversion of 89 % was achieved at catalyst:oil ratio of 1.5:1 while the least FFA conversion rate of 78 % was gotten at the catalyst:oil ratio of 2:0. Though FFA conversion at 2.5:1 is also high, a catalyst:oil ratio of 1.5:1 is preferred for economic reasons [24].

2) Effect of reaction temperature

Fig. 4(b) depicts the influence of reaction temperature (°C) on FFA conversion (%) when the catalyst:oil ratio was maintained at 2.5:1, reaction time at 125 min, catalyst particle size at 75 µm and methanol:oil ratio at 4:1. FFA conversion reduced after the temperature of 50 °C. The highest and least FFA conversion was achieved at 90 °C and 75 °C respectively. The reaction temperature of 90 °C, which is higher than the boiling point of methanol can only be achieved if the reacting container is covered to prevent the evaporation of methanol thereby decreasing the methanol concentration in the reacting mixture [25].

3) Effect of reaction time

Fig. 4(c) shows the effects of reaction time on FFA conversion when catalyst:oil ratio was maintained at 2.5:1, reaction temperature at 60 °C, catalyst particle size at 75 µm and methanol:oil ratio at 4:1. The FFA conversion increases with the increase in reaction time. Bokhari et al. [26] advocated sufficient residence time to allow for the reactants to interrelate. However, with the use of a catalyst and the reversibility of the transesterification process, prolonging the reaction time might be costly and not advisable. A good balance between reaction time and the temperature is recommended for economical transesterification process [22].

4) Effect of catalyst particle size

With a catalyst:oil ratio of 2.5:1, reaction time of 125 mins, a reaction temperature of 60 °C and methanol:oil ratio of 4:1, maximum FFA conversion of 80 % were recorded at 55 µm and 75 µm as shown in fig. 4(d). The four particle sizes of the catalyst resulted in high FFA conversion as a result of an increase in the surface contact area.
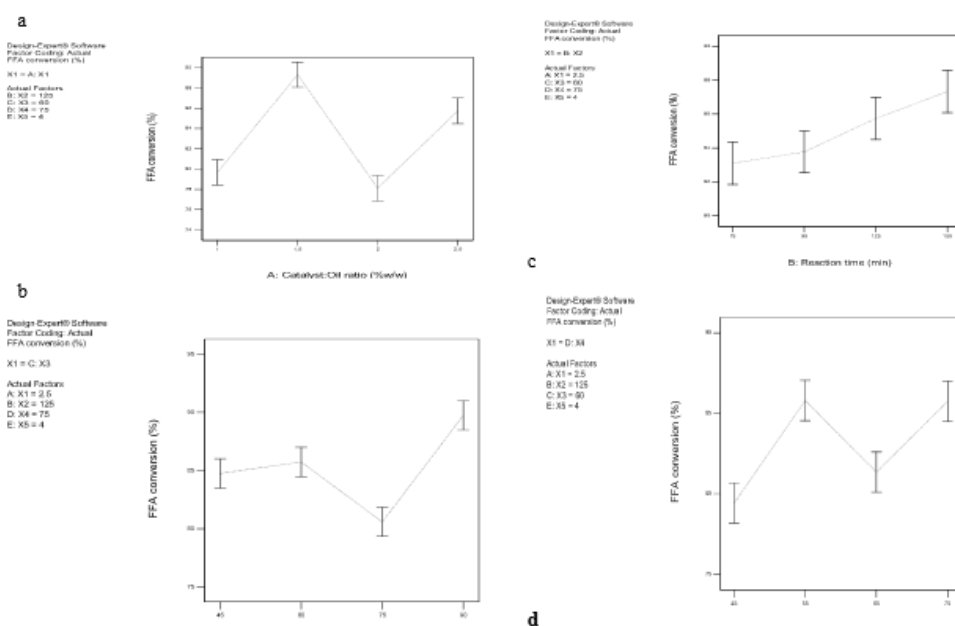
Fig. 4: Effect of (a) catalyst:oil ratio (b) reaction temperature (c) reaction time (d) catalyst particle size on FFA conversion (%)

F. Characterization of the eggshell catalyst

The waste chicken eggshell powder was calcined at 900 ^{o}C for 3 hours and the ensuing powder was characterized. Fig 5 shows the XRD pattern and SEM image of the calcined Eggshell powder. The XRD pattern of the calcined waste chicken eggshell powder reveals that it contained 63.8 % lime (CaO), 24.9 % portlandite (Ca(OH)$_2$), 10.9 % calcium oxalate (C$_2$H$_2$CaO$_5$) and 0.4 % calcite (CaCO$_3$). The high CaO content is as a result of high-temperature calcination which has decomposed the CaCO$_3$ to CaO and CO$_2$. The presence of Ca(OH)$_2$ might be due to atmospheric exposure during storage and analysis while the presence of 0.4 % CaCO$_3$ might be due to incomplete decomposition of CaCO$_3$ to CaO [27]. The SEM image shows that the calcined waste chicken eggshell powder showed irregular shape bonded together as aggregates with high specific surface area. The high surface area will enhance transesterification reaction and consequently improved FFA conversion than uncalcined eggshell powder [28].

G. FFA composition of FAME

The acid value of the waste sunflower oil was found to be 0.72 mg/g, making it suitable for the transesterification process. The outcome of transesterification of waste sunflower oil to waste sunflower methyl ester (WSME) using calcined waste chicken eggshell was subjected to GCMS analysis to determine its free fatty acid composition. Fig. 6 shows the chromatograph of the WSME to determine the FA composition. The peaks in the chromatograph indicate the individual FA. The WSME contains 73.72 % unsaturated FA and 26.28 % saturated FA as shown in Table V.
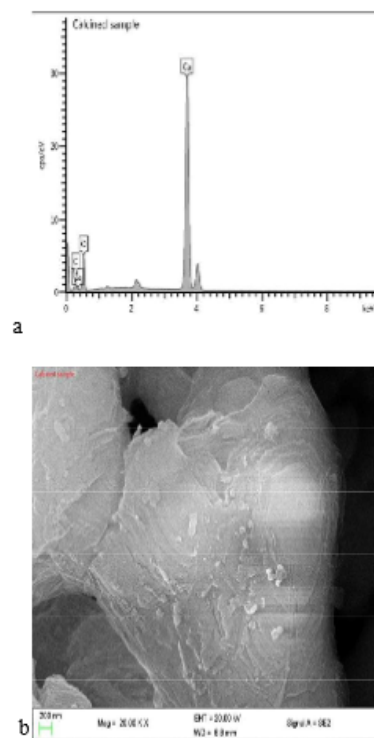
Fig. 5: (a) XRD pattern (b)SEM image of calcined waste chicken eggshell

WCE 2019
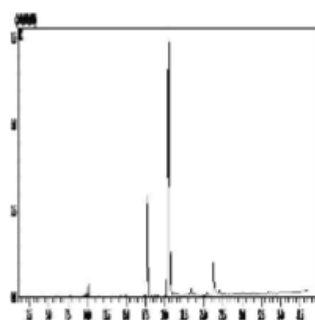
Fig. 6: Chromatograph of the FA composition of FAME from GCMS

TABLE V
RESULT OF THE FA COMPOSITION OF WSME

Name	% Composition (WSME)
Palmitic acid	15.10
Linoleic acid	84.16
Behenic acid	0.73
Saturated fatty acid	26.28
Unsaturated fatty acid	73.72
Total	100

IV. CONCLUSION

The L16 Taguchi design has been applied to optimize the FFA conversion in the transesterification process of WSFO to WSME using calcined waste chicken eggshell. The model has been adjudged significant and regression model equation has predicted the response with 95 % assurance. The actual FFA conversion and the predicted FFA conversion has been found to be in agreement. The ANOVA results showed the coefficient of correlation and adjusted coefficient of correlation are 0.9945 and 0.9724 respectively. Also, the significant process parameters and their contribution factor have been found to be catalyst:WSFO ratio of 49.04 %, reaction temperature of 25.32 %, catalyst particle size of 18.44 % and reaction time of 6.65 %.

The optimum operating conditions for FFA conversion was found to be 2.5:1 catalyst:WSFO ratio, reaction time of 75 min, reaction temperature of 90 $^{\circ}$C, catalyst particle size of 55 µm and methanol:WSFO ratio of 8:1. The XRD and SEM analyses of the eggshell catalyst showed the effectiveness of high-temperature calcination in decomposing $CaCO_3$ to CaO for effective transesterification reaction. The application of Taguchi OA has reduced the number of experimental runs to 16 and ensure a cost-effective transesterification of waste sunflower oil to FAME when compared with the conventional one-variable-at-a-time method.

ACKNOWLEDGMENT

REFERENCES

[1] P. Vijayashree and V. Ganesan, "Oxygenated Fuel Additive Option for PM Emission Reduction from Diesel Engines—A Review," in *Engine Exhaust Particulates*: Springer, 2019, pp. 141-163.

[2] B. Zielinska, S. Samy, J. McDonald, and J. Seagrave, "Atmospheric transformation of diesel emissions," *Research report (Health Effects Institute)*, no. 147, pp. 5-60, 2010.

[3] H. Song, E. Dotzauer, E. Thorin, and J. Yan, "Techno-economic analysis of an integrated biorefinery system for poly-generation of power, heat, pellet and bioethanol," *International Journal of Energy Research*, vol. 38, no. 5, pp. 551-563, 2014.

[4] P. Verma and M. P. Sharma, "Review of process parameters for biodiesel production from different feedstocks," *Renewable and Sustainable Energy Reviews*, vol. 62, pp. 1063-1071, 2016/09/01/ 2016.

[5] H. M. Mahmudul, F. Y. Hagos, R. Mamat, A. A. Adam, W. F. W. Ishak, and R. Alenezi, "Production, characterization and performance of biodiesel as an alternative fuel in diesel engines – A review," *Renewable and Sustainable Energy Reviews*, vol. 72, pp. 497-509, 2017/05/01/ 2017.

[6] A. K. Azad, M. Rasul, M. M. K. Khan, S. C. Sharma, and M. Hazrat, "Prospect of biofuels as an alternative transport fuel in Australia," *Renewable and Sustainable Energy Reviews*, vol. 43, pp. 331-351, 2015.

[7] F. Moazeni, Y.-C. Chen, and G. Zhang, "Enzymatic transesterification for biodiesel production from used cooking oil, a review," *Journal of Cleaner Production*, vol. 216, pp. 117-128, 2019/04/10/ 2019.

[8] A. Azad, S. A. Uddin, and M. Alam, "Mustard oil, an alternative Fuel: An experimental investigation of Bio-diesel properties with and without Trans-esterification reaction," *Global advanced research journal of engineering, technology and innovation*, vol. 1, no. 3, pp. 075-084, 2012.

[9] N. Mansir *et al.*, "Modified waste egg shell derived bifunctional catalyst for biodiesel production from high FFA waste cooking oil. A review," *Renewable and Sustainable Energy Reviews*, vol. 82, pp. 3645-3655, 2018/02/01/ 2018.

[10] E. M. Vargas, M. C. Neves, L. A. C. Tarelho, and M. I. Nunes, "Solid catalysts obtained from wastes for FAME production using mixtures of refined palm oil and waste cooking oils," *Renewable Energy*, vol. 136, pp. 873-883, 2019/06/01/ 2019.

[11] T. T. V. Tran *et al.*, "Green biodiesel production from waste cooking oil using an environmentally benign acid catalyst," *Waste management*, vol. 52, pp. 367-374, 2016.

[12] M. K. Akalın, S. Karagöz, and M. Akyüz, "Supercritical ethanol extraction of bio-oils from German beech wood: Design of experiments," *Industrial Crops and Products*, vol. 49, pp. 720-729, 2013/08/01/ 2013.

[13] R. Leardi, "Experimental design in chemistry: A tutorial," *Analytica Chimica Acta*, vol. 652, no. 1, pp. 161-172, 2009/10/12/ 2009.

[14] A. Buasri, P. Worawanitchaphong, S. Trongyong, and V. Loryuenyong, "Utilization of Scallop Waste Shell for Biodiesel Production from Palm Oil – Optimization Using Taguchi Method," *APCBEE Procedia*, vol. 8, pp. 216-221, 2014/01/01/ 2014.

[15] T. S. Singh and T. N. Verma, "Taguchi design approach for extraction of methyl ester from waste cooking oil using synthesized CaO as heterogeneous catalyst: Response surface methodology optimization," *Energy Conversion and Management*, vol. 182, pp. 383-397, 2019/02/15/ 2019.

[16] A. P. Bora, S. H. Dhawane, K. Anupam, and G. Halder, "Biodiesel synthesis from Mesua ferrea oil using waste shell derived carbon catalyst," *Renewable Energy*, vol. 121, pp. 195-204, 2018/06/01/ 2018.

[17] G. Singh, S. K. Mohapatra, S. S. Ragit, and K. Kundu, "Optimization of biodiesel production from grape seed oil using Taguchi's orthogonal array," *Energy Sources, Part A: Recovery, Utilization, and Environmental Effects*, vol. 40, no. 18, pp. 2144-2153, 2018.

[18] S. K. Sharma, "Use of Taguchi Method for Optimization of Biodiesel Production from Waste Cooking Oil," *Invertis Journal of Renewable Energy*, vol. 8, no. 2, pp. 59-63, 2018.

[19] *AOCS Official Method Ca 5a-40 in Official Methods and Recommended Practices of the AOCS. 7th edition*, 2017.

[20] O. Awogbemi, F. L. Inambao, and E. I. Onuh, "Development and Characterization of Chicken Eggshell waste as Potential Catalyst for Biodiesel Production," *International Journal of Mechanical Engineering and Technology*, vol. 9, no. 12, pp. 1329 - 1346, 2018.

[21] M. Kılıç, B. B. Uzun, E. Pütün, and A. E. Pütün, "Optimization of biodiesel production from castor oil using factorial design," *Fuel processing technology*, vol. 111, pp. 105-110, 2013.

[22] B. Karmakar, S. H. Dhawane, and G. Halder, "Optimization of biodiesel production from castor oil by Taguchi design," *Journal of*

Environmental Chemical Engineering, vol. 6, no. 2, pp. 2684-2695, 2018/04/01/ 2018.

[23] S. H. Dhawane, T. Kumar, and G. Halder, "Parametric effects and optimization on synthesis of iron (II) doped carbonaceous catalyst for the production of biodiesel," *Energy conversion and management,* vol. 122, pp. 310-320, 2016.

[24] R. Arora, V. Kapoor, and A. P. Toor, "Esterification of free fatty acids in waste oil using a carbon-based solid acid catalyst," in *2nd International Conference on Emerging Trends in Engineering and Technology (ICETET'2014), London (UK),* 2014.

[25] N. Tshizanga, E. F. Aransiola, and O. Oyekola, "Optimisation of biodiesel production from waste vegetable oil and eggshell ash," *South African Journal of Chemical Engineering,* vol. 23, pp. 145-156, 2017.

[26] A. Bokhari, L. F. Chuah, S. Yusup, J. J. Klemeš, and R. N. M. Kamil, "Optimisation on pretreatment of rubber seed (Hevea brasiliensis) oil via esterification reaction in a hydrodynamic cavitation reactor," *Bioresource technology,* vol. 199, pp. 414-422, 2016.

[27] J. Goli and O. Sahu, "Development of heterogeneous alkali catalyst from waste chicken eggshell for biodiesel production," *Renewable Energy,* vol. 128, pp. 142-154, 2018.

[28] A. Piker, B. Tabah, N. Perkas, and A. Gedanken, "A green and low-cost room temperature biodiesel production method from waste oil using egg shells as catalyst," *Fuel,* vol. 182, pp. 34-41, 2016/10/15/ 2016.

CHAPTER 3 ARTICLE 2: Modelling and Optimization of Transesterification of Waste Sunflower Oil to Fatty Acid Methyl Ester: A Case of Response Surface Methodology vs Taguchi Orthogonal Approach

Modelling and Optimization of Transesterification of Waste Sunflower Oil to Fatty Acid Methyl Ester: A case of Response Surface Methodology vs Taguchi Orthogonal Approach

Awogbemi, Omojola*, Inambao, FL and Onuh EI

Green Energy Solutions Research Group, Discipline of Mechanical Engineering, Howard College, University of KwaZulu-Natal, Durban 4041, South Africa
*jolawogbemi2015@gmail.com. *ORCID: 0000-0001-6830-6434

Abstract:

Determining the cost-effective process combinations that will achieve prime fatty acid methyl ester (FAME) is laborious, onerous and time-wasting using the experimental process; this has necessitated the need for modelling and optimization tools. This research study, utilizes and compares regression models developed by central composite design of randomized response surface methodology (RSM) and L16(4^15) Taguchi orthogonal approach for the optimization of five process parameters to predict FAME yield (%) for the transesterification of waste sunflower oil (WSFO). The process was catalyzed by calcium oxide developed from high temperature calcination of waste chicken eggshell powder. RSM predicted an optimum FAME yield of ~91 % at process parameters of 1.5 %w/w catalyst: WSFO ratio, catalyst particle size of 50 μm for a reaction time of 60 min, reaction temperature of 55 ºC; and, methanol: WSFO ratio of 6:1 in 32 runs. Taguchi, on the other hand, predicted a prime FAME yield of ~61 % under process operating parameters of catalyst: WSFO ratio = 1:1 %w/w, catalyst particle size = 75 μm, reaction time = 45 min, reaction temperature = 45 °C; and, methanol: WSFO ratio = 4:1 in 16 runs. The calculated coefficient of determination (R), adjusted R, and coefficient of variance were found to be 0.8167 %, 0.7743 % and 3.83 % respectively for the RSM method and 0.9085 %, 0.7711 % and 4.03 % respectively for the Taguchi method. RSM predicted marginally higher FAME yield but Taguchi was substantially more cost-effective owing to 50 % fewer number of runs.

Keywords: ANOVA, FAME yield, optimization, response surface methodology, Taguchi

I. INTRODUCTION

Global warming, increased concern about emission of greenhouse gas, air pollution, explosive population growth, rapid industrial development, continuous depletion of petroleum fuel sources and the need for locally available energy sources has necessitated the quest for countries to survey alternative energy sources that are feasible, affordable, beneficial, and sustainable. The target energy sources are expected not only to minimize air pollution, slash global warming emissions,

generate new jobs, create new industries in the value chain, expand power and energy supply, lessen reliance on coal and other fossil fuel sources but also to steer nations towards a cleaner, safer and healthier fuel and energy future. In order to meet this goal of switching from traditional pollution causing petroleum-based fuels, researchers have paid a great deal of attention to development and testing of renewable energy sources. Biofuel, consisting mainly of bioethanol and biodiesel, produced 2.8 % of world energy consumption in 2015 and 3.1 % in 2017 [1] and is projected to increase to 3.8 % by 2023 [2]. Various countries, have through their renewable energy policy, set targets for renewable energy application. Usage and applicability of renewable energy in transport increased from 2.6 % in 2011 to 3.4 % in 2018 and is projected to increase to 3.8 % in 2023 as shown in Fig 1. In the same vein, biodiesel production is projected to continue to increase, particularly for the United States of America, Indonesia, Brazil, Malaysia between 2017 and 2023 as shown in Fig 2.
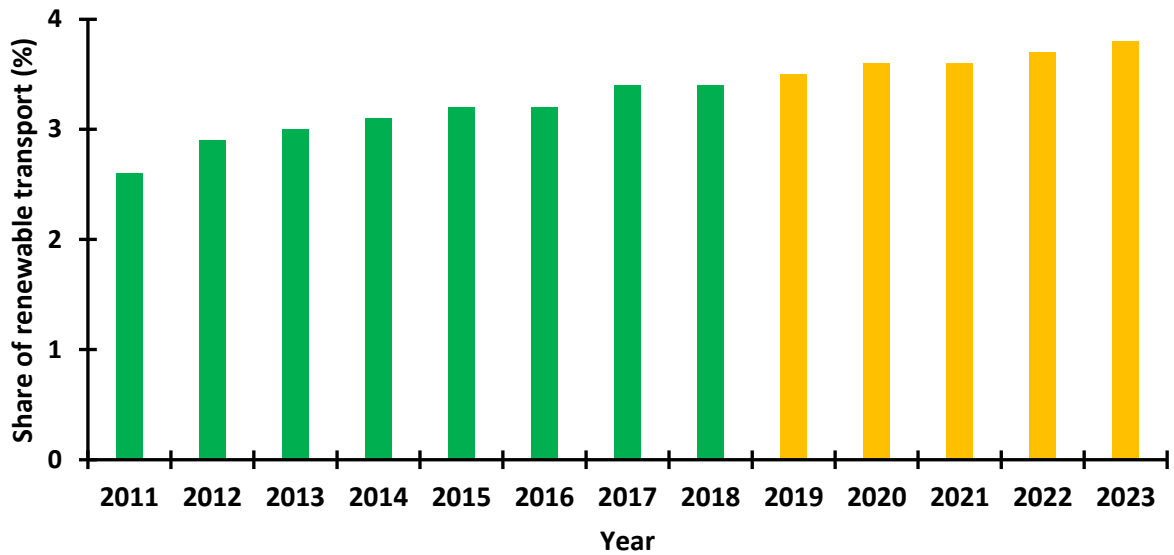
Figure 1. Global share of renewable transport (%) 2011 - 2023 [2].
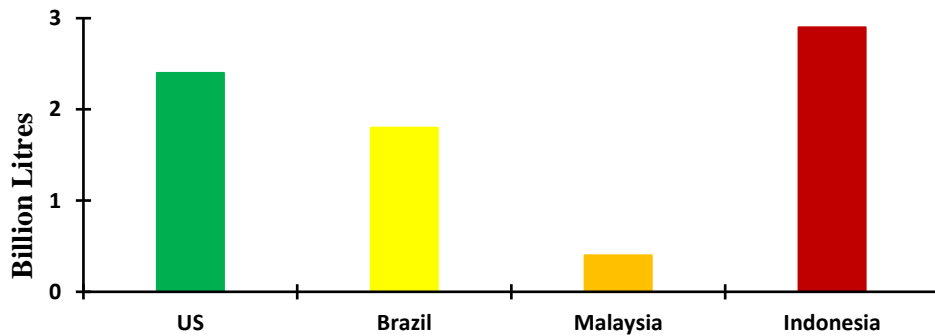
Figure 2. Projected change in biodiesel generation between 2017 and 2023 [103].

Biodiesel, which is usually referred to as fatty acid methyl esters (FAME), is not only a renewable, friendly, easy to produce, but also environmentally pleasant fuel for compression ignition (CI) engines. It is generally produced from a range of feedstock including animal fats, algae, vegetable oils, and other renewable biological sources. Among the proven methods of FAME production, namely, thermal cracking (pyrolysis) [3], microemulsion [4], hydrocarbon blending [5] etc., transesterification is the most common due to its simplicity, low equipment outlay and higher conversion efficiency [6]. The transesterification process is a reversible chemical reaction process where glyceride reacts with alcohol to generate biodiesel with or without catalysts. The alcohol can either be methanol or ethanol while the catalytic process is enhanced by acid, alkaline or enzymatic catalysts. After transesterification, the crude biodiesel must be purified to comply with international standards such as EN 14214 or ASTM D6751. Major benefits of biodiesel include its similar cetane number compared to petrol based diesel (PBD) fuel which allows high combustion efficiency, 90 % biodegradability within 21 days, reduced emission of hydrocarbon (UHC), carbon monoxide (CO), particulate matters (PM), sulphur oxide (SO_2), and aromatic compounds, and, compared to PBD fuel, low toxicity, high lubricity, more complete combustion and engine performance, safe handling, conversion of waste to fuel as well as other social, and economic benefits. In spite of these advantages, increased NOx emissions, high production cost, food security threat, etc. are among the shortcomings in the application of biodiesel [7, 8]. The application of used or waste cooking oil (WCO) to synthesize biodiesel will assuage the almost prohibitive cost of feedstock, prevent food crises arising from the utilization of edible vegetable oil as feedstock, as well as help in the proper disposal of WCO thereby preventing contamination of aquatic and terrestrial habitats.

Various techniques including response surface methodology (RSM), Taguchi orthogonal array [9], artificial neural networks (ANN) [10], matrix laboratory (MATLAB), Simulink, adaptive neuro-fuzzy inference systems (ANFIS) [11], Box-Behnken design [12], and genetic algorithm (GA) [13] have been engaged to optimize the transesterification of vegetable oil to FAME. These techniques can be used individually, in combination or comparison with other techniques using soft computing methods to optimize FAME production. The employment of RSM and Taguchi for the modelling and optimization of the transesterification process are documented in the literature. Karmakar et al. [14] explored the Taguchi orthogonal design to optimize biodiesel generation using castor oil as feedstock and reported that the tool yielded an affordable and sustainable optimization technique for synthesizing biodiesel from castor oil. Dhawane et al. [15] also employed the Taguchi orthogonal approach for the parametric optimization of generation of FAME using edible vegetable oil as feedstock and reported that the approach was easy and productive. Other research has supported the efficacy and effectiveness of Taguchi to successfully optimize the transesterification process and to achieve the lowest cost possible [16, 17]. RSM has been employed to design experiments, develop empirical models, and perform optimization of transesterification of oil to biodiesel as well as for property prediction [18-21].

Najafi et al. [22] applied a combination of ANN, ANFIS and RSM to estimate, predict and optimize the parametric factors that influence biodiesel yield during transesterification and reported that the models successfully predicted biodiesel yield and the outcomes were validated

by the experimental data. The application of Taguchi method to predict and optimize the biodiesel production parameters has been reported to yield acceptable conditions for the economical generation of biodiesel from various feedstocks through the transesterification process [14, 15, 23]. Tan et al. [9] used the RSM and Taguchi methods for the optimization of transesterification of WCO to biodiesel and reported that the statistical tools provided favorable prediction outcomes and experimental validation of biodiesel yield. In general, the application of modelling, optimization tools and other soft computing techniques in the transesterification of WCO to biodiesel has been found to be cost effective and saves time, are less laborious, innovative, flexible, prevents multiple experimental processes, offers better understanding of the process and have the capability to forecast and predict "what-if" scenarios. Some of the parameters that influence biodiesel yield include reaction temperature, alcohol/feedstock molar ratio, catalyst concentration, reaction time, etc. [24-27].

The economics and cost analysis of FAME production has shown that cost of feedstock gulps over 70 % of the production expenses while raw materials and other consumables jointly take up 86 % of the production cost. Raw materials for transesterification process include the oil feedstock, catalyst, alcohol, and purification medium. The cost of input and other materials is a substantial part of the operating cost [28, 29]. The use of the experimental processes, also known as the one-variable-at-a-time (OVAT) experimental technique, is not just expensive, onerous, burdensome, time-consuming, requires huge laboratory architecture but also consumes a high volume of materials. Materials are wasted in trying to determine the optimal parameters combinations for best yield. These identified drawbacks can be overcome by the use of optimization techniques with the capability of providing the required information from minimum runs by concurrently altering all the process factors. The use of design-of-experiment software reduces experimental runs, saves time, saves raw materials, and uncovers the mutual interactions going on among the various process independent parameters (inputs) and dependent variable (output) [30-32].

With the use of WCO as feedstock for transesterification gaining traction, the relevant questions that remain unanswered and which serve as the justification for this effort relate to the necessary conditions that facilitate the optimum biodiesel yield and catalyst recovery in the shortest time and lowest cost. The current study aims to use a combination of experimental and statistical techniques to interrogate the optimal operating parameters aimed at the transesterification of waste sunflower oil (WSFO) to biodiesel using calcium oxide (CaO) developed from calcined waste chicken eggshell (WCE) powder. The motivation is to investigate parameters that will ensure optimum FAME yield using both the RSM and Taguchi optimization methods.

The effects and influences of catalyst concentration, catalyst particle size, methanol to waste oil mole ratio, experimental reaction temperature and reaction time on FAME yield and FAME conversion were investigated and analyzed. The specific objectives were: (i) production of biodiesel from WSFO using CaO derived from calcined WCE powder; (ii) evaluation of the effects of the listed factors of biodiesel yield; (iii) comparison of the experimental FAME yield with the predicted FAME yield using RSM and Taguchi methods. The parameters studied were catalyst: WSFO ratio (%w/w), catalyst particle size (µm), reaction temperature (°C), reaction time

(min) and methanol: WSFO ratio. Also, the interrelationship among these identified process parameters were studied using three-dimensional (3D) surface plots of RSM, ramps and other plots. The established models using the Taguchi orthogonal and RSM methods were appraised using statistical parameters including standard error, sum of squares, correlation coefficient (R), F- and p-values, standard deviation, coefficient of determination (R^2), and adjusted R^2 (R_{adj}^2).

II. MATERIALS AND METHODS

II.I. Materials collection

Waste Sunflower oil (WSFO) sample was sourced and collected from take away outlets close to Howard College campus, University of KwaZulu-Natal (UKZN), Durban, at the point of disposal. Available information showed that the waste oil had been used repeatedly for 14 days to fry potato chips. WCE was collected from restaurants within Howard College, UKZN. Methanol uniVAR (analytical grade) at 99.5 % purity was procured from Merck.

II.II. Materials treatment and preparation

The WSFO was heated in an electric heated to 120 °C for 90 min to eliminate water and sieved via vacuum filtration to remove food particles and other solids in the oil and later analyzed to determine the acid value, molecular weight and iodine number. The procedure for the preparation CaO catalyst via high temperature calcination of WCE powder has been described in our earlier work [33]. The eggshell powder was classified by using sieves of different pore sizes.

II.III. Transesterification process

The acid value of WSFO allows for a one stage transesterification process. The filtered WSFO, methanol and CaO derived from WCE shell powder were emptied into a round bottom flask and heated to a predetermined temperature and time and mixed at a predetermined speed (rpm) maintained by a magnetic stirrer. A digital thermocouple was utilized to verify the temperature of the reacting solution throughout the duration of the experiment. Different catalyst concentrations, catalyst particle size, reaction temperature and methanol:WSFO mole oil ratio were used during each batch of the transesterification process as shown in Table 1. A medium sized magnetic stirrer was employed to guarantee adequate and homogeneity of the reacting mixture maintained at a predetermined temperature, time and stirring speed throughout the process. The resulting solution was thereafter filtered in a vacuum filtration set up to recover the catalyst. The filtered mixture was transmitted into clean separating funnel and left to stay overnight. Glycerol was seen coagulated beneath the separating funnel. Thereafter, the coagulated glycerol was drained out while the remaining crude before the crude biodiesel was decanted and transferred into a glass container for further purification and analysis.

The FAME yield (%) of WSFO to biodiesel were estimated by Equation (1):

$$FAME\ yield\ \% = \frac{Weight_{Biodiesel}}{Weight_{Oil}} \times 100\% \tag{1}$$

II.IV. Modeling and optimization by RSM

The optimization of biodiesel yield and catalyst recovery arising from transesterification of WSFO into FAME was conducted by applying the central composite design (CCD) of the response surface methodology version of design of experiment (DoE) available on the Design-Expert software. The CCD of a randomized RSM is a very popular and effective optimization tool with full or fractional factorial point, axial point and centre point that can be duplicated for every combination of categorical factor level. In order to use DoE, several experiments are conducted to ascertain the prime factors for the best outcomes. RSM was later engaged to form a mathematical model to validate the outcomes of the experiments. The process parametric factors investigated for the optimization of the transesterification process of WSFO were catalyst weight: WSFO ratio, reaction time, reaction temperature, particle size of the catalyst and methanol-to-WSFO molar ratio as shown in Table 1. A total of 24 non-center points and 6 center points and alpha of 2 gave rise to a total of 32 runs. The choice of this method was dictated by the number of variables and levels [34]. The data collected from 32 experimental runs were analyzed by RSM CCD by Design Expert Software10.0.8.0 version.

Table 1. Investigated parameters, notations and coded levels

Variable	Units	Notation	Coded factors level				
			-2	-1	0	1	2
Catalyst:WSFO	%w/w	X_1	0.5	1	1.5	2	2.5
Particle size of catalyst	µm	X_2	50	75	90	125	150
Reaction time	min	X_3	30	45	60	75	90
Reaction temperature	ºC	X_4	35	45	55	65	75
Methanol:WSFO ratio		X_5	2	4	6	8	10

II.V. Modeling and Optimization by Taguchi

Application of the Taguchi orthogonal array (OA), developed by Dr. Genichi Taguchi, allows for the investigation of every likely permutation of parameters, minimizes the number of tests and identifies and quantifies the interactive impacts of the parameters on a process by substantially reducing the cumbersome optimization procedure. Taguchi OA reduces the number of experiments without negatively affecting the operating parameters while retaining all the required details [35, 36]. Taguchi OA allows the implementation of various design designation from L4 (2^3), L8 (2^7) and up to L64(4^21). In this study, the L16(4^15) design was chosen which allows four levels and five parameters in the Taguchi technique. The number of runs, N, were estimated by means of Equation (2):

$$N = (L - 1)P + 1 \tag{2}$$

Where P and L indicate number of parameters and levels, respectively. From Equation (2), the number of runs, using Taguchi OA, is 16 runs.

Table 2 shows the experimental design matrix developed by the Taguchi design. Experimental outcomes were analyzed via signal-to-noise (S/N) ratio for estimating the effect of the factors on FAME yield. The difference between the response and the anticipated result was calculated by S/N ratio as:

$$\frac{S}{N} = -10 log_{10} \left(\frac{\Sigma \left(\frac{1}{y_i^2} \right)}{n} \right) \tag{3}$$

Where y_i = response value, and n = number of experimental runs.

Analysis of variance

The evaluation, prediction and measurement of the effects of parametric factors on the transesterification process by determining the effects of key factors i.e. the best factor levels from the tested factor levels for the optimal process parameters for the transesterification process are conducted by analysis of variance (ANOVA) or S/N ratio. However, S/N ratio is unable to identify the impact of these factors on the response, unlike ANOVA. The influence of each parameter in generating the response can be determined by calculating the contributing factor.

$$\% \, Contributing \, factor = \frac{Sum \, of \, squares \, of \, the \, particular \, variable \, (SS_f)}{Sum \, of \, squares \, of \, all \, the \, variable \, (SS_{r)}} \times 100 \tag{4}$$

ANOVA is targeted at increasing the percentage of FAME yield. The parameter with the highest percentage contribution factor is also reflected in the regression model equation employed to predict and validate the model from the RSM analysis of the actual data obtained from the actual experimental runs [37].

Table 2. Experimental design matrix generated by Taguchi

Run	X_1	X_2	X_3	X_4	X_5	FAME Yield %
1	1.5	75	60	65	10	85.43
2	2	125	45	55	10	86.76
3	2	150	60	45	8	78.32
4	1	150	90	75	10	69.45
5	1	90	60	55	6	82.5
6	2.5	125	60	75	4	71.68
7	2.5	90	75	45	10	73.78
8	2.5	150	45	65	6	85.51
9	2,5	75	90	55	8	70.86
10	1.5	150	75	55	4	75.45

11	2	75	75	75	6	87.54
12	1	75	45	45	4	81.66
13	1.5	90	45	75	8	70.55
14	1.5	125	90	45	6	84.66
15	1	125	75	65	8	76.58
16	2	90	90	65	4	87.54

III. RESULTS AND DISCUSSIONS

III.I. Response Surface Method statistical analysis

Table 3 presents the results of the transesterification of WSFO to FAME using RSM via CCD experimental design. The experimental (actual) FAME yield varied between 69.45 % and 90.55 %. The actual yields were evaluated to produce a suitable and workable regression model. An appropriate model was selected from mean, linear, quadratic, cubic, quartic etc. A cubic regression model was generated and employed to predict optimal parameters for the transesterification of WSFO to biodiesel by the software. The best fit model for FAME yield is as shown in Equation (5).

$$y = 127.84 + 7.41X_1 - 1.86X_2 - 0.25X_3 + 0.22X_4 + 6.23X_5 - 0.11X_1X_4 + 0.028X_3X_5 - 0.019X_4X_5 - 1.38X_1^2 + 0.018X_2^2 - 0.51X_5^2 - 0.000051X_2^3 \quad (5)$$

Where y is the FAME yield (%), the catalyst WSFO ratio, particle size of catalyst, experimental reaction time, process reaction temperature, and methanol:WSFO ratio are denoted by X_1, X_2, X_3, X_4, and X_5, respectively. The interaction terms are X_3X_5 and X_4X_5, and X_1^2, X_2^2, X_5^2, and X_2^3 are quadratic (cubic) terms of the independent variables. Parameters with positive coefficients (linear, interaction or quadratic) have a desirable effect on FAME yield while those with a negative coefficient negatively affected FAME yield.

Table 3. Actual and predicted of FAME yield (%) by RSM

Run	X_1	X_2	X_3	X_4	X_5	FAME yield (%)	
						Actual	Predicted
1	0.5	150	30	75	10	85.43	86.34
2	1.5	100	90	55	6	86.76	83.12
3	2.5	150	30	75	2	78.32	79.28
4	2.5	50	90	75	2	69.45	67.44
5	1.5	100	60	65	6	82.5	84.74
6	3.5	100	60	55	6	71.68	73.83
7	0.5	50	90	35	2	73.78	73.29
8	1.5	100	60	55	6	85.51	85.45
9	1.5	200	60	55	6	70.86	70.86
10	1.5	100	60	55	2	75.45	74.16
11	0.5	100	60	55	6	87.54	86
12	1.5	100	60	95	6	81.66	82.62

13	2.5	150	90	35	2	70.55	72.14
14	0.5	50	30	35	10	84.66	87.3
15	0.5	150	90	75	2	76.58	78.47
16	0.5	150	90	35	10	87.54	89.85
17	2.5	50	30	35	2	80.51	83.27
18	1.5	100	60	55	6	90.43	85.45
19	0.5	50	90	75	10	89.54	88.18
20	0.5	150	30	35	2	87.59	85.13
21	1.5	100	60	55	6	81.54	85.45
22	2.5	150	30	35	10	90.54	86.15
23	1.5	100	60	55	6	89.51	85.45
24	1.5	100	60	55	6	81.87	85.45
25	2.5	50	30	75	10	76.66	75.31
26	1.5	100	60	55	6	87.56	85.45
27	1.5	100	30	55	6	79.65	80.8
28	2.5	50	90	35	10	89.65	87.99
29	1.5	50	60	55	6	88.65	91.07
30	0.5	50	30	75	2	90.55	89.6
31	1.5	100	60	55	10	76.76	80.46
32	2.5	150	90	75	10	78.67	77.86

As shown in Table 3, the highest FAME yield, as predicted by RSM regression model, of 91.07 %, was obtained with catalyst:WSFO ratio = 1.5 %w/w, particle size of catalyst = 50 µm, reaction time = 60 min, process reaction temperature = 55 °C and methanol:WSFO ratio = 6:1, with reaction time being the most important parameter that influences FAME yield.

The model equation was appraised for statistical importance using the ANOVA test, R^2 and R^2_{adj}. The accuracy, and efficiency of the regression model in predicting the response were tested by ANOVA and the outcomes are shown in Table 4. The F-value and p-value of the model was estimated to be 9.86 and < 0.0001 respectively, indicating that the model was statistically significant at 95 % CI level ($p < 0.05$) [38]. In that scenario, X_1, X_2, X_3, X_4, X_4, $X_1 X_4$, $X_3 X_5$, X_1^2, X_2^2, X_5^2, and X_2^3 are statistically significant model terms while X_4 and X_5 are insignificant. The variable X_3 with the highest F-test value of 29.53, $p < 0.0001$ was the most statistically significant parameter indicating that reaction time was the most significant parameter for FAME yield. The F-value of 0.58 for the lack of fit denotes that it was not significant compared to the pure error. In addition, it was discovered that there is 80.58 % prospect that a Lack of Fit F-value of 0.58 could be instigated by noise. It is advantageous to have a non-significant Lack of Fit (Table 4).

Table 5 depicts the outcomes of test for significance of the model. Though the standard error of the intercept is high, the standard errors of most of the parameters are < 1 and the degree of freedom (df) associated with the parameters are 1. The measure of accuracy and precision of the model were ascertained by the R^2 and R^2_{adj} values. An R^2 value of 0.8617 reveals that 86.17 % of the entire data were consistent with the predicted data and variability [39]. R^2_{adj} of 0.7743 indicates an acceptable fitness for the model. An adequate precision (S/N ratio) above than 4 has been found to be desirable and advantageous. The S/N ratio of 11.789 is a pointer to the suitability

of the model to traverse the design space and a further proof that the generated model is statistically significant [40] (Table 6). A standard deviation of 3.14 was recorded and the low value of coefficient of variation (CV) of 3.83 % is a sign of good accuracy and dependability of this model [41].

The highest FAME production yield of 91.07 % forecasted by the RSM model was accomplished at a catalyst: WSFO ratio of 1.5 %w/w, particle size of catalyst of 50 µm, a reaction time of 60 min, a reaction temperature of 55 °C and a methanol: WSFO ratio of 6:1, with reaction time being the most important parameter that influenced FAME yield, as clearly displayed in Table 3.

Table 4. ANOVA for FAME yield

Source	Sum of Squares	df	Mean Square	F Value	p-value Probability > F	
Model	1170.13	12	97.51	9.86	< 0.0001	significant
Linear						
Catalyst:WSFO ratio (X_1)	65.77	1	65.77	6.65	0.0184	
Particle size of catalyst (X_2)	159.62	1	159.62	16.15	0.0007	
Reaction time (X_3)	291.98	1	291.98	29.53	< 0.0001	
Reaction temperature (X_4)	56.33	1	56.33	5.70	0.0275	
Methanol: WSFO ratio (X_4)	145.88	1	145.88	14.76	0.0011	
Interaction						
$X_1 X_4$	84.09	1	84.09	8.51	0.0089	
$X_3 X_5$	187.14	1	187.14	18.93	0.0003	
$X_4 X_5$	37.70	1	37.70	3.81	0.0657	
Quadratic						
X_1^2	53.67	1	53.67	5.43	0.0310	
X_2^2	172.06	1	172.06	17.40	0.0005	
X_5^2	170.97	1	170.97	17.29	0.0005	
X_2^3	188.72	1	188.72	19.09	0.0003	
Residual	187.84	19	9.89			
Lack of Fit	116.30	14	8.31	0.58	0.8058	not significant
Pure Error	71.54	5	14.31			
Total	1357.97	31				

Table 5. Test of significance

Factor	Coefficient Estimate	df	Standard Error	95% CI Low	95% CI High	VIF
Intercept	127.84	1	13.52	99.55	156.13	
Linear						
Catalyst:WSFO ratio (X_1)	7.41	1	2.87	1.40	13.43	20.05
Particle size of catalyst (X_2)	-1.86	1	0.46	-2.83	-0.89	1133.89
Reaction time (X_3)	-0.25	1	0.046	-0.34	-0.15	3.94
Reaction temperature (X_4)	0.22	1	0.091	0.027	0.41	6.66
Methanol:WSFO ratio (X_5)	6.23	1	1.62	2.84	9.63	76.71

Interaction						
$X_1 X_4$	-0.11	1	0.039	-0.20	-0.032	15.16
$X_3 X_5$	0.028	1	0.0066	0.015	0.042	8.41
$X_4 X_5$	-0.019	1	0.0098	-0.040	0.0014	12.33
Quadratic						
X_1^2	-1.38	1	0.59	-2.63	-0.14	8.78
X_2^2	0.018	1	0.0042	0.0088	0.026	4546.17
X_5^2	-0.51	1	0.12	-0.76	-0.25	65.75
X_2^3	-0.000051	1	0.000012	-0.000075	-0.000026	1242.64

Table 6. ANOVA of regression equation

Parameter	Value	Parameter	Value
Standard Deviation	3.14	R^2	0.8617
Mean	82.12	Adj R^2	0.7743
C.V. %	3.83	Predicted R^2	N/A
PRESS	N/A	Adequate Precision	11.789
-2 Log Likelihood	147.45	BIC	192.50
		AICc	193.67

Process parameters interactions

Design expert version 10 was applied to produce 3D response surface plots in order to comprehend the connections, interrelationship, and interactions among the process variables affecting the selected process response (FAME yield) as generated by Equation 4. The response surface plots show the interactions, relationships and correlations of two different variables in the study while maintaining the other variables at a fixed value. Figure 2 shows the 3D plots with the y axis offset from the x axis at a value of 20.

a. Influence of methanol:WSFO ratio and reaction time on FAME yield

Figure 2a shows the relationship between reaction time and methanol:WSFO ratio against FAME yield (%) while keeping catalyst:WSFO ratio, particle size of catalyst, reaction temperature constant as 2.5:1 %w/w, 50 µm and 35 °C in that order. As the methanol to WSFO ratio increases from 2:1 to 8:1, the proportion of FAME yield increases from 70 % to 90 % but decreases to 82 % when the methanol to WSFO ratio increases beyond 8:1. This confirms earlier reports that sufficient methanol to oil ratio positively impact on FAME yield in the production of biodiesel through transesterification reaction. A higher methanol to oil ratio will also precipitate more FAME formation [42]. Similarly, as the process reaction time increases from 30 min to 90 min, FAME yield increases. This may be attributable to sufficient contact time between the reactants which results in higher yield [43]. The interaction of methanol: WSFO ratio and process reaction time have negative impacts on FAME yield (Table 5).

b. Influence of catalyst to WSFO ratio and reaction temperature on FAME yield

The interactions between reaction temperature and catalyst: WSFO ratio against FAME yield at constant catalyst particle size, reaction time, and methanol to WSFO ratio of 150 µm, 30 min and 2:1 respectively is displayed in Figure 2b. From the plot, the highest proportion of FAME generation of about 92 % was achieved at 95 °C and 0.5 %w/w catalyst to WSFO ratio while the least FAME yield of 78 % was recorded at 95 °C and 2.5:1 catalyst: WSFO ratio. FAME yield decreases from 92 % to 77 % when the catalyst: WSFO improved from 0.5 %w/w to 2.5 %w/w. When the transesterification process reaction temperature was escalated from 35 °C to 95 °C the FAME production yield reduced from 84 % to 78 %. The catalyst to WSFO ratio had more of an effect on FAME yield than reaction temperature. The combination of these two variables had negative effects on FAME yield (Table 5).

c. Influence of methanol to WSFO ratio and reaction temperature on FAME yield

The mutual interaction between the methanol to WSFO ratio and process reaction temperature on FAME yield is depicted in Figure 2c. Catalyst: WSFO ratio, particle size of catalyst and reaction time were kept constant at 0.5 %w/w, 50 µm and 90 min respectively to adequately show the interaction between these two variables. As shown in Tables 4 and 5, the combination of methanol to WSFO ratio and reaction temperature had a negative but insignificant impact on FAME yield. As shown in the plot, the highest FAME yield was attained at a methanol: WSFO oil ratio of 6:1 and reaction temperature of 95 °C, while the least FAME yield was achieved at 2:1 methanol: WSFO ratio and 35 °C reaction temperature. An increase in reaction temperature from 35 °C to 88 °C resulted in a slight reduction in FAME yield from 92 % to 86 %, while an increase in methanol: WSFO ratio from 2:1 to 8:1 led to an increment in FAME yield from 73 % to 90 %. A further increment in methanol:WSFO ratio, to 10:1, however, caused a reduction in FAME yield to 88 %. The effect of methanol:WSFO ratio was more pronounced than that of reaction temperature.
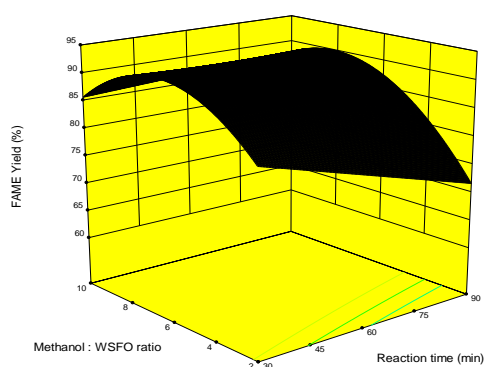
(a)
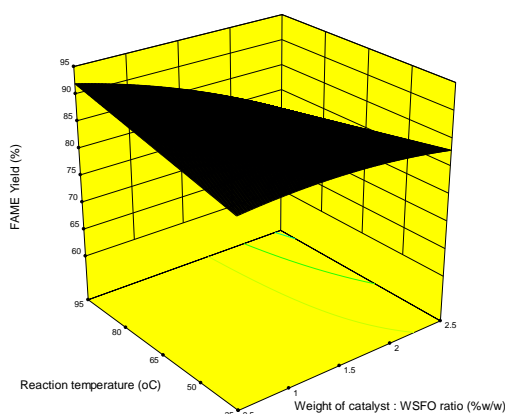
(b)
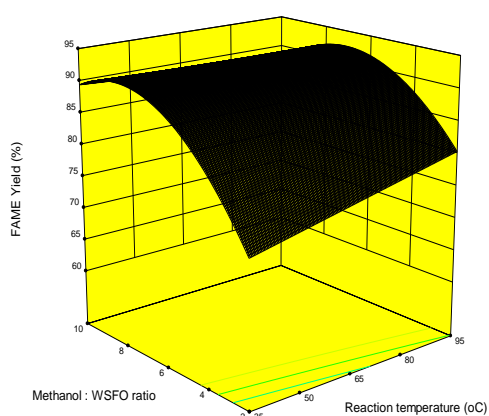
(c)

Figure 2. 3D response surface plots for (a) methanol: WSFO ratio and reaction time (b) catalyst:WSFO ratio and reaction temperature (c) methanol:WSFO and reaction temperature.

III.II. Taguchi method

a. Analysis of variance (ANOVA)
The outcomes and consequences of the prediction of FAME yield from the transesterification process using the L16 Taguchi orthogonal approach is depicted in Table 7. The F-value and the sum of squares are estimated and applied to determine the influence of the parameters on the response.

In this study, with the sum of squares of 607.44 and mean square of 67.49, the model is considered significant. The F-value and p-value of 6.62 and 0.0161 respectively corroborates that the model generated by Taguchi method is significant. Also, the p-value shows that there is only 1.61 % likelihood that the value of the F-value achieved occurred due to the preponderance of noise. Consequently, the model is considered fit and significant enough for the optimization of FAME yield of the transesterification process of WSFO within the selected process parameters. From the ANOVA study, it has been shown that only three out of the five process parameters,

namely, catalyst:WSFO (%w/w), reaction temperature (°C), and methanol:WSFO ratio, have a substantial influence on the dependent variable (response). The effects of reaction time and particle size of the catalyst was negligible. Among the three parameters having significant influence, the methanol: WSFO ratio with F-value and the sum of squares value of 7.92 and 242.43 respectively showed the highest influence on FAME yield. The significance of each process parameters was further authenticated by calculating the contribution factor (CF) of each significant parametric factor in the process. Equation (4) was employed to calculate the contribution factors. The methanol:WSFO ratio, catalyst:WSFO ratio and reaction temperature contribute 36.26 %, 30.42 % and 24.16 % respectively to FAME yield through transesterification process as shown in Table 8. The contribution factor result agrees with the ANOVA result showing that the methanol: WSFO ratio has the highest influence on FAME yield.

Table 7. Analysis of variance (ANOVA of model and process parameters

Source	Sum of Squares	Degree of freedom	Mean Square	F Value	p-value Prob > F	
Model	607.44	9	67.49	6.62	0.0161	significant
X_1: Catalyst:WSFO (%w/w)	203.43	3	67.81	6.65	0.0246	
X_4: Reaction temperature (°C)	161.58	3	53.86	5.28	0.0404	
X_5: Methanol:WSFO ratio	242.43	3	80.81	7.92	0.0165	
Residual	61.21	6	10.20			
Total	668.64	15				

Table 8. Contribution factor the significant parameter on FAME yield

Parameter (unit)	Contribution factor (%)
Catalyst:WSFO (%w/w)	30.42
Reaction temperature (°C)	24.16
Methanol:WSFO ratio	36.26
Residual	9.15

From the parameters estimated from the analysis of variance, as shown in Table 9, R^2 was found to be 0.9085. The R^2 value, being close to unity, shows its linearity and fitness for the selected model. The value obtained for R^2_{adj} was found to be 0.7711 while the predicted R^2 was 0.349 for the preferred model. Adequate precision is a degree of the S/N ratio and as shown in Table 9, the adequate precision value obtained was 7.914 which is almost double the required tolerable accuracy of 4 for any model. The adequate precision of 7.914 shows that the model has the capability to forecast the dependent variable and adequately optimize FAME yield. Furthermore, the standard deviation was estimated to be 3.19 while the coefficient of variance was 4.03 % which confirmed the capability of the model to predict the optimum parameters with satisfactory precision [15, 44].

Table 9. Statistical parameters estimated from ANOVA

Parameter	Value	Parameter	Value
Standard Deviation	3.19	R^2	0.9085
Mean	79.27	Adjusted R^2	0.7711
C.V. %	4.03	Predicted R^2	0.3490
PRESS	435.26	Adequate Precision	7.914
-2 Log Likelihood	66.87	BIC	94.60
		AICc	130.87

b. Regression model equation from Taguchi method

ANOVA was used to develop a model and identify the individual parameters that were significant to the generation of the desired response. Significant parameters were considered and escalated while the insignificant parameters were relegated. The CI of the model parameters are 95 % which indicated a very high assurance level of the mathematical model to forecast the FAME yield. The Taguchi method mathematical model equation (Equation (6)) relate the three parameters that are significant in predicting the response.

$$y = 79.27 - 1.72X_1[1] - 0.24X_1[2] + 5.77X_1[3] + 0.34X_4[1] - 0.34X_4[2] + 5.5X_4[3] - 0.18X_5[1] + 5.79X_5[2] - 5.19X_5[3] \quad (6)$$

Where y = FAME yield (%), $X_1[1]$, $X_1[2]$ and $X_1[3]$ are the weight of catalyst:WSFO ratio, $X_4[1], X_2[2]$ and $X_4[3]$ are reaction temperature, and $X_5[1], X_5[2]$ and $X_5[3]$ are the methanol:WSFO ratio as shown in Table 10.

The degree of freedom for the model is unity while the CI is 95 % and the standard error of the parameters is 1.38 (Table 10). The linear regression model equation has the capacity to predict FAME yield using the parameters and data given in Table 2. The influence of the three significant parameters on the biodiesel yield is displayed in Fig 3 (a, b, c).

Table 10. Coefficients in terms of coded for categoric factors and actual for other factors

Term	Coefficient Estimate	df	Standard Error	95% CI Low	95% CI High
Intercept	79.27	1	0.80	77.31	81.22
$X_1[1]$	-1.72	1	1.38	-5.10	1.66
$X_1[2]$	-0.24	1	1.38	-3.63	3.14
$X_1[3]$	5.77	1	1.38	2.39	9.16
$X_4[1]$	0.34	1	1.38	-3.05	3.72
$X_4[2]$	-0.37	1	1.38	-3.76	3.01
$X_4[3]$	4.50	1	1.38	1.11	7.88
$X_5[1]$	-0.18	1	1.38	-3.57	3.20
$X_5[2]$	5.79	1	1.38	2.40	9.17
$X_5[3]$	-5.19	1	1.38	-8.57	-1.81

[1], [2] and [3] represent first, second and third level respectively

III.III. Effect of individual significant parameters on FAME yield predicted by Taguchi method

Three process parameters have significant influence on FAME yield as predicted by Taguchi method. The three parameters are represented in Equation (6) while their individual contribution factors are shown in Table 8.

a. Effect of catalyst:WSFO ratio

At reaction time of 45 min, catalyst particle size of 125 µm and reaction temperature of 55 °C, the effect of catalyst:WSFO ratio was measured. As shown in Fig 3a, maximum FAME yield of 84 % was attained with a catalyst:WSFO ration of 2:1. A higher concentration of the resulted in a drastic reduction in FAME yield. This may be a direct consequence of excessive catalyst loading which could accelerate the reverse reaction during transesterification. Comparable outcomes have earlier been reported by Sirisomboonchai et al. [45] and Gupta and Ratho [46].

b. Effect of reaction temperature

The proportion of FAME yield was studied at four different temperature levels, namely 45 °C, 55 °C, 65 °C and 75 °C. As shown in Fig 3b the maximum FAME yield of 89 % was accomplished

at a reaction temperature of 65 °C when the catalyst: WSFO ratio, catalyst particle size, reaction time and methanol: WSFO ratio were maintained at 2:1 %w/w, 125 µm, 45 min and 10:1 respectively. A further improvement of the reaction temperature to 75 °C reduced the FAME yield to 80 %. This is due to the fact that at high temperatures methanol is lost due to evaporation and this impedes the transesterification reaction which alters the methanol to oil ratio resulting in saponification. Reaction temperature above methanol boiling point (65 °C) is counterproductive [47, 48]. Outcomes of previous research by Maneerung et al. [49], Dhawane et al. [15], Karmakar et al. [14] supported the results of this study in this regard.

c. Effect of methanol:WSFO ratio

Methanol: WSFO ratio is the most important factor in FAME yield (Table 8). Under the reaction conditions of catalyst: WSFO ration of 2 %w/w, catalyst particle size of 125 µm, reaction time of 45 min, and reaction temperature of 55 °C, the highest FAME yield of 90 % was obtained at a methanol: WSFO ratio of 6:1. Theoretically, a methanol: oil ratio of 3:1 is a prerequisite to producing biodiesel and water. However, careful adjustment of molar ratio can result in optimum use of alcohol and formation of more product. Excessive methanol to oil ratio impedes FAME yield, especially when the catalyst concentration is kept constant [50, 51].
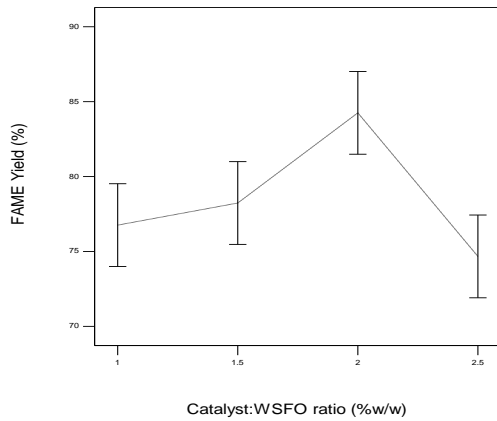
(a)
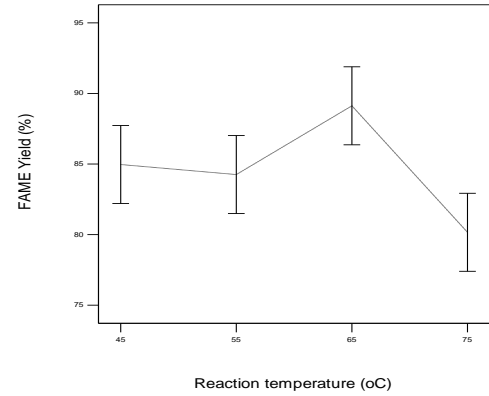
(b)
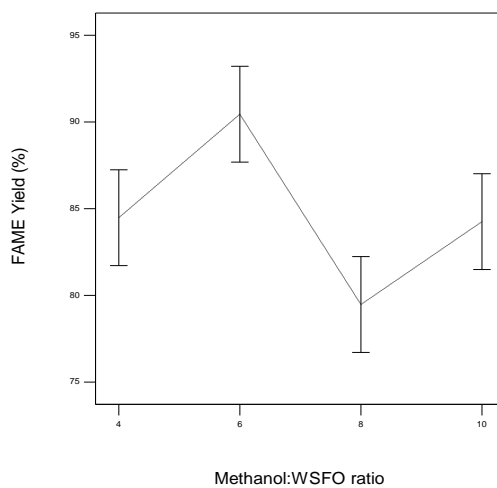
(c)

Figure 3. (a) Effect of catalyst: WSFO ratio (%w/w), (b) reaction temperature (°C), and (c) methanol:WSFO ratio of FAME yield (%)

III.III. Comparison of RSM and Taguchi method

99

In this present study, the outcome of prediction of FAME yield using RSM optimization technique was compared with that of Taguchi OA method. The results of the two optimization techniques are similar and in agreement. Both techniques threw up the significant parameters for the prediction of FAME yield with the set factors and levels. The two techniques formulated model equations based on the significant factors they predicted. There are agreements in the parameters that RSM and Taguchi method found to be significant to the models. In this regard, catalyst: WSFO ratio, reaction temperature, and methanol: WSFO ratio were found to be dominant. In terms of number of data, the Taguchi method required lesser experimental data and always utilized linear regression, while RSM could also use quadratic or cubic regression [9, 52].

As shown in Fig 4a and Fig 4b, the pattern of the predicted and actual FAME yield was similar, indicating agreement between the two optimization techniques [14, 53]. As shown in Fig 5, the actual and RSM predicted data agreed to a large extent, indicating the accuracy of RSM in predicting the response. However, more pronounced deviations between the actual and predicted yield were noticed between runs 17 and 24. This can be attributed to the outcome of the different interactions among the process parameters. The lower and upper constraints of the range for all the investigated process parameters were contained in the optimization process. With the FAME yield maximized, the optimal value of the parametric factors which engender a desirability function of unity are shown in Fig 6a and Fig 6b. Maximized FAME yields of 93.42 % and 89.13 % were obtained from the RSM and Taguchi orthogonal methods respectively. The desirability function of the RSM and Taguchi method were within the span of the optimum operating process conditions for the response within the range of level of factors. The import of the desirability function was to obtain an optimal response from the model. Table 11 presents a comparison between the outcomes of the utilization of the response surface methodology and Taguchi methods to optimize FAME yield. While the RSM models obtained five significant parameters that can influence FAME yield, Taguchi presented only three. The Optimum FAME yield predicted by RSM was higher than that predicted by Taguchi. The parameter which had the highest influence on FAME yield according to RSM and Taguchi were reaction time and methanol: WSFO ratio respectively.

(a)   (b)
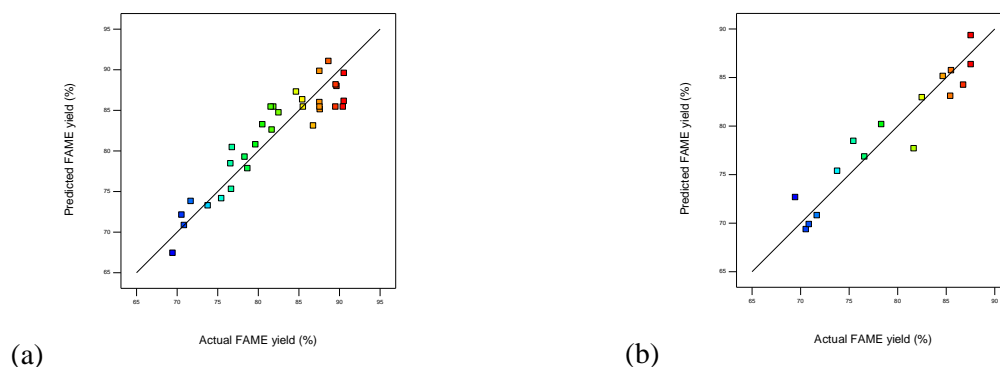
Figure 4. Predicted vs actual FAME yield (a) RSM (b) Taguchi method
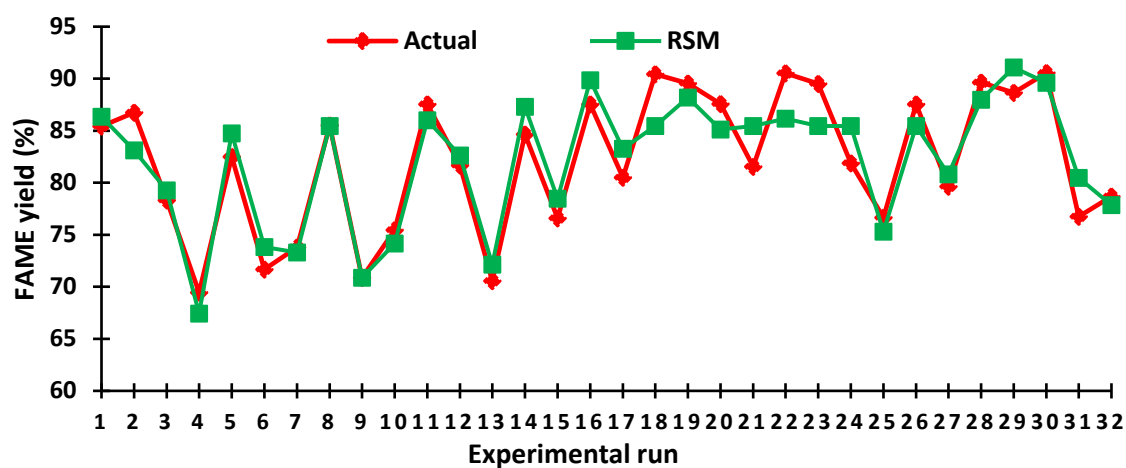
Figure 5. A plot of FAME yield (%) against actual and RSM predicted data
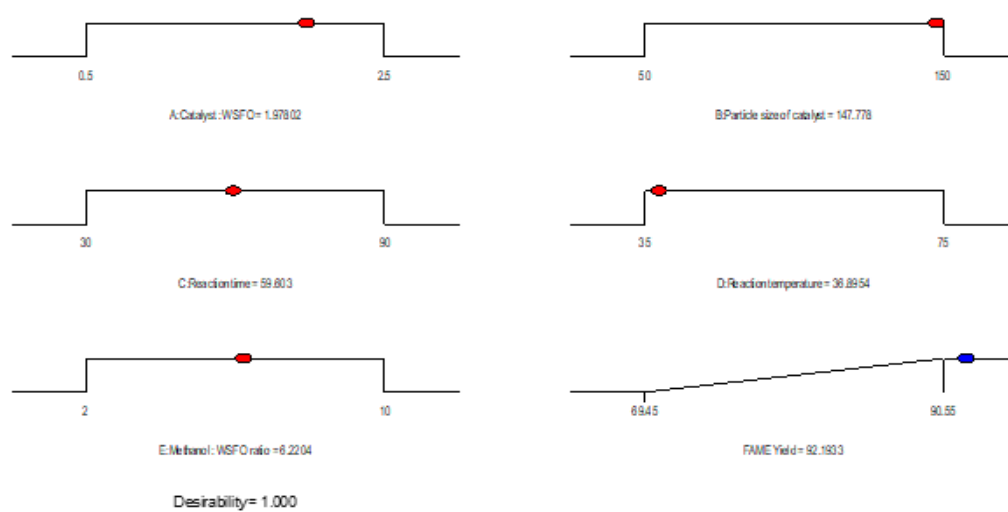
(a)
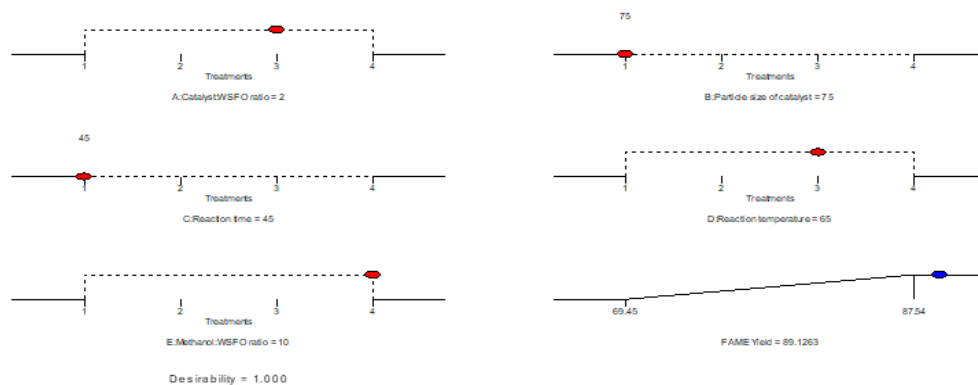
(b)

Figure 6. The optimal reaction condition through (a) RSM, (b) Taguchi method

101

Table 11. Comparison of Optimum conditions for RSM and Taguchi

Criteria	RSM	Taguchi
Catalyst:WSFO ratio (%w/w)	1.5:1	1:1
Reaction temperature (°C)	55	75
Reaction time (min)	60	45
Particle size of catalyst (μm)	50	45
Methanol:WSFO ratio	6:1	4:1
Predicted highest FAME yield (%)	91.07	61.16
Significant parameters	- Catalyst:WSFO ratio (%w/w) - Methanol:WSFO ratio - Reaction time (min) - Reaction temperature (°C) - Particle size of catalyst (μm)	- Reaction temperature (°C) - Catalyst:WSFO ratio (%w/w) - Methanol:WSFO ratio
Most significant parameter	Reaction time	Methanol:WSFO ratio
No of runs	32	16
R^2	0.8617	0.9085
R^2_{adj}	0.7743	0.7711
C V (%)	3.83	4.03

IV. CONCLUSION

In this study, the RSM and Taguchi orthogonal methods, both from Design Expert version 10, were adapted to model and optimize the transesterification of WSFO using WCE powder prepared through high temperature calcination. Using the statistical parameters of R^2, R^2_{adj}, CF, and CV, the outcome of RSM and Taguchi predictions were compared to establish which was the more accurate and cost effective method between the two. The following outcomes are worth highlighting:

i. The models generated by the RSM and Taguchi methods were significant and the model equations derived therefrom predicted FAME yield within acceptable error.

ii. The optimum FAME yield predicted by RSM was higher than that predicted by Taguchi, showing RSM to be a better optimization technique.

iii. RSM predicted FAME yield of 91.07 % with optimum operation condition of 1.5 %w/w catalyst:WSFO ratio, process time of 60 min, catalyst particle size of 50 μm, reaction temperature of 55 °C and methanol:WSFO ratio of 6:1. Taguchi, on the other hand, predicted a FAME yield of 61.16 % under optimum operating parameters of 1.1 %w/w catalyst to WSFO ratio, reaction time of 45 min, reaction temperature of 45 °C, 75 μm catalyst particle size and methanol:WSFO ratio of 4:1.

iv. The five tested parameters were discovered to be significant by the RSM model with reaction time (min) predicted as the most statistically significant parameter. Of the three parameters predicted to be significant by Taguchi method, methanol: WSFO ratio was the most significant since it had the highest F-value.

v. From the analysis of variance for FAME yield, both the R^2 and R^2_{adj} showed that the models were validated and consistent with the predicted value confirming the acceptability and adequacy of the models.

vi. Though RSM was found to be more accurate, the Taguchi method with 16 runs was observed to be more cost effective and less time consuming than RSM with 32 runs.

From the foregoing, it is safe to conclude that both the RSM and Taguchi methods are useful, efficient, and effective for the optimization of FAME yield in a transesterification process of waste sunflower oil. RSM is more reliable especially in handling more parameters with nonlinear relationship among the process parameters and response because it predicted higher yield and more value for money. However, Taguchi is more cost effective in the handling processes with a linear relationship between the parameters and the response.

REFERENCES

[1] REN21. Renewables 2018 Global Status Report. Available online: http://www.ren21.net/wp-content/uploads/2018/06/17-8652_GSR2018_FullReport_web_final_.pdf (accessed on 14 Feb. 2019).

[2] International, Energy, and Agency. Renewables 2018. Market Analysis and Forecast from 2018 to 2023. Available online: https://www.iea.org/renewables2018/ (accessed on14 Feb. 2019).

[3] Zhao, C.; Yang, L.; Xing, S.; Luo, W.; Wang, Z.; Lv, P. Biodiesel Production by a Highly Effective Renewable Catalyst from Pyrolytic Rice Husk. *J. Cleaner Prod.* **2018**, *199*, 772–780,. https://doi.org/10.1016/j.jclepro.2018.07.242

[4] Leng, L.; Han, P.; Yuan, X.; Li, J.; Zhou, W. Biodiesel Microemulsion Upgrading and Thermogravimetric Study of Bio-oil produced by Liquefaction of Different Sludges. *Energy* **2018**, *153*, 1061-1072, https://doi.org/10.1016/j.energy.2018.04.087.

[5] Abbaszaadeh, A.; Ghobadian, B.; Omidkhah, M.R.; Najafi, G. Current Biodiesel Production Technologies: A Comparative Review. *Energy Convers. Manage.* **2012**, *63*, 138-148, 2012/11/01/, https://doi.org/10.1016/j.enconman.2012.02.027

[6] Baskar, G.; Aiswarya, R.; Trends in Catalytic Production of Biodiesel from Various Feedstocks. *Renewable and Sustainable Energy Rev*. **2016**, *57*, 496-504. DOI: 10.1016/j.rser.2015.12.101

[7] Santana, H. S.; Tortola, D. S.; Reis, É. M.; Silva, J. L.; Taranto, O. P. Transesterification Reaction of Sunflower Oil and Ethanol for Biodiesel Synthesis in Microchannel Reactor: Experimental and Simulation Studies. *Chem. Eng. J*. **2016**, *302*, 752-762. https://doi.org/10.1016/j.cej.2016.05.122

[8] Tan, Y. H.; Abdullah, M. O.; Nolasco-Hipolito, C. The Potential of Waste Cooking Oil-Based Biodiesel using Heterogeneous Catalyst Derived from Various Calcined Eggshells Coupled with an Emulsification Technique: A Review on the Emission Reduction and Engine Performance. *Renewable and Sustainable Energy Rev.* **2015**, *47*, 589-603. https://doi.org/10.1016/j.rser.2015.03.048

[9]   Tan, Y. H.; Abdullah, M. O.; Nolasco-Hipolito, C.; Zauzi, N. S. A. Application of RSM and Taguchi Methods for Optimizing the of Waste Cooking Oil Catalyzed by Solid Ostrich and Chicken-Eggshell Derived CaO. *Renewable Energy* **2017**, *114*, 437-447. https://doi.org/10.1016/j.renene.2017.07.024

[10]   Sarve, A.; Sonawane, S. S.; Varma, M. N. Ultrasound Assisted Biodiesel Production from Sesame (Sesamum indicum L.) Oil using Barium Hydroxide as a Heterogeneous Catalyst: Comparative Assessment of Prediction Abilities between Response Surface Methodology (RSM) and Artificial Neural Network (ANN). *Ultrason. Sonochem.* **2015**, *26*, 218-228. https://doi.org/10.1016/j.ultsonch.2015.01.013

[11]   Mostafaei, M.; Javadikia, H.; Naderloo, L. Modeling the Effects of Ultrasound Power and Reactor Dimension on the Biodiesel Production Yield: Comparison of Prediction Abilities Between Response Surface Methodology (RSM) and Adaptive Neuro-Fuzzy Inference System (ANFIS). *Energy* **2016**, *115*, 626-636. https://doi.org/10.1016/j.energy.2016.09.028

[12]   Veljković, V. B.; Veličković, A. V.; Avramović, J. M. Stamenković, O. S. Modeling of Biodiesel Production: Performance Comparison of Box–Behnken, Face Central Composite and Full Factorial Design. *Chinese J. Chem. Eng*. **2018**. https://doi.org/10.1016/j.cjche.2018.08.002

[13]   Corral Bobadilla, M.; Fernández Martínez, R.; Lostado Lorza, R.; Somovilla Gómez, F.; Vergara González, E. Optimizing Biodiesel Production from Waste Cooking Oil Using Genetic Algorithm-Based Support Vector Machines. *Energies* **2018**, *11*, 2995. https://doi.org/10.3390/en11112995

[14]   Karmakar, B.; Dhawane, S. H.; Halder, G. Optimization of Biodiesel Production from Castor Oil by Taguchi Design. *J. Environ. Chem. Eng*. **2018**, *6*, 2684-2695.

[15]   Dhawane, S. H.; Karmakar, B.; Ghosh, S., Halder, G. Parametric Optimisation of Biodiesel Synthesis from Waste Cooking Oil via Taguchi Approach. *J. Environ. Chem. Eng*. **2018**, *6*, 3971-3980. https://doi.org/10.1016/j.jece.2018.05.053

[16]   Hassan S. Z.; Vinjamur, M. Parametric Effects on Kinetics of Esterification for Biodiesel Production: A Taguchi Approach. *Chem. Eng. Sci.* **2014**, *110*, 94-104.

[17]   Sharma, S. K. Use of Taguchi Method for Optimization of Biodiesel Production from Waste Cooking Oil. *Invertis J. Renewable Energy* **2018**, *8*, 59-63.

[18]   Patrick, M. J. A.; Whitcomb, J. *RSM Simplified: Optimizing Processes Using Response Surface Methods for Design of Experiments*. CRC Press: Boca Raton, FL, USA, 2004.

[19]   Sulaiman, N. F.; Bakar, W. A.; Toemen, S.; Kamal, N. M.; Nadarajan, R. In depth Investigation of Bi-Functional, Cu/Zn/γ-Al2O3 Catalyst in Biodiesel Production from Low-Grade Cooking Oil: Optimization using Response Surface Methodology. *Renewable Energy*, **2019**, *135*, 408-416. https://doi.org/10.1016/j.renene.2018.11.111

[20]   Nguyen, H.; Huong, D.; Juan, H.-Y.; Su, C.-H.; Chien, C.-C. Liquid Lipase-Catalyzed Esterification of Oleic Acid with Methanol for Biodiesel Production in the Presence of Superabsorbent Polymer: Optimization by using Response Surface Methodology. *Energies*, **2018**, *11*, 1085. https://doi.org/10.3390/en11051085

[21] Anwar, M.; Rasul, M. G.; Ashwath, N. Production Optimization and Quality Assessment of Papaya (Carica papaya) Biodiesel with Response Surface Methodology. *Energy Convers. Manage.* **2018**, *156*, 103-112. DOI: 10.1016/j.enconman.2017.11.004

[22] Najafi, B.; Faizollahzadeh Ardabili, S.; Shamshirband, S.; Chau, K.-w.; Rabczuk, T. Application of ANNs, ANFIS and RSM to Estimating and Optimizing the Parameters that affect the Yield and Cost of Biodiesel Production. *Eng. Appl. Comput. Fluid Mech.* **2018**, *12*, 611-624.

[23] Adewale, P.; Vithanage, L. N.; Christopher, L. Optimization of Enzyme-Catalyzed Biodiesel Production from Crude Tall Oil using Taguchi Method. *Energy Convers. Manage.* **2017**, *154*, 81-91. DOI: 10.1016/j.enconman.2017.10.045

[24] Na, J. W.; Lee, J.-C.; Kim, H.-W. Biodiesel Production from Waste Cooking Grease: Optimization and Comparative Productivity Assessment. *KSCE J. Civ. Eng.* **2019**, *23*, 1000. https://doi.org/10.1007/s12205-019-0827-2

[25] Aghbashlo, M.; Hosseinpour, S.; Tabatabaei, M.; Soufiyan, M. M. Multi-Objective Exergetic and Technical Optimization of a Piezoelectric Ultrasonic Reactor Applied to Synthesize Biodiesel from Waste Cooking Oil (WCO) using Soft Computing Techniques. *Fuel*, **2019**, 235, 100-112. https://doi.org/10.1016/j.fuel.2018.07.095

[26] Esonye, C.; Onukwuli, O. D.; Ofoefule, A. U. Optimization of Methyl Ester Production from Prunus Amygdalus Seed Oil Using Response Surface Methodology and Artificial Neural Networks. *Renewable Energy*, **2019**, *130*, 61-72. https://doi.org/10.1016/j.renene.2018.06.036

[27] Kurniasih E.; Pardi, P. Analysis of Process Variables on Biodiesel Transesterification Reaction using Taguchi Method. *IOP Conf. Ser.: Mater. Sci. Eng.* **2018**, 420, 012034. doi:10.1088/1757-899X/420/1/012034

[28] Skarlis, S.; Kondili, E.; Kaldellis, J. K. Small-Scale Biodiesel Production Economics: A Case Study Focus on Crete Island. *J. Cleaner Prod.* **2012**, *20*, 20-26. https://doi.org/10.1016/j.jclepro.2011.08.011

[29] Sun J. et al. Microalgae Biodiesel Production in China: A Preliminary Economic Analysis. *Renewable and Sustainable Energy Rev.* **2019**, *104*, 296-306. https://doi.org/10.1016/j.rser.2019.01.021

[30] Akalın, M. K.; Karagöz, S.; Akyüz, M. Supercritical Ethanol Extraction of Bio-Oils from German Beech Wood: Design of Experiments. *Ind. Crops Prod.* **2013**, *49*, 720-729. https://doi.org/10.1016/j.indcrop.2013.06.036

[31] Gebremariam S. N.; Marchetti, J. M. Economics of Biodiesel Production: Review. *Energy Convers. Manage*, **2018**, *168*, 74-84. https://doi.org/10.1016/j.enconman.2018.05.002

[32] Joshi, S.; Hadiya, P.; Shah, M.; Sircar, A. Techno-Economical and Experimental Analysis of Biodiesel Production from Used Cooking Oil. *BioPhysical Economics Resource Quality*, **2019**, *4*, 2. DOI: 10.1007/s41247-018-0050-7

[33] Awogbemi, O.; Inambao, F. L.; Onuh, E. I. Development and Characterization of Chicken Eggshell waste as Potential Catalyst for Biodiesel Production. International Journal of Mechanical Engineering and Technology, **2018**, *9*, 1329-1346.

[34] Bu, X.; Xie, G.; Peng, Y.; Chen, Y. Kinetic Modeling and Optimization of Flotation Process in a Cyclonic Microbubble Flotation Column using Composite Central Design Methodology. *Int. J. Miner. Process*. **2016**, *157*, 175-183. https://doi.org/10.1016/j.minpro.2016.11.006

[35] Kumar, R. S.; Sureshkumar, K.; Velraj, R. Optimization of Biodiesel Production from Manilkara zapota (L.) Seed Oil using Taguchi Method. *Fuel*, **2015**, *140*, 90-96. https://doi.org/10.1016/j.fuel.2014.09.103

[36] Singh T. S.; Verma, T. N. Taguchi Design Approach for Extraction of Methyl Ester from Waste Cooking Oil using Synthesized CaO as Heterogeneous Catalyst: Response Surface Methodology Optimization. *Energy Convers. Manage*, **2019**, *182*, 383-397. https://doi.org/10.1016/j.enconman.2018.12.077

[37] Dhawane, S. H.; Kumar, T.; Halder, G. Biodiesel Synthesis from Hevea brasiliensis Oil Employing Carbon Supported Heterogeneous Catalyst: Optimization by Taguchi Method. *Renewable Energy* **2016**, *89*, 506-514, https://doi.org/10.1016/j.renene.2015.12.027

[38] Veličković, A. V.; Stamenković, O. S.; Todorović, Z. B.; Veljković, V. B. Application of the Full Factorial Design to Optimization of Base-Catalyzed Sunflower Oil Ethanolysis. *Fuel* **2013**, *104*, 433-442. https://doi.org/10.1016/j.fuel.2012.08.015

[39] Betiku E.; Ajala, S. O. Modeling and Optimization of Thevetia peruviana (yellow oleander) Oil Biodiesel Synthesis via Musa paradisiacal (plantain) Peels as Heterogeneous Base Catalyst: A Case of Artificial Neural Network vs. Response Surface Methodology. *Ind. Crops Prod.* **2014**, *53*, 314-322. https://doi.org/10.1016/j.indcrop.2013.12.046

[40] Pandit P. R.; Fulekar, M. H. Egg Shell Waste as Heterogeneous Nanocatalyst for Biodiesel Production: Optimized by Response Surface Methodology. *J. Environ. Manage*. **2017**, *198*, 319-329. https://doi.org/10.1016/j.jenvman.2017.04.100

[41] Namwong, S.; Punsuvon, V.; Arirop, W. Process Optimization of Ethyl Ester Biodiesel Production from Used Vegetable Oil under Sodium Methoxide Catalyst and its Purification by Ion Exchange Resin. *Applied Mech Materials*, **2017**, *873*, 89-94. https://doi.org/10.4028/www.scientific.net/AMM.873.89

[42] Betiku, E.; Akintunde, A. M.; Ojumu, T. V. Banana Peels as A Biobase Catalyst for Fatty Acid Methyl Esters Production Using Napoleon's plume (Bauhinia monandra) Seed Oil: A Process Parameters Optimization Study. *Energy*, **2016**, 103, 797-806. https://doi.org/10.1016/j.energy.2016.02.138

[43] Olutoye, M. A.; Lee, S. C.; Hameed, B. H. Synthesis of Fatty Acid Methyl Ester from Palm Oil (Elaeis Guineensis) with Ky(MgCa)2xO3 as Heterogeneous Catalyst. *Bioresour. Technol*. **2011**, *102*, 10777-10783. DOI: 10.1016/j.biortech.2011.09.033

[44] Kılıç, M.; Uzun, B. B.; Pütün, E.; Pütün, A. E. Optimization of Biodiesel Production from Castor Oil Using Factorial Design. *Fuel Process. Technol,* **2013**, *111*, 105-110. https://doi.org/10.1016/j.fuproc.2012.05.032

[45] Sirisomboonchai S. et al. Biodiesel Production from Waste Cooking Oil Using Calcined Scallop Shell as Catalyst. *Energy Convers. Manage* **2015**, *95*, 242-247, https://doi.org/10.1016/j.enconman.2015.02.044

[46] Gupta A. R.; Rathod, V. K. Waste Cooking Oil and Waste Chicken Eggshells Derived Solid Base Catalyst for The Biodiesel Production: Optimization and Kinetics. *Waste Manage.* **2018**, *79*, 169-178, 2018/09/01/ 2018. https://doi.org/10.1016/j.wasman.2018.07.022

[47] Pradhan, S.; Madankar, C.; Mohanty, P.; Naik, S. Optimization of Reactive Extraction of Castor Seed to Produce Biodiesel Using Response Surface Methodology. *Fuel*, **2010**, *97*, 848-855. https://doi.org/10.1016/j.fuel.2012.02.052

[48] Tshizanga, N.; Aransiola, E. F.; Oyekola, O. Optimisation of Biodiesel Production from Waste Vegetable Oil and Eggshell Ash. *S. Afr. J. Chem. Eng*, **2017**, *23*, 145-156. https://doi.org/10.1016/j.sajce.2017.05.003

[49] Maneerung, T.; Kawi, S.; Dai, Y.; Wang, C.-H. Sustainable Biodiesel Production via Transesterification of Waste Cooking Oil by using Cao Catalysts Prepared from Chicken Manure. *Energy Convers. Manage* **2016**, *123*, 487-497. https://doi.org/10.1016/j.enconman.2016.06.071

[50] Bokhari, A.; Chuah, L. F.; Yusup, S.; Klemeš, J. J.; Kamil, R. N. M. Optimisation on Pretreatment of Rubber Seed (Hevea brasiliensis) Oil via Esterification Reaction in a Hydrodynamic Cavitation Reactor. *Bioresour. Technol*. **2016**, *199*, 414-422. https://doi.org/10.1016/j.biortech.2015.08.013

[51] Jazie, A.; Pramanik, H.; Sinha, A.; Jazie, A. Egg Shell as Eco-Friendly Catalyst for Transesterification of Rapeseed Oil: Optimization for Biodiesel Production. *Int. J. Sustainable Dev. Green Econ.* **2013**, *2*, 27-32.

[52] Varatharajulu, M.; Jayaprakash, G.; Baskar, N.; Kumar, B. S. Comparison of Response Surface Methodology and Taguchi Analysis for Determining Appropriate Drilling Parameters of Duplex 2205. *Asian J. Res. Soc. Sci. and Human.* **2017**, *7*, 1237-1251.

[53] Dhawane, S. H.; Kumar, T.; Halder, G. Central Composite Design Approach Towards Optimization of Flamboyant Pods Derived Steam Activated Carbon for its use as Heterogeneous Catalyst in Transesterification of Hevea brasiliensis oil. *Energy Convers. Manage.* **2015**, *100*, 277-287. https://doi.org/10.1016/j.enconman.2015.04.083

CHAPTER 3 ARTICLE 3: Application of Multiple Linear Regression for the Prediction of Some Properties of Biodiesel Using Fatty Acid Compositions

---

Application of Multiple Linear Regression for the Prediction of some properties of Biodiesel using Fatty Acid Compositions

Awogbemi Omojola*, Inambao Freddie and Onuh Emmanuel Idoko

Green Energy Solutions Research Group, Discipline of Mechanical Engineering,

Howard College, University of KwaZulu-Natal, Durban 4041, South Africa

*Corresponding author E-mail: jolawogbemi2015@gmail.com

Abstract: The quest for renewable, cost-effective, environmentally friendly and sustainable alternative fuels to run compression ignition (CI) engines has escalated the tempo of research in biodiesel over the last decades. Investigations targeted towards improving combustion, engine performance, and emission characteristics of CI engines fuelled with fatty acid methyl ester (FAME) have increased substantially in recent years. Properties of biodiesel are key parameters in the engine performance, emission characteristics, and its suitability as CI engine fuel, which are influenced by its fatty acid (FA) compositions. In order to overcome the complexities in the real-time experimental determination of biodiesel properties, prediction techniques have been used. This current effort explores multiple linear regression (MLR) to formulate linear correlations for the prediction of the density, cetane number (CN), calorific value (CV), and kinematic viscosity (KV) of biodiesel using five commonest FAs (palmitic, stearic, oleic, linoleic and linolenic). Input data were sourced from literature to formulate linear relations for these interesting FAME fingerprints and the outcome subjected to statistical analysis. The predictive capabilities of the models were verified using other experimental data mined from various sources. The outcomes of the analysis show that the adjusted R square and maximum absolute errors are 83 % and 0.35 % for density, 84.3 % and 1.72 % for CN, 43 % and 0.98 % for CV, and 68.3 %, and 4.33 % for KV. It is evident that linear correlations established from five FAs are highly successful in predicting density, CN, CV and KV of biodiesel from a wide range of feedstocks

Keywords: FAME, fatty acid compositions, linear correlations, property prediction

1. INTRODUCTION

As a result of the global population explosion, rapidly expanding urbanization, industrial revolution and economic development, global energy demand and consumption has continued to increase, with a huge chunk of the energy sourced from nonrenewable sources. Fossil fuel contributed 86.9 %, 82.67 % and 85 % to the global energy consumption in 2010, 2013, and 2016 respectively. Similarly, in 2013, crude oil and coal contributed 30.92 % and 28.95 % to global energy consumption while the figure became 33 % for crude oil and 28 % for coal in 2016 [1]. Over the past 15 years, oil has contributed a third of the global energy consumption, closely followed by coal and natural gas, in that order [2]. Products of refining of fossil fuels are used to power internal combustion engines, particularly compression ignition (CI) engines, have found invaluable usefulness in our daily life and continue to contribute significantly to industrial growth, economic and commercial growth, agricultural sector development, social and household needs,

as well as transportation of goods and services. Generally, global primary energy consumption has continued to increase and has projected to continue to increase (Figure 1) [3].
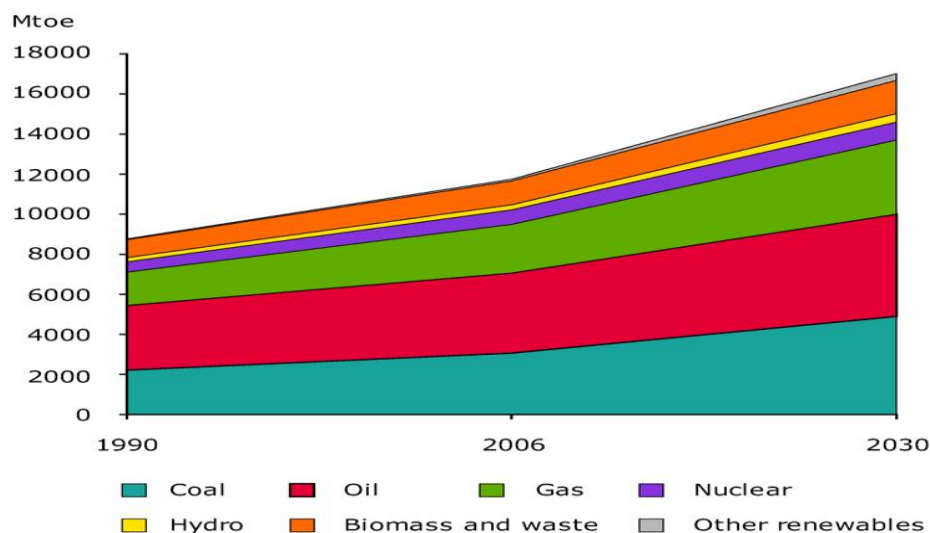
Figure 1. Global Total Primary Energy Consumption by fuel

Transport sector consumes about 28 % of total global energy and contributes 24 % of global carbon dioxide (CO_2) emissions in the year 2016 [4]. According to the United States Environmental Protection Agency [5], transport vehicles contributed 71 % of total greenhouse gas emissions globally in 2010. The panacea to this disturbing trend is to develop cleaner and affordable alternative fuels to reduce dependence on fossil fuels, guarantee amicable coexistence of human and environment and ensure sustainable economic growth. Reducing the use of fossil-based fuel will ensure that air quality, particularly around high-density traffic residential areas, is maintained within the World Health Organization standards to safeguard human health and maintain environmental clemency [6].

Biodiesel, a renewable fuel, comprised of mono-alkyl/methyl esters of long chain fatty acids obtained from various feedstocks including neat vegetable oils, used vegetable oils, microalgae, animal fats, etc. Biodiesel, also known as fatty acid methyl ester (FAME), are generated by various techniques, including, pyrolysis, dilution or blending of oils, micro-emulsification and transesterification and are dried to ensure compliance with standards. Internationally acceptable specifications for FAME are well documented in the American Standard for Testing and Materials (ASTM) and European Union (EN) documents, like ASTM D6751 and EN 14214 respectively. Different countries set up their own standards from these two standards as it relates to their peculiar geographical locations and in line with international protocols [7-9]. According to the United States Energy Information Administration, global biodiesel generation grew from 25.46 thousand barrels per day (mbpd) in 2002 to 123.9 mbpd in 2006 and further to 432.9 mbpd in 2012. Consumption was reported to be 22.26, 118.1, and 419.9 mbpd in 2002, 2006 and 2012 respectively and still increasing [10]. Replacement of petroleum-based diesel (PBD) fuel with biodiesel offers technical, economic, sanitation, and economic benefits, notably simpler refining process, cheaper feedstock, veritable means of waste disposal, better engine performance and

reduction in the emission of GHGs and other hazardous gases. FAME is considered to be the most widely used liquid renewable fuel in Europe, accounting for about 80 % of biofuel market share, owing to its non-toxicity, biodegradability, and renewability [11].

There is a near consensus among fuel refiners, and engine researchers on the importance of fuel properties in determining fuel quality, fuel mixing, ease of ignition, fuel combustion, and other activities in the combustion chambers. Properties like oxygen content, density, cetane number (CN), kinematic viscosity (KV), flash point (FP), cold filter plugging point (CFPP), cloud point (CP), heating values (HHV), pour point (PP) have been highlighted to influence fuel quality, handling, safety, transportation, combustion, engine performance and emission characteristics [12, 13]. Fatty acid (FA) compositions of FAME have been an important factor in the determination of its fingerprint properties, quality, storage capacity, engine performance, and emission characteristics. Put modestly, FA composition determines the properties of FAME.

Experimental, numerical, simulation and statistical investigations have been used to exploit the nexus between FA composition of biodiesel and some of its properties to predict these important properties. Specifically, cold flow properties, KV, CN, and other biodiesel fingerprint are significantly influenced by fatty acid composition, branching, chain length, number and position of double bonds. Samavi et al. [14] predicted the KV and FP of FAME as a function of its FA composition and verified the outcome with experimental data. Giakoumis and Sarakatsanis [15] estimated the CN, KV, and density of biodiesel from its FA compositions. The outcomes of the predictions were compared with experimental value given rise to the low value of relative error. Multiple Linear regression (MLR) analysis have been employed to develop compositional-based models to predict biodiesel properties from various feedstocks with considerable accuracy because the derived correlations possess sound theoretical basis [16-19]. Statistical investigations were successfully carried out to predict the density, CN, KV, FP, CFPP, CP and PP of FAME based on the degree of saturation and FA composition [19]. MLR, Artificial neural network (ANN), and other machine learning techniques were used to forecast the properties of FAME based on their FA compositions. The outcome of the investigations shows that these techniques are able to predict some important properties of the FAME samples [18, 20-22].

In determining the most occurring FAs in biodiesel, FA composition of 123 samples of biodiesel were studied from various literature and were found to comprise of 13 methyl esters, namely: palmitic acid (C16:0), stearic (C18:0), oleic acid (C18:1), linoleic acid (C18:2), linolenic acid (C18:3), arachidic acid (C20:0), palmitoleic acid (C16:1), lauric acid (C12:0), myristic acid (C14:0), eicosenic acid (C20:1), behenic acid (C22:0), erucic acid (C22:1), and lignoceric acid (C24:0). Available information shows that C16:0, C18:0, C18:1, C18:2, and C18:3 are the most common FAs in the biodiesels [20, 23-25].

With the increased visibility of compositional-based models for the prediction of major FAME properties, the relevant questions begging for informed answers and which serve as the motivation for this effort is whether biodiesel properties can be accurately predicted using linear correlations developed from five methyl esters. The aim of this investigation, therefore, is to use multiple linear regression techniques to formulate predictive correlations based on five methyl esters to predict density, CN, and KV. The predictive capability of MLR derived-correlations for

fingerprint prediction using compositional-based models using five methyl esters as inputs will be tested and verified from data mined from literature. This current effort will be limited to the application of MLR to predict the density, CN, and KV of unblended FAME derived from various feedstocks using C16:0, C18:0, C18:1, C18:2, and C18:3.

2. MATERIALS AND METHOD

Inputs for the formulation of a reliable correlation for the prediction of biodiesel properties based on weight composition of five methyl esters requires a large and widely spread experimental data reported in the literature for the correlations to have a broad-based effect, irrespective of the type of feedstock, location, production technique, and purification methods [15, 26, 27]. The chosen five fatty acids have been found to occur in most of the GCMS analysis of biodiesels, cutting across saturated, monounsaturated, and polyunsaturated fatty acids. The general equation adopted for the MLR analysis is given by Equation 1. The predicted data for each property are plotted against the experimental data to appraise the predictive capability of the model using statistical indices. The correlations are used to predict the outcome of another set of data from the literature, different from the data used to formulate the correlation and the absolute errors calculated.

$$y = A + a_1X_1 + a_2X_2 + a_3X_3 + a_4X_4 + a_5X_5 \qquad \text{(Equation 1)}$$

Where:

− $\quad$ y = the dependent variable to be predicted

− $\quad$ A = the intercept

− $\quad$ a_1 to a_5 = the coefficients of each independent variable

− $\quad$ X_1 to X_5 = the percentage composition of each FA in the sample

For this analysis, 1 to 5 represent C16:0, C18:0, C18:1, C18:2, and C18:3 respectively which represent the independent variables.

3. RESULTS AND DISCUSSIONS

3.1 Density

The density of a material, measured in kg/m^3, is expressed as the mass per unit volume of the material. The quantity of fuel admitted into the combustion chamber is influenced by the density of the fuel, an indication that density has a direct impact on the fuel injection process, combustion, engine performance, and emission characteristics of FAME. Density also has strong correlations with KV, CN, and heating value affect the air-fuel ratio and energy content of fuel injected into the engine, degree of saturation, number of double bonds, molecular weight, and chain length [28, 29].

The data for the generation of the model were sourced from various literature [15, 27, 30]. The MLR model equation is as represented by Equation 2 while table 1 shows the independent variables, the experimental dependent variables, and the predicted density. The predicted data is generated by the linear correlations among the FA compositions.

$$Density = 914 - 0.52X_1 - 0.54X_2 - 0.34X_3 - 0.25X_4 - 0.14X_5 \qquad \text{(Equation 2)}$$

The intercept value of 914 achieved by this effort is comparably higher than 869 reported by Giakoumis [19] but lower than the 923 established by Giakoumis and Sarakatsanis [15] for comparable investigations. The statistical indices show that the R-value is 0.927 while the R2 of 0.859 shows that the predicted dependent variable can be attributed to 85.9 % of the independent variables in 30 observations (table 2). A standard error of 1.9 is suggestive of a satisfactory correlation between the model equation and the experimental data, confirming the capability of the model equation to adequately predict the dependent variable.

The model was tested on a new set of experimental values, different from those used in table 1, in order to ascertain the predictive reliability of the model using equation 2. As shown in table 3, a negligible error was established, with a maximum of 0.35 %. The predictive capability of the model is shown by plotting the experimental data with the predicted data (Figure 2). The predictive capability of this model gave a higher R2-value than the outcome of a similar prediction by Pratas et al. [31].

Table 1: Data for Density prediction

S/N	Source	C16:0	C18:0	C18:1	C18:2	C18:3	Exp. Density	Pred. Density
1	Beef tallow	24.39	19.08	41.65	5.91	0.72	874.3	875
2	Canola	4.51	2	60.33	21.24	9.49	881.6	883.3
3	Chicken fat	24.06	6.42	41.43	18.83	1.06	876.3	878.9
4	Corn	11.81	2.13	27.35	57.74	0.63	882.2	882.8
5	Cottonseed	25.93	1.74	15.98	55.12	0.16	879	880.2
6	Croton	7.25	3.43	10.8	77.25	5.4	883.2	884.6
7	Hazenut	6.36	3.71	79.17	10.67	0.15	877.9	879
8	Jatropha	14.42	5.82	42.81	35.38	0.23	878.7	879.8
9	Karanja	10.89	7.89	53.56	21.34	2.09	882.9	880.1
10	Linseed	5.18	3.26	19.04	16.12	54.54	891.5	891.1
11	Mahua	22.23	22.49	39.01	14.87	0.1	874.5	873
12	Neem	17.57	16.6	45.83	17.79	0.72	876.2	875.5
13	Olive	11.47	2.83	74.52	9.54	0.51	881.2	878.6
14	Palm	42.39	4.2	40.91	9.7	0.29	874.7	873.1
15	Peanut	10.33	2.79	47.63	31.52	0.64	882.9	882.8
16	Rapeseed	4.07	1.55	62.24	20.61	8.72	882.2	883.4
17	Rice barn	18.12	2.17	42.35	34.84	0.93	880.9	880
18	Rubber seed	9.39	9.41	24.22	38.12	17.54	882.3	883.6
19	Safflower	7.42	2.38	14.41	75.31	0.09	883.8	885.1
20	Soybean	11.44	4.14	23.47	53.46	6.64	882.8	883.4
21	Sunflower	6.26	3.93	20.77	67.75	0.15	882.9	884.5
22	Soybean	15.69	6.14	42.84	29.36	2.03	880.6	880.2
23	Sunflower	25.1	13.23	44.36	12.06	1.18	873	875.3
24	Karanja	10.74	6.8	50.24	17.21	3.47	880.5	882.7
25	Karanja	8.38	5.32	40.54	14.91	2.84	890.6	888.7
26	Ibicella lutea	9.1	2.33	52.36	35.88	0.33	882.4	881.1
27	Onopordum nervosum	9.08	2.57	27.02	60.34	10.23	885.4	882.1
28	Peganum harmala	4.02	2.57	26.93	53.62	2.44	890.1	887.5
29	Smymium olusatrum	5.26	1.07	74.14	14.1	0.48	880.3	881.8
30	Solanum elaeagnifolium	9.86	4.24	20.92	63.32	1.07	885.9	883.4

Table 2: Statistical indices of the MLR model for density

Regression Statistics	
Multiple R	0.927
R^2	0.859
Adjusted R^2	0.83
Standard Error	1.9
Observations	30

Table 3: Density model verification

Biodiesel	Ref	Exp. value	Pred. value	Error (%)
RME	[32]	882	882.81	0.09
SFME	[32]	885	884.82	0.02
SME	[32]	886	883.4	0.29
CSME	[32]	882	879.06	0.33
HME	[33]	874.07	877.11	0.35
PBME	[34]	869.5	867.96	0.18
JBME	[34]	880.3	879.19	0.13
ALBME	[34]	875.7	877.04	0.15
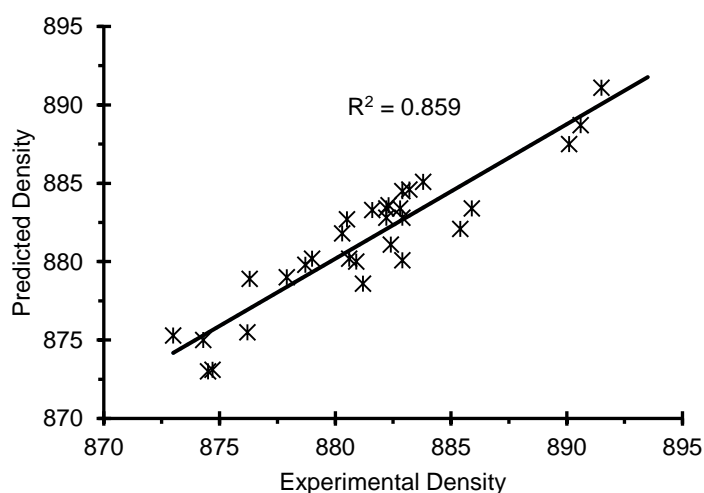
Figure 2. The predictive capability of the density model

3.2 Cetane Number

Cetane number (CN) is a dimensionless parameter and one of the most important properties of fuel that relates to its self-ignitability and ignition delay characteristics in CI engines. FAME structure, FA composition, number and position of double bonds, chain length, degree of saturation/unsaturation, boiling point, the heat of vaporization, the heat of combustion, etc have been reported to substantially affect CN. Engine combustion noise level, vibration, heat release rate, engine performance and generation of pollutants are influenced by the CN of FAME. Higher CN is believed to be a precursor for less ignition delay time, lower combustion noise, higher power, as well as less emission of soot, NOx, CO, and SO2 [35, 36].

Bamigboye and Hansen [16], Tong et. al. [37], Ramadhas et al.[38], Gerhard Knothe [39] and Piloto-Rodríguez et al. [18] among other researchers have estimated CN using a percentage of FA compositions as inputs by MLR/ANN or both but with a higher number of methyl esters (> 5 methyl esters). This present effort is limited to the use of the five most common FAs as input.

The general linear regression equation (equation 1) is transformed into Equation 3 through MLR for the prediction of the CN. The intercept value of 61.84 is comparable with values of 61.1 predicted by Bamigboye and Hansen [16], and 62.2 predicted by Gopinath et al. [17].

$$\text{Cetane number} = 61.84 + 0.07X_1 + 0.01X_2 - 0.05X_3 - 0.22X_4 - 0.51X_5 \qquad \text{(Equation 3)}$$

Table 4 shows the FA and cetane number measured from experimental data sourced from literature [19, 37] and the dependent output predicted by the model. A total of 30 input data was used to generate the model. The source of the data covers a wide range of feedstock type to ensure the model has a wide range of applications in view of the variability of CN with feedstock type. Table 6 illustrates the statistical indices of the model. The developed model was found to be significant and competent to adequately predict the dependent variable. The R-value of 0.918 and R2 value of 0.843 indicating that 84.3 % of the independent variable determined the outcome of the model. A standard error of 2.55 displays a good statistical correlation between the model equation and the experimental data.

Table 4. Measured and predicted data for Cetane number

S/N	Source	C16:0	C18:0	C18:1	C18:2	C18:3	Exp. CN	Pred. CN
1	Aphanamixis polystachya Park	23.1	12.8	21.5	29	13.6	48.52	49.5
2	Azadirachta indica	14.9	14.4	61.9	7.5	0	57.83	58.68
3	Moringa oleifera Lam	9.1	2.7	79.4	0.7	0.2	56.66	58.67
4	Mesua ferrea Linn	10.8	12.4	60	15	0	55.1	56.8
5	Corylus avellana	3.1	2.6	88	2.9	0	54.5	57.44
6	Basella rubra Linn	19.7	6.5	50.3	21.6	1.1	54	55.83
7	Ervatamia coronaria Stapf	24.4	7.2	50.5	15.8	0.6	56.33	57.7
8	Aleurites moluccana wild	5.5	6.7	10.5	48.5	28.5	34.18	36.75
9	vallaria solanacea Kuntzc	7.2	14.4	35.3	40.4	0	50.26	52.15
10	Holoptelia integrifolia	35.1	4.5	53.3	0	0	61.22	62.08
11	Mappia foetida Milers	7.1	17.7	38.4	36.8	0	50.7	52.83
12	Swietenia mahagoni Jacq	9.5	18.4	56	0	16.1	52.26	52.02
13	madhuca indicai JF Gmel	17.8	14	46.3	17.9	0	56.61	57.34
14	Anamirta cocculus Wight & Hrn	6.1	47.5	46.4	0	0	64.26	60.8
15	Broussanetia papyrifera Vent	4	6.1	14.8	71	1	41.25	45.56
16	Beef tallow	24.39	19.02	41.65	5.91	0.72	60.9	60.35
17	Canola	4.51	2	60.33	21.24	9.49	54.8	49.97
18	Chicken fat	24.06	6.42	41.43	18.83	1.06	57	57.18
19	Coconut	9.69	0	2.83	6.83	0	61	60.95
20	Corn	11.81	2.13	27.35	57.74	0.63	52.5	48.6
21	Cottonseed	25.93	1.74	15.98	55.12	0.16	53.3	50.98
22	Hazelnut	6.32	3.71	79.17	10.67	0.15	53.8	56.33
23	Jatropha	14.42	5.82	42.81	35.38	0.23	55.7	53.21
24	Karanja	10.89	7.89	53.56	21.34	2.09	55.4	54.59

25	Mahua	22.23	22.49	39.01	14.87	0.1	56.9	58.72
26	Olive	11.47	2.83	74.52	9.54	0.51	58.9	56.98
27	Palm	42.39	4.2	40.91	9.7	0.29	61.2	60.93
28	Peanut	10.33	2.79	47.63	31.52	0.64	54.9	53.27
29	Rapeseed	4.07	1.55	62.24	20.61	8.72	54.1	50.38
30	Waste cooking	15.69	6.14	42.84	29.36	2.03	56.2	53.7

The model was tested to predict the CN of other reported experimental data available in the literature, apart from those used in table 4, as a way to verify the predictive capability of the model. As shown in table 6, the highest error obtained was 1.72 % which can be adjudged a good result considering the wide variability of the feedstock. Figure 3 shows the plot of experimental data against predicted data to show the predictive capability of the model.

Table 5: Statistical indices of the MLR model for Cetane number

Regression Statistics	
Multiple R	0.918
R Square	0.843
Adjusted R Square	0.81
Standard Error	2.55
Observations	30

Table 6. Cetane number model verification

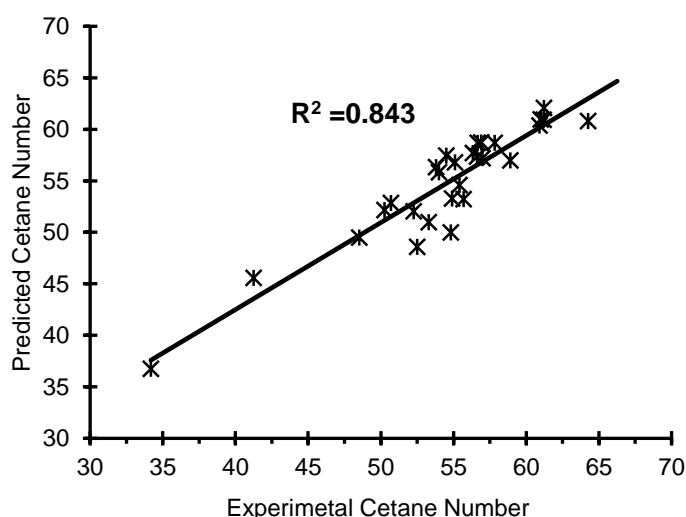| Source	Ref.	Exp. value	Pred. value	Error (%)
HME	[33]	55.66	55.79	0.23
JBME	[34]	53.50	53.67	0.32
ALBME	[34]	55.50	55.11	0.72
Madhuca butyracea Mac	[37]	65.27	64.46	1.26
Basella rubra Linn	[37]	56.33	56.99	1.15
Ervatamia coronaria Stapf	[37]	56.33	57.31	1.72

Figure 3. The predictive capability of the cetane number model

3.3 Kinematic viscosity

Kinematic Viscosity (KV) is a degree of the resistance of fluid flow as a result of the internal friction of a layer of fluid flowing over another layer and has been found to affect fuel injection, fuel atomization, among other critical fuel behavior properties. The high value of KV predisposes the fuel into large droplet size, enhanced polymerization reaction, more carbon deposits, poorer vaporization, small injection spray angle, and better in-cylinder penetration of the fuel spray. Increased KV often leads to weaker fuel combustion, higher oil dilution, and increased emission of smoke and other pollutants. KV is closely related to density, specific gravity, degree of unsaturation, location of double bonds, and molecular weight [40, 41]. At low temperatures, fuels with high KV pose critical challenges while too low KV can cause insufficient lubrication in fuel pumps, increased leakage and wear [42].

The model correlation is as shown in Equation 4 is arrived at from the general format stated in Equation 1. The model is significant and sufficient to predict the dependent variable within an acceptable standard. Table 7 depicts the FA composition, the experimentally measured KV sourced from literature, and the MLR predicted data. With the R2 of 0.683, 68.3 % of the independent variable contributed to the prediction of the dependent variable. The R-value of 0.83 and standard error of 0.33, though with five methyl esters, is comparable to the outcome of similar research by Giakoumis and Sarakatsanis [15] with eight methyl esters.

$$\text{Kinematic Viscosity} = 1.22 + 0.03X_1 + 0.07X_2 + 0.04X_3 + 0.03X_4 + 0.02X_5 \quad \text{(Equation 4)}$$

Compared with the capability of MLR to predict CN, the model was not as accurate as of that of CN but was significant enough to predict the dependent variable within reasonable error. The predictive capability of the model was tested with experimental data, apart from the data used in table 7 and the outcome of the verification of the predictive capability model is shown in table 9. The model verification presented a maximum error of 4.33 %. Though this current presented higher error figures compared with absolute error for density and CN in the preceding sections, it is however lower than similar results available in the literature.

Table 7. Experimental and predicted data for kinematic viscosity

S/N	Source	C16:0	C18:0	C18:1	C18:2	C18:3	Exp. KV	Pred. KV
1	Beef tallow	24.39	19.08	41.65	5.91	0.72	4.83	4.96
2	Canola	4.51	2	60.33	21.24	9.49	4.4	4.48
3	Chicken fat	24.06	6.42	41.43	18.83	1.06	4.81	4.44
4	Corn	11.81	2.13	27.35	57.74	0.63	4.32	4.26
5	Cottonseed	25.93	1.74	15.98	55.12	0.16	4.7	4.19
6	Croton	7.25	3.43	10.8	77.25	5.4	4.48	4.23
7	Hazenut	6.36	3.71	79.17	10.67	0.15	4.55	4.84
8	Jatropha	14.42	5.82	42.81	35.38	0.23	4.72	4.56
9	Karanja	10.89	7.89	53.56	21.34	2.09	5.04	4.65
10	Linseed	5.18	3.26	19.04	16.12	54.54	4.06	4.06
11	mahua	22.23	22.49	39.01	14.87	0.1	5.06	5.25
12	Neem	17.57	16.6	45.83	17.79	0.72	4.72	5.05
13	Olive	11.47	2.83	74.52	9.54	0.51	5.05	4.75
14	Palm	42.39	4.2	40.91	9.7	0.29	4.61	4.60
15	Peanut	10.33	2.79	47.63	31.52	0.64	4.77	4.31
16	Rapeseed	4.07	1.55	62.24	20.61	8.72	4.63	4.47
17	Rice barn	18.12	2.17	42.35	34.84	0.93	4.7	4.42
18	Rubber seed	9.39	9.41	24.22	38.12	17.54	4.79	4.46

19	Safflower	7.42	2.38	14.41	75.31	0.09	4.1	4.11
20	Soybean	11.44	4.14	23.47	53.46	6.64	4.29	4.28
21	Sunflower	6.26	3.93	20.77	67.75	0.15	4.53	4.22
22	RME	3.57	0.87	65.18	22.27	8.11	4.556	4.55
23	SMEA	10.49	4.27	24.2	51.36	7.48	3.67	4.25
24	SMEB	10.81	4.54	24.96	50.66	7.27	4.41	4.28
25	GMSME	3.97	2.99	82.54	4.98	3.7	4.87	4.77
26	YGME	17.44	12.38	54.67	7.96	0.69	5.02	4.82
27	GP	10.57	2.66	41.05	36.67	7.1	3.96	4.36
28	PBME	38.1	4.1	44.2	11	0.3	4.56	4.61
29	JBME	17.1	6.4	41.8	32.9	0.2	4.27	4.58
30	Coconut	13.83	3.94	14.3	4.73	0	2.45	2.52
31	Cottonseed	24.09	2.56	15.74	56.99	0	3.99	4.22
32	ALBME	14.8	16	41.3	26.6	0.2	5.38	4.97
33	Soy A	16.18	3.82	28.2	50.46	0	3.74	4.34
34	Rapeseed	5.26	1.63	62.94	20.94	6.99	3.942	4.51
35	Soy B	10.18	3.82	28.5	35.46	0	3.96	4.34

Table 8: Statistical indices of the MLR model for kinematic viscosity

Regression Statistics	
Multiple R	0.83
R Square	0.683
Adjusted R Square	0.629
Standard Error	0.33
Observations	35

Table 9. Kinematic viscosity model verification

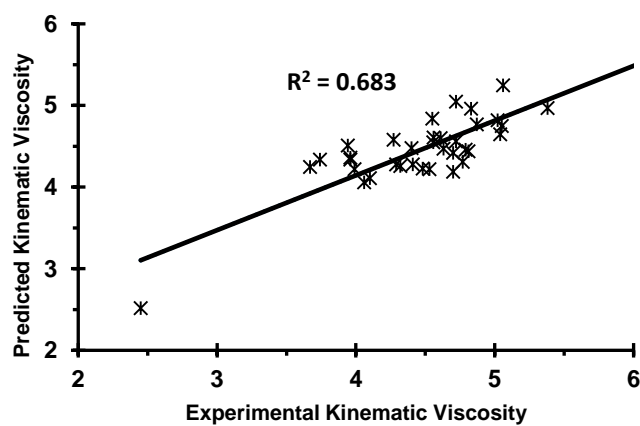| Source	Ref.	Exp. value	Pred. value	Error (%)
Rapeseed	[43]	4.67	4.84	3.57
POME	[44]	4.61	4.79	3.72
Soybean	[45]	4.04	4.2	3.86
Sunflower	[45]	4.55	4.61	1.24
Jatropa curcas	[45]	4.46	4.28	4.33

Figure 4. The predictive capability of the Kinematic viscosity model

3.4 Calorific Value

The calorific value (CV) of a fuel is a measure or degree of its heating capacity. A CV is measured in kilojoule per kg (kJ/kg) and is commonly defined as the quantity of energy generated by the

complete combustion of a known volume of fuel under stipulated conditions. The gross calorific value, also known as higher heating value (HHV) is measured of the fuel's heat of combustion when the water's heat of combustion is completely condensed and the heat contained in the water vapor is fully retrieved [46]. The net calorific value, also known as the lower heating value (LHV) is measured when the product of the fuel's combustion includes water vapor and the heat in the water vapor is not retrieved. The difference between the HHV and LHV is termed the heat of vaporization of water. FAME is reputed to contain higher oxygen content than petroleum-based diesel fuel (PBDF), it follows that FAME has lower heating values than PBDF. This fact accounts for the higher quantity of FAME injected for combustion to achieve the required engine power [47]. An increment in the chain length of fuel molecules and carbon/nitrogen to nitrogen/oxygen ratio of FAME result in higher CV [48, 49].

Without a doubt, higher CV is needed for effective combustion of FAME in an unmodified CI engine because of its desirable effects on combustion of IC engines. The lowest recommended value for the CV of biodiesel fuel for heating purpose as specified by EN 14213 is 35 MJ/kg [50, 51]. Apart from oxygen content, other factors that influence the heating value of FAME include the degree of saturation, number of double bonds, C:O ratio, C:H ratio, and feedstock [23]. Some properties like cloud point, density, flash point, and KV have been found to have strong correlations with heating values. In terms of emission, a higher quantity of FAME that needed to be injected into the combustion chamber to meet up with the required engine power has been found to affect PM and NOx emissions, particularly under exhaust gas recirculation system [52, 53].

It is believed that heating values can be predicted using the FA composition of FAME. Only a few citations are available in referred literature to establish a linear correlation to link heating values with FA composition, as far as the authors know. Specifically, Sanli et al. [49], Giakoumis [19], and Giakoumis and Sarakatsanis [15] have predicted the heating values using a percentage of FA compositions as inputs but with more than five methyl esters. This present effort is limited to the use of the five most common FAs as input, using the MLR approach. Input data are sourced from the data set available in the literature [15, 49].

The model correlation, shown in Equation 5 is arrived at from the general format (Equation 1). The model is found to be significant and adequate to predict the CV within an acceptable standard. Table 7 shows the five FA compositions, the experimentally determined CV (MJ/kg) sourced from literature, and the MLR predicted data. Equation 5 was arrived at by generating a linear correlation between the experimentally measured CV and the MLD predicted CV. The intercept was found to be 40.144 while C16:0 and C18:1 had a very minimum but negative effect on the output data. The predictive capability of the model is shown in figure 5.

$$\text{Calorific Value} = 40.144 - 0.02X_1 + 0.017X_2 - 0.001X_3 + 0.004X_4 + 0.005X_5 \text{ (Equation 5)}$$

The statistical analysis (table 11) shows that the model is significant with the R2 of 0.43. This implies that 43 % of the independent variable (input) contributed to the prediction of the dependent variable (output). The R-value of 0.66 and standard error of 0.33, though with five methyl esters, is comparable to the outcome of similar research [15, 40, 49]. The model was verified with a different set of data sourced from literature and was found to satisfactorily predict

the CV despite the diverse nature of the FAME source. The difference between the measure and predicted CV was negligible and within acceptable standards (table 12).

Table 10. Experimental and predicted data for Calorific value

S/N	Source	C16:0	C18:0	C18:1	C18:2	C18:3	Exp. CV	Pred. CV
1	Corn	11.81	2.13	27.35	57.74	0.63	40.19	40.163
2	Cottonseed	25.93	1.74	15.98	55.12	0.16	40.48	39.879
3	Croton	7.25	3.43	10.8	77.25	5.4	40.28	40.401
4	Hazelnut	6.32	3.71	79.17	10.67	0.15	39.8	40.04
5	Jatropha	14.42	5.82	42.82	35.38	0.23	40.38	40.062
6	Karanja	10.89	7.89	53.56	21.34	2.09	40.275	40.106
7	Peanut	10.33	2.79	47.63	31.52	0.64	39.93	40.071
8	Rapeseed	4.07	1.55	62.24	20.61	8.72	40.335	40.154
9	Rice bran	18.12	2.17	42.35	34.84	0.93	40.475	39.929
10	Rubber seed	9.39	9.41	24.22	38.12	17.54	40.35	40.349
11	Beef tallow	24.39	19.08	41.65	5.91	0.72	40.04	39.976
12	Canola	4.51	2	60.33	21.24	9.49	39.975	40.162
13	Chicken fat	24.06	6.42	41.43	18.83	1.06	39.89	39.821
14	Lard	25.1	13.23	44.36	12.06	1.18	39.95	39.887
15	Olive	11.47	2.83	74.52	9.54	0.51	40.28	39.926
16	Neem	17.57	16.6	45.83	17.79	0.72	39.96	40.112
17	Mahua	22.23	22.49	39.01	14.87	0.1	40.18	40.114
18	Safflower	7.42	2.38	14.41	75.31	0.09	40.155	40.339
19	Waste frying oil	25.043	4.283	37.942	30.032	0.19	39.223	39.811
20	Waste frying oil	25.95	3.899	43.574	23.637	0.265	39.833	39.754
21	Waste frying oil	27.614	3.93	42.754	22.805	0.281	39.312	39.719
22	Waste frying oil	29.117	4.375	37.455	26.233	0.21	39.259	39.717
23	Waste frying oil	25.645	3.863	43.228	24.306	0.271	39.441	39.762
24	Waste frying oil	41.438	4.775	40.636	10.293	0.182	39.741	39.413
25	Waste frying oil	40.637	3.369	42.104	9.958	0.173	39.336	39.401

Table 11: Statistical indices of the MLR model for Calorific Value

Regression Statistics	
Multiple R	0.66
R Square	0.43
Adjusted R Square	0.28
Standard Error	0.33
Observations	25

Table 12. Calorific Value model verification

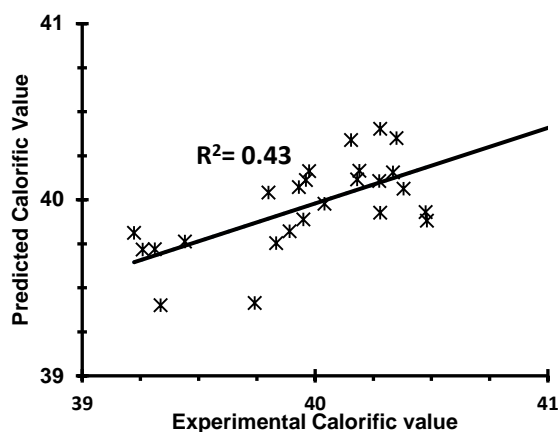| Source	Ref	Exp. value	Pred. value	Error (%)
Jatropha	[54]	40.536	40.501	0.09
Palm	[55]	39.907	39.863	0.11
Corn	[56]	39.93	39.538	0.98
Canola	[40]	39.64	39.615	0.06
Soybean oil	[40]	40.04	39.907	0.33
Grape Seed	[40]	39.82	39.968	0.37
Karanja	[57]	39.66	39.542	0.3

Figure 5. The predictive capability of the Calorific Value model

4. Conclusion

One of the motivations for the use of FAME as CI engine fuel is safer handling, improved engine performance, and mitigated emissions. Experimental determination of FAME fingerprint, which is a key determinant for the behavior, handling, storage, transportation, performance and emissions of the fuel, is onerous, laborious, requires costly laboratory architecture and highly technical personnel. Appropriately developed models and prediction correlations are considered to be a faster, cheaper and easier method of determining these properties based on certain criteria and conditions. The degree of saturation, chain length, branching, number and position of double bonds are key parameters in the performance of biodiesel. FA compositions of biodiesel are dependent on the type of feedstock, and to some extent on its production parameters and technique and greatly influence the properties of FAME based on the proportion of the methyl esters present in the biodiesel.

This current effort employed the five most common methyl esters, namely palmitic acid (C16:0), stearic acid (C18:0), oleic acid (C18:1), linoleic acid (C18:2), and linolenic acid (C18:3) to predict density, KV, CN, and CV of FAME using the MLR approach. A linear correlation was generated for the individual fingerprints and employed to predict the output using data extracted from the literature. The model was analyzed statistically to determine the standard error and other statistical indices. The predictive capability and model verification were carried out to test the competency and accuracy of the model within acceptable limits. Conclusively, the following points can be deduced:

- Some FAME properties can be predicted by the proportion of methyl esters as a panacea for difficulties in the experimental determination of the properties.
- Five FAs are enough to generate a linear correlation using MLR to accurately predict the density, KV, CN and CV of FAME.
- The outcome of the model verification shows that the correlation generated by this research can be relied upon to correctly predict the dependent outcomes being sought.

Going forward, a more accurate prediction correlations and models should be developed for predicting properties, performance, fuel mixing, combustion, and emission characteristics with linear and nonlinear relations. This will eliminate the cumbersome experimental determinations of these parameters with a view to advancing capacities in engine research.

REFERENCES

[1] BP. Statistical Review of World Energy. Available on https://www.bp.com/en/global/corporate/energy-economics/statistical-review-of-world-energy.html.

[2] H.-W. Schiffer. World Energy Resources by World Energy Council. Available on https://www.worldenergy.org/wp-content/uploads/2016/10/World-Energy-Resources-Full-report-2016.10.03.pdf .

[3] EEA. Global Total Primary Energy Consumption by fuel. Available on https://www.eea.europa.eu/data-and-maps/figures/global-total-primary-energy-consumption-by-fuel-1 .

[4] Statista. Global CO2 emissions share from fuel combustion by sector 2016. Available on https://www.statista.com/statistics/270527/distribution-of-worldwide-co2-emissions-by-sector/.

[5] EPA. (2017). Climate Change Indicators: Global Greenhouse Gas Emissions. Available: https://www.epa.gov/climate-indicators/climate-change-indicators-global-greenhouse-gas-emissions.

[6] WHO, Air quality guidelines: global update 2005: particulate matter, ozone, nitrogen dioxide, and sulfur dioxide. World Health Organization, 2006.

[7] H. Jääskeläinen. Biodiesel Standards & Properties. Available : https://www.dieselnet.com/tech/fuel_biodiesel_std.php .

[8] Biodiesel Standards. Available on https://www.biofuelsystems.com/specification.htm .

[9] Worldwide Fuel Charter. Available on http://www.oica.net/wp-content/uploads//WWFC5-2013-Final-single-page-correction2.pdf, 2013.

[10] EIA. World Biodiesel Production and Consumption by Year. Available on https://www.indexmundi.com/energy/?product=biodiesel&graph=production+consumption

[11] L. Zhu, Y. K. Nugroho, S. R. Shakeel, Z. Li, B. Martinkauppi, and E. Hiltunen, "Using microalgae to produce liquid transportation biodiesel: What is next?," Renewable and Sustainable Energy Reviews, vol. 78, pp. 391-400, 2017.

[12] H. K. Imdadul et al., "Higher alcohol–biodiesel–diesel blends: An approach for improving the performance, emission, and combustion of a light-duty diesel engine," Energy Conversion and Management, vol. 111, pp. 174-185, 2016.

[13] M. S. M. Zaharin, N. R. Abdullah, G. Najafi, H. Sharudin, and T. Yusaf, "Effects of physicochemical properties of biodiesel fuel blends with alcohol on diesel engine performance and exhaust emissions: A review," Renewable and Sustainable Energy Reviews, vol. 79, pp. 475-493, 2017.

[14] M. Samavi, B. Ghobadian, M. Ardjmand, and A. Seyfkordi, "Prediction of biodiesel properties and its characterization using fatty acid profiles," Korean Journal of Chemical Engineering, vol. 33, no. 7, pp. 2042-2049, 2016.

[15] E. G. Giakoumis and C. K. Sarakatsanis, "Estimation of biodiesel cetane number, density, kinematic viscosity and heating values from its fatty acid weight composition," Fuel, vol. 222, pp. 574-585, 2018.

[16] A. Bamgboye and A. Hansen, "Prediction of cetane number of biodiesel fuel from the fatty acid methyl ester (FAME) composition," International Agrophysics, vol. 22, no. 1, p. 21, 2008.

[17] A. Gopinath, S. Puhan, and G. Nagarajan, "Theoretical modeling of iodine value and saponification value of biodiesel fuels from their fatty acid composition," Renewable Energy, vol. 34, no. 7, pp. 1806-1811, 2009.

[18] R. Piloto-Rodríguez, Y. Sánchez-Borroto, M. Lapuerta, L. Goyos-Pérez, and S. Verhelst, "Prediction of the cetane number of biodiesel using artificial neural networks and multiple linear regression," Energy Conversion and Management, vol. 65, pp. 255-261, 2013.

[19] E. G. Giakoumis, "A statistical investigation of biodiesel physical and chemical properties, and their correlation with the degree of unsaturation," Renewable Energy, vol. 50, pp. 858-878, 2013.

[20] A. O. Barradas Filho et al., "Application of artificial neural networks to predict viscosity, iodine value and induction period of biodiesel focused on the study of oxidative stability," Fuel, vol. 145, pp. 127-135, 2015.

[21] D. A. Saldana, L. Starck, P. Mougin, B. Rousseau, N. Ferrando, and B. Creton, "Prediction of density and viscosity of biofuel compounds using machine learning methods," Energy & Fuels, vol. 26, no. 4, pp. 2416-2426, 2012.

[22] R. M. Balabin, E. I. Lomakina, and R. Z. Safieva, "Neural network (ANN) approach to biodiesel analysis: analysis of biodiesel density, kinematic viscosity, methanol and water contents using near infrared (NIR) spectroscopy," Fuel, vol. 90, no. 5, pp. 2007-2015, 2011.

[23] S. K. Hoekman, A. Broch, C. Robbins, E. Ceniceros, and M. Natarajan, "Review of biodiesel composition, properties, and specifications," Renewable and sustainable energy reviews, vol. 16, no. 1, pp. 143-169, 2012.

[24] X. Meng, M. Jia, and T. Wang, "Neural network prediction of biodiesel kinematic viscosity at 313K," Fuel, vol. 121, pp. 133-140, 2014.

[25] N. Moradi-kheibari, H. Ahmadzadeh, M. A. Murry, H. Y. Liang, and M. Hosseini, "Chapter 13 - Fatty Acid Profiling of Biofuels Produced From Microalgae, Vegetable Oil, and Waste Vegetable Oil," in Advances in Feedstock Conversion Technologies for Alternative Fuels and Bioproducts, M. Hosseini, Ed.: Woodhead Publishing, 2019, pp. 239-254.

[26] E. G. Giakoumis, "Analysis of 22 vegetable oils' physico-chemical properties and fatty acid composition on a statistical basis, and correlation with the degree of unsaturation," Renewable Energy, vol. 126, pp. 403-419, 2018.

[27] B. Jeeva and C. Rajashekar, "Investigating the Role of Fatty Acid Methyl Ester Composition on Engine Performance and Emission Characteristics," International Journal of Vehicle Structures & Systems (IJVSS), vol. 10, no. 4, 2018.

[28] G. Sakthivel and M. Ilangkumaran, "Optimisation of compression ignition engine performance with fishoil biodiesel using Taguchi-Fuzzy approach," International Journal of Ambient Energy, vol. 38, no. 2, pp. 146-160, 2017.

[29] G. Knothe, J. Krahl, and J. Van Gerpen, The biodiesel handbook. Elsevier, 2015.

[30] T. Houachri et al., "Fatty acid methyl esters (FAME) from oleaginous seeds grown in arid lands. Part II: Ibicella lutea, Onopordum nervosum, Peganum harmala, Smyrnium olusatrum and Solanum elaeagnifolium," Energy Sources, Part A: Recovery, Utilization, and Environmental Effects, vol. 40, no. 12, pp. 1434-1441, 2018.

[31] M. J. Pratas, S. V. Freitas, M. B. Oliveira, S. C. Monteiro, Á. S. Lima, and J. A. Coutinho, "Biodiesel density: experimental measurements and prediction models," Energy & Fuels, vol. 25, no. 5, pp. 2333-2340, 2011.

[32] Z. Zhang et al., "Effects of fatty acid methyl esters proportion on combustion and emission characteristics of a biodiesel fueled marine diesel engine," Energy Conversion and Management, vol. 159, pp. 244-253, 2018.

[33] M. Gülüm and A. Bilgin, "Measurements and empirical correlations in predicting biodiesel-diesel blends' viscosity and density," Fuel, vol. 199, pp. 567-577, 2017.

[34] M. A. Ruhul et al., "Impact of fatty acid composition and physicochemical properties of Jatropha and Alexandrian laurel biodiesel blends: An analysis of performance and emission characteristics," Journal of Cleaner Production, vol. 133, pp. 1181-1189, 2016.

[35] B. Sajjadi, A. A. A. Raman, and H. Arandiyan, "A comprehensive review on properties of edible and non-edible vegetable oil-based biodiesel: Composition, specifications and prediction models," Renewable and Sustainable Energy Reviews, vol. 63, pp. 62-92, 2016.

[36] S. Mishra, K. Anand, and P. S. Mehta, "Predicting the cetane number of biodiesel fuels from their fatty acid methyl ester composition," Energy & Fuels, vol. 30, no. 12, pp. 10425-10434, 2016.

[37] D. Tong, C. Hu, K. Jiang, and Y. Li, "Cetane number prediction of biodiesel from the composition of the fatty acid methyl esters," Journal of the American Oil Chemists' Society, vol. 88, no. 3, pp. 415-423, 2011.

[38] A. S. Ramadhas, S. Jayaraj, C. Muraleedharan, and K. Padmakumari, "Artificial neural networks used for the prediction of the cetane number of biodiesel," Renewable Energy, vol. 31, no. 15, pp. 2524-2533, 2006.

[39] G. Knothe, "Dependence of biodiesel fuel properties on the structure of fatty acid alkyl esters," Fuel processing technology, vol. 86, no. 10, pp. 1059-1070, 2005.

[40] I. K. Hong, G. S. Jeon, and S. B. Lee, "Prediction of biodiesel fuel properties from fatty acid alkyl ester," Journal of Industrial and Engineering Chemistry, vol. 20, no. 4, pp. 2348-2353, 2014.

[41] P. Saxena, S. Jawale, and M. H. Joshipura, "A review on prediction of properties of biodiesel and blends of biodiesel," Procedia Engineering, vol. 51, pp. 395-402, 2013.

[42] R. M. Joshi and M. J. Pegg, "Flow properties of biodiesel fuel blends at low temperatures," Fuel, vol. 86, no. 1-2, pp. 143-151, 2007.

[43] S. Geacai, O. Iulian, and I. Nita, "Measurement, correlation and prediction of biodiesel blends viscosity," Fuel, vol. 143, pp. 268-274, 2015.

[44] O. M. Ali, R. Mamat, N. R. Abdullah, and A. A. Abdullah, "Analysis of blended fuel properties and engine performance with palm biodiesel–diesel blended fuel," Renewable Energy, vol. 86, pp. 59-67, 2016.

[45] G. Martínez, N. Sánchez, J. Encinar, and J. González, "Fuel properties of biodiesel from vegetable oils and oil mixtures. Influence of methyl esters distribution," Biomass and Bioenergy, vol. 63, pp. 22-32, 2014.

[46] M. Kaisan, F. Anafi, J. Nuszkowski, D. Kulla, and S. Umaru, "Calorific value, flash point and cetane number of biodiesel from cotton, jatropha and neem binary and multi-blends with diesel," Biofuels, pp. 1-7, 2017.

[47] A. Atabani and A. da Silva César, "Calophyllum inophyllum L.–A prospective non-edible biodiesel feedstock. Study of biodiesel production, properties, fatty acid composition, blending and engine performance," Renewable and Sustainable Energy Reviews, vol. 37, pp. 644-655, 2014.

[48] L. F. Ramírez-Verduzco, J. E. Rodríguez-Rodríguez, and A. del Rayo Jaramillo-Jacob, "Predicting cetane number, kinematic viscosity, density and higher heating value of biodiesel from its fatty acid methyl ester composition," Fuel, vol. 91, no. 1, pp. 102-111, 2012.

[49] H. Sanli, M. Canakci, and E. Alptekin, "Predicting the higher heating values of waste frying oils as potential biodiesel feedstock," Fuel, vol. 115, pp. 850-854, 2014.

[50] K. Muralidharan, D. Vasudevana, and K. N. Sheeba, "Performance, emission and combustion characteristics of biodiesel fuelled variable compression ratio engine," (in eng), Energy, vol. 36, no. 8, p. 5385, 2011.

[51] U. Rashid, F. Anwar, and G. Knothe, "Evaluation of biodiesel obtained from cottonseed oil," Fuel Processing Technology, vol. 90, no. 9, pp. 1157-1163, 2009.

[52] C. D. Rakopoulos and E. G. Giakoumis, Diesel engine transient operation: principles of operation and simulation analysis. Springer Science & Business Media, 2009.

[53] E. G. Giakoumis, C. D. Rakopoulos, A. M. Dimaratos, and D. C. Rakopoulos, "Exhaust emissions of diesel engines operating under transient conditions with biodiesel fuel blends," Progress in Energy and Combustion Science, vol. 38, no. 5, pp. 691-715, 2012.

[54] M. Mofijur, H. Masjuki, M. Kalam, and A. Atabani, "Evaluation of biodiesel blending, engine performance and emissions characteristics of Jatropha curcas methyl ester: Malaysian perspective," Energy, vol. 55, pp. 879-887, 2013.

[55] A. E. Atabani, A. S. Silitonga, I. A. Badruddin, T. Mahlia, H. Masjuki, and S. Mekhilef, "A comprehensive review on biodiesel as an alternative energy resource and its characteristics," Renewable and sustainable energy reviews, vol. 16, no. 4, pp. 2070-2093, 2012.

[56] M. Gülüm and A. Bilgin, "Density, flash point and heating value variations of corn oil biodiesel–diesel fuel blends," Fuel Processing Technology, vol. 134, pp. 456-464, 2015.

[57] T. K. Jose and K. Anand, "Effects of biodiesel composition on its long term storage stability," Fuel, vol. 177, pp. 190-196, 2016.

CHAPTER 4: OPTIMIZATION OF FAME COMPOSITION FOR IMPROVED ENGINE PERFORMANCE AND EMISSIONS REDUCTION

This chapter presents the results of the numerical technique to find an optimal FAME candidate to ensure improved engine performance and mitigated emission. Linear mathematical correlations were derived using five FA compositions to compute certain properties. A numerical approach (MATLAB) was adopted to solve the resulting equations resulting in the parameters of the optimal candidate in terms of five FAME compositions only. The outcome has been submitted to the *International Journal of Low-Carbon Technologies*.

Awogbemi, O., Inambao F., Onuh E. I. (2019). "Optimization of FAME Composition for Improved Engine Performance and Emissions Reduction," International Journal of Low-Carbon Technologies. Oxford University Press

Optimization of FAME Composition for Improved Engine Performance and Emissions Reduction

Omojola Awogbemi [a], Freddie Inambao[b] and Emmanuel I. Onuh [c]

Discipline of Mechanical Engineering, University of KwaZulu Natal, Durban 4041, South Africa

[a] Corresponding Author: 217080448@stu.ukzn.ac.za. ORCID = 0000-0001-6830-6434.

[b] inambaof@ukzn.ac.za

[c] onuhe@ukzn.ac.za. ORCID = 0000-0002-3891-222X.

Abstract: Detrimental environmental effects of diesel fuel have stimulated investigation into the utilization of biodiesel as an alternative fuel for compression ignition (CI) engine. This present work employed MATLAB to solve linear equations generated for biodiesel properties using fatty acid (FA) composition for the determination of an optimal FAME candidate. Transesterification of waste vegetable oil employed to experimentally produce the fatty acid methyl ester (FAME) candidate generated through numerical intervention. The gas chromatography-mass spectrometer analysis of the resulting FAME revealed that the type of used vegetable oil, the food the oil was used to fry, and catalyst particle size influenced the FA composition of the FAME. Numerical evaluation of the objective function and the constraints yielded a FAME candidate with palmitic and oleic acids at 36.4 % and 59.8 % respectively. The resulting FAME candidate is expected to produce optimal engine performance and mitigate emissions in an unmodified CI engine.

Keywords: Engine performance; FAME; MATLAB; optimal candidate; waste cooking oil

1. Introduction

Globally, there is a growing utilization of biodiesel in the internal combustion (IC) engine, particularly in the fuel and power generation application sectors. This has led to an increased global demand for biodiesel with the United States of America, Germany, Argentina, Thailand, Belgium, and Canada topping the list of world producers as of 2016. By 2025 global biodiesel consumption is expected to swell by between 4.4 % to 5.4 % with a market value in the region of US$ 53.6 billion [1, 2]. World consumption of biofuel is predicted to reach 129.7 million metric tons of oil equivalent (Mtoe) from a paltry 59.7 Mtoe in 2010 as shown in Figure 1 [3]. This underscores the importance of biodiesel in the new global effort to enhance energy sustainability and reduce environmental pollution. Interest in biodiesel has compelled further studies in all facets of the fuel, predominantly in cost reduction, advancing engine performance and mitigating emissions for all categories of on-road and off-road compression ignition (CI) engines. Research in the conversion of used vegetable oil from households and restaurants to biodiesel is gaining ground by the day. This is due to its numerous advantages including a cleaner environment as a result of proper disposal, conversion of waste to fuel, reduction in the cost of biodiesel production, and generation of more income for households and small-scale businesses, among others [4].
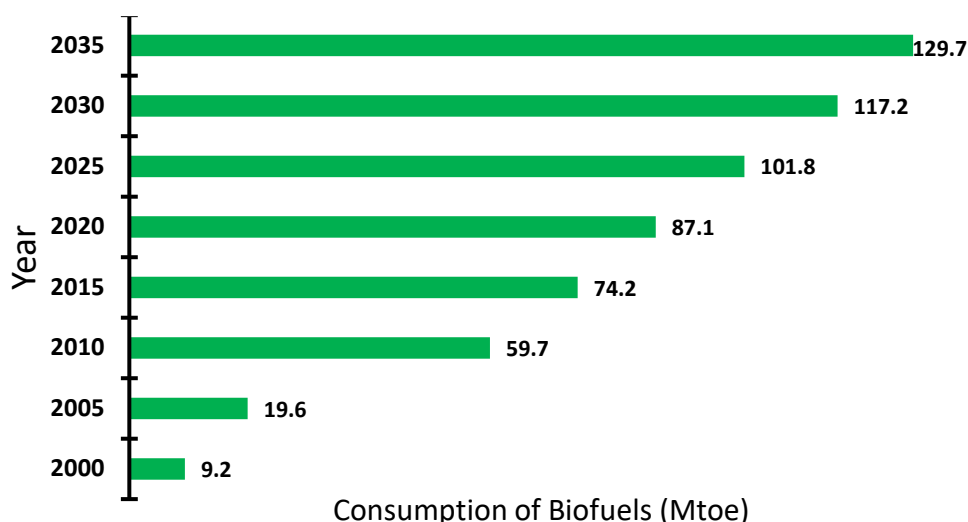
Fig. 1. World consumption of biofuel, including estimate to the year 2035

Over the years, particularly in the last few decades, many researches have been carried out with a view to upgrading the engine performance significantly and cutting down the emission characteristics of CI engines fueled with biodiesel, otherwise referred to as fatty acid methyl esters (FAME) with appreciable success. Amongst others, hybridization of feedstock, exhaust gas recirculation, low-temperature combustion, and other fuel injection and combustion strategies have been modestly effective in this regard. However, in the author's informed opinion, no attempt has been made to establish the FAME mix that gives the best possible engine performance and reduced emissions. Biodiesel consists of different esters and fatty acids (FAs) which are the major constituents and determinant of the behavior and performance of the fuel.

The source of the feedstock of biodiesel, whether fat or oil, has placed an inherent constraint on the composition of FAME. This is so because each source has its own unique fingerprint and composition. An optimal mix of FAME, therefore, is capable of enhancing performance and mitigating emissions of harmful gasses from CI engines fueled with biodiesel since the fuel's property is dependent on FAME mix. The motivation for this current effort is to engineer an acceptable FAME mix for CI engine application.

The significance of this present research arises from the need to explore FAME composition and the major fingerprints of biodiesel as a basis for obtaining a FAME candidate with improved performance and reduced emissions. Such a

relationship depends on the FA composition and the fingerprints of FAME. This study used compositional models to predict the major properties of biodiesel so as to deduce an optimal FAME candidate. The numerically generated FAME candidate will be produced experimentally by transesterification which can then be used to verify the outcome of the linear equation model. Such an optimal mix is expected to give the best possible performance and reduced emission of unblended FAME (B100) use in unmodified and an unmodified CI engine.

2. Background of Study

The inherent properties of FAME are a function of several factors including chain length and branching, the degree of saturation, number as well as position of double bonds [5], while it's quality and behavior are influenced by feedstock, production technique, handling, and storage processes.

FA composition is a major factor that determines the properties of FAME. FA composition is measured by gas chromatography-mass spectrometry (GC-MS). FAs are categorized as either saturated fatty acids (SFAs) or unsaturated fatty acids (USFAs). SFAs contain single carbon-carbon bonds while USFAs contain a single or multiple double carbon-carbon bonds in the chain. USFA can either be monounsaturated or polyunsaturated fatty acids. Table 1 compares SFAs and USFAs.

Table 1. Comparison of SFA and USFA

Factor	Saturated fatty acids	Unsaturated fatty acids
Structure	COOH—C—C—C—C—C—C—H (with H atoms on each carbon, all single bonds)	COOH—C—C—C—C=C—C—H (with H atoms, one double bond between carbons)
Type of Bond	Single bond between carbon atoms (C-C)	Minimum of one double bond between carbon atoms (C=C)
Examples	Palmitic acid, Stearic acid, Lauric acid, Myristic acid, Caprylic acid, Behenic acid, Arachidic acid	Oleic acid, Eladic acid, Palmitoleic acid, Linoleic acid, Linolenic acid, etc
Reactivity	Less reactive	Highly reactive
Stability	More stable	Less stable
Physical appearance	Solid at ambient temperature	Liquid at ambient temperature
Type of chain	Straight	Branch, at double bond
Melting point	Comparatively higher	Comparatively lower
Hydrogen atom per carbon atom	Have more hydrogen atoms per carbon atom	Have a comparatively less number of hydrogen atoms per carbon atom
Sources	Animal fats, palm oil, coconut oil.	Plant oil, vegetable oil, and fish oil
Solubility	Soluble in vitamins	Insoluble in vitamins
Effect of hydrogenation	Without effect	They are converted into saturated state by hydrogenation.
Shelf life/oxidative stability	Have a high oxidative stability index	Have a low oxidative stability index

Experimental determination of properties of FAME requires intricate procedures and techniques, a high degree of technical equipment, reagents, and personnel. It is time-consuming, expensive and exposes personnel to possible laboratory mishaps and hurts. This has led to the use of mathematical models and correlations over the last few decades. The deployment of mathematical models and correlations are cost-effective, timesaving, less laborious, innovative, flexible, safe and require no reagents, chemicals and specialized equipment [6]. Predictions arising from mathematical models have often been validated by experimental results in compliance with accepted standards. The two widely recognized standard requirements and test methods for B100 FAME are the European standard (EN) and the United States (US) standard represented by EN 14214 and D6751 respectively [7]. Table 2 shows details of methods and limits for major properties of B100 FAME.

There are some property prediction models for biodiesel employed produced by various authors. The empirical-based prediction models are believed not to have not produced satisfying outcomes in relation to biodiesel. The application of the vapour pressure based model is restricted to ideal solutions, though it can be extended to biodiesel, its accuracy is in doubt. The Liaw's model, a form of activity coefficient-based model, is mainly used for all flammable mixtures and not strictly for methyl esters. Molecular structure-based models rely on structural specifications and configurations like chain length, the position of double bonds, etc., of compounds. It, however, fails with the increased molecular weight associated with a fatty acid or the ester. Double-bond based models are contingent upon the number of double bonds available in the FAME which is considered not comprehensive enough to make an informed and all-encompassing forecast. Models/correlations based on combustion reactions, molecular weight, electron numbers and those centered on the physical properties and behavior of FAME are not individually comprehensive, inclusive, and far-reaching enough to accommodate all categories of esters. Thermodynamic-based models, though successfully predicting the properties of saturated fatty acids, have, however, showed a large error with unsaturated FAME [8].

The use of thermodynamic and other correlative models are appealing and unsophisticated, but they fail the test of precision and are often deficient in terms of theoretical footing [9]. These models cannot produce a candidate for the optimization problem because they do not derive their models from the composition of FAME. Composition-based models are not only straightforward, they also take

into consideration the distinctive fingerprints and FA composition of individual FAMEs. FAME composition has great influence and produces a more acceptable outcome so as to predict the optimal mix to enhance engine performance in addition to lowering the emission characteristics of CI engines [10].

Table 2. Limits and test methods of properties of B100 FAME

Standards	Europe EN 14214		US ASTM D 6751	
	Limits	Methods	Limits	Methods
Acid no (mgKOH/g, max)	0.5	EN 14104	0.5	D664
Carbon residue (wt. %, max)			0.05	D4530
Cetane no. (min)	51	EN ISO 5165	47	D613
CFPP (°C, max)	-5 to -44	EN 116		
Cloud point(°C, max)	Variable	EN 23015	Report	D2500
Copper strip corrosion (3 hr, at 50 °C, max)	No 1	EN ISO 2160	No. 3	D130
		EN ISO 3675		
Density (Kg/m^3)	860-900	EN ISO 12185		
Distillation (T90, °C, max)			360	D1160
Ester content (wt. %, min)	96.5	EN 14103		
Flash point (°C, max)	101	EN ISO 2719	93	D93
Monoglycerides (wt, %, max)	0.7	EN 14105	0.40	D6584
Diglycerides (wt, %, max)	0.2	EN 14105		
Triglycerides (wt, %, max)	0.2	EN 14105		
		EN 14105	0.02	D6584
Free glycerol (wt, %, max)	0.02	EN 14106		
Total glycerol (wt, %, max)	0.25	EN 14105	0.24	D6584
		EN 14111		
Iodine number (gl$_2$/100 g, max)	120	EN 16300		
Kinematic Viscosity @ 40 °C (mm^2/s)	3.5-5.0	EN ISO 3104	1.9-6.0	D445
Linolenic acid methyl esters (wt. %, max)	12.0	EN 14103		
Metal (Ca+Mg), ppm, max	5.0	EN 14538	5.0	EN 14538
		EN 14108	5.0	EN 14538
		EN 14109		
Metal (Na+K), ppm, max	5.0	EN 14538		
Methanol, (wt, %, max)	0.2	EN14110	0.20	EN 14110
Oxidation stability (hrs @ 110 °C, min)	6	EN 14112	3	EN 14112
	4.0	EN 14107	0.001% wt	D4951
Phosphorus (max)	mg/kg	PrEN 16294		
Polyunsaturated acid methyl esters (wt. %, max)	1.0	EN 15779		
Sulfated ash (wt. %, max)	0.02	ISO 3987	0.02	D874
Total contamination (mg/kg, max)	24	EN 12662		
		EN ISO 20846	15 ppm	D5453
		EN ISO 20884		
Total sulphur (max)	10 mg/kg	EN ISO 13032		
Water and sediment (% vol., max)			0.05	D2709
Water, (ppm, max)	500	EN ISO 12937		

2.1. Cetane Number

As opposed to a spark ignition engine, CI engine is a self-ignition engine where the charge inside the combustion chamber of the engine is projected to be self-ignited. Cetane number (CN) is an important dimensionless property of fuel that is capable of determining auto-ignition, the fuel

quality and fuel ignition delay time [11, 12]. A higher value of CN is connected with a shorter fuel ignition delay time so that the fuel is combusted timeously and completely, smooth running, engine stability, less noise, better engine performance and emissions mitigation [13, 14]. Thus, CN is recognized as the most important property of FAME for effective combustion, better engine performance, and reduced emissions. An increment in the chain length, number of carbon atom chains, and a decrease in the mean degree of saturation causes in an increase in the CN of B100 FAME [15, 16]. Recommended specifications and test methods for CN for both the EN 14214 and ASTM D 6751 are shown in Table 2.

2.2. Density

The density of a given matter, or substance is the mass per unit volume of the substance. Density directly impacts the process and quantity of the fuel admitted into the engine's combustion chamber for effective combustion. It has an explicit effect on the operation and operation of pumps, nozzle injectors, and other fuel injection architecture. The density of FAME has been reported to be dependent on FA composition, feedstock, and to a large extent the production techniques [17]. Kinematic viscosity (KV), increase in pressure, reduction in temperature, CN, the degree of unsaturation, heating value, and higher unsaturation have been found to increase the value of fuel density, while increased chain length is believed to lead to a reduced density of FAME [8, 9]. For this study, density was the objective function and was maximized between 860 kg/m3 and 900 kg/m3 as recommended by EN 14214, which is the specification for biodiesel from most third generation feedstock, including waste cooking oil (WCO). The density fingerprint of FAME affects fuel atomization, engine operation, and thermal efficiency of a CI engine [18, 19].

2.3. Kinematic Viscosity

Kinematic Viscosity (KV) remains a vital fluid fingerprint that determines the degree of resistance/easiness to the flow of a portion of a given fluid over another and is attributable to internal friction in the fluid. High KV causes poor fuel atomization, slimmer injection spray, and precipitates fatter droplet size which ensures in poor fuel injection, the formation of engine deposits, decreased thermal efficiency, inferior

fuel combustion and higher emissions. Conversely, lower KV precipitates better quality fuel droplets and enhanced performance of the fuel injector. This ensures the injecting of the required quantity of fuel into the combustion chamber. Chain length, branching, number and position of double bonds of FAME influence the KV and other properties of biodiesel [18, 20, 21]. Compared with petroleum-based diesel fuel, FAME has superior chemical structure, molecular mass, and hence higher KV [22]. The value of KV not greater than 4.5 mm2/s, measured at 40 °C, was used in this study as the constraint for the regression analysis.

2.4. Calorific Value

Calorific value (CV), otherwise referred to as higher heating value, has been more accurately described in terms of the measure of the energy content of fuels, and depicts the quantity of heat given out when one gram of fuel is combusted to generate carbon dioxide and water at initial temperature. An increment in the chain length of fuel molecules and carbon to oxygen ratio of FAME results in a higher CV [15, 21]. A higher CV is needed for effective combustion of FAME in an unmodified CI engine because of its desirable effects on combustion of IC engines. The lowest recommended value for the CV of biodiesel fuel for heating purpose as specified by EN 14213 is 35 MJ/kg [23, 24]. As one of the constraints, a CV of between 34.4 MJ/kg and 45.2 MJ/kg was employed in this study for analysis as a desirable factor for the combustion of fuel.

2.5. Cold Filter Plugging Point

One of the issues inhibiting the utilization of FAME in CI engines is its cold flow properties, particularly in low-temperature countries. Cold filter plugging point (CFPP) signifies the least temperature whereupon a known quantity (20 mL) of biodiesel flows pass a standardized filtration gadget (45-micron screen) in a stipulated period of time, usually 1 minute, when cooled in a defined condition [8]. CFPP measures the ease of operation of fuels under low-temperature climatic conditions. It is the temperature of the fuel which signals the onset of fuel crystallization or gelling, clogging of fuel filters, and other fuel line architecture. The consequence of a high CFPP of FAME is clogging of the fuel filter, lines and hose more easily due to the rapid crystallization of the fuel [14, 18]. Long-chain saturated FAME,

especially palmitic acid and stearic acid, have been found to contribute to high CFPP in fuel, much more than unsaturated FAME. The chain length saturated factor is employed to correlate the CFPP of FAME. Generally, chain length, the intensity of unsaturation, and branching, etc., affect the CFPP of FAME [25]. CFPP, due to its importance in fuel performance at low temperature, was chosen as a constraint. In line with EN 14214 and ASTM D 6751 standards, CFPP was set between -15 °C and -5 °C to incorporate extreme low-temperature conditions.

2.6. Cloud Point

The cloud point (CP) is described as the least temperature that facilitates the formation of clusters of wax quartzes of about 0.5 μm in diameter resulting in the appearance of a murky solution. It triggers the formation of biowax within the FAME leading to the blocking of fuel hoses, lines, filters, and injectors in FAME-fueled engines [26, 27]. The nature and quantity of saturated fatty acids compounds, the source of the FAME, the location of double bonds, in addition to the length and linearity of carbon chains, affect the CP of biodiesel. The FAME obtained from animal fats or oils with double bonds situated near carbon chain ends, etc., precipitates elevated CP [8, 28]. Although both EN 14214 and ASTM D 6751 do not give definite specifications for CP, the constraints in this study were set at between -25 °C and 26 °C to cater for a wide range of temperature conditions.

3. Review of Literature

FA composition has been explored to predict some properties of biodiesel as a result of the fundamental importance of FA composition, degree or intensity of saturation or unsaturation, and carbon chain length, in addition to the position, number, and configuration of double bonds in the carbon chain [29, 30]. The impact of carbon chain length and intensity of saturation on some physical properties of FAME has been affirmed by some research [30, 31]. FA compositional models have been exploited to predict the KV, CN, density, higher heating value [32], iodine value, CP, saponification value, pour point [33], flash point [34][38], and cold filter plugging point [35]. Various numerical techniques and correlations, including empirical equations [36], adaptive-network-based fuzzy inference system [33],

multiple linear regression analysis [32], least squares regression method [37], least squares support vector machine model [38], artificial neural network [39] etc., have been employed by various researchers to predict fuel properties of FAME and its blends using FA composition.

The outcomes of the research of many scholars have indicated that the application of FAME as CI engine fuel results in better engine performance, reduced PM, smoke, UHC, and CO emissions in general but increased NOx emission in some cases. The outcomes of those researches showed that the application of biodiesel fuel is capable of improving the performance characteristics of the diesel engine, drastically reducing CO emissions and lessening NOx emissions [40-42]. Researchers have predicted the performance and emission characteristics of FAME and its blends with varying outcomes. Biodiesels with higher saturated FA (palmitic acid, stearic acid) composition have been reported to exhibit higher CN which tends to improve combustion activities within the combustion chamber and produce reduced brake specific fuel consumption (BSFC), higher brake thermal efficiency (BTE), higher exhaust gas temperature (EGT), as well as less smoke and NOx. Generally, the degree of saturation, chain length, number and location of double bonds influence the CN which affects the combustion activities and the emission characteristics [43, 44]. Jiaqiang [45] explored KIVA-4 in conjunction with CHEMKIN II code to stimulate and validate the emission characteristics of a CI engine under variable load conditions fueled by FAME produced from vegetable oil. They reported that changes in the percentage of palmitic, stearic and oleic acids in the FAME influenced the fuel-air mixing, evaporation break up, combustion efficiency, engine performance, and emission of regulated gases. Similar work by authors showed that soot and NOx emissions of CI engine energized by FAME are affected by changing FA methyl ester proportions [45]. Similarly, Zhang et al. [46] investigated the effects of the proportion of FA composition of FAME on engine performance and emission characteristics of biodiesel fueled CI engine. They reported that a rise in the proportion of linoleic acids resulted in superior BSFC while an increase in the proportion of oleic, stearic, and palmitic acids lowered the indicated power.

There is near consensus of opinion that the proportion of the five major FAs in FAME, i.e.

stearic, palmitic, oleic, linoleic and linolenic acids affects the activities of fuel within the combustion chambers and greatly influences the engine performance and emission of regulated pollutants of an unmodified CI engine fueled by FAME. The relevant questions to ask, therefore, are: what is the best proportion of the five FAs that can improve engine performance and reduce emission of regulated gases in an unmodified conventional CI engine, and how can this proportion be determined? This present effort is aimed at exploring the use of mathematical and numerical tools to determine the optimal FA mix that will produce the best FAME candidate for improved engine performance and mitigated emission in an unmodified CI engine. The motivation for this investigation is to assist biodiesel refiners, engine manufacturers, combustion and emission researchers in their efforts to improve fuel combustion with a view to enhancing engine performance and lessening the obnoxious emissions. This current work is limited to effect of the five most common FAs, namely palmitic acid (C16:0), stearic acid (C18:0), oleic acid (C18:1), linoleic acid (C18:2), and linolenic acid (C18:3), on engine performance and emission characteristics.

4. Methods

An optimal mix FAME candidate was determined using a numerical solution which was verified by the FA composition of biodiesel produced from WCO by transesterification process.

4.1. Numerical Method

This study employed the application of a compositional model using some major properties to unveil an optimal candidate mix using linear regression equations. This arose from the need to explore mathematical tools to solve a series of linear equations arising from the compositional models of some critical FAME properties. The compositional models are products of the strategy for property prediction of FAME using the FA composition of biodiesel as determined by GC-MS analysis.

Linear correlations of major fingerprints that are crucial to engine performance and emission generation in an unmodified CI engine fuelled with FAME were mined from literature. CN was chosen

as an objective function and maximized, while density, KV, calorific value, cold filter plugging point, and CP were taken to be constraints. Compositional based models for these properties were compiled from literature as shown in Table 3 and formed into equations (1) to (6). The established linear correlations were reduced to contain the five most commonly occurring FAs for each of the considered properties. The five most occurring FAs from the literature surveyed were palmitic, oleic, stearic, linoleic, and linolenic acids [47-50]. This section is divided into subheadings and provides concise and precise descriptions of the experimental results, their interpretation as well as the experimental conclusions that can be drawn.

The resulting linear equations (7) to (12) are solved, using MATLAB according to the flowchart shown in Figure 2, bearing in mind that the outcome of the numerical evaluation agrees with the EN 14214 and ASTM D 6751 standards. Transesterification of WCO feedstock with a variety of catalyst particle sizes was carried out to produce various FAME with FA compositions and properties to meet the specifications arrived at by the numerical interventions. The optimal FAME candidate produced from WCO was used to verify the outcome of the linear equation model.

4.2. Experimental method

4.2.1. Material collection and treatment

Waste vegetable oil samples were collected from takeaway restaurants in central Durban. Methanol (analytical grade, 99.5 %) was used as alcohol. Activated magnesium silicate, commercially known as Magnesol® (analytical grade, 60-100 mesh, M_w of 100.39 g/mol) was used as an absorbent. Magnesol® is hygroscopic and contact with eyes must be avoided. The container must always be kept airtight. The waste vegetable oils were heated to 110 °C in a beaker in an electric heater for 15 min to remove moisture and filtered to eliminate every food residue and other suspended solid particle in the used vegetable oils. Some important properties of the WPO were also determined by using standard methods. Chicken waste eggshells were collected from Butterfield Bakery, Reddy's Bakery, and Nubbile's Bakery in central Durban.

Table 3. Composition-based models for the prediction of some FAME properties

Property	Correlation	Definition of unknowns	Ref
Cetane number (CN)	$CN = 56.16 + (0.07La) + (0.1M)i$ $+ (0.15P) - (0.05Pt)$ $+ (0.23S) - (0.03O)$ $- (0.19Li) - (0.31Ln)$ $+ (0.08Ei) + (0.18Er)$ $- (0.1Ot)$	La = Lauric, M=Myristic, P=Palmitic, Pt=Palmitoleic, S=Stearic, O=Oleic, Li=Linoleic, Ln=Linolenic, Ei=Eicosanoic, Er=Erucic and Ot=others	[16]
Density (DN)	$DN = 2204.5 - 13.2P - 1.4PL - 16S$ $- 13.8OL - 13.3L$ $- 3.717LL + 39.7A$ $+ 72.2Oth$	P = Palmitic, PL = Palmitoleic, S = Stearic, OL = Oleic, L = Linoleic, LL = Linolenic, A = Arachidic, Oth = Others [all values in Percentage weight].	[51]
Kinematic Viscosity (KV)	$KV = 373.4774 - 3.7096P - 0.0993PL$ $- 3.812S - 3.7431OL$ $- 3.6808L - 3.717LL$ $+ 0.1131A$ $- 10.8943Oth$	P = Palmitic, PL = Palmitoleic, S = Stearic, OL = Oleic, L = Linoleic, LL = Linolenic, A = Arachidic, Oth = Others [all values in Percentage weight].	[51]
Calorific value (CV)	$CV = 32629.061 + 57.390a + 71.795b$ $+ 231.631c$ $+ 16.913d + 66.268e$ $+ 70.501f$ $+ 387.989g$ $+ 1228.692h$ $- 115.455i$	a–i : mass fractions (wt.%) of the fatty acids C14:0, C16:0, C16:1, C18:0, C18:1, C18:2, C18:3, C20:0, C22:0, respectively	[21]
Cold filter plugging point (CFPP)	$CFPP = 3.1417LCSF - 16.477$ $LCSF = 0.1C_{16:0} + 0.5C_{18:0} + 1C_{20:0}$ $+ 1.5C_{22:0} + 2C_{24:0}$	LCSF: The long-chain saturated factor for C16:0-C24:0 C: Mass fraction of saturated fatty acid (wt%)	[35]
Cloud point (CP)	$CP = -40.278 + 0.514C_{16:0} +$ $0.6364C_{18:0} + 0.38363C_{18:1} +$ $0.35362C_{18:2} + 0.26341C_{18:3} +$ $0.58623C_{22:1}$	C16:0, C18:0, C18:1, C18:2, C18:3, C22:1¼Mass percentage in biodiesel	[34]

Where X_1 = Palmitic acid (C16:0), X_2 = Stearic acid (C18:0), X_3 = Oleic acid (C18:1), X_4 = Linoleic acid (C18:2), X_5 = Linolenic acid (C18:3), X_6 = Arachidic acid (C20:0), X_7 = Palmitoleic acid (C16:1), X_8 = Lauric acid (C12:0), X_9 = Mytristic acid (C14:0), X_{10} = Eicosenoic acid (C20:1), X_{11} = Behenic acid (C22:0), X_{12} = Erucic acid (C22:1), X_{13} = Lignoceric acid (C24:0), X_{14} = Others.

CN: $56.16 + 0.07X_1 + 0.1X_2 + 0.15X_3 - 0.05X_4 + 0.23X_5 - 0.03X_6 - 0.19X_7 - 0.31X_8 + 0.08X_9 + 0.18X_{10} - 0.1X_{14} = 45 \leq CN \leq 51$ (1)

DN: $2204.5 - 13.2X_3 - 1.4X_4 - 16X_5 - 13.8X_6 - 13.3X_7 - 3.717X_8 + 39.7X_9 + 72.2X_{14} = 860 \leq DN \leq 900$ (2)

KV: $337.4774 - 3.7096X_3 - 0.0993X_4 - 3.812X_5 - 3.743X_6 - 3.6808X_7 - 3.717X_8 + 0.1131X_9 - 10.8943X_{14} = KV \leq 4.$ (3)

$32629.061 + 57.390X_2 + 71.795X_3 + 231.631X_4 + 16.913X_5 + 66.268X_6 + 70.501X_7 + 387.989X_8 + 1228.692X_9 - 115.455X_{11} = 34.4 \leq CV \leq 45.2$ (4)

CFPP: $-16.447 + 0.3141X_3 + 1.57085X_5 + 3.1417X_9 + 4.71255X_{12} + 6.2834X_{13} = -5 \leq CFPP \leq -15$ (5)

CP: $-40.278 + 0.514X_3 + 0.6364X_5 + 0.38363X_6 + 0.35362X_7 + 0.26341X_8 + 0.58623X_{12} = -25 \leq CP \leq 26$ (6)

$CN = 56.16 + 0.15X_1 + 0.23X_2 - 0.03X_3 - 0.19X_4 - 0.31X_5$ (7)

$DN = 2204.5 - 13.2X_1 - 16X_2 - 13.8X_3 - 13.3X_4 - 3.717X_5$ (8)

$$KV = 337.4774 - 3.7096X_1 - 3.812X_2 - 3.743X_3 - 3.6808X_4 - 3.717X_5 \qquad (9)$$

$$CV = 32629.061 + 71.795X_1 + 16.913X_2 + 66.268X_3 + 70.501X_4 + 387.989X_5 \qquad (10)$$

$$CFPP = -16.447 + 0.3141X_1 + 1.57085X_2 \qquad (11)$$

$$CP = -40.278 + 0.514X_1 + 0.6364X_2 + 0.38363X_3 + 0.35362X_4 + 0.26341X_5 \qquad (12)$$

The unknowns (X_1, X_2, X_3, X_4, and X_5) are non-negative and vary between 0 and 100 steps of 0.01.

4.2.2. FAME production

The collected waste chicken eggshells were washed with hot water and rinsed several times with distilled water to ensure absolute cleanliness and converted into CaO as described in our previous work [52]. Figure 3 depicts the transesterification process for converting WCO to WCOME. A waterless purification method was adopted to prevent wastewater and the attendant cost of disposal and treatment, while used Magnesol® was recycled as compost and animal feed. Magnesol® at 1 % (magnesol:biodiesel) was added to the crude biodiesel maintained at 65 °C for 30 min and stirred by a magnetic stirrer at 600 rpm. This was to allow evaporation of excess methanol trapped in the crude biodiesel and to ensure adequate contact between the absorbent and the crude biodiesel. The mixture was then subjected to centrifuge at 400 rpm for 20 min at ambient temperature. The decanted biodiesel was polished using a 0.45 µm syringe filter. The clean FAME was stored in a clean glass vial for analysis.

4.2.3. Characterization of FAME

The FA composition of the biodiesel samples was determined by a gas chromatograph-mass spectrometer (GC-MS) fitted with an ultra-alloy-5 capillary column and GCMS-QP2010 Plus software. Table 4 shows the GCMS configuration used for the analysis of FAME samples. The total time for the GC-MS analysis was 39.81 min.

5. Results and discussions

5.1. Numerical solution

The composition of FAME and some properties that are able to give optimal engine performance and mitigated emissions were revealed and are shown in Table 5. The optimal candidate was the FAME with palmitic acid 36.4 % and oleic acid of 59.8 %. This candidate was arrived at when the CN, CP, density, KV, calorific

value, and the cold flow plug point (CFPP) met both the EN 14214 and ASTM D 6751 standards. The CN, because of its importance in combustion, engine performance and emission generation, was maximized. The other candidates for an optimal candidate also provided satisfactory outcomes. Palmitic acid and oleic acid, being SFAs
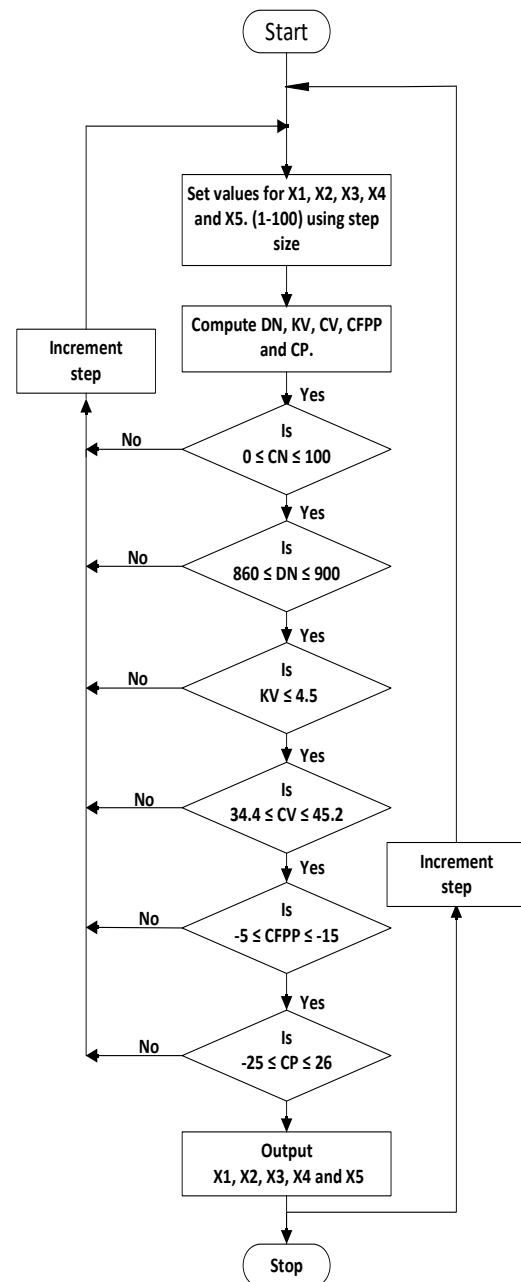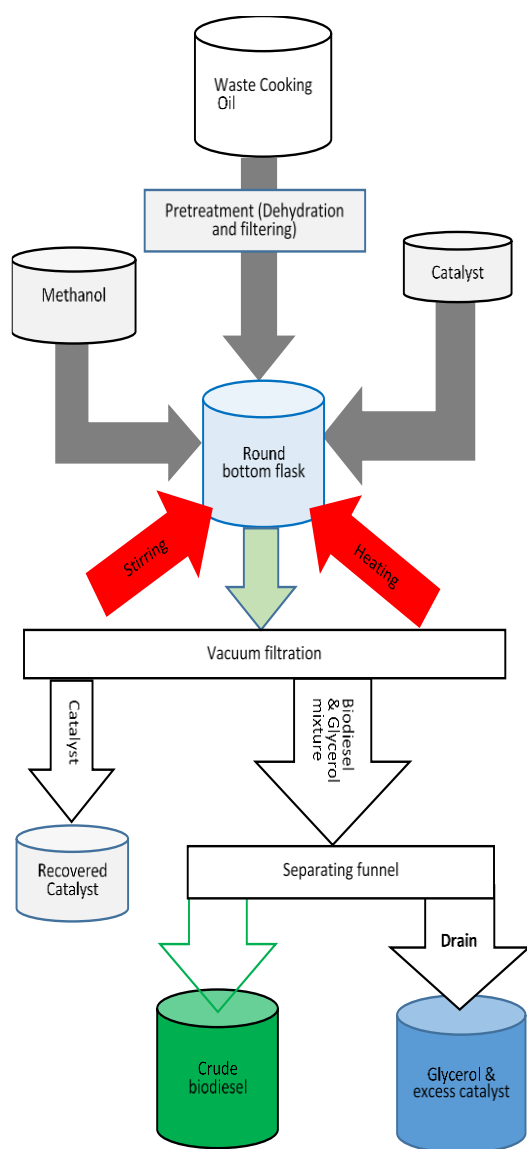

Fig. 2. The flowchart for solving the equations

Fig. 3. Transesterification process flowchart

Injector	
Inlet temperature	250 °C
Carrier gas	Helium
Sample size	2 μL
Injection mode	splitless
Column temperature	50 °C

Detector	
Type	GCMS
Interface temperature	280 °C
Detector gain	1.08 kV + 0.00 kV

Oven temperature program		
Rate	**Temperature (°C)**	**Hold time (min)**
-	50	1
15.00	180	1
7.00	230	1
5.00	350	5

Column	
Type	Ultra alloy -5(MS/HT)
Specification	30 m, 0.25 mm ID, 0.25 μm
Flow rate	3.0 mL/min
Total flow	4.9 mL/min
Column flow	0.95 L/min

and MUFAs respectively, were the dominant percentage while stearic, linoleic and linolenic acids which are PUFAs had a combined composition of less than 2 %. The optimal candidate, being defined in terms of its FA compositions will be tested in an unmodified CI engine and reported in our next publication. However, going by the outcome of engine performance and emission characteristics of similar FAME were found to present encouraging performance parameters and mitigated emissions [53-56].

Table 5. Outcomes of linear algebra to determine an optimal candidate

C16:0	C18:0	C18:1	C18:2	C18:3	CN	CP (°C)	ρ (kg/m³)	KV (mm²/s)	CV (MJ/kg)	CFPP (°C)
36.4	0	59.7	0.9	0.1	59.63	1.68	887.81	4.69	39300.85	-5.01
36.4	0	59.7	1	0	59.64	1.69	886.86	4.69	39269.1	-5.01
36.4	0	59.7	1	0.1	59.61	1.71	886.49	5.06	39307.9	-5.01
36.4	0	59.7	1.1	0	59.62	1.72	885.53	5.06	39276.15	-5.01
36.4	0	59.7	1.2	0	59.60	1.76	884.2	5.43	39283.2	-5.01
36.4	**0**	**59.8**	**0**	**0**	**59.83**	**1.37**	**898.8**	**4.4**	**39205**	**-5.01**
36.4	0	59.8	0	0.1	59.80	1.40	898.41	4.76	39244.02	-5.01
36.4	0	59.8	0	0.2	59.76	1.43	898.04	4.13	39282.82	-5.01
36.4	0	59.8	0	0.3	59.73	1.45	897.66	4.50	39321.62	-5.01
36.4	0	59.8	0	0.4	59.7	1.49	897.29	4.87	39360.42	-5.01
36.4	0	59.8	0	0.5	59.67	1.51	896.92	5.24	39399.22	-5.01

Table 6. Properties of waste cooking oil samples

Source	Waste cooking oil			Test method
	Sunfoil (WSFO)	Palm oil (WPO$_{FC}$)	Palm oil (WPO$_{SC}$)	
Food items	Chips	Fish and chips	Chips and sausages	N/A
Usage (Days)	14	14	14	N/A
Acid value (mgKOH/g)	0.72	0.66	1.13	AOCS Ca 4a-40
Density @ 20 °C (kg/m³)	919.8	904.3	913.7	ASTM D 1298
Iodine value (cg/g)	116.7	81.7	54.2	AOCS Cd 1B-87
Kinematic Viscosity @ 40 °C (mm²/s)	43.521	44.254	38.407	ASTM D445

5.2. Analysis of the Optimal Candidate

WCOs were adopted as a feedstock due to their affordability, availability and environmental advantages over other types of feedstocks. Waste sunflower oil (WSO), waste palm oil (WPO) used to fry fish and chips (WPO$_{FC}$) and WPO used to fry sausages and chips (WPO$_{SC}$) were used as feedstock. Table 6 shows the details and properties of the waste cooking oil samples. The acid value of the samples shows the suitability of the transesterification process for their conversion to FAME. The effect of the food items the palm oil fried is manifested in the variations in their properties. Sausage was found to increase the density of the palm oil sample when compared to the sample used to fry fish. The iodine value and kinematic viscosity of the waste palm oil used to fry fish and chips were higher than that used to fry sausages and chips. WSO presented higher density and iodine values than the waste palm oil samples.

The transesterification of WSO, WPO$_{FC}$, and WPO$_{SC}$ into waste sunflower oil methyl esters (WSOME), waste palm oil methyl ester fish and chips (WPOME$_{FC}$), and waste palm oil methyl ester sausage and chips (WPOME$_{SC}$) respectively using varying catalyst particle size, namely 75 µm, 90 µm, 125 µm, and 150 µm, were subjected to GC-MS analysis. As shown in Table 7, catalyst particle size affects FA composition and the degree of saturation of FAME. For the WSOME samples, SFA varied between 37.18 % and 36.66 %. SFA increased with a reduction in catalyst particle size from 37.87 % for 75 µm catalyst particle size to 38.66 % for 150 µm particle size but reduced to but reduced to 37.81 % for 150 µm catalyst particle size.at 150 µm catalyst particle size produced the least SFA but the highest (61.29 %) MUFA. The highest PUFA of 0.52 % was recorded at 125 µm catalyst particle size.
The effect of the food item the neat palm oil was used to fry did not only affect its properties but also the FA composition and degree of saturation. The WPOME$_{FC}$ consisted of about 61 % MUFA, 38 % SFA and 1 % PUFA. The percentage of MUFA reduced with an increment in the catalyst particle size, with the least PUFA occurring at 150 µm

catalyst particle size. PUFA for WPOME$_{FC}$ were noticed to increase with the increment in the catalyst particle size, rising from 0 % for 75 µm catalyst particle size to 1.97 % for 150 µm particle size. The percentage of MUFA in WPOME$_{SC}$ reduced as the catalyst particle size increased. At 90 µm catalyst particle size, the WPOME$_{SC}$ presented the least SFA but the highest PUFA. Conversely, SFA and PUFA were noticed to increase with an increment in the catalyst particle size used to produce WPOME$_{SC}$.

In general, oleic and palmitic acids were common FAs to all the samples, irrespective of the feedstock and catalyst particle size, while linolenic, palmitoleic, stearic, linoleic, arachidic lauric and behenic acids appeared in trace percentages. The different surface area size of the catalyst was believed to be responsible for the different FA compositions. According to [57], the particle size of the solid catalyst influences catalytic behavior and performance. Different catalytic activity influenced by catalyst particle size and surface area is likely to affect the degree of saturation, the position of carbon—carbon double bond and, ultimately, the FA composition.

From Table 5 it is evident that the two major FAs are palmitic and oleic acids and can be produced experimentally. Monirul et al. [53] and Ozsezen et al. [54] produced FAME from waste palm oil with palmitic and oleic acid of 38.4 % and 44.3 % and 39 % and 43.69 % respectively. Ozsezen et al. [58] produced WPOME with palmitic and oleic acids of 39 % and 43.65 % respectively and tested the WPOME in an unmodified CI engine. The outcome of the emission characteristics showed that the CO, CO2, HC, and smoke opacity reduced by 88.89 %, 1.74 %, 14.29 %, and 67.65 % respectively while NOx increased by 22.13 % at full load in contrast with petroleum-based diesel (PBD) fuel. The result of the engine performance test showed that the BSFC (g/kWh) increased by 6.93 %, brake power (kW) reduced by 2.64 % and the brake thermal efficiency reduced by 1.44 % at full load when compared with PBD fuel.

Table 7. Result of GCMS analysis of FAME samples

Fatty acid	Structure	WSOME @ different catalyst particle size (%)				WPOME$_{FC}$ @ different catalyst particle size (%)				WPOME$_{SC}$ @ different catalyst particle size (%)			
		75 μm	90 μm	125 μm	150 μm	75 μm	90 μm	125 μm	150 μm	75 μm	90 μm	125 μm	150 μm
Oleic acid	C18:1	60.43	60.41	60.82	60.75	60.96	60.85	60.43	59.67	61.56	60.75	59.82	59.35
Palmitic acid	C16:0	36.16	36.61	36.63	36.28	37.72	36.24	37.52	37.32	36.35	36.26	36.71	36.51
Linolenic	C18:3	1.25	1.12	-	0.62	-	-	0.13	1.64	0.32	0.47	0.85	0.12
Palmitoleic	C16:1	-	-	-	0.54	0.62	0.65	0.25	-	-	0.57	0.56	0.43
Stearic acid	C18:0	0.54	0.61	1.01	0.78	-	0.15	0.26	1.04	0.91	-	0.75	1.17
Linoleic acid	C18:2	0.45	0.53	0.52	0.91	-	1.24	0.95	0.33	0.12	0.07	0.55	0.89
Arachidic acid	C20:0	0.66	-	0.5	-	0.12	-	-	-	-	1.27	0.79	1.05
Lauric acid	C12:0	0.45	0.15	-	-	0.44	1.07	0.46	-	0.74	-	0.52	0.06
Behenic acid	C22:0	0.06	0.57	0.52	0.12	0.14	-	-	-	-	0.61	-	0.42
Saturated FA (%)		37.87	37.94	38.66	37.18	38.42	37.46	38.24	38.36	38	38.14	38.77	39.21
Monounsaturated FA (%)		60.43	60.41	60.82	61.29	61.58	61.5	60.68	59.67	61.56	61.32	60.38	59.78
Polyunsaturated FA (%)		1.7	1.65	0.52	1.53	-	1.04	1.08	1.97	0.44	0.54	0.85	1.01
Total (%)		100	100	100	100	100	100	100	100	100	100	100	100

6. Conclusion

The optimal candidate to engender better engine performance and mitigate emissions has been numerically determined. Major FAME fingerprints that influence engine performance and emission were estimated within acceptable standards using linear algebra based on FA composition. The numerically generated FAME was produced by the transesterification of WSO and WPO using five different catalyst particle sizes of CaO produced from high-temperature calcination of waste chicken eggshells. The outcome of the application of MATLAB to solve the ensuing linear equation consisting of the objective function and the constraints yielded a FAME candidate with palmitic and oleic acids of 36.4 % and 59.8 % respectively.

Although the actual candidate could not be produced experimentally, a candidate with similar characteristics and FA in the range of the optimal FAME candidate was generated. The types of feedstock, the food items fried in the oil, as well as the different particle sizes, were ascertained to have an effect on the FA composition of the FAME produced through the transesterification process. Going forward, the FAME candidates should be tested on an unmodified CI engine to measure engine performance and emissions.

However, a research gap still exists on the modalities to produce the exact FAME candidate. Specifically, more investigations should be carried out on the hybridization of feedstock or mixing of FAME from the various feedstocks. Also, the actual effect of catalyst particle size and other parametric factors that can affect the FA composition of FAME should be thoroughly investigated.

Conflict of Interest

The authors declare no conflict of interest.

References

[1] G. Dwivedi and M. P. Sharma, "Impact of cold flow properties of biodiesel on engine performance," *Renewable and Sustainable Energy Reviews,* vol. 31, pp. 650-656, 2014.

[2] L. Wood. (2017) Global Biodiesel Market Forecasts to 2025. Available on https://www.researchandmarkets.com/research/cc7mbw/global_biodiesel. *Research and Markets.*

[3] Statista. Biofuels: global consumption 1990-2035. Available on https://www.statista.com/statistics/243942/worldwide-consumption-of-biofuels/.

[4] E. Onuh, F. Inambao, and O. Awogbemi, "Performance and emission evaluation of biodiesel derived from waste restaurant oil and Moringa oleifera: A comparative study," *International Journal of Ambient Energy,* no. just-accepted, pp. 1-15, 2019.

[5] E. Onuh and F. L. Inambao, "A comparative evaluation of biodiesel derived from waste restaurant oil and Moringa," in*, 2017 International Conference on Domestic Use of Energy (DUE)*, 2017, pp. 210-218: IEEE.

[6] P. Pranav, T. Patel, and K. P. Singh, "Development of database and mathematical models for predicting engine performance parameters using biodiesel," *International Journal of Agricultural and Biological Engineering,* vol. 10, no. 3, p. 121, 2017.

[7] H. Jääskeläinen. Research Engines for Optical Diagnostics. Available on https://www.dieselnet.com/tech/diesel_comb_res.php#tech .

[8] B. Sajjadi, A. A. A. Raman, and H. Arandiyan, "A comprehensive review on properties of edible and non-edible vegetable oil-based biodiesel: Composition, specifications and prediction models," *Renewable and Sustainable Energy Reviews,* vol. 63, pp. 62-92, 2016.

[9] G. R. Stansell, V. M. Gray, and S. D. Sym, "Microalgal fatty acid composition: implications for biodiesel quality," *Journal of Applied Phycology,* journal article vol. 24, no. 4, pp. 791-801, August 01 2012.

[10] S. Pinzi, P. Rounce, J. M. Herreros, A. Tsolakis, and M. Pilar Dorado, "The effect of biodiesel fatty acid composition on combustion and diesel engine exhaust emissions," *Fuel,* vol. 104, pp. 170-182, 2013.

[11] S. M. Miraboutalebi, P. Kazemi, and P. Bahrami, "Fatty Acid Methyl Ester (FAME) composition used for estimation of biodiesel cetane number

employing random forest and artificial neural networks: a new approach," *Fuel,* vol. 166, pp. 143-151, 2016.

[12] M. Balat and H. Balat, "Progress in biodiesel processing," *Applied Energy,* vol. 87, no. 6, pp. 1815-1835, 2010.

[13] G. Knothe, J. Krahl, and J. Van Gerpen, *The biodiesel handbook*. Elsevier, 2015.

[14] A. Atabani *et al.*, "Non-edible vegetable oils: a critical evaluation of oil extraction, fatty acid compositions, biodiesel production, characteristics, engine performance and emissions production," *Renewable and Sustainable Energy Reviews,* vol. 18, pp. 211-245, 2013.

[15] L. F. Ramírez-Verduzco, J. E. Rodríguez-Rodríguez, and A. del Rayo Jaramillo-Jacob, "Predicting cetane number, kinematic viscosity, density and higher heating value of biodiesel from its fatty acid methyl ester composition," *Fuel,* vol. 91, no. 1, pp. 102-111, 2012.

[16] R. Piloto-Rodríguez, Y. Sánchez-Borroto, M. Lapuerta, L. Goyos-Pérez, and S. Verhelst, "Prediction of the cetane number of biodiesel using artificial neural networks and multiple linear regression," *Energy Conversion and Management,* vol. 65, pp. 255-261, 2013.

[17] M. J. Pratas, S. V. Freitas, M. B. Oliveira, S. C. Monteiro, Á. S. Lima, and J. A. Coutinho, "Biodiesel density: Experimental measurements and prediction models," *Energy & Fuels,* vol. 25, no. 5, pp. 2333-2340, 2011.

[18] R. Sakthivel, K. Ramesh, R. Purnachandran, and P. M. Shameer, "A review on the properties, performance and emission aspects of the third generation biodiesels," *Renewable and Sustainable Energy Reviews,* 2017.

[19] E. Alptekin, M. Canakci, and H. Sanli, "Biodiesel production from vegetable oil and waste animal fats in a pilot plant," *Waste Management,* vol. 34, no. 11, pp. 2146-2154, 2014.

[20] P. Saxena, S. Jawale, and M. H. Joshipura, "A Review on Prediction of Properties of Biodiesel and

Blends of Biodiesel," *Procedia Engineering,* vol. 51, pp. 395-402, 2013.

[21] H. Sanli, M. Canakci, and E. Alptekin, "Predicting the higher heating values of waste frying oils as potential biodiesel feedstock," *Fuel,* vol. 115, pp. 850-854, 2014.

[22] A. E. Atabani, "A comprehensive review on biodiesel as an alternative energy resource and its characteristics," (in eng), *Renewable and Sustainable Energy Reviews,* vol. 16, no. 4, p. 2070, 2012.

[23] K. Muralidharan, D. Vasudevana, and K. N. Sheeba, "Performance, emission and combustion characteristics of biodiesel fuelled variable compression ratio engine," (in eng), *Energy,* vol. 36, no. 8, p. 5385, 2011.

[24] U. Rashid, F. Anwar, and G. Knothe, "Evaluation of biodiesel obtained from cottonseed oil," *Fuel Processing Technology,* vol. 90, no. 9, pp. 1157-1163, 2009.

[25] F. Al-Shanableh, E. Ali, and M. A. Savaş, "Fuzzy logic model for prediction of cold filter plugging point of biodiesel from various feedstock," *Procedia Computer Science,* vol. 120, pp. 245-252, 2017.

[26] P. A. Leggieri, M. Senra, and L. Soh, "Cloud point and crystallization in fatty acid ethyl ester biodiesel mixtures with and without additives," *Fuel,* vol. 222, pp. 243-249, 2018.

[27] M. A. Wakil, M. A. Kalam, H. H. Masjuki, A. E. Atabani, and I. M. Rizwanul Fattah, "Influence of biodiesel blending on physicochemical properties and importance of mathematical model for predicting the properties of biodiesel blend," *Energy Conversion and Management,* vol. 94, pp. 51-67, 2015.

[28] G. Knothe and L. F. Razon, "Biodiesel fuels," *Progress in Energy and Combustion Science,* vol. 58, pp. 36-59, 2017.

[29] G. Knothe and K. R. Steidley, "Kinematic viscosity of biodiesel fuel components and related compounds. Influence of compound structure and

comparison to petrodiesel fuel components," *Fuel,* vol. 84, no. 9, pp. 1059-1065, 2005.

[30] P. S. Mehta and K. Anand, "Estimation of a lower heating value of vegetable oil and biodiesel fuel," *Energy & Fuels,* vol. 23, no. 8, pp. 3893-3898, 2009.

[31] S. Pinzi, D. Leiva, G. Arzamendi, L. Gandia, and M. Dorado, "Multiple response optimization of vegetable oils fatty acid composition to improve biodiesel physical properties," *Bioresource Technology,* vol. 102, no. 15, pp. 7280-7288, 2011.

[32] E. G. Giakoumis and C. K. Sarakatsanis, "Estimation of biodiesel cetane number, density, kinematic viscosity and heating values from its fatty acid weight composition," *Fuel,* vol. 222, pp. 574-585, 2018.

[33] M. Mostafaei, "Prediction of biodiesel fuel properties from its fatty acids composition using ANFIS approach," *Fuel,* vol. 229, pp. 227-234, 2018.

[34] M. Agarwal, K. Singh, and S. Chaurasia, "Prediction of biodiesel properties from fatty acid composition using linear regression and ANN techniques," *Indian Chemical Engineer,* vol. 52, no. 4, pp. 347-361, 2010.

[35] M. J. Ramos, C. M. Fernández, A. Casas, L. Rodríguez, and Á. Pérez, "Influence of fatty acid composition of raw materials on biodiesel properties," *Bioresource Technology,* vol. 100, no. 1, pp. 261-268, 2009.

[36] L. F. Ramírez-Verduzco, J. E. Rodríguez-Rodríguez, and A. d. R. Jaramillo-Jacob, "Predicting cetane number, kinematic viscosity, density and higher heating value of biodiesel from its fatty acid methyl ester composition," *Fuel,* vol. 91, no. 1, pp. 102-111, 2012.

[37] M. Gülüm and A. Bilgin, "Measurements and empirical correlations in predicting biodiesel-diesel blends' viscosity and density," *Fuel,* vol. 199, pp. 567-577, 2017.

[38] R. Razavi, A. Bemani, A. Baghban, A. H. Mohammadi, and S. Habibzadeh, "An insight into the estimation of fatty acid methyl ester based biodiesel properties using a LSSVM model," *Fuel,* vol. 243, pp. 133-141, 2019.

[39] F. Al-Shanableh, A. Evcil, and M. A. Savaş, "Prediction of Cold Flow Properties of Biodiesel Fuel Using Artificial Neural Network," *Procedia Computer Science,* vol. 102, pp. 273-280, 2016.

[40] J. Li, W. Yang, and D. Zhou, "Modeling study on the effect of piston bowl geometries in a gasoline/biodiesel fueled RCCI engine at high speed," *Energy Conversion and Management,* vol. 112, pp. 359-368, 2016.

[41] K. Ryu, "Effects of pilot injection pressure on the combustion and emissions characteristics in a diesel engine using biodiesel–CNG dual fuel," *Energy Conversion and Management,* vol. 76, pp. 506-516, 2013.

[42] W. Tutak, A. Jamrozik, M. Pyrc, and M. Sobiepański, "A comparative study of co-combustion process of diesel-ethanol and biodiesel-ethanol blends in the direct injection diesel engine," *Applied Thermal Engineering,* vol. 117, pp. 155-163, 2017.

[43] T. Selvan and G. Nagarajan, "Combustion and emission characteristics of a diesel engine fuelled with biodiesel having varying saturated fatty acid composition," *International Journal of Green Energy,* vol. 10, no. 9, pp. 952-965, 2013.

[44] P. Tamilselvan and G. Nagarajan, "Combustion and emission characteristics of a diesel engine fuelled with biodiesel having varying palmitic acid, stearic acid and oleic acid in their fuel composition," *International Journal of Oil, Gas and Coal Technology,* vol. 8, no. 3, pp. 353-368, 2014.

[45] E. Jiaqiang, T. Liu, W. Yang, J. Li, J. Gong, and Y. Deng, "Effects of fatty acid methyl esters proportion on combustion and emission characteristics of a biodiesel fueled diesel engine," *Energy Conversion and Management,* vol. 117, pp. 410-419, 2016.

[46] Z. Zhang *et al.*, "Effects of fatty acid methyl esters proportion on combustion and emission

characteristics of a biodiesel fueled marine diesel engine," *Energy Conversion and Management,* vol. 159, pp. 244-253, 2018.

[47] A. O. Barradas Filho *et al.*, "Application of artificial neural networks to predict viscosity, iodine value and induction period of biodiesel focused on the study of oxidative stability," *Fuel,* vol. 145, pp. 127-135, 2015.

[48] S. K. Hoekman, A. Broch, C. Robbins, E. Ceniceros, and M. Natarajan, "Review of biodiesel composition, properties, and specifications," *Renewable and Sustainable Energy Reviews,* vol. 16, no. 1, pp. 143-169, 2012.

[49] X. Meng, M. Jia, and T. Wang, "Neural network prediction of biodiesel kinematic viscosity at 313K," *Fuel,* vol. 121, pp. 133-140, 2014.

[50] N. Moradi-kheibari, H. Ahmadzadeh, M. A. Murry, H. Y. Liang, and M. Hosseini, "Chapter 13 - Fatty Acid Profiling of Biofuels Produced From Microalgae, Vegetable Oil, and Waste Vegetable Oil," in *Advances in Feedstock Conversion Technologies for Alternative Fuels and Bioproducts*, M. Hosseini, Ed.: Woodhead Publishing, 2019, pp. 239-254.

[51] S. Mitra, P. Bose, and S. Choudhury, "Mathematical Modeling for the Prediction of Fuel Properties of Biodiesel from their FAME Composition," in *Key Engineering Materials*, 2011, vol. 450, pp. 157-160: Trans Tech Publ.

[52] O. Awogbemi, F. L. Inambao, and E. I. Onuh, "Development and Characterization of Chicken Eggshell waste as Potential Catalyst For Biodiesel Production," *International Journal of Mechanical Engineering and Technology,,* vol. 9, no. 12, pp. 1329 - 1346, 2018.

[53] I. M. Monirul *et al.*, "Assessment of performance, emission and combustion characteristics of palm, jatropha and Calophyllum inophyllum biodiesel blends," *Fuel,* vol. 181, pp. 985-995, 2016.

[54] A. N. Ozsezen, M. Canakci, A. Turkcan, and C. Sayin, "Performance and combustion characteristics of a DI diesel engine fueled with waste palm oil and canola oil methyl esters," *Fuel,* vol. 88, no. 4, pp. 629-636, 2009.

[55] M. Serrano, A. Bouaid, M. Martínez, and J. Aracil, "Oxidation stability of biodiesel from different feedstocks: influence of commercial additives and purification step," *Fuel,* vol. 113, pp. 50-58, 2013.

[56] I. M. Rizwanul Fattah, H. H. Masjuki, M. A. Kalam, M. Mofijur, and M. J. Abedin, "Effect of antioxidant on the performance and emission characteristics of a diesel engine fueled with palm biodiesel blends," *Energy Conversion and Management,* vol. 79, pp. 265-272, 2014.

[57] D. Kumar and A. Ali, "Nanocrystalline K–CaO for the transesterification of a variety of feedstocks: Structure, kinetics and catalytic properties," *Biomass and Bioenergy,* vol. 46, pp. 459-468, 2012.

[58] A. N. Ozsezen and M. Canakci, "Determination of performance and combustion characteristics of a diesel engine fueled with canola and waste palm oil methyl esters," Energy Conversion and Management, vol. 52, no. 1, pp. 108-116, 2011.

CHAPTER 5: PERFORMANCE AND EMISSION EVALUATION OF BIODIESEL DERIVED FROM WASTE RESTAURANT OIL AND MORINGA OLEIFERA: A COMPARATIVE STUDY

This chapter examines the performance and emission characteristics of a CI engine fuelled with biodiesel synthesis from waste cooking oil (WCO) and *Moringa oleifera* oil. The article, among other things, compared FAME composition of neat *Moringa oleifera* oil and palm oil with the biodiesel derived from *Moringa* oil and WCO, showcased and compared the engine performance and emission of moringa oleifera methyl ester (MOME) and waste *oleifera* methyl ester (WOME). The outcome of the experimental investigation was published in the International Journal of Ambient Energy, Taylor and Francis Publishers.

Taylor & Francis
Taylor & Francis Group

Check for updates

Performance and emission evaluation of biodiesel derived from waste restaurant oil and *Moringa oleifera*: a comparative study

E. I. Onuh ⬥, F. Inambao and O. Awogbemi ⬥

Mechanical Discipline, School of Engineering, University of Kwazulu-Natal, Durban, South Africa

ABSTRACT

Biodiesel as an alternative to fossil-based diesel has shown great promise but, sustainable feedstock source remains a challenge. Biodiesel produced from waste restaurant oil and *Moringa oleifera* had their thermophysical and engine characteristics evaluated in a validated property prediction scheme and a 3.5-kW direct injection compression ignition engine. Results revealed that waste restaurant oil biodiesel with a relatively higher palmitate of 20% (saturated fatty acid methyl ester [FAME]) and oleic of 52.8% (unsaturated FAME) had a 5% higher brake thermal efficiency (BTE) at peak load, a 65% lower brake specific fuel consumption (BSFC) across the load spectrum and 5% to 10% lower brake specific carbon monoxide (BSCO) than Moringa biodiesel which had 6.5% palmitate and 72.2% oleic. Regarding brake specific NOx (BSNO$_X$) emission, Moringa biodiesel showed a lower level of 6.2% across the full load spectrum.

1. Introduction

Pressure continues to mount globally on the need to substitute finite fossil sourced transportation fuel with renewable alternatives for several reasons, the most compelling being environmentally dangerous emissions and their impact on the global climate (Balat 2011). As a result, biofuel has gained traction as a strategy of choice to confront these challenges in the energy sector, particularly in the transport sub-sector. This choice presents considerable advantages for developing countries because they are relatively cheap to produce due to cheap labour costs and access to land resources (Balat 2011). Biodiesel production is quite modern and has been successfully commercialised in several countries. As a result, standards to ensure quality control have been extensively developed. These include: (i) American Society for Testing and Materials (ASTM) ASTM D6751 (ii) European Standard EN 14214 (Knothe 2006). Biodiesel is often blended with diesel; in Europe it is mostly up to 5%. It is predominantly used as blend of up to 20% with diesel storage devices and does not require any engine modification. Pure (100%) biodiesel can also be used in many engines with little or no modification, particularly in farm power equipment (Raheman, Jena, and Jadav 2013). Biodiesel advantages include: (i) liquid nature-portability (ii) ready availability (iii) renewability (iv) higher combustion efficiency (v) low sulphur and aromatic content (vi) higher cetane number (vii) biodegradability. On the other hand, its disadvantages include: (i) higher viscosity (ii) lower energy content (iii) high cloud point and pour point (iv) high NOx (v) injector coking (vi) higher engine wear (Raheman, Jena, and Jadav 2013).

Biodiesel feedstock has been generally obtained from a wide range of sources. The first-generation biodiesel was produced from seed oils such as soy beans, rapeseed etc., but concerns about its sustainability were raised because of food security issues, particularly in developing countries. As at 2010, 95% of the world biodiesel production was from edible oil (Balat 2011). Between 2004 and 2007, vegetable oil production globally increased by 6.6 million tons, 34% of this increase being attributed to biodiesel use (Mitchell 2008). Between 2005 and 2017, biodiesel use of edible oil accounted for a third of the growth in edible oil production (Aransiola et al. 2014). These increases are expected to put enormous strain on the use of land resources; in the US and EU it is unlikely that there will be sufficient land available to meet the growing demand for the production of biodiesel (Gibbs et al. 2008). Already, as at 2007, 7% of global edible oil production was being used for biodiesel production. It is self-evident that a combination of a rapidly growing world population and growing demand for biodiesel is set to raise concerns regarding food security and increase resistance against the use of edible oil for fuel production, especially considering that nearly 60% of the global human population is currently malnourished and the need for food and basic crops is critical. Therefore, suitable alternative feedstock should be found for fuel, which do not compete directly as a food source.

Besides the obvious challenges associated with the use of edible oil, the current cost of using edible oil for biodiesel production is unsustainable and this gives a comparative advantage to conventional diesel. Biodiesel from edible oil usually costs over US $0.5 per litre compared to diesel which cost US $ 0.35 per litre as at 2010 (Zhang et al. 2003). The price of biodiesel varies depending on base stock, geography and variability of crop from season to season. These and other reasons make a compelling case for the use of non-edible feedstock for the production of biodiesel. Non-edible oil seed crops such as *Jatropha*, *Karanja*, tobacco seed, rice bran, rubber plant, castor, linseed

and micro-algae have all been extensively explored as potential sources of biodiesel production (Balat 2011). Within the context of South Africa, it is the author's opinion that waste cooking oil (WCO) in the form of waste restaurant oil holds the most potential and benefits as a source of non-edible biodiesel. Exotic oils such as Moringa oil have also been suggested in some form as a possible alternative, hence the need of a comparative analysis.

In the case of waste restaurant oil, an entire industry already exists for the production of WCO by default, mainly being the food industry, the hospitality industry, and households. Prior to its use as a biodiesel, the product has been regarded as waste at the end of the supply chain and is discarded. Nahman et al. (2012) estimated that food waste accounts for 4.14% of GDP in South Africa, of which WCO is a significant component. An estimated 200,000 tons of WCO are generated but uncollected annually in South Africa. This uncollected WCO contributes to soil and water contamination, sewage blockages, and damage to aquatic life (Hamze, Akia, and Yazdani 2015). A number of enterprises have been set up to take advantage of this opportunity, including Green Tech in the Eastern Cape, Environ diesel in Cape Town, and Khezi oil in KwaZulu-Natal (Brand South Africa 2016). Moringa oil is extracted from *Moringa oleifera* and has many useful properties thus its commercial production will have many associate benefits. The oil has excellent therapeutic properties and is used in the following areas (i) antioxidant (ii) anti-inflammatory (iii) anti-ageing (iv) anti-microbial (v) disinfectant (vi) hepatoprotective (vii) emollient (viii) preservative (ix) exfolient (x) effleurage. Moringa is made up of mainly monounsaturated fatty acid and saturated fats, and contains about 70% oleic acid. Clearly, a well calibrated legislative framework is needed to ring-fence the industry to enable it to thrive. This is an imperative because of South Africa's current challenge with meeting base demand for diesel.

South Africa's production of petrol and diesel has decreased marginally from 20.2 billion litres in 2002 to 19.7 billion litres in 2013 due to capacity constraints, but consumption has grown at 3% annually during the same period (Brand South Africa 2016). There are fears that the widening gap between production and consumption could potentially inhibit economic growth if local solutions are not found. As at 2013, the gap between demand and supply for diesel is about half a billion litres. The key questions, going forward, will then be: of the various options available for sourcing biodiesel from nonedible sources, which sources hold the most economic benefit and at the same time meet sustainability criteria. But more importantly, from a technical point of view, which of the options will enhance engine performance at acceptable emission levels. And where emission and performance gaps exist, can local regulations be developed to guarantee standards and mitigate likely defects in production process. It is against this background that this work set out to conduct a comparative study of Moringa biodiesel (Moringa methyl ester [MOME]) and waste restaurant oil (waste oil methyl ester [WOME]).

The fuel samples were produced by means of conventional methods. Their thermophysical properties were experimentally determined and subsequently matched with results obtained from a validated property prediction scheme to identify production process gaps in the conventional methods. Subsequently, the fuels were then evaluated in a 3.5 kW diesel engine to

determine their engine performance and emissions using the ISO 8178-4 engine test protocol (Knothe, Van Gerpen, and Krahl 2005). Whereas some studies have suggested a direct correlation between free fatty acid susceptibility to oxidation and its level of unsaturation, others have submitted that the reverse is the case under certain conditions (Schonborn et al. 2009). Part of the focus of this study was to experimentally investigate that relationship. This investigation sought to determine whether WCO combusted more efficiently in a compression ignition (CI) engine than unused (virgin) vegetable oil or vice versa. If a complimentary relationship is established, it could assuage some of the concern regarding food security.

2. Theory and experimental method

The combustion characteristics, performance and emissions of biodiesel in a CI engine is largely determined by the thermophysical and transport properties of the FAME composition of the fuel and the engine configuration. Properties like density, heating value, viscosity, cetane number and cold flow properties are influenced by FAME composition and can be predicted (Onuh and Inambao 2016a). Fuel chemistry therefore plays an important role and since biodiesel is essentially a mixture of different compositions of FAME, the aggregate composition determines the engine outcome. Typically, if the experimental process is of highest quality and the numerical fidelity is maintained, the results of the experimental property determination and the theoretical property prediction will converge. The first approach in this study was to employ the routine experimental methods prescribed by the ASTM code to determine the properties and subsequently use the validated prediction scheme to measure gaps in the experiment. The extent of the gaps and measures to cover them can be sued to define the standards to be recommended to provide the platform for industrial grade biodiesel production. The second approach was to evaluate (using ISO 8178-4 engine test protocol) the two fuel samples (MOME and WOME) in a CI engine with the aim of comparing their performance and emission outcomes.

2.1. Experimental property determination

The fatty acid (FA) composition of the neat Moringa oil and WCO samples were determined by pyrolysis gas chromatography mass spectrometer (PYGCMS) on a Shimadzu Gas Chromatograph Mass Spectrometer using an ultra-alloy-5 capillary column and GCMS-QP2010 Plus software. The choice of PYGCMS as against the normal GCMS was due to the low volatility nature of the samples which might clog the column of the GCMS machine. The adopted method was as shown in Table 1.

Trans-esterification was achieved with methanol using potassium oxide as an alkaline catalyst. The resulting biodiesel was processed and tested. The standards proposed by regulation and which were adopted in determining the properties are stated in ASTM D6751.

2.2. FAME composition and property correlations

Biodiesel FAME compositions were analysed using gas chromatography (GC). The compositions were obtained from secondary sources with similar sample backgrounds. MOME FAME

Table 1. GCMS test configuration.

Carrier gas		Helium
Injection volume		2 µL
Column oven temperature		40.0°C
Injection temperature		240°C
Injection mode		Split
Flow control mode		Pressure
Pressure		100.0 kPa
Total flow		58.2 mL/min
Column flow		1.78 mL/min
Linear velocity		48.1 cm/sec
Purge flow		3.0 mL/min
Split ratio		30.0
Oven temperature program		
Rate (°C/min)	Temperature (°C)	Hold time (min)
–	40.0	5.00
5.00	125.0	0.00
3.00	285.0	0.00
5.00	320.0	10.00
Ion source temperature		200.00°C
Interface temperature		250.00°C
Solvent cut time		1.00 min
Start time		1.00 min
End time		92.33 min

Table 2. Sample FAME composition.

FAME	WOME (%)	MOME (%)
Myristic (C14:0)	0.9	
Palmitic (C16:0)	20.4	6.5
Palmitoleic (C16:1)	4.6	2.0
Stearic (C16:0)	4.8	6.0
Oleic (C18:1)	52.9	72.2
Linoleic (C18:2)	13.5	1.0
Linolenic (C18:3)	0.8	
Arachidic (C20:0)	0.12	4.0
Eicosenic (C20:1)	0.84	2.0
Behenic (C22:0)	0.03	6.74
Erucic (C22:1)	0.07	
Tetracosanic (C24:0)	0.04	
U_{FAME}	72.01	77.0

composition was obtained from the work of Azad et al. (2015) and WOME from Chhetri, Watts, and Islam (2008). Details are given in Table 2.

FAME properties are influenced by carbon chain length and the degree of unsaturation (number of double or more bonds).

Table 3 gives detail of linear correlations used to predict the properties. Where ρ_i, z, M_i N_c, U_{FAME} and N_{DB} are the density, ratio of given FAME composition, molecular weight of ith FAME, carbon chain length, total unsaturated FAME and the average weighted number of double bonds respectively. n is the number of experimental or data points, and f_{iexp} and f_{ical} represent the function that determines the experimental and calculated properties of individual FAME or biodiesel properties. An algorithm to predict WOME and MOME properties using the FAME composition 'fingerprint' and the correlations in Tables 2 and 3 respectively was then implemented using C+ code. The objective of the scheme was to predict seven properties of biodiesel derived from MOME and WOME using four independent variables obtained from a single experiment.

2.3. Engine test protocol

The test protocol was ISO 8178-4: 2007 with a test cycle categorisation range of between C1, C2, E1, E2, F, G, G3 and H which

Table 3. Correlation predicting FAME property.

Property	Correlation
Density (ρ_i)–(kg/m³)	$\rho_i = 0.8463 + \frac{4.9}{M_i} + 0.0118 N_{DB}$
Higher heating value (δ_i)–(kJ/kg)	$\delta_i = 49.19 - \frac{1794}{M_i} - 0.2 N_{DB}$
Kinematic viscosity (η-cSt)	$\eta = 0.235 N_c - 0.468 N_{DB}$
Cetane number (CN)	$CN = 3.930 N_c - 15.936 N_{DB}$
Flash point (T_f)–(°C)	$T_f = 23.362 N_c + 4.854 N_{DB}$
Cloud point, C_p (°C)	$C_p = 18.134 N_c - 0.790 (U_{FAME})$
Pour point, P_p (°C)	$P_p = 18.880 (N_c) - 1.00 (U_{FAME})$
Cold flow plugging point (CFPP) – (°C)	$CFPP = 18.019 N_c - 0.804 (U_{FAME})$
Mixing rule	$f_b = \sum_{i=1}^{n} z_i f_i$
Average relative deviation (ARD)	$ARD = \frac{1}{n}\left(\sum_{i=1}^{n}\left\lvert \frac{(f_{iexp} - f_{ical})}{f_{iexp}} \times 100 \right\rvert\right)$

covers the broad range of engine application types currently in use (International Standards Organization 2007). This test protocol gives specific detail about loading profile, speed range, test cycle duration, etc.

The test engine was a 3.5 kW rated, direct injection (DI), single-cylinder diesel engine. Selected test speeds were 1800, 2500 and 3600 rpm. Each test cycle at selected torque consisted of running the engine for 1 min at idle speed and 9 min at selected load in accordance with test cycle G3 of ISO 8178-4. The engine rated power was taken as 100% load. The SV-5Q exhaust gas analyzer was deployed in accordance with ND112 (nondispersive infrared) via micro computer analysis to measure the thickness of unburnt hydrocarbon (HC), carbon monoxide (CO) and carbon dioxide (CO_2) in the exhaust gas and to inspect the density of NO_X and O_2 via electrochemical sensors. The excess air coefficient, λ was also computed automatically by the analyzer. HC and NO_X were measured in ppm whereas CO, CO_2 and O_2 were measured in percentages. Given the standard measures stipulated by ISO 8178-4, it was necessary to convert these measurements into g/kWh using the air and fuel flow method (National Center for Biotechnology Information 2018). The prevailing ambient temperature at the time of the test ranged between 30°C and 33°C and the relative humidity between 71% and 75%. Recorded atmospheric pressure was 92 kPa, air density 1.208 kg/m³ and absolute humidity, 0.022 kg/m³. From these data, the specific humidity and kH were computed. An exhaust gas sampling probe inserted in the exhaust line drew exhaust gas through a filter enroute to the gas analyzer. The particulate matter (PM) was measured by trapping it with a filter (which was replaced at the end of every test cycle) which was weighed to obtain a direct mass measurement on a weighting device with a 1 µg resolution. This method was adopted because mass-based PM is the regulated format by the United States Environmental Protection Agency (EPA) and the European Union (EU).

3. Result and discussion

Results of the pyrolysis gas chromatography mass spectrometer (PYGCMS) for the MOME and WOME are shown in Table 4. Substances harmful to human consumption, found in the test of the WCO (Table 5), clearly established the unsuitability of WCO for human consumption.

Table 4. PYGCMS of feedstock.

Common name	Formula	Fatty acid Acronym	MOME	WOME
Oleic acid	$CH_3(CH_2)_7CH = CH(CH_2)_{11}COOH$	C18:1	0.24	14.39
Palmitic acid	$CH_3(CH_2)_{14}COOH$	C16:0	35.77	40.21
Linoleic acid	$CH_3(CH_2)_4CH = CHCH_2CH = CH(CH_2)_7COOH$	C18:2	16.18	
Erucic acid	$CH_3(CH_2)_7CH = CH(CH_2)_{11}COOH$	C22:1		
Caprylic acid	$CH_3(CH_2)_6COOH$	C8:0		
Enanthic acid	$CH3(CH2)5COOH$	C7:0	0.18	
Capric acid	$CH3(CH2)8COOH$	C10:0	0.41	
Undecylic acid	$CH_3(CH_2)_9COOH$	C11:0		
Stearic acid	$CH_3(CH_2)_{16}COOH$	C18:0	12.87	
Myristic acid	$CH_3(CH_2)_{12}COOH$	C14:0		17.04
Nonadecylic acid	$CH_3(CH_2)_{17}COOH$	C19:0		
	Saturated Fatty Acid, SFA (%)		74.99	80
	Monounsaturated Fatty Acid, MUFA (%)		0.37	20

Table 5. Harmful chemicals found in waste cooking oil.

2,3-Dihydroxypropyl elaidate	$C_{21}H_{40}O_4$	Harmful if swallowed Causes serious eye irritation	National Center for Biotechnology Information (2018)
1-Hexanol	$C_6H_{14}O$	Harmful if swallowed or in contact with skin Causes serious eye irritation	Ditto
Palmitic acid	$C_{16}H_{32}O_2$	Causes acute skin, eye and respiratory irritations Harmful to aquatic life with long lasting effects	Ditto
Linoleic acid	$C_{18}H_{32}O_2$	Causes skin, eye and respiratory irritations May cause long lasting harmful effects to aquatic life	Ditto
i-Propyl 14-methyl-pentadecanoate	$C_{16}H_{32}O_2$	Toxic to aquatic organisms and wildlife habitat Causes eye and skin irritations and lung injury Long-term negative health effects Acute mammalian inhalation toxicity	Ditto
1-Heptene	C_7H_{14}	Highly flammable liquid and vapour May be fatal if swallowed and enters airways Very toxic to aquatic life with long lasting effects	Ditto
cis-9-Hexadecenal	$C_{16}H_{30}O$	Causes skin, acute eye, and respiratory irritations Harmful if inhaled Very toxic to aquatic life	Ditto

The predicted properties using the code base on correlations are given in Table 3, and the experimentally determined properties using the ASTM test method and the average relative deviation (ARD) estimate obtained by comparing the computed results with a range of experimental data, are all shown in Table 6.

Following the engine test protocol mentioned in 2.3, the performance and emission profile for the fuel samples were evaluated and the outcomes are presented in Figures 2–7. The results are discussed below.

3.1. Predicted and experimental properties

As shown in Table 5, seven properties were simultaneously predicted and experimentally determined. The density, calorific value and cetane number for both WOME and MOME showed results that fell within the ASTM standard for CI engine fuel within acceptable limits of ≤ 5% (Cornell 2015). The transport and cold flow properties such as viscosity, pour point and cold flow plugging point all failed the ARD test when the predicted results were compared with the experimental results. The likely cause of these discrepancies have to do with the sensitivity of these properties with a variety of conditions, namely, the process of production, level of impurities and property altering ambient conditions due to the varying nature of the fuel samples (unsaturated FAME are susceptible to oxidative polymerisation, post-processing) (Cornell 2015).
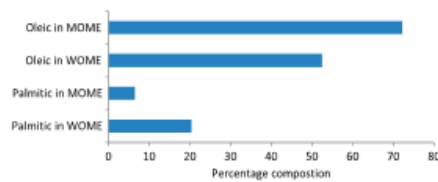
Typically, the production process of biodiesel is such that a complete removal of all impurities is not practicable. These impurities include excess methanol, free glycerin, mono- and diglyceride, metal contaminants, free fatty acids (FFA) and soaps (Banga and Varshney 2010). The presence of these impurities along with the unsaturated nature of the FAME fuel samples leads to deterioration and unpredictability of these properties. The more double bonds and unsaturation that exist, the larger the variation in these properties (Banga and Varshney 2010). This can be seen in Table 2 for MOME and WOME (the former having more double bonds and unsaturation than the latter) where ARDs for almost all the properties were higher in MOME. The implication is that property predictability and stability is more guaranteed for biodiesel obtained from WCO because of its reduced susceptibility to oxidative polymerisation. Another inference drawn from this result is that property prediction tools along with ASTM (or any other biodiesel standard) can be used as a means of universal quality assurance for biodiesel regardless of the feedstock source.

3.2. Engine performance

Brake thermal efficiency (BTE) and brake specific fuel consumption (BSFC) are some of the important gauges for evaluating engine performance of fuel samples (Onuh and Inambao 2016b). Figure 1 shows the composition of palmitic and oleic in both fuel samples, giving an indication of what to expect from the

Table 6. Properties of resulting biodiesel.

Property	Comp. data		ARD (%)		Exp. data	
	MOME	WOME	MOME	WOME	MOME	WOME
Density @40°C(kg/m^3)	832.6	864.09	4.07	1.49	892.98	874.20
Viscosity @40°C(cSt)	3.887	3.911	17.9	18.3	5.10	4.2
Calorific value (kJ/kg)	41.31	42.90	3.82	3.25	40.05	39.4
Cetane number	58.52	58.28	4.9	4.45	–	–
Flash point (°C)	146.78	152.40	9.3	7.0	215	219
Pour point (°C)	−4.14	2.94	3.8	–	1	6
Cold flow plugging point (°C)	−5.34	1.009	–	–	–	–

Figure 1. FAME profile of combustion determinants.

Figure 2. Brake thermal efficiency (BTE).

Figure 3. Brake specific fuel consumption (BSFC).

engine test evaluation. This is because saturated straight chain palmitic has a paraffinic characteristic that easily initiates and sustains both auto-ignition and late-stage combustion heat release which is governed by the $CO + O \rightarrow CO_2$ reaction in CI engines (Salamanca et al. 2012). Double bond unsaturated oleic, on the other hand, slows the start of ignition by attacking the CH_2O, HO_2 and O radicals that drives the low-temperature reaction (LTR) and as a result, the reaction process side steps this vital heat release process by initiating a recombination reaction to form poly-aromatic hydrocarbons (PAH), the precursor of soot (Salamanca et al. 2012).

Figure 2 shows the BTE profile for the two fuel samples for loads ranging from 16.7% to 100%. As expected, efficiency rose from a low base to peak at between 30% and 35% for both samples, depicting a typical performance characteristic for CI engines. It could also be observed that BTE, which is a measure of how efficient the heat release rate for useful work is in an engine, indicated that the WOME profile gave a better performance than MOME for the entire load profile. The difference varied from 20% to about 16% of peak performance, indicating that the band narrowed as engine activity approached optimal level. A slightly higher viscosity for MOME of 5.10 cst compared to WOME of 4.2 cst is partly responsible for this difference but they do not sufficiently explain a double-digit difference in BTE across the entire load spectrum. This significant improvement in BTE of WOME over MOME is clearly explained by the difference in the composition of palmitic and oleic in both the fuel samples (Schonborn et al. 2009). As stated earlier, paraffinic palmitic, which acts as a promoter of auto-ignition and late-stage heat release agent, is approximately three times greater in WOME when compared to MOME 6.5% palmitic. This explains why the viscosity disadvantage of WOME did not diminish its BTE performance. This finding largely agrees with related works in literature (Zheng et al. 2008). Oleic, which had the opposite effect of palmitic, was found to be approximately 40% greater in MOME, further making it easy for WOME BTE performance to trump that of MOME BTE.
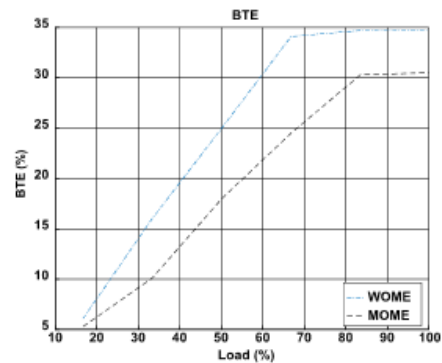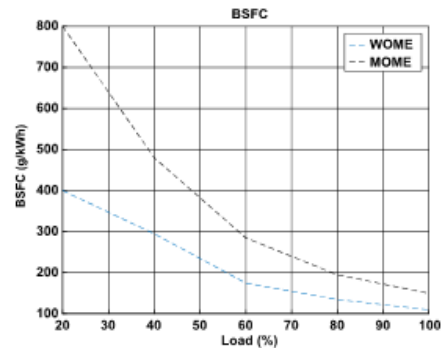
This fact is further revealed by the BSFC of the two fuel samples as shown in Figure 3. In this profile, despite MOME's diminished BTE, its fuel consumption for the entire loading profile was more than that of WOME, decreasing from a 100% difference at idle load (20%) to about 25% difference at peak load (100%).

3.3. Engine emission

Figures 4–7 show the different emission profiles obtained for both fuel samples and the general observation is that the emission increase in brake specific format reveals a consistently downward trend as the engine revs-up through idle load to peak
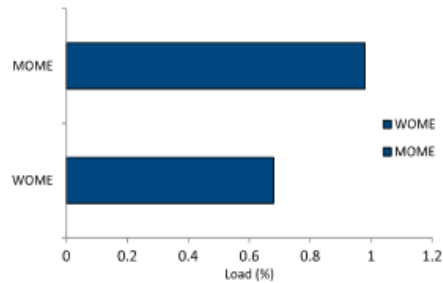
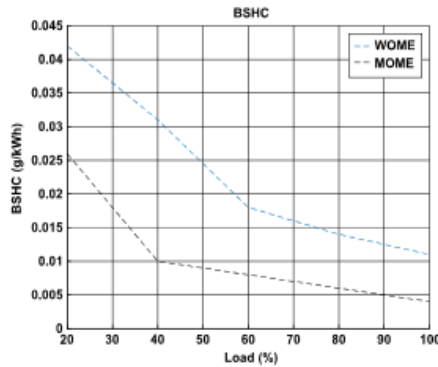**Figure 4.** Brake specific particulate matter (BSPM-soot).

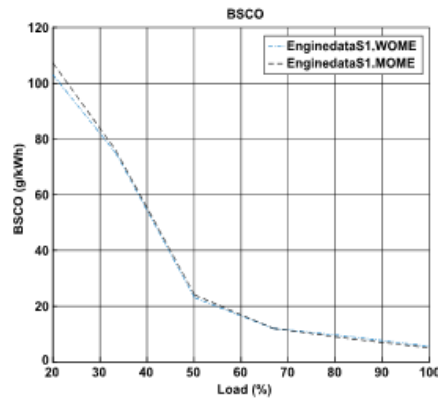**Figure 5.** Brake specific unburnt hydrocarbon (BSHC).

Figure 6. Brake specific carbon monoxide (BSCO).

Figure 7. Brake specific nitrogen oxide (BSNO$_X$).

load. An inverse relationship can be observed between BTE and brake specific emission, that is, optimal engine performance is near impossible for engines at idle to low load. This has a direct impact on clogged traffic intra-city commuting. This trend is generic to CI engines regardless of fuel type (Buyukkaya 2010).
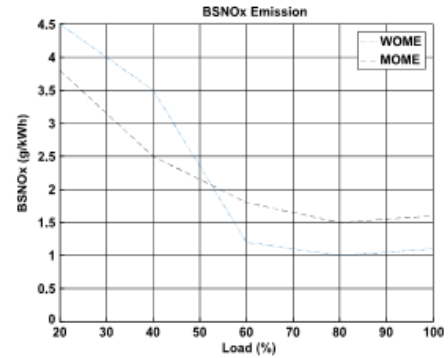
With regard to the emission limit set by the EPA and the EU, the samples showed a varied outcome (Buyukkaya 2010). The brake specific particulate matter (BSPM) results indicated that the EPA and EU limit of 0.4 and 0.5 g/kWh respectively were breached by MOME (Figure 3.4). WOME only passed the EPA limit of 1.5 g/kWh and the EU limits of 1.3 g/kWh (Onuh and Inambao 2016b). Both WOME and MOME only stayed below the EPA and EU limits of 8.0 and 6.5 g/kWh for brake specific carbon monoxide (BSCO) at load limit exceeding 6.5%. Surprisingly, both samples' brake specific NOx (BSNOx) emissions stayed significantly below the EPA and EU limits of 9.5 and 9.2 g/kWh. This can be explained by the fact that thermal NOx production in CI engines is triggered by temperatures above 1560 °k and facilitated by excess air (oxygen specifically). The prevailing temperatures were below this limit and this helped in curtailing the production of NOx.

Specific focus on the various pollutant emissions brings to the fore the role of FAME composition on emissions of the fuel samples. Figure 4 depicts the average BSPM emission for WOME and MOME. WOME's BSPM averaged of 0.68 g/kWh across the entire load spectrum and was less than MOME's emission average by 30.6%. In the diffuse, turbulent and stratified charge/thermal environment of the CI engine, particulate matters (the precursors of soot) are formed and promoted when low-temperature combustion (LTC) is stifled by the inadequacies of straight chain hydrocarbons like the palmitic structure, and the late stage heat release reaction of $CO + O \rightarrow CO_2$ is sabotaged by the recombination reaction of unsaturated double bonds to form poly-aromatic hydrocarbons (PAH) (Salamanca et al. 2012). This phenomenon has been reported in several studies with a similar charge and thermal profiles (Yao, Zheng, and Liu 2009). The inference from this is that oils rich in unsaturated FFA (which are good antioxidants and are therefore healthy food sources for humans) perform poorly when converted to fuel for use in CI engines.

Figure 5 gives the outcome of the emission evaluation of the brake specific unburnt hydrocarbon (BSHC) for the two fuel samples. In the figure, WOME's BSHC can be seen to exceed those of MOME by an average of about 40% across the entire load spectrum. In this result, it may appear as if MOME performed better,

but it should be noted that this is a measure of fuel that did not partake in the combustion reaction, and, as such, the heat content was lost. But when this is added to the BSPM emission where PM are produced by subtracting heat from the engine, it can be clearly seen that BSPM has twice the same effect as BSHC because not only is the heat release potential of BSPM lost, but its production further removes heat from the engine because of the pyrolysis and recombination reaction that produces PAH is endothermic (Schonborn et al. 2009). Typically, BSHC emissions are determined by thermal and charge stratification and the high viscosity of biodiesel makes mixing, droplet formation and evaporation prior to auto-ignition difficult. This is why the emission is highest at idle load and reduces as the engine warms up and picks up speed/power. This also, evidently, accounts for the BSCO emission shown in Figure 6 for the fuel samples. Incomplete combustion normally produces BSHC and BSCO emission simultaneously; one is the mirror of the other, particularly in biodiesel combustion where thermal dissociation of CO_2 is not common (Onuh and Inambao 2016b).

The brake specific NOx (BSNOx) emissions are shown in Figure 7. It can be seen here that between idle and mid-point load, the BSNOx for WOME exceeded those of WOME by about 20%, but from 60% load upward, MOME's BSNOx exceeded WOME's by about 30%. Higher combustion efficiency facilitated by better auto-ignition and heat release rate in WOME at idle to mid-load created better thermal conditions, and, since NO_X production in CI engine is governed by the Zeldovich mechanism, the higher the temperature, the higher the NO_X particularly for oxygenated fuels (Brakora, Ra, and Reitz 2011). But beyond the mid-load point, the higher BSFC MOME combining with a warmer engine resulted in a good fuel oxidation which sufficiently increased the thermal condition leading to higher NO_X production. It is important to note that the level of NO_X production was nevertheless relatively low.

4. Conclusion

This study has revealed that biodiesel derived from waste restaurant oil and moringa seed oil can be used in CI engines with comparatively good results in terms of performance and emissions. The results showed a better outcome for WOME because by default substantial pyrolysis has resulted in the breaking of double bonds and extensive re-use of the restaurant oil has led to saturation, forming straight chain paraffinic hydrocarbons that are well suited for CI engines. The comparative evaluation also revealed that WOME, because of its higher level of saturation and single bonds is more stable and its properties more predictable and as a result, gives better engine performance as well as better emissions than MOME. This is an indication that it is better to use monounsaturated oil as food before converting it into waste form for fuel. The study also revealed that biodiesel, because of its unsaturated FAME structure, continues to have fuel property stability challenges resulting from post-processing susceptibility to oxidation, thus reducing the capacity of engineers to control its properties in storage. The study also reveals the unsuitability of re-packaging of waste cooking oil for re-use (a practice common in poor communities).

References

Aransiola, E. F., T. V. Ojumu, O. O. Oyekola, T. F. Madzimbamuto, and D. I. O. Ikhu-Omoregbe. 2014. "A Review of Current Technology for Biodiesel Production: State of the Art." *Biomass and Bioenergy* 61: 276–297. doi:10.1016/j.biombioe.

Azad, A. K., M. G. Rasul, M. M. K. Khan, C. S. Sharmal, and R. Islam. 2015. "Prospect of Moringa Seed Oil as a Sustainable Biodiesel Fuel in Australia: A Review." *Procedia Engineering* 105: 601–606. doi:10.1016/j.proeng.2015.05.037.

Balat, M. 2011. "Potential Alternatives to Edible Oils for Biodiesel Production – A Review of Current Work." *Energy Conversion and Management* 52 (2): 1479–1492. doi:10.1016/j.enconman.2010.10.011.

Banga, S., and P. K. Varshney. 2010. "Effect of Impurities on Performance of Biodiesel: A Review." *Journal of Scientific and Industrial Research* 69: 575–579. http://hdl.handle.net/123456789/9968.

Brakora, J. L., Y. Ra, and R. D. Reitz. 2011. "Combustion Model for Biodiesel-Fueled Engine Simulations Using Realistic Chemistry and Physical Properties." *SAE International Journal of Engines* 4 (1): 931–947. doi:10.4271/2011-01-0831.

Brand South Africa. 2016. Accessed October 29. http://www.energy.gov.za/files/media/explained/Overview-of-petrol-and-diesel-market-in-SA-between2002-and-2013.pdf.

Buyukkaya, E. 2010. "Effects of Biodiesel on a DI Diesel Engine Performance, Emission and Combustion Characteristics." *Fuel* 89: 3099–3105. doi:10.1016/j.fuel.2010.05.034.

Chhetri, A. B., K. C. Watts, and M. R. Islam. 2008. "Waste Cooking Oil as an Alternate Feedstock for Biodiesel Production." *Energies* 1: 3–18. doi:10.3390/en1010003.

Cornell. 2015. http://www.Law.cornell.edu./cfr/text/40.91.

Gibbs, H. K., M. Johnson, J. A. Foley, T. Holloway, C. Monfreda, N. Ramankutty, and D. Zaks. 2008. "Carbon Payback Times for Crop-Based Biofuel Expansion in the Tropics: The Effects of Changing Yield and Technology." *Environmental Research Letters* 3 (3): 034001. doi:10.1088/1748-9326/3/3/034001.

Hamze, H., M. Akia, and F. Yazdani. 2015. "Optimization of Biodiesel Production From the Waste Cooking oil Using Response Surface Methodology." *Process Safety and Environmental Protection* 94: 1–10. doi:10.1016/j.psep.2014.12.005.

International Standards Organization. 2007. "Reciprocating Internal Combustion Engines: Exhaust Emission Measurement. Part 4: Steady-state and transient test cycles for different engine applications." ISO 8178-4:2007.

Knothe, G. 2006. "Analyzing Biodiesel: Standards and Other Methods." *Journal of the American Oil Chemists' Society* 83: 822–833. doi:10.1007/s11746-006-5033-y.

Knothe, G., J. Van Gerpen, and J. Krahl, eds. 2005. "Basics of the Transesterification Reaction." In *The Biodiesel Handbook*. Urbana, IL: AOCS Press.

Mitchell, D. 2008. "A Note on Rising Food Prices." 2008. World Bank Policy Research Working Paper No. 4682. Washington, DC: World Bank Policy Development Economics Group (DEC). Accessed June 21, 2016. http://documents.worldbank.org/curated/en/229961468140943023/A-note-on-rising-food-prices.

Nahman, A., W. de Lange, S. Oelofse, and L. Godfrey. 2012. "The Costs of Household Food Waste in South Africa." *Waste Management* 32 (11): 2147–2153. doi:10.1016/j.wasman.2012.04.012.

National Center for Biotechnology Information. 2018. PubChem Compound Database; CID = 5364833. Accessed October 14. https://pubchem.ncbi.nlm.nih.gov/compound/5364833.

Onuh, E. I., and F. Inambao. 2016a. "A Property Prediction Scheme for Biodiesel Derived from Non-Edible Feedstock". In; 2016 *International Conference on the Domestic Use of Energy (DUE)*. doi:10.1109/DUE.2016.7466718.

Onuh, E. I., and F. Inambao. 2016b. "Performance and Emission Evaluation of Pure Biodiesel From Non-Edible Feedstock and Waste Oil in a Diesel Engine." *African Journal of Science, Technology, Innovation and Development*, doi:10.1080/20421338.2016.1219483.

Raheman, H., P. C. Jena, and S. S. Jadav. 2013. "Performance of a Diesel Engine With Blends of Biodiesel (From a Mixture of Oils) and High-Speed Diesel." *International Journal of Energy and Environmental Engineering* 4 (6), doi:10.1186/2251-6832-4-6.

Salamanca, M., J. R. Mondragon, P. Agudelo, F. Benjumea, and A. Santamaria. 2012. "Variations in the Chemical Composition and Morphology of Soot Induced by the Unsaturation Degree of Biodiesel and a Biodiesel Blend." *Combustion and Flame* 159: 1100–1108. doi:10.1016/j.combustflame. 2011.10.011.

Schonborn, A., N. J. Ladommatos, R. Williams, A. J. Allan, and J. Rogerson. 2009. "The Influence of Molecular Structure of Fatty Acid Monoalkyl Esters on Diesel Combustion." *Combustion and Flame* 156: 1396–1412. doi:10.1016/j.combustflame.2009.03.011.

Yao, M., Z. Zheng, and H. Liu. 2009. "Progress and Recent Trends in Homogeneous Charge Compression Ignition (HCCI) Engines." *Progress in Energy and Combustion Science* 35: 398–437. doi:10.1016/j.pecs.2009.05.001.

Zhang, Y., M. A. Dube, D. D. McLean, and M. Kates. 2003. "Biodiesel Production From Waste Cooking oil: 1. Process Design and Technological Assessment." *Bioresource Technology* 89: 1–16.

Zheng, M., M. C. Mulenga, G. T. Reader, M. Wang, D. S. K. Ting, and J. Tjong. 2008. "Biodiesel Engine Performance and Emissions in Low Temperature Combustion." *Fuel* 87 (6): 714–722. doi:10.1016/j.fuel.2007.05.039.

CHAPTER 6: DEVELOPMENT AND APPLICATION OF ARTIFICIAL NEURAL NETWORK FOR THE PREDICTION OF ENGINE PERFORMANCE AND EMISSION CHARACTERISTICS OF DIESEL ENGINE USING FATTY ACID COMPOSITIONS

In this chapter, an artificial neural network was developed, trained and applied to predict the performance and emission characteristics of CI engine using FA composition as inputs. Two FAs, namely palmitic acid (C16:0) and stearic acid (C18:0), were used as input parameters on a NNTool platform using a back-propagation (BP) algorithm with a Levenberg-Marquardt (LM) learning algorithm to predict BSFC (g/kWhr), BTE (%), EGT (^{o}C), brake mean effective pressure (BMEP) (bar), CO (%), smoke intensity, NOx (ppm), and UHC (ppm) for a conventional CI engine. The predictive capacity of the model and statistical error parameters such as correlation coefficient, mean square error, root mean square error, and the mean absolute percentage error were evaluated. The outcome of the prediction has been accepted by the *International Journal of Engineering Research and Technology* for publication.

Development and Application of Artificial Neural Network for the Prediction of Engine Performance and Emission Characteristics of Diesel Engine from Fatty Acid Composition

Omojola AWOGBEMI[1], Freddie INAMBAO[2], Emmanuel I, ONUH[3]

Discipline of Mechanical Engineering, Howard College Campus,

University of KwaZulu-Natal, Durban 4041, South Africa.

[1]jolawogbemi2015@gmail.com, orcid = 0000-0001-6830-6434 (Corresponding author)

[2]inambaof@ukzn.ac.za, [3]onuhe@ukzn.ac.za, orcid = 0000-0002-3891-222X

Abstract

The utilization of artificial neural networks (ANN) for the prediction of biofuel properties, engine performance parameters, and emission of gases within statutory regulations in engine research has been topical in recent times and is predicted to replace the cumbersome and highly technical requirements of real-time engine testing. This study developed an ANN model to predict the engine performance and emission parameters of an unmodified compression ignition (CI) engine fueled with biodiesel using two fatty acid compositions as inputs. The ANN model adopted the backpropagation with Levenberg-Marquardt algorithm, tangent-sigmoid transfer function comprising two, eight, and eight nodes as input, hidden, and output layers respectively. The overall regression coefficient (R) was found to be 0.9998 while the R-value for predicted outputs ranged between 0.9966 and 0.9997, the root mean square error varied between 0.01834 and 0.1725, and the mean absolute percentage error was reported to be between 1.6243 % and 4.546 % showing an acceptable prediction accuracy. It was found that the MATLAB NNTool is a reliable and effective tool for the prediction of engine performance parameters and emission of CI engines using two fatty acid compositions as inputs thereby minimize the time, cost, and infrastructural requirements of a real-time engine test.

Keywords: ANN, engine performance, emission, FAME, prediction

I. INTRODUCTION AND BACKGROUND

The rise in population, growing depletion of crude oil deposits, constrained refining infrastructure, and environmental pollution, especially emissions from transport vehicles, has placed enormous pressure on stakeholders to develop renewable and biodegradable alternatives. This has increased research for affordable, renewable, biodegradable, and environmentally amenable options which include biofuel, hydrogen, electric cars, and vegetable oil-based fuels. Various researchers [1-5] have, in their investigations, enumerated the damaging effects of the application of petroleum-based diesel (PBD) fuel in internal combustion engines to include environmental, performance, combustion, emissions, and health effects.

155

According to the researchers, the environmental effects include the greenhouse effect, increased global temperature, and rapid climate change. Infection and inflammation of airways, risk of asthma, bronchitis, eye irritation, and lung cancer and carcinogenic effects on humans and animals' health are some of the health effects of the use of PBD fuel. In terms of performance, PBD fuel provides incomplete combustion resulting in the emission of high volumes of carbon monoxide. Biodiesel, as an alternative fuel, has been found to offer enormous advantages such as non-toxicity, renewability, biodegradability, higher lubricity, high cetane number, high flash point, positive energy balance, low to zero sulphur, and safer handling compared to PBD fuel. However, biodiesel suffers from certain demerits including poor cold flow properties, lower volatility, higher kinematic viscosity, higher NOx emission, more prone to corrosion, damaging effects on automobile parts and concrete and auto-oxidation characteristics [6-9]. The initial challenge of high production cost is being overcome by the application of waste vegetable oil and waste animal fats as feedstock. The adaptation of waste cooking oil (WCO) has been reported to cause a 60 % to 90 % reduction in the production cost of biodiesel [10, 11].

Available statistics from the International Energy Agency [12] reveal that the current global biofuel production is not increasing rapidly enough to meet the transport biofuel consumption required as specified by the Sustainable Development Scenario (SDS). Biofuel demand in shipping and aviation has continued to increase and it is projected to triple by 2030 as shown in Fig. 1. Deliberate investment and targeted research are required in the areas of feedstock development, production infrastructure, deployment of numerical and optimization techniques in the production process, and improvement of performance and emission indices towards meeting the SDS. Meeting optimal engine performance and stringent emission requirements for compression ignition (CI) engines prescribed by regulatory bodies for CI engines fueled with fatty acid methyl ester (FAME) requires testing the fuels at various engine speeds and loads, among other parameters. This entails enormous resources, time, technicality, and personnel. One of the ways to deal with these challenges is the application of high-speed computers in numerical simulation and optimization of the production, process and utilization parameters to explore and discover optimal scenarios.
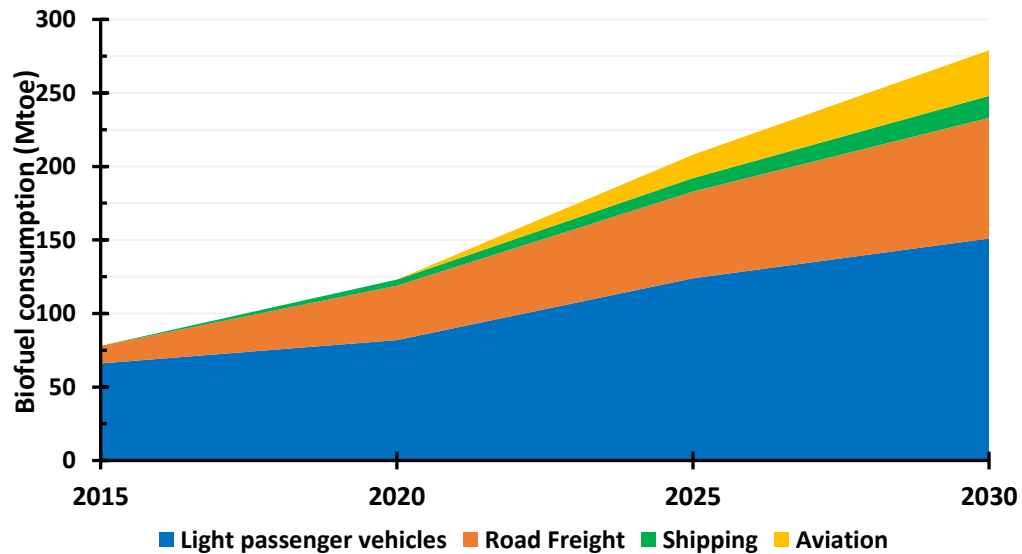
Fig. 1. Biofuel consumption breakdown in the SDS

In order to overcome the strenuous, time consuming, costly and intricate engine test experimentation involved in the determination of performance and emission parameters, researchers have adopted various numerical prediction tools to execute these important tasks. Linear prediction models have been widely used in predicting FAME properties but have been deficient in estimating engine performance and emission parameters because of their nonlinearity orientation. Artificial neural networks (ANN) have found wide application in business, medicine, engineering, image and voice recognition, with appreciable success, particularly where the traditional modeling techniques proved ineffective. ANN has been deployed for the purpose of predicting engine performance and emission of internal combustion engines [13]. An ANN uses the information presented to it to learn, relearn, and understand the correlation between the input and the output data. Using those established relationships, the ANN can predict responses from a new set of independent variables, drawing from its learning experience. A properly trained ANN possesses a high predictive capability and the ability to learn, unlearn, and relearn to improve the quality and integrity of the output if a different array of data is made available The preference of the ANN model over other prediction techniques is due to its adaptability and capability to learn then relearn nonlinear progressions and its uncomplicated adaptation to real-time data fluctuations. A well-trained ANN is faster, simpler, and more accurate than other conventional simulation techniques or mathematical models which require extensive computations, long iterations, and complex differential equations [14]. Major advantages of ANNs include high processing speed, ability to capture nonlinearities between predictors and outcomes as well as the capability to learn and model linear, nonlinear, and complex correlations. Though ANNs are trained on

a case by case basis which cannot be transferred for usage to other applications, this approach has continued to find applications in pattern classification, scheduling, intrusion detection, financial analysis as well as in control and optimization [15-20].

Due to its obvious benefits, researchers have employed well-trained ANN models to forecast and estimate engine performance parameters and release of emission gases on CI engines including torque, engine power, brake specific fuel consumption (BSFC), brake thermal efficiency (BTE), exhaust gas temperature (EGT), thermal efficiency, carbon dioxide (CO_2), nitric oxide (NO), nitrogen oxides (NOx), unburnt hydrocarbon (UHC), and smoke intensity under different engine speed and loading situations. The outcomes of the prediction exercises have agreed with real-time experimental engine test results, thereby meeting the primary purpose of its deployment.

Bearing in mind the importance of fatty acid (FA) composition in the handling, storage, performance, combustion, properties, and emissions of biodiesel fuel, a lot of resources and efforts are being deployed for the prediction of engine performance parameters as well as the emission based on its FA compositions. These efforts need to be improved upon and strengthened, hence the present intervention. In this research, the pertinent question to ask, and which forms the motivation for this research, is whether the numerically determined optimal FAME candidate can advance engine performance and tone down the emission characteristics of an unmodified of CI engine.

The object of the present effort, therefore, is to develop and train an ANN model with the capacity to predict the engine performance parameters and emission characteristics of an unmodified CI engine fueled with an optimal FAME candidate determined in terms of two FA

compositions with the aim of unearthing an appropriate biodiesel fuel that will advance engine performance and mitigate emission characteristics. This investigation is limited to the use of C16:0 and C18:1 percentage concentrations as input variables to develop an ANN model capable of training, testing and predicting the BSFC, BMEP, BTE, EGT, CO, smoke intensity, UHC, and NOx of an unmodified CI engine fueled by unblended FAME.

The application of ANN in biofuel study has been well documented owing to the obvious derivable advantages, which include simplicity, adaptability, and manoeuvrability [21]. ANN has been applied on many occasions to predict biodiesel properties, engine performance, fuel mixing and combustion parameters, and emission characteristics. Filho et al. [22], Hosseinpour et al. [23], Oliveira et al. [24], and Rocabruno-Valdes et al. [25] utilized a well-trained ANN model to predict some properties of FAME. The outcome of their investigations revealed that the predicted data agreed with the experimental data. Taghavifar et al. [26] engaged ANN to predict the heat flux of a CI engine using spray characteristics such as crank angle, temperature, and pressure as inputs with acceptable output. Rao et al. [27], Javed et al. [28], and Kshirsagar and Anad [29] used ANN prediction modeling to predict BTE, BSFC, EGT, CO, CO_2, UHC, NOx, and soot using blending ratios as inputs with reasonable outputs. Çay et al. [30], and Kumar et al. [31] developed standard backpropagation algorithms on a MATLAB platform to predict the engine performance of a CI engine powered with biodiesel and compared the predicted results with experimental results. Bietresato et al. [32] evaluated the effectiveness of ANN models of sigmoidal and Gaussian algorithms to demonstrate their predictive capabilities for engine performance and emission characteristics in a farm tractor.

Other researchers have used various parameters, including temperature, number of carbon and hydrogen atoms as inputs for the prediction of properties, engine performance and emission parameters of a conventional CI engine. The use of fatty acid (FA) compositions have not been widely and adequately exploited. Ramadhas et al. [33], Filho et al. [22], Piloto-Rodriguez et al. [34], and Sara et al. [35] have at various times used FA composition as input variables to predict the properties, engine performance and emission characteristics of FAME. A painstaking and exhaustive search of literature, comprising over 120 biodiesel samples, revealed that palmitic acid (C16:0), stearic (C18:0), oleic acid (C18:1), linoleic acid (C18:2), and linolenic acid (C18:3) are the most popular FAs in biodiesel among the 13 FAs [22, 36-38]. Myristic acid (C14:0), C16:0, C18:0, C18:1, and C18:2 were adopted by Menon et al. [39] as input variables to predict various parameters of CI engine fueled with biodiesel using ANN, thereby developing an optimal biodiesel fuel candidate based of FA composition and degree of saturation/unsaturation of the fuel.

II. MATERIAL AND METHODS

In this section, we discuss the experimental and the numerical methods employed in carrying out the research. The experimental method involves the production of an optimal FAME candidate through the transesterification of waste palm oil (WPO) and the GCMS analysis of the samples to reveal the FA composition. The development and training of an ANN model to predict the engine performance and emission characteristics parameters of unmodified CI engine fueled with FAME is categorized by means of numerical techniques using advances in software computing.

II.I. Production of Optimal FAME Biodiesel from WPO and Determination of FA Composition

The WPO sample was collected from a local owner-operated restaurant at the point of disposal near the university campus while waste chicken eggshells were obtained from eateries at the University of KwaZulu-Natal, Durban, cafeteria. The waste chicken eggshells were converted to a CaO catalyst through high-temperature calcination at 900 ºC as described by our earlier work [40]. The WPO was pretreated by removing food debris and moisture before subjecting it to a one-stage transesterification process since the acid value was found to be 0.66 mgKOH/g.

The clean feedstock was mixed with methanol and calcined CaO catalyst in a flat-bottomed flask in the required quantity and heated on an electric cooker with a magnetic stirrer maintained at 1200 rpm while a digital thermocouple was used to authenticate the reaction temperature throughout the process. A reaction temperature of 60 ºC, methanol to oil ratio of 6:1, the catalyst particle size of 75 µm, 1 % w/w catalyst: oil ratio, and total reaction time of 90 min were selected as process parameters. The ensuing mixture was subsequently filtered in a Buchner funnel filtration system assembled to retrieve the catalyst. The filtered mixture was transmitted to a separating funnel for the glycerol to coagulate at the base of the separating funnel where it was tapped off. The crude biodiesel was purified using magnesol. The purified FAME was subjected to FA characterization in a GCMS.

II.II. Development of ANN Model

ANN, available on MATLAB platform, is a parallel distributed processing computer system modeled on the functioning of the human brain with the capacity to generate, form and discover new knowledge without any help, based on the information presented to it. It comprises a number of linked and interconnected processing elements known as neutrons or nodes. The neutrons are linked with each other by synaptic weights through which signals are passed from one neuron to the other in accordance with the connecting weights. The weight of the signal is determined by the knowledge acquired in the course of the training, testing, and validation. The neutron processes information presented to it based on its dynamic state. The neuron receives input from external sources, analyzes such information, and executes non-linear operations based on it and generates an output [41, 42]. Figure 2 shows the network configuration of a typical ANN model used for this study.
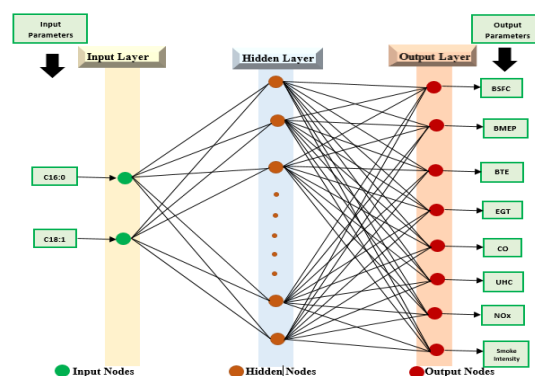
Fig. 2. The ANN structure

In order to develop and improve an ANN model, the network is exposed to the training or learning phase and the testing or validation stage. During the learning phase, the network studies the input data and estimates the output variables. In the test stage, the network stops learning and estimates the output data using the knowledge gained during the training stage. Training is programmed to terminate when the testing error attains the previously set tolerance and the preferred epoch number is reached in relation to the error value [43].

II.III. Determination of the Model Parameters

For the present research, a MATLAB R2017b NNTool was used to develop the model [44]. The back-propagation (BP)

algorithm with a Levenberg-Marquardt (LM) learning algorithm was applied because of its high robustness, fault tolerance, self-learning, self-adaptability and reputation for good prediction accuracy [45, 46]. Despite this advantage, BPA has been found to be susceptible to slow convergence, fluctuations, and severe oscillations particularly during the training stage [47, 48]. Tangent-sigmoid (TANSIG) is adopted as the transfer function.

The number of nodes at the input and output layers were selected as stated on the research objective which is to use C16:0 and C18:1 as inputs to estimate the engine performance and emission characteristics of an unmodified CI engine. For this research, the selected engine performance output parameters were BSFC, BMEP, BTE, and EGT, while the emission characteristics were CO, smoke intensity, UHC, and NOx. Hence, two nodes were selected for input layers while eight nodes were selected for output layers.

A single hidden layer can sufficiently predict any non-linear relations or functions using the BPA neural network. Since there are few nodes in the input layer in the proposed model, the network did not require any complex arrangement. Hence one hidden layer was adopted for the model. The number of nodes in the hidden layer (p) was selected based on the Kolmogorov theorem and neural network theory [49]. p was estimated by Eq. 1 [50].

$$p < \sqrt{n + m} + a \qquad (1)$$

Where n is the total number of nodes in the input layer, m is the total number of nodes in the output layer and a is a positive integer $(a < 10)$. The a must be strategically chosen to get a reasonable p. An excessively low p will reduce the accuracy of the network approximation of the model thereby leading to increased prediction error, while an excessively large p will make the network unnecessarily complex requiring longer training time

[51]. With n *value* of 2, m *value* of 3, and a *value* of 7, p was set to 10. The learning rate and target error were both set at 0.01 based on the experience of continuous testing.

The minimum gradient of 10^{-7} was set as part of the stopping criteria. Other factors to be considered for the design of the ANN model are depicted in Table 1. Also, as shown in Table 2, there were 125 experimental datasets mined from the literature. The FA compositions were obtained from GCMS analysis while the engine performance and emission characteristics were gotten from real-time engine tests [52-55]. 70 % (95 patterns) of the data were chosen for training the model, 15 % (15 patterns) for validation while 15 % (15 patterns) were used for testing the prediction capability of the trained network. The developed, trained, and validated model was used to predict the engine performance and emission characteristics of FAME candidates with C16:0 and C18:1 concentration of 36.4 % and 59.8 % respectively. The flow chart representing the developed ANN algorithm is shown in Fig. 3. The performance of the developed ANN model was examined by correlation coefficient (R), while the errors were evaluated using statistical error parameters, namely, Mean Square Error (MSE), Root Mean Square Error (RMSE), and the Mean Absolute Percentage Error (MAPE). The R, MSE, RMSE, and MAPE were calculated using the Eqs. 2-5 [41, 56, 57].

Table 1. Details of the neural network model

Factors	Value
Input layer	2
Hidden Layer	1
Output layer	8
Number of neutrons in the hidden layer	10
Number of epoch	10000
Number of iterations	69

$$R = 1 - \left\{ \frac{\sum_{i=1}^{n}(A_t - F_t)^2}{\sum_{i=1}^{n}(F_t)^2} \right\} \quad (2)$$

$$MSE = \frac{\sum_{i=1}^{n}(A_t - F_t)^2}{n} \quad (3)$$

$$RMSE = \sqrt{\frac{\sum_{i=1}^{n}(A_t - F_t)^2}{n}} \quad (4)$$

$$MAPE = \frac{\sum_{i=1}^{n}\left|\frac{A_t - F_t}{A_t}\right|}{n} \times 100\ \% \quad (5)$$

Where 'n' is the number of the patterns in the dataset, 'A_t' is the actual output, and 'F_t' is the predicted output value.

The R, MSE, RMSE, and MAPE were applied to measure the accuracy of the model. The ANN model was set to terminate the iteration when $R > 98, MSE < 0.001, and MAPE < 5\ \%$. The RMSE measures the variation between the predicted data and the experimental data while the MSE denotes the standard deviation of the difference between the predicted value and the experimental value for the data. A smaller RMSE symbolizes accurate outputs and model.

Table 2. Datasets for the ANN model

S/N	C16:0	C18:1	BSFC (g/kWhr)	BTE (%)	EGT (ºC)	BMEP (bar)	CO (%)	Smoke intensity	NOx (ppm)	UHC (ppm)
1	20.8	58.4	266.13	33.8	408	11.92	0.07	40	451	43
2	24.5	62.6	233.31	38.58	398	12.31	0.058	43	750	55
3	31.4	58.4	325.67	27.62	466	8.91	0.026	50	543	40
4	30.6	60.3	285.14	31.55	483	9.27	0.023	56	723	35
5	21.9	57.4	280.47	32.08	449	11.15	0.21	60	468	20
6	36.3	58.4	252.18	35.68	468	11.79	0.21	54	483	34
7	23.4	70.3	231.96	38.79	400	12.17	0.069	55	459	40
8	34.5	68.4	310.43	28.98	477	9.22	0.21	58	425	50
9	36.5	57.6	272.59	33.12	459	11.64	0.049	49	471	55
10	35.6	62.4	294.53	30.55	497	10.08	0.018	42	455	53
11	34.8	60.7	257.24	34.97	430	11.38	0.04	54	460	45
12	35.8	59.3	229.81	39.15	396	12	0.07	62	446	43
13	28.5	70.6	278.83	32.27	437	10.62	0.16	66	465	50
14	43.6	56.2	255.79	35.17	431	12.17	0.032	43	675	32
15	34.8	55.9	230.03	39.11	389	12.31	0.07	45	447	34
16	26.4	65.4	279.63	32.17	494	10.9	0.13	56	456	18
17	23.6	65.3	242.07	37.17	434	12.25	0.032	48	467	32
18	26.1	65.8	226.24	39.77	388	12.39	0.01	39	478	28
19	26.7	56.5	246.55	32.43	380	12.67	0.06	30	290	34
20	34.6	54.2	246.78	40.43	342	10.56	0.05	58	875	32
21	34.3	51.6	355.74	32.76	250	9.65	0.03	62	650	28
22	24.5	49.5	290.52	43.24	245	11.89	0.04	54	473	28
23	23.6	60.5	270.74	40.21	370	10.45	0.18	48	478	19
24	29.5	61.7	355.61	32.65	290	16.32	0.07	54	660	25
25	23.5	55.8	322.79	31.35	287	11.04	0.03	50	456	28

26	22.5	54.7	250.62	33.65	370	12.76	0.12	61	476	26
27	23.6	44.7	261.78	32.67	400	10.45	0.16	34	821	43
28	29.4	58.4	276.85	23.65	468	9.43	0.04	38	448	50
29	43.48	41.13	280.54	27.43	280	10.45	0.02	43	650	51
30	42.45	40.32	278.54	23.54	460	12.03	0.03	41	720	40
31	40.21	50.35	300.45	30.78	380	9.32	0.12	40	459	39
32	39.43	55.43	285.05	32.76	380	10.45	0.21	42	700	52
33	42.56	50.45	260.45	22.09	410	15.23	0.07	60	710	48
34	37.16	46.93	290.54	35.05	420	9.05	0.04	57	651	27
35	35.76	50.43	315.85	35.87	410	10.45	0.12	43	552	40
36	40.42	49.32	250.45	34.53	358	10.25	0.08	38	460	48
37	43.56	42.46	260.48	22.87	330	11.35	0.15	28	570	28
38	35.32	50.32	270.41	28.54	450	11.21	0.21	40	592	28
39	38.43	39.45	301.45	27.91	510	10.35	0.05	50	702	34
40	45.21	55.32	310.65	32.56	350	9.25	0.13	61	810	28
41	42.75	45.55	317.23	38.21	420	12.25	0.17	52	830	54
42	34.52	42.59	260.54	28.45	470	10.27	0.13	58	750	43
43	53.7	22.8	270.4	23.54	400	11.45	0.12	42	453	40
44	52.9	22.2	230.2	30.43	398	12.43	0.089	45	650	52
45	51.83	24.13	332.4	26.54	453	9.43	0.012	51	542	43
46	53	23.3	280.4	32.54	498	8.56	0.032	54	732	51
47	22.19	48.2	276.1	32.65	453	10.43	0.22	52	487	43
48	53.3	25	321.3	34.67	487	11.76	0.21	52	505	56
49	13.31	50.76	324.8	40.32	421	11.43	0.045	48	476	34
50	55.53	23.26	265.3	28.43	487	10.21	0.27	51	432	45
51	52.5	24.8	234.5	32.54	462	10.43	0.047	47	480	48
52	54.1	22.6	301.2	29.56	487	10.04	0.012	41	440	47
53	48.9	23.18	261.4	33.06	442	11.25	0.05	51	455	51
54	73.73	16.93	230	39.54	398	11.54	0.081	60	475	48
55	66.02	20.43	265.1	33.65	436	10.56	0.127	53	432	53
56	69	23.87	223.5	35.91	429	12.15	0.034	56	624	46
57	67.7	20.5	230.03	39.23	387	12.23	0.068	45	654	32
58	63.29	23.68	267.3	33.09	492	10.45	0.014	51	562	27
59	77.89	32.78	243.1	37.43	431	12.56	0.043	49	467	54
60	63.5	24	276.3	37.89	342	12.54	0.015	46	480	34
61	42.8	40.5	254.3	31.65	380	13.21	0.06	41	431	43
62	42.6	40.5	265.3	39.02	371	11.54	0.08	61	657	30
63	42.7	40.9	342.1	32.94	278	10.41	0.043	57	567	36
64	44.81	39.99	287.3	43	263	11.54	0.023	52	680	25
65	43.32	40.57	276.3	40.43	381	9.43	0.143	52	623	20
66	40.2	43.3	344.9	32.65	301	12.54	0.043	58	560	27
67	47.9	37	312.4	31.54	297	11.27	0.078	56	467	30
68	43.9	39	265.1	33.89	385	12.54	0.17	59	651	24
69	39.5	43.2	253.87	32.76	402	11.48	0.042	37	605	40
70	23.3	42.4	265.32	24.5	458	10.21	0.054	31	458	42
71	25.2	48.9	276.21	28.54	320	11.24	0.027	45	620	35

72	23.1	45.8	265.32	23.87	430	12.38	0.04	53	680	43
73	23.9	43.9	299.3	31.5	341	10.34	0.014	48	461	47
74	24.34	42.23	300	31.65	374	10.5	0.043	54	680	41
75	20.1	55.2	267.3	24.65	403	13.78	0.052	61	520	56
76	28.7	57.4	297	35.78	415	10.54	0.05	54	670	43
77	11.67	57.51	312.34	33.87	407	10.68	0.14	48	550	40
78	28.33	57.51	243.43	35.05	372	9.98	0.065	35	535	41
79	20.6	52.5	260.45	23.55	350	12.21	0.18	30	555	32
80	22.9	54.2	265.43	28.94	448	11.12	0.27	38	610	28
81	11.38	48.28	300.2	27.54	471	10.58	0.052	47	700	43
82	11.4	48.3	312.45	33.56	378	10.76	0.076	60	750	26
83	11.2	45.5	317.43	39.84	425	11.35	0.17	54	652	44
84	10.4	47.1	276.4	29.4	446	10.46	0.173	51	690	32
85	23.6	44.2	265.43	34	400	10.57	0.045	49	475	24
86	25.5	47.1	235.53	37.98	389	12.89	0.072	40	705	32
87	24.49	38.32	321.54	28.54	476	10.54	0.045	45	530	38
88	20.6	64	287.43	32.04	473	10.43	0.043	59	710	43
89	22.3	64.1	280.11	33.41	450	11.28	0.28	61	480	25
90	22.3	64.4	250.12	34.14	470	11.54	0.32	57	503	36
91	20.6	61.6	231.07	35.8	405	12.05	0.076	61	470	43
92	20.6	61.5	308.05	28.98	465	10.21	0.32	53	443	56
93	46.36	32.38	278.5	34.65	450	11.56	0.045	52	472	45
94	69.07	18.97	298.32	30.55	475	10	0.048	48	485	51
95	43.08	40.55	254.43	34	420	11.35	0.064	52	605	60
96	23.88	45.25	228.57	38.45	400	12.58	0.023	60	621	42
97	55.72	40.23	278.43	31	435	11.43	0.182	54	710	38
98	32.14	47.23	254.65	36.41	420	12.56	0.132	47	540	54
99	26.03	45.43	234.61	38.5	385	11.67	0.126	48	462	32
100	21.28	63.12	276.54	32.81	490	11.68	0.023	55	440	26
101	23.1	63.2	234.54	37	441	10.43	0.043	45	445	55
102	20.43	61.9	234.78	40.33	398	18.45	0.05	46	465	43
103	10.12	79.4	200.54	31.56	379	12.5	0.06	47	367	56
104	24.32	62.05	220.56	40.34	337	11.65	0.056	35	761	34
105	15.05	75.32	340.54	24	248	10.03	0.132	37	658	37
106	34.54	50.3	300	51	271	11.32	0.231	41	456	54
107	35.65	50.5	267.05	40.05	375	10.76	0.16	42	571	39
108	23.67	58.23	340.54	36.02	271	13.28	0.17	40	665	28
109	26.76	46.55	342	38.87	300	10.43	0.034	55	456	34
110	30.65	53.3	256.54	33.13	362	11.32	0.172	42	467	53
111	27.54	58.43	270	33.76	389	9.47	0.166	48	749	48
112	34.32	46.5	256.43	30.19	465	11.78	0.074	41	450	65
113	20.43	46.3	278.54	28.78	300	9.68	0.023	50	630	31
114	26.43	57.84	260	24.67	487	13.43	0.056	44	726	27
115	54.32	26.89	310.65	30.56	381	15.32	0.183	54	471	41
116	46.32	34.54	290.5	33.81	345	18.01	0.124	60	704	28
117	20.56	60.33	267.54	26.5	389	16.55	0.23	46	723	44

118	43.65	34.59	284.65	33.89	400	13.65	0.124	59	456	47
119	32.65	50.05	312.54	33.71	421	11.45	0.043	44	443	34
120	25.21	52.65	260.67	37.2	430	9.67	0.012	51	506	49
121	42.39	34.56	239.05	24.54	327	10.32	0.043	39	561	28
122	41.65	50.05	289.12	29.55	437	10.43	0.312	45	604	38
123	44.54	45.5	310.32	28.57	505	11.59	0.043	50	673	43
124	32.89	44.65	309.65	33.65	355	10.54	0.23	48	782	26
125	27.35	56.43	278.09	35.18	430	9.26	0.176	51	774	41

III. RESULTS AND DISCUSSION

We developed an ANN model to predict the engine performance and emission characteristics of an unmodified CI engine with C16:0 and C18:1 as inputs using the BP-LM algorithm. The predicted engine performance was BSFC, BMEP, BTE, and EGT, while four emission characteristics, namely CO, smoke intensity, UHC, and NOx were predicted. The two input parameters were palmitic and oleic acids. Figure 4 shows the structure of ANN consisting of input, hidden, and output layers and their respective number of nodes generated by the ANN model developed on a MATLAB R2017b NNTool. Data were sourced from literature for the training and validation of the model while the engine performance and emission characteristics of optimal FAME candidate produced by the transesterification of WPO and analyzed by GCMS were predicted by the trained ANN model. The overall correlation coefficient of the ANN model is shown in Fig. 5. The regression coefficient of the training, validation, and test data gave satisfactory value, an indication of high predictive proficiency of the established model. The outcome of the overall correlation coefficient for the present model is an improvement on the outcome of similar efforts [58-60].

The performance indices of the trained ANN model using regression and other statistical error parameters as well as comparison of the predicted data with experimental data for 15 different test cases are presented in Fig. 5–14. The prediction of output parameters yielded impressive outcomes for BSFC, BMEP, BTE, CO, EGT, UHC, NOx, and smoke intensity with commendable and reliable values of R, MSE, RMSE, and MAPE for each parameter. This indicates the accuracy, sensitivity, capacity, and capability of the developed model to simultaneously predict important engine performance and emission parameters that can be relied upon.
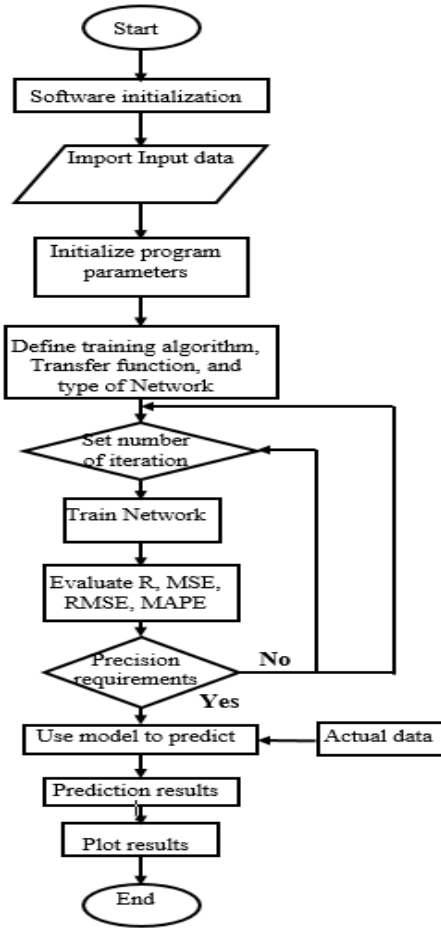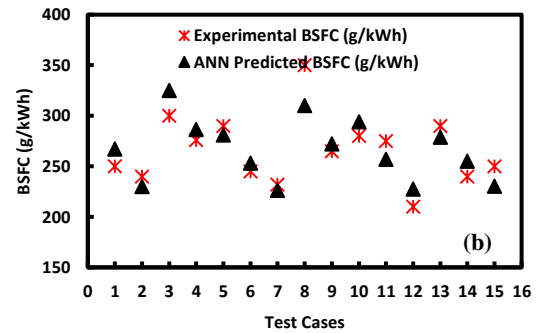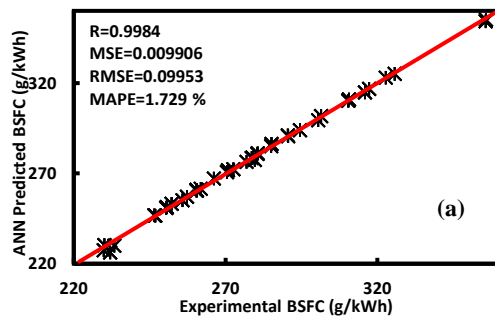
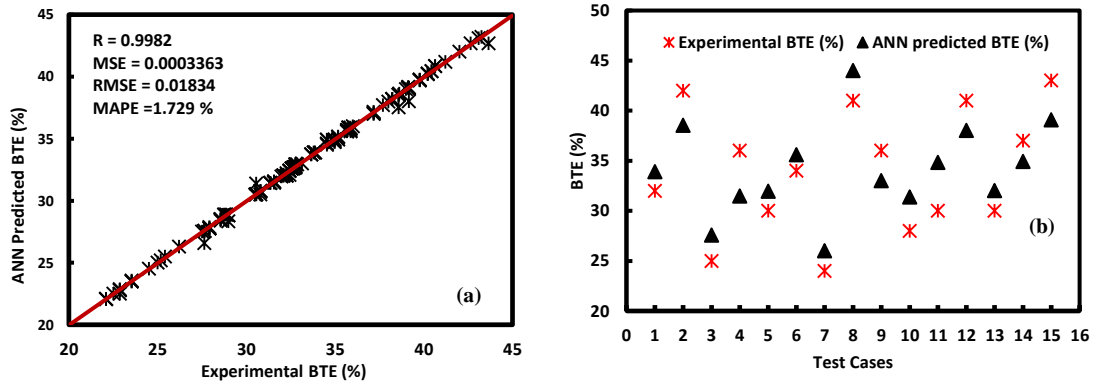**Fig. 3.** Flow chart of ANN model
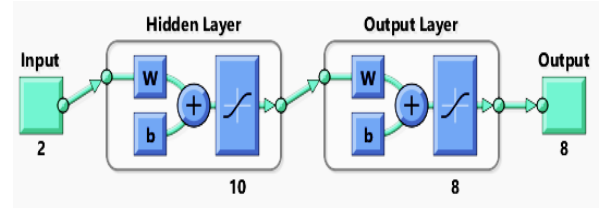
Fig. 4. Neural network model created using NNTool box [44]

Fig. 5. The overall correlation coefficient of the ANN model.

R=0.9984
MSE=0.009906
RMSE=0.09953
MAPE=1.729 %

(a)

(b)
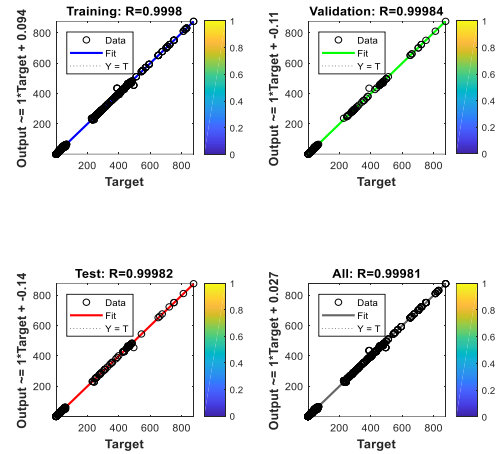
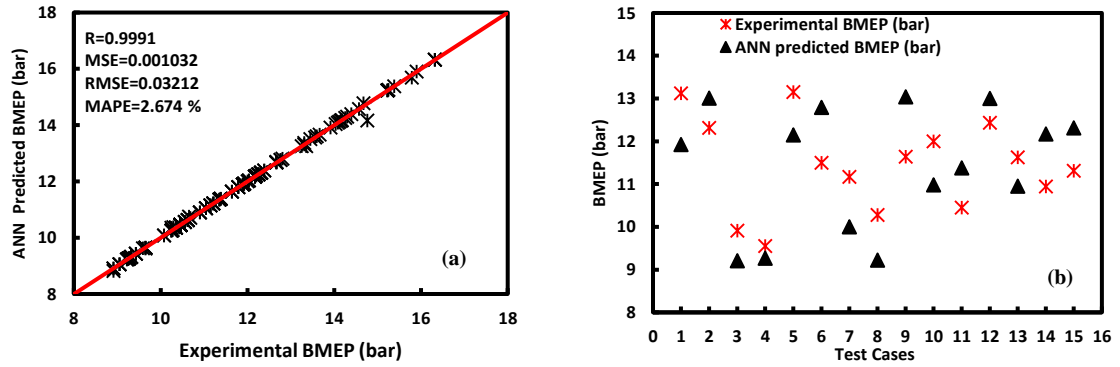**Fig. 6.** (a) Regression plot for BSFC (b) Comparison of experimental and ANN predicted BSFC

Fig. 7. (a) Regression plot for BTE (b) Comparison of experimental and ANN predicted BTE

Figure 6a compares the ANN predicted data with the experimentally measured data. With R-value of 0.9984, MSE, RMSE, and MAPE values of 0.009906, 0.09953 g/kWh, and 1.729 % respectively, the model performed acceptably. The model was also applied to predict the BSFC of some FAME samples. This result is comparable to the correlation coefficient of 0.9968, and MSE of 0.0177 reported by Syed et al. [61]. The outcome, as shown in Fig. 6b, was commendable and can be relied upon to arrive at a sound decision on the fuel. Bearing in mind the importance of BSFC as an engine performance parameter, and the relationship between fuel consumption, power output and efficiency of an oxygenated fuel like FAME, this model will be useful to determine the behavior of FAME from its palmitic and oleic acid concentrations. Figures 7a and 7b illustrate the ANN predicted BTE versus experimental BTE and the outcome of the predicted data for 15 experimental test cases. With R of 0.9982, MSE of 0.0003363, RMSE of 0.09953 % and MAPE of 1.729 %, the developed ANN model was satisfactory

and acceptable. These results were comparable with the outcome of similar investigations reported in the literature [59, 62].

The correlation coefficient and other statistical errors of the developed ANN model for BMEP were found to be within acceptable levels throughout the investigation despite the nonlinear relationship between BMEP and the FA composition of biodiesel. As shown in Fig. 8a and 8b, the model provided a satisfactory outcome with statistical errors within acceptable limits. The R-value of 0.9991, MSE value of 0.001032, RMSE value of 0.03212 bar and MAPE value of 2.674 % showed good predictive capabilities of the model. Figure 9a and 9b show the relationship between the experimental and ANN predicted data of EGT. The performance index of the model indicates an R of 0.999 and RMSE of 0.03212. This result is comparable with the R-values of 0.9995 reported by Syed et al. [61] and 0.99754 reported by Javed et al. [28].
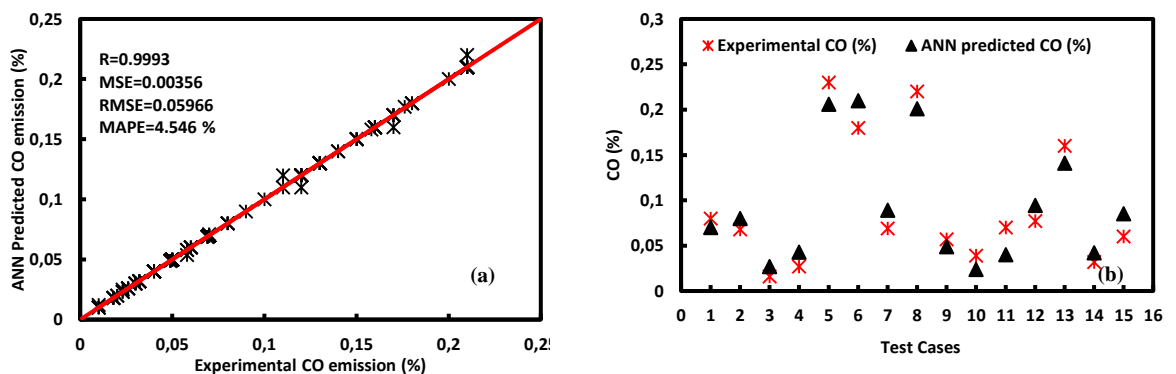
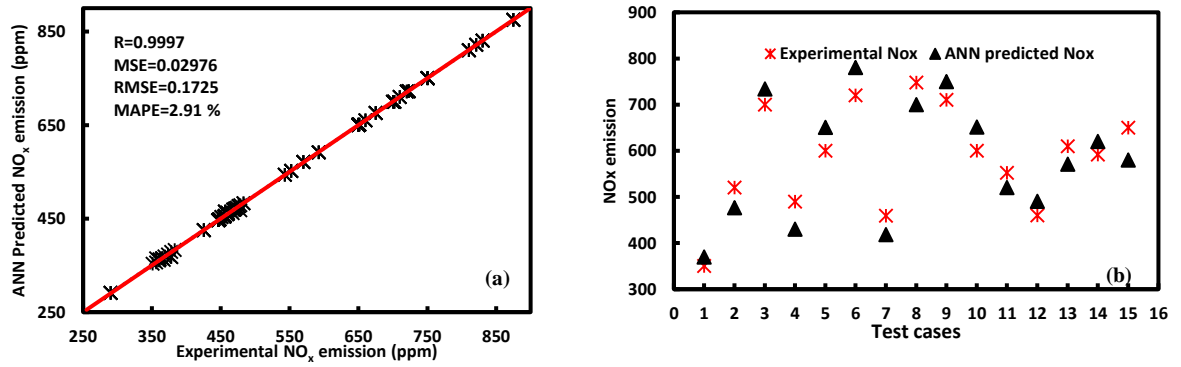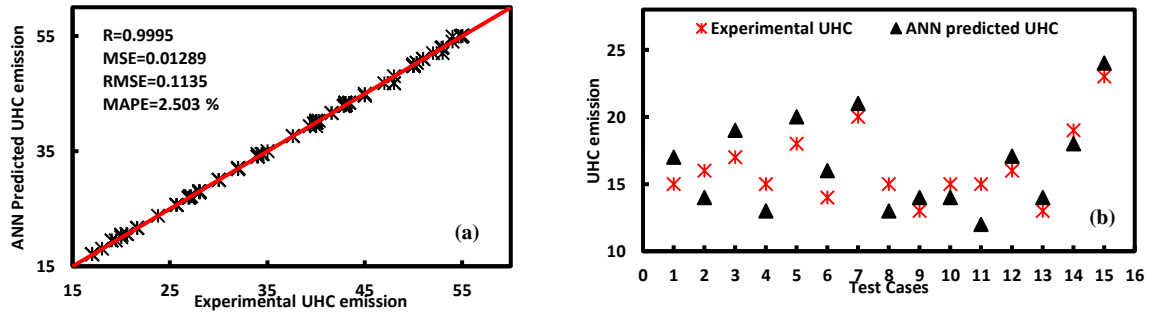**Fig. 8** (a) Regression plot for BMEP (b) Comparison of experimental and ANN predicted BMEP
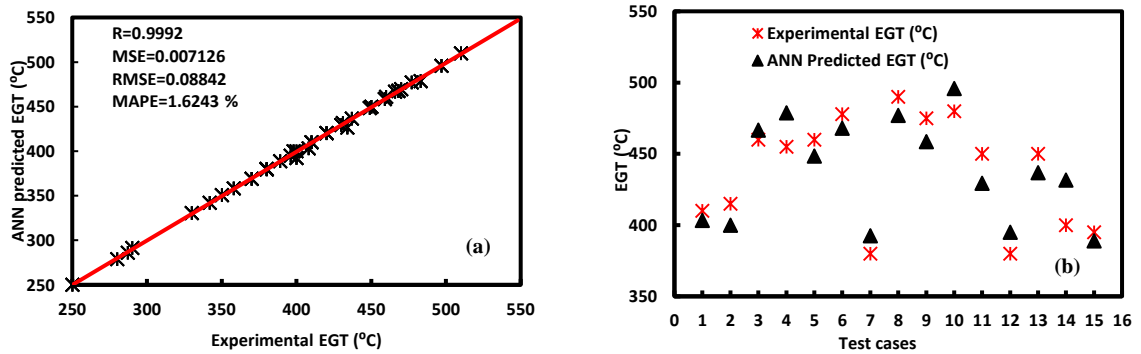
Fig. 9. (a) Regression plot for EGT (b) Comparison of experimental and ANN predicted EGT

The developed model predicted CO and NOx within acceptable limits. The predicted CO and NOx were close to the experimentally measured values. This is shown by the R-value near 1. The value of MSE, RMSE, and MAPE show the high prediction accuracy of the model. As shown in Fig. 10a and b, and 11a and b the gap between the experimentally determined and ANN predicted values are negligible for CO and NOx emissions. Due to the effects of CO emission on humans and the environment the parameters need to be accurately predicted so as to be able to drastically reduce CO emissions. High emissions of NOx in a CI engine remains one of the drawbacks for the application of FAME as a CI engine fuel. Researchers are still working on lowering the NOx emission in line with standards. This model accurately predicts the emissions of CO and NOx gases thereby making real-time engine tests unnecessary. This result is an improvement on the outcome of similar studies available in the literature [62, 63].

Fig. 10. (a) Regression plot for CO (b) Comparison of experimental and ANN predicted CO
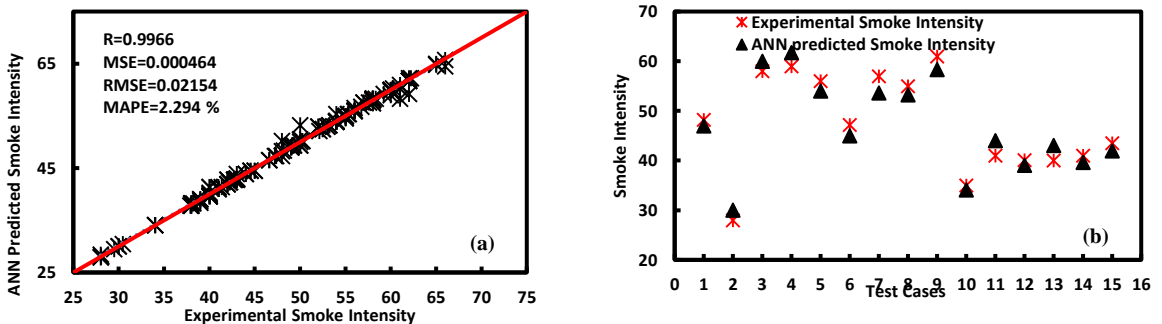

Fig. 11. (a) Regression plot for NOx (b) Comparison of experimental and ANN predicted NOx

It can be deduced from the outcomes of the model prediction that the ANN predicted values agree well with the experimentally measured values. This reveals that the developed ANN model has satisfactorily determined the UHC and smoke intensity of CI engine fueled with FAME. The R-value was found to be 0.9995 and 0.9966 for UHC and smoke intensity, respectively. The closeness of these R values to 1 signifies the high accuracy of the prediction. For the UHC emissions the RMSE value is 0.1135 and MAPE value is 2.503 % (Fig. 12a and 12b) and for the smoke intensity the RMSE is 0.02154 and the MAPE is 2.294 % (Figure 13a and 13b). These small RMSE and MAPE values are indicative of the high accuracy of the developed model [41, 61, 63].

Fig. 12. (a) Regression plot for UHC (b) Comparison of experimental and ANN predicted UHC

Fig. 13. (a) Regression plot for Smoke intensity (b) Comparison of experimental and ANN predicted Smoke intensity

Table 3. Comparison of outcome of this research with other results

Parameter	unit	Present research	Arunkumar et al. [64]	Sanli et al. [65]	Subramaniam et al. [66]	Singh et al. [67]
BSFC	g/kWh	205	750	230 to 247	400 to 460	300 to 500
BTE	%	30	28	-	24 to 26	0 to 30
BMEP	bar	45	-	38 to 42	-	-
EGT	ºC	260	300	-	-	150 to 380
CO	%	0.05	0.07	700 to 6000(ppm)	-	0.05 to 0.09
NOx	ppm	400	470	1400 to 1550	300 to 900	350 to 980
UHC	ppm	18	35	22 to 26	-	70 to 110
Smoke intensity	-	50	55	-	72 to 102	9 to 50

III.I. Prediction of Engine Performance and Emissions of Optimal FAME

A well-trained ANN model was deployed to predict the BSFC, BMEP, BTE, CO, EGT, UHC, NOx, and smoke intensity of CI engine fueled with the optimal FAME candidate produced to certain configurations. The two most important FA composition identified were C16:0 and C18:1 and these were used as inputs. The outcomes of the ANN predictions were compared with the outcomes of real-time CI engine tests from the literature as shown in Table 3. In terms of engine performance, the optimal candidates delivered encouraging performance parameters when compared with similar research outcomes. The BSFC was lower whereas the BTE was relatively high but at a lower EGT. The CO, NOx, UHC and smoke opacity emissions were found to be lower than all the outcomes of comparable investigations. The oxygenated fingerprint of the FAME candidate ensured better combustion which was reflected in the low CO emission. The low EGT also resulted in low NOx emissions. These outcomes show that the computed optimal FAME candidates yielded better engine performance and emitted less regulated gases, thereby meeting the objective of developing a new fuel.

IV. CONCLUSION

In this study, ANN was developed and trained using secondary data mined from literature for the simulation and prediction of engine performance and emission characteristics. The validated model was used to predict the engine performance and emission of a computed optimal FAME mix. The MATLAB ANN model based on BP-LM algorithms with tangent-sigmoid transfer function was developed to predict engine performance and emission parameters of an unmodified CI engine fueled with FAME. We employed two input layers, one hidden layer with ten neutrons, and eight output layers using NNTool techniques to determine the BSFC, BMEP, BTE, CO, EGT, UHC, NOx, and smoke intensity.

The outcomes of the developed ANN model were evaluated using regression coefficient and other statistical error platforms as well as other performance metrics to compare the experimental data with ANN predicted data. A total of 749 data were mined from literature and used to train the model while the FA composition of the optimal FAME candidates were produced through the transesterification of WPO. Going by the results, the model performed very well with the experimental data matching the ANN predicted data with an overall regression coefficient (R) of 0.9998. For the engine performance

parameters, R varied between 0.9982 and 0.9991 while the RMSE and MAPE ranged between 0.01834 and 0.09953, and 1.729 % and 2.674 % respectively. The R, RMSE, and MAPE for the emission parameters varied from 0.9966 to 0.9997, 0.02154 to 0.1725, and 1.6443 % to 4.546 % respectively.

From the foregoing, the optimal FAME candidates, namely, C16:0 with results of 36.4 % and C18:1 with 59.8 % demonstrated better engine performance and mitigated emission characteristics. The developed model accurately and reliably predicted the performance and emission parameters within acceptable limits. Thus, these two FAs are sufficient to accurately predict the engine performance and emission characteristics of a conventional and unmodified CI engine. Thus, FAME with concentrations of C16:0 and C18:1 can be trusted to perform optimally and generate mitigated emissions. It is thus safe to conclude that the developed ANN model has been able to reliably and conveniently imitate real engine performance and emission characteristics within satisfactory prediction accuracy and efficiency.

Going forward, this narrative should be stretched further to include the use of FA compositions of various feedstocks to predict, within reasonable accuracy, combustion, fuel mixing, and heat release rate with a view to evaluating their influence on engine performance, combustion, and emission characteristics of an unmodified CI engine.

REFERENCES

[1] Yildiz, I. Açıkkalp, E. Caliskan, H. and Mori, K. Environmental pollution cost analyses of biodiesel and diesel fuels for a diesel engine. Journal of Environmental Management, 2019, 243: 218-226. doi: 10.1016/j.jenvman.2019.05.002.

[2] Chrysikou, L. P., Dagonikou, V., Dimitriadis, A. and Bezergianni, S. Waste cooking oils exploitation targeting eu 2020 diesel fuel production: environmental and economic benefits. Journal of Cleaner Production, 2019, 219: 566-575, 2019. https://doi.org/10.1016/j.jclepro.2019.01.211

[3] Hosseinzadeh-Bandbafha, H., Tabatabaei, M., Aghbashlo, M., Khanali, M. and Demirbas, A. A comprehensive review on the environmental impacts of diesel/biodiesel additives. Energy Conversion and Management, 2018, 174: 579-614. https://doi.org/10.1016/j.enconman.2018.08.050

[4] Dias, D., Antunes, A. P. and Tchepel, O. Modelling of emissions and energy use from biofuel fuelled vehicles at urban scale. Sustainability. 2019, 11(10): 2902.

[5] Kharina, A., Searle, S., Rachmadini, D., Kurniawan, A. A. and Prionggo, A. The potential economic, health and greenhouse gas benefits of incorporating used cooking oil into Indonesia's biodiesel. White Paper, 26, 2018.

[6] Kinnal, N., Sujaykumar, G., D'costa, S. W. and Girishkumar, G. Investigation on the performance of diesel engine by using waste chicken fat biodiesel. IOP Conference Series: Materials Science and Engineering, 2018, 376(1): 012012.

[7] Samuel O. D. and Gulum, M. Mechanical and corrosion properties of brass exposed to waste sunflower oil biodiesel-diesel fuel blends. Chemical Engineering Communications, 2019, 206(5): 682-694. https://doi.org/10.1080/00986445.2018.1519508

[8] Appavu, P., Madhavan, V. R., Venu, H. and Jayaraman, J. Experimental investigation of an unmodified diesel engine operated with ternary fuel. Biofuels, 2019. https://doi.org/10.1080/17597269.2019.1600454

[9] Mohd Noor, C. W., Noor, M. M. and Mamat, R. Biodiesel as alternative fuel for marine diesel engine applications: a review. Renewable and Sustainable Energy Reviews, 2018, 94: 127-142. https://doi.org/10.1016/j.rser.2018.05.031

[10] Lee S. Y. et al., Waste to Bioenergy: A review on the recent conversion technologies. BMC Energy, 2019, 1(1): 4.

https://doi.org/10.1186/s42500-019-0004-7

[11] Joshi, S., Hadiya, P., Shah, M. and Sircar, A. Techno-economical and experimental analysis of biodiesel production from used cooking oil. Biophysical Economics and Resource Quality, 2019, 4(1): 2. https://doi.org/10.1007/s41247-018-0050-7

[12] International Energy Agency. Transport biofuels. tracking clean energy progress, 2019. https://www.iea.org/tcep/transport/biofuels/

[13] Walczak, S. Artificial Neural Networks. in Advanced Methodologies and Technologies in Artificial Intelligence, Computer Simulation, and Human-Computer Interaction. Philadelphia: IGI Global, 2019, pp. 40-53.

[14] Zhang, Z. Artificial Neural Network. in Multivariate Time Series Analysis in Climate and Environmental Research. Berlin: Springer, 2018.

[15] Ayer, T., Chen, Q. and Burnside, E. S. Artificial neural networks in mammography interpretation and diagnostic decision making. Computational and Mathematical Methods in Medicine, 2013, 2013. http://dx.doi.org/10.1155/2013/832509

[16] Behrooz, F., Mariun, N., Marhaban, M., Mohd Radzi, M. and Ramli, A. Review of control techniques for HVAC Systems—nonlinearity approaches based on fuzzy cognitive maps. Energies, 2018, 11(3): 495. https://doi.org/10.3390/en11030495

[17] Dumitru C. and Maria, V. Advantages and Disadvantages of Using Neural Networks for Predictions. Ovidius University Annals, Series Economic Sciences, 2013, 13(1).

[18] El-Shahat, A. Advanced Applications for Artificial Neural Networks. BoD–Books on Demand, 2018.

[19] Rabuñal, J. R. Artificial Neural Networks in Real-Life Applications. Philadelphia: IGI Global, 2005.

[20] Kishore, D. S. C., Rao, K. P., Basha, S. M. J. and Rao, B. J. P. Investigation of surface roughness in turning of in-situ Al6061-TiC metal matrix composite by taguchi and prediction of response by ANN. Materials Today: Proceedings, 2018, 5(9, Part 3): 18070-18079. https://doi.org/10.1016/j.matpr.2018.06.141

[21] Barradas Filho A. O. Viegas, and I. M. A. Applications of Artificial Neural Networks in Biofuels. Advanced Applications for Artificial Neural Networks. IntechOpen, 2017. https://doi.org/10.5772/intechopen.70691

[22] Barradas Filho A. O. et al. Application of artificial neural networks to predict viscosity, iodine value and induction period of biodiesel focused on the study of oxidative stability. Fuel, 2015, 145: 127-135. https://doi.org/10.1016/j.fuel.2014.12.016

[23] Hosseinpour, S., Aghbashlo, M., Tabatabaei, M. and Khalife, E. Exact estimation of biodiesel cetane number (cn) from its fatty acid methyl esters (fames) profile using partial least square (pls) adapted by artificial neural network (ANN). Energy Conversion and Management, 2016, 124: 389-398. https://doi.org/10.1016/j.enconman.2016.07.027

[24] De Oliveira F. M. et al. Predicting cetane index, flash point, and content sulfur of diesel–biodiesel blend using an artificial neural network model. Energy & Fuels, 2017, 31(4): 3913-3920. https://doi.org/10.1021/acs.energyfuels.7b00282

[25] Rocabruno-Valdés, C., Ramírez-Verduzco, L. and Hernández, J. Artificial neural network models to predict density, dynamic viscosity, and cetane number of biodiesel. Fuel, 2015, 147: 9-17. https://doi.org/10.1016/j.fuel.2015.01.024

[26] Taghavifar, H., Taghavifar, H., Mardani, A., Mohebbi, A. and Khalilarya, S. A Numerical investigation on the wall heat flux in a DI diesel engine fueled with N-heptane using a coupled CFD and ANN approach. Fuel, 2015, 140: 227-236. https://doi.org/10.1016/j.fuel.2014.09.092

[27] Prasada Rao, K., Victor Babu, T., Anuradha, G. and Appa Rao, B. V. IDI

diesel engine performance and exhaust emission analysis using biodiesel with an artificial neural network (ANN). Egyptian Journal of Petroleum, 2017, 26(3): 593-600. https://doi.org/10.1016/j.ejpe.2016.08.006

[28] Javed, S., Satyanarayana Murthy, Y. V. V., Baig, R. U. and Prasada Rao, D. Development of ANN model for prediction of performance and emission characteristics of hydrogen dual fueled diesel engine with Jatropha methyl ester biodiesel blends. Journal of Natural Gas Science and Engineering, 2015, 26: 549-557. https://doi.org/10.1016/j.jngse.2015.06.041

[29] Kshirsagar C. M. and Anand, R. Artificial neural network applied forecast on a parametric study of Calophyllum Inophyllum methyl ester-diesel engine out responses. Applied Energy, 2017, 189: 555-567. https://doi.org/10.1016/j.apenergy.2016.12.045

[30] Çay, Y., Çiçek, A., Kara, F. and Sağiroğlu, S. Prediction of engine performance for an alternative fuel using artificial neural network. Applied Thermal Engineering, 2012, 37: 217-225. https://doi.org/10.1016/j.applthermaleng.2011.11.019

[31] Kumar, D. V., Kumar, P. R. and Kumari, M. S. Prediction of performance and emissions of a biodiesel fueled lanthanum zirconate coated direct injection diesel engine using artificial neural networks. Procedia Engineering, 2013, 64: 993-1002. https://doi.org/10.1016/j.proeng.2013.09.176

[32] Bietresato, M. Calcante, A. and Mazzetto, F. A Neural network approach for indirectly estimating farm tractors engine performances. Fuel, 2015, 143: 144-154. https://doi.org/10.1016/j.fuel.2014.11.019

[33] Ramadhas, A., Jayaraj, S., Muraleedharan, C. and Padmakumari, K. Artificial neural networks used for the prediction of the cetane number of biodiesel. Renewable Energy, 2006, 31(15): 2524-2533. https://doi.org/10.1016/j.renene.2006.01.009

[34] Piloto-Rodríguez, R., Sánchez-Borroto, Y., Lapuerta, M., Goyos-Pérez, L. and Verhelst, S. Prediction of the cetane number of biodiesel using artificial neural networks and multiple linear regression. Energy Conversion and Management, 2013, 65: 255-261. https://doi.org/10.1016/j.enconman.2012.07.023

[35] Pinzi, S., Rounce, P., Herreros, J. M., Tsolakis, A. and Pilar Dorado, M. The effect of biodiesel fatty acid composition on combustion and diesel engine exhaust emissions. Fuel, 2013, 104: 170-182. https://doi.org/10.1016/j.fuel.2012.08.056

[36] Hoekman, S. K., Broch, A., Robbins, C., Ceniceros, E. and Natarajan, M. Review of biodiesel composition, properties, and specifications. Renewable and Sustainable Energy Reviews, 2012, 16(1): 143-169. https://doi.org/10.1016/j.rser.2011.07.143

[37] Meng, X., Jia, M. and Wang, T. Neural network prediction of biodiesel kinematic viscosity at 313K. Fuel, 2014, 121: 133-140. https://doi.org/10.1016/j.fuel.2013.12.029

[38] Moradi-Kheibari, N., Ahmadzadeh, H., Murry, M. A., Liang, H. Y. and Hosseini, M. Fatty Acid Profiling of Biofuels Produced from Microalgae, Vegetable Oil, and Waste Vegetable Oil. In M. Hosseini (Ed). Advances in Feedstock Conversion Technologies for Alternative Fuels and Bioproducts, Cambridge: Woodhead Publishing, 2019, pp. 239-254.

[39] Menon P. R. and Krishnasamy, A. A composition-based model to predict and optimize biodiesel-fuelled engine characteristics using artificial neural networks and genetic algorithms. Energy & Fuels, 2018, 32(11): 11607-11618. https://doi.org/10.1021/acs.energyfuels.8b02846

[40] Awogbemi, O., Inambao, F. L. and Onuh, E. I. Development and characterization of chicken eggshell waste as potential catalyst for biodiesel production.

International Journal of Mechanical Engineering and Technology, 2018, 9(12): 1329-1346.

[41] Uslu, S. and Celik, M. B. Prediction of engine emissions and performance with artificial neural networks in a single cylinder diesel engine using diethyl ether. Engineering Science and Technology, 2018, 21(6): 1194-1201. https://doi.org/10.1016/j.jestch.2018.08.0 17

[42] Atik, K., Kahraman, N. and Çeper, B. A. Prediction of performance and emission parameters of an SI Engine by using artificial neural networks. Isi Bilimi ve Teknigi Dergisi-Journal of Thermal Science and Technology, 2013, 33(20): 57-64.

[43] Yang, I.-H., Yeo, M.-S. and Kim, K.-W. Application of artificial neural network to predict the optimal start time for heating system in building. Energy Conversion and Management, 2003, 44(17): 2791-2809. https://doi.org/10.1016/S0196-8904(03)00044-X

[44] MathWorks MATLAB. 2017. http://www.mathworks.com.

[45] Xu, B., H. Zhang, Z. Wang, H. Wang, and Y. Zhang, Model and algorithm of BP neural network based on expanded multichain quantum optimization. Mathematical Problems in Engineering, 2015, 2015. http://dx.doi.org/10.1155/2015/362150

[46] Jia, W., Zhao, D., Shen, T., Ding, S., Zhao, Y. and C. Hu, An optimized classification algorithm by BP neural network based on PLS and HCA. Applied Intelligence, 2015, 43(1): 176-191. https://doi.org/10.1007/s10489-014-0618-x

[47] Ahmad, M. W., Mourshed, M., Yuce, B. and Rezgui, Y. Computational intelligence techniques for HVAC systems: a review. Building Simulation, 2016, 9(4): 359-398. https://doi.org/10.1007/s12273-016-0285-4

[48] Bocheng, Z., Kuo, L., Dinghao, L., Jing, L. and Xuan, F. Short-term prediction of building energy consumption based on GALM neural network. International Conference on Advances in Mechanical

Engineering and Industrial Informatics, 2015, pp. 867-71. https://doi.org/10.2991/ameii-15.2015.161

[49] Kůrková, V. Kolmogorov's theorem and multilayer neural networks. Neural Networks, 1992, 5(3): 501-506. https://doi.org/10.1016/0893-6080(92)90012-8

[50] Ye Z. and Kim, M. K. Predicting electricity consumption in a building using an optimized back-propagation and Levenberg–Marquardt back-propagation neural network: case study of a shopping mall in China. Sustainable Cities and Society, 2018, 42: 176-183. https://doi.org/10.1016/j.scs.2018.05.050

[51] Zhong T. and Xie, T. Application and simulation of MATLAB neural network tool NNTool. Computer and Modernization, 2012, 12.

[52] Monirul I. M. *et al.*, Assessment of Performance, emission and combustion characteristics of Palm, Jatropha and Calophyllum inophyllum biodiesel blends. Fuel, 2016, 181: 985-995. https://doi.org/10.1016/j.fuel.2016.05.01 0

[53] Ozsezen, A., Canakci, N. M., Turkcan, A. and Sayin, C. Performance and combustion characteristics of a DI diesel engine fueled with waste palm oil and canola oil methyl esters. Fuel, 2009, 88(4): 629-636. https://doi.org/10.1016/j.fuel.2008.09.02 3

[54] Ileri, E., Karaoglan, A. D. and Atmanli, A. Response surface methodology based prediction of engine performance and exhaust emissions of a diesel engine fuelled with canola oil methyl ester. Journal of Renewable and Sustainable Energy, 2013, 5(3): 033132. https://doi.org/10.1063/1.4811801

[55] Sharon, H., Jayaprakash, R., Karthigai Selvan, M., Soban kumar, D. R., Sundaresan, A. and Karuppasamy, K. Biodiesel production and prediction of engine performance using SIMULINK model of trained neural network. 2012, Fuel, 99: 197-203. https://doi.org/10.1016/j.fuel.2012.04.01 9

[56] Pai and P. S., Rao, B. S. Artificial Neural Network based prediction of performance and emission characteristics of a variable compression ratio CI engine using WCO as a biodiesel at different injection timings. Applied Energy, 2011, 88(7): 2344-2354. https://doi.org/10.1016/j.apenergy.2010.12.030

[57] Najafi, B., Faizollahzadeh Ardabili, S., Mosavi, A., Shamshirband, S. and Rabczuk, T. An intelligent artificial neural network-response surface methodology method for accessing the optimum biodiesel and diesel fuel blending conditions in a diesel engine from the viewpoint of exergy and energy analysis. Energies, 2018, 11(4): 860. https://doi.org/10.3390/en11040860

[58] Roy, S., Banerjee, R. and Bose, P. K. Performance and exhaust emissions prediction of a CRDI assisted single cylinder diesel engine coupled with EGR using artificial neural network. Applied Energy, 2014, 119: 330-340. https://doi.org/10.1016/j.apenergy.2014.01.044

[59] Roy, S., Banerjee, R., Das, A. K. and Bose, P. K. Development of an ANN based system identification tool to estimate the performance-emission characteristics of a CRDI assisted CNG dual fuel diesel engine. Journal of Natural Gas Science and Engineering, 2014, 21: 147-158. https://doi.org/10.1016/j.jngse.2014.08.002

[60] Hamouda M. and Számel, L. Optimum control parameters of switched reluctance motor for torque production improvement over the entire speed range. Acta Polytechnica Hungarica, 16(3), 2019.

[61] Syed, J., Baig, R. U., Algarni, S., Murthy, Y. V. V. S., Masood, M. and Inamurrahman, M. Artificial Neural network modeling of a hydrogen dual fueled diesel engine characteristics: an experiment approach. International Journal of Hydrogen Energy, 2017, 42(21): 14750-14774. https://doi.org/10.1016/j.ijhydene.2017.04.096

[62] Javed, S., Murthy, Y. S., Baig, R. U. and Rao, D. P. Development of ANN model for prediction of performance and emission characteristics of hydrogen dual fueled diesel engine with Jatropha methyl ester biodiesel blends. Journal of Natural Gas Science and Engineering, 2015, 26: 549-557. https://doi.org/10.1016/j.jngse.2015.06.041

[63] Dharma S. *et al.*, Experimental study and prediction of the performance and exhaust emissions of mixed Jatropha curcas-Ceiba pentandra biodiesel blends in diesel engine using artificial neural networks. Journal of Cleaner Production, 2017, 164: 618-633. https://doi.org/10.1016/j.jclepro.2017.06.065

[64] Arunkumar, M., Kannan, M. and Murali, G. Experimental studies on engine performance and emission characteristics using castor biodiesel as fuel in CI engine. Renewable Energy, 2019, 131: 737-744. https://doi.org/10.1016/j.renene.2018.07.096

[65] Sanli, H., Canakci, M., Alptekin, E., Turkcan, A. and Ozsezen, A. N. Effects of waste frying oil based methyl and ethyl ester biodiesel fuels on the performance, combustion and emission characteristics of a DI diesel engine. Fuel, 2015, 159: 179-187. https://doi.org/10.1016/j.fuel.2015.06.081

[66] Subramaniam, D., Murugesan, A. and Avinash, A. Performance and emission evaluation of biodiesel fueled diesel engine abetted with exhaust gas recirculation and Ni coated catalytic converter. Journal of Renewable and Sustainable Energy, 2013, 5(2): 023138. https://doi.org/10.1063/1.4802943

[67] Singh, P., Chauhan, S. R. and Goel, V. Assessment of Diesel engine combustion, performance and emission characteristics fuelled with dual fuel blends. Renewable Energy, 2018, 125: 501-510. https://doi.org/10.1016/j.renene.2018.02.105

CHAPTER 7: DEVELOPMENT AND CHARACTERIZATION OF CHICKEN EGGSHELL WASTE AS POTENTIAL CATALYST FOR BIODIESEL PRODUCTION

This chapter presents strategies for the development and characterization of chicken eggshell waste as a catalyst for biodiesel production. In the article, the process for the collection, cleaning and preparation of chicken eggshell waste to powder form, calcination, and characterization (TGA, FTIR, XRD, SEM, TEM) of raw uncalcined, boiled uncalcined, and raw calcined chicken eggshell waste powder are extensively discussed and conclusions drawn. Synthetic CaO costs in excess of USD 230/ton, whereas the conversion of chicken eggshell waste collected freely from bakeries cost less than USD 10/ton, expended only on transportation. The article has been published in the *International Journal of Mechanical Engineering and Technology*, IAEME Publications.

To cite this article: Awogbemi, O., Inambao F., Onuh E. I. (2019). "Development and Characterization of Chicken Eggshell waste as Potential Catalyst for Biodiesel Production," International Journal of Mechanical Engineering and Technology, Volume 9, number 12, pp. 1329-1346.

The link to this article:

http://www.iaeme.com/MasterAdmin/UploadFolder/IJMET_09_12_134/IJMET_09_12_134.pdf

DEVELOPMENT AND CHARACTERIZATION OF CHICKEN EGGSHELLWASTE AS POTENTIAL CATALYST FOR BIODIESEL PRODUCTION

OmojolaAwogbemi, Freddie L. Inambao, and Emmanuel I. Onuh

Green Energy Solutions Research Group, Discipline of Mechanical Engineering,
Howard College, University of KwaZulu-Natal, Durban 4041, South Africa

ABSTRACT

An average of 369800 cases of chicken eggsare consumed per week in South Africa. Disposal of the resultant shells, which constitute about 10% by weight of eggs, has been problematic and costly. Conversion of chicken eggshell waste to useful substances has engaged the attention of researchers in recent years. This work is geared towards exploring chicken eggshell waste as allow cost, sustainable, and readily available source of calcium oxide (CaO) for use as a possible catalyst for biodiesel production. Raw, boiled and calcined eggshell 75μmpowder were prepared and characterized. The results of the X-ray diffraction (XRD) showed that while raw and boiled chicken eggshell contained 79.3% and 99% calcite (calcium carbonate [$CaCO_3$]) respectively, whereas eggshell powder calcined at $900^\circ C$ for 3h contained 63.8% lime (CaO). This wasdue to the thermal decomposition of $CaCO_3$ to CaO and portlandite (Ca $(OH)_2$) during calcination. Thermogravimetric analysis (TGA) revealed a 44.5% and 42% weight loss of the boiled and raw eggshell samples respectively, which occurred between $700^\circ C$ and $900^\circ C$, whereas the calcined powder sample only witnessed 5.5% weight loss at $400^\circ C$. Scanning electron microscope (SEM) analysis showed that raw, boiled, and calcined eggshell samples contained 41.31%, 21.91%, and 46.08% of calcium, 14.93%, 26.40% and 6.22% of carbon, and 43.76%, 51.68%, and 47.70% of oxygen respectively. The results of transmission electron microscopy (TEM) image analysis and Fourier-transform infrared spectroscopy (FTIR) revealed that boiling has no significant effect on the structure, composition and thermal degradation of waste chicken eggshell, unlike calcination. Complete conversion of $CaCO_3$to CaO through calcination enhances the properties and usefulness of waste chicken eggshell powder as a heterogeneous catalyst for biodiesel production.

Keywords: Calcination, Characterization Chicken Eggshells, Heterogeneous Catalyst.

1. INTRODUCTION

Affordability and access to energy are some of the key indicators of enhanced quality of life. The quest for comfortable living has caused humans to desire a safe, affordable, and environmentally friendly energy source to meet their ever-increasing energy needs. Fossil fuels and their derivative shave, over the years, been used to heat homes, provide lighting and power internal combustion (IC) engines for households, commercial and industrial purposes. With an upsurge in population, urbanization, modernization, and industrialization, the demand for energy has increased geometrically without a commensurate increment in the energy supply[1]. According to the International Energy Outlook report for 2017, the cumulative global energy consumption was projected to increase by 28%, rising from 575 quadrillion British thermal units (Btu) in 2015 to 736 quadrillion Btu in 2040, with China and India accounting for more than 50% of the total global increase within that period[2].Available statistics how that primary energy consumption and global energy related carbon dioxide (CO_2) emissions have continued to increase across all regions globally between year 2010 and 2017, as shown in Figure 1[3, 4].
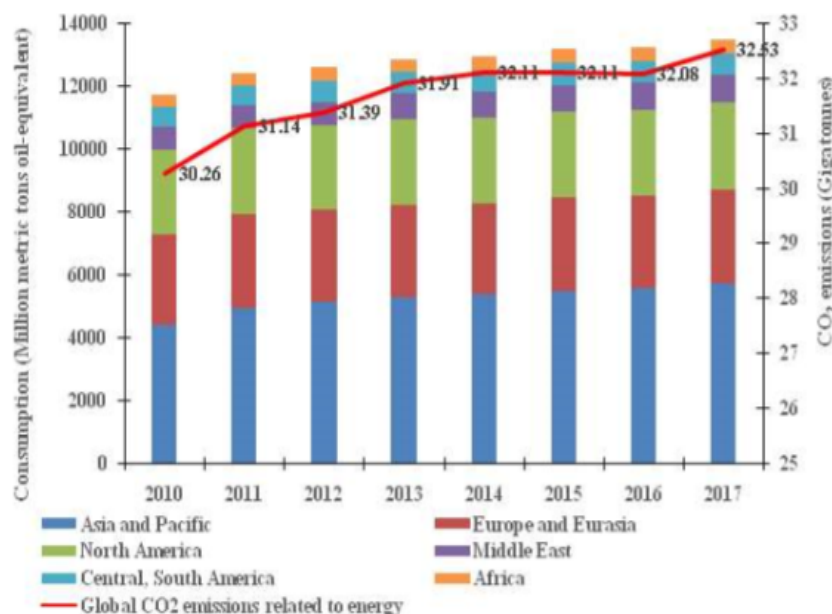
Figure 1. Global primary energy consumption (in million metric tons oil-equivalent)and Energy related carbon dioxide emissions (in gigatonnes) between 2010 and 2017, by region

Environmental concerns, rate of depletion of fossil fuel deposits, high cost of exploration, continuous unpredictability in the global oil price, and emission of hazardous gases have made the use of renewable energy a viable substitute[5, 6]. Of all the renewable energy

sources of fuels for IC engines, biofuels, consisting of biodiesel, green diesel, bioethanol, etc., are considered to be among the most promising alternatives. Biodiesel, also known as fatty acid methyl ester (FAME), is considereda sustainable candidate to replace petroleum-based diesel (PBD) fuel in unmodified compression ignition (CI) engines owing to its similarity to PBD fuel in terms of its properties and miscibility. Among the important properties of FAME are that it is biodegradable, non-poisonous, and sulfur-free, has a better cetane number, lower CO_2 emissions, enhanced lubricity, and is easy to produce domestically. It also possesses similar physico-chemical fingerprints to PBD fuel[7, 8].

FAME are produced when vegetable oils (sunflower oil, jatropha oil, palm oil, rubber seed oil, soybean oil etc.) or animal fats are trans-esterified using an alcohol, preferably methanol, in the presence of a catalyst (homogenous or heterogeneous) with glycerol as a by-product [9, 10]. Unaffordability, interference with food security, absence of land mass for growing non-edible feedstock, among other reasons, has made the use of used restaurant oil, also known as waste cooking oil (WCO), anacceptable feedstock for FAME production. The benefits of utilizing WCO as feedstock for FAME production includes its easy availability, non-interference with food chain, converts waste to fuel, provides additional income to households, prevents illegal disposal into drainages and rivers, preserves aquatic lives, etc.[11-14].

The application of homogeneous basic catalystssuch as NaOH, KOH, etc.can be problematic because they: (i)involve the use of a large volume of water for washing, (ii) arecostly, (iii) corrode the reactor, (iv) require treatment of the waste water produced, (v) require numerous purification processes, and(vi) inability to reuse, recover and regenerate the catalyst [15-17].Calcium oxide (CaO), an example of a heterogeneous catalyst, can be derived from calcium carbonate ($CaCO_3$), which is a major constituent of chicken eggshells. The advantages of a heterogeneous catalystsynthesized from chicken eggshell waste include:(a) conversion of waste to beneficial applications, (b) the biodiesel produced requires little further cleaning, (c) can be effortlessly separated, recovered, reused and regenerated, (d) produces uncontaminated glycerol as a by-product, (e) no adverse impact on the environment, (f) less energy and water consumption, (g) relativelycost-effective, (h) high basicity, (i) non toxicity[9, 13, 18-20]. However, heterogeneous catalysts produced from chicken eggshell waste have some setbacks including low specific activity, and absence of satisfactory stability during usage. CaO is reported to be one of the most active heterogeneous catalysts for transesterification of feedstock to biodiesel and has been widely used due to its availability, ease of production, affordability, non-toxicity, high basicity and high regeneratability. CaO is ideal as a catalyst due to its high surface area and the highnumber of pores available on the surface[21-23], andhas been used as a catalyst for FAME production with satisfactory success and high yield[24]. CaO has been reported to occur in significant proportions in some low cost material including chicken eggshell waste, fish scalewaste, cockle shellwaste, ostrich shellswaste, mud scrub shellwaste, and animal bone waste [9, 25].Chicken eggshellwaste which represents nearly10% of a chicken egg by weight, is generated when an egg is cracked and the egg yolk and egg white removed as well as after hatching of an incubated egg [26].

The United Nations Food and Agricultural Organization (FAO) reported that China is the world's highest producer of eggs with 24.8 billion kilograms, followed by the United States of America, India, and Japan with 5.6 billion kilograms, 3.8 billion kilograms, and 2.522 billion kilograms respectively. China's production is projected by the FAO to become34.2 metric tons of eggs per year by 2020 [27]. According to a report published by the South Africa Poultry Association, an average of 378 940 cases of eggs were consumed in South Africa per week in 2017 while the figure decreased to 369800 cases of eggs per week in March 2018[28].Among the various food wastes, eggshells have many bioactive compounds and

other useful minerals of high economic value but which can constitute a health and environmental menace if not well disposed of and managed[29]. The application of chicken eggshellwaste as a heterogeneous catalyst for FAME production would significantly reduce the cost of disposing of such waste (especially those produced by bakeries),improve sanitation by keeping the environment clean, and reduce waste disposed to landfills.

Chicken eggshell waste has attracted considerable interest in recent times due its potential utilization as:a heterogeneous catalyst [7, 19, 30-35], a durable and effective protection fromultravioletradiation[36], a component in paper treatment[37], ceramic raw material for tiles and sanitary sectors[29], animal feed [38], absorbent [39, 40], fertilizer [41], a component in glass foam production [42], abrasive material [43] among other uses. Chicken eggshell waste can be treated (calcined) to enhance its usefulness and improve its efficiency. Outcomes of researches have shown that chicken eggshells can be recovered, reused and regenerated [22, 44, 45] with improved efficiency.

Despite the recognized application of eggshells, the relevant question to ask arehow far have these pre-treatment procedures and processes affected its usefulness and applications, particularly as a catalyst for biodiesel production, in view of the advantages derivable from its treatment and usage? The motivation for this research is the conversion of chicken eggshells, which have hitherto been regarded as waste and an environmental nuisance, into an economically and scientifically useful product. The aim of this present work, therefore, wasto develop CaO from three forms of chicken eggshell waste, namely, raw chicken eggshell, boiled chicken eggshell and calcined eggshell and characterize the resultant chicken eggshell powder. The scope of the research waslimited to collection, cleaning and pre-treatment, development and characterization of the chicken eggshellwaste. To this end, chicken eggshell waste waspre-treated, pulverized and subjected to characterization to determine the effects of boiling and calcination.

2. MATERIAL AND METHODS

2.1 Raw Material Collection and Preparation

Chicken eggshell waste was collected from Butterfield Bakery, Reddy's Bakery, and Nubbile's Bakery, all located in central Durban. The chicken eggshell waste was washed with hot water to eliminate any dirt, sand or other foreign objects (including the inner white membrane) clinging to the shells. The shells were rinsed several times with distilled water to ensure absolute cleanliness. The clean eggshells were divided into three equal parts. One part was boiled on the electric stove for 0.5 h then the shells were dried in an oven at 100 °C for 3h to remove any moisture.

OmojolaAwogbemi, Freddie L. Inambao, and Emmanuel I. Onuh
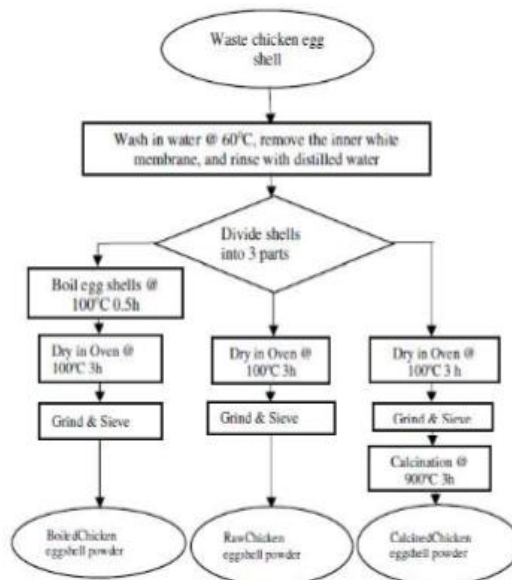
Figure 2. Flowchart of production of egg shell catalysts

The oven-dried eggshells were subsequently crushed by mortar and pestle then pulverized into a fine powder with an electric coffee grinder and passed through a 75 μm meshsieve. The second part was calcined at 900°C for 3 h to convert the calcium tri oxo carbonate IV ($CaCO_3$) into CaO. The raw chicken eggshell powder, boiled chicken eggshell powder, and calcined chicken eggshell powder were thereafter stored in sealed glass vials, labeled appropriately, and placed in desiccators to guard against contamination and oxidation. The flowchart of the catalyst preparation is shown in Figure 2 while Figure 3 shows the state of the shells at the different stages of catalyst preparation.

Figure 3.Conversion of eggshells to powdery form

2.1. Catalyst Characterization

The eggshell powder developed from chicken eggshell waste were characterized through X-ray diffraction (XRD) using a PAN alytical Empyrean diffractometer with HighScore Plus software version 3.0d.The samples were prepared on a Quorum Q150A ES sputtering

http://www.iaeme.com/ IJMET/index.asp 1333   editor@iaeme.com

180

machine before transferring to the Zeiss Ultra Plus in field emission gun scanning electron microscope (FEGSEM) for morphology analysis of the powder sample. A JEOL JEM-2100 operating at an accelerating voltage of 20 kV was used for the high-resolution transmission electron microscopy (TEM) analysis. Fourier-transform infrared spectroscopy (FTIR) was determined using a Perkin-Elmer Spectrum 100 spectrometer, while the thermogravimetric analysis (TGA) was determined using a Perkin-Elmer Simultaneous Thermal Analyzer STA 6000with Nitrogen gas at 20 ml/min for the analysis and at a temperature from $100^{\circ}C$ to $1000^{\circ}C$ at $20^{\circ}C/min$.

3. RESULTS AND DISCUSSION

The three samples exhibited different colors after preparation. The raw chicken eggshell powder appeared greyish white while the calcinedegg shell powder appeared lighter and whiter. The change in color after calcination may be due to the conversion of $CaCO_3$to CaO and the departure of CO_2 from the carbonate, as reported by Cree and Rutter [46] and Salaudeen et al.[47].The outcome of characterization of raw, boiled and calcined chicken eggshell powder by XRD, FTIR, TGA, SEM, TGA, TEM and the image analysis are described below.

3.1. XRD analysis

The X-ray diffraction patterns of the raw, boiled and calcined chicken eggshell samples are shown in Figure 4, while Figure 5 shows the pattern of the three samples in stacked form. The spectrometry of the raw and boiled eggshell samples have their peaks at the same location, testifying to the insignificant effect of boiling. As shown in Table 1, raw and boiled chicken eggshell contains 77.9 % and 99.2 % of calcite ($CaCO_3$) respectively while the $CaCO_3$ has been converted to lime (CaO) in the calcined sample. At a calcination temperature of $900^{\circ}C$ for 3h, the $CaCO_3$ decomposed to CaO and CO_2 which accounted for a high percentage of CaO in the calcined sample as reported by Goli and Sahu[48], Piker et al.[49] and Tan et al.[19]. The formation of portlandite ($Ca(OH_2)$) in the calcined chicken eggshell sample is as a result of the interaction of CaO with atmospheric air during storage and analysis as confirmed by Lesbani et al.[50]. The 0.4% of calcite in the calcined sample might be due to incomplete decomposition of $CaCO_3$ to CaO, while the 0.5% graphite in the raw eggshell sample might be attributed to the presence of impurity. The 20.2% calcite magnesium in the raw chicken eggshell is considered to be mainly calcite while the magnesium oxide is expected to be in trace quantity as reported by Goli and Sahu [48] and Ayodeji et al.[51].
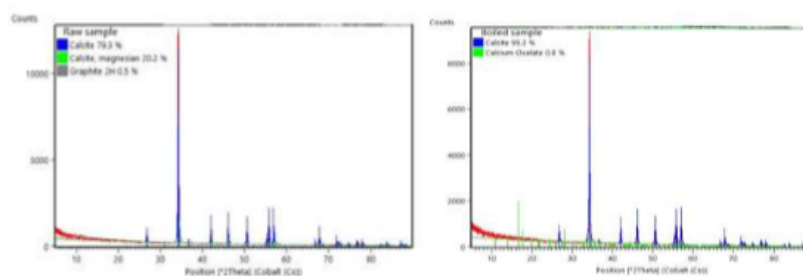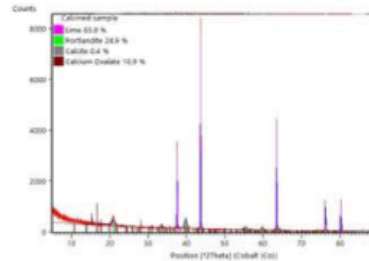
Figure 4.XRD spectrometry of raw, boiled and calcined chicken eggshells
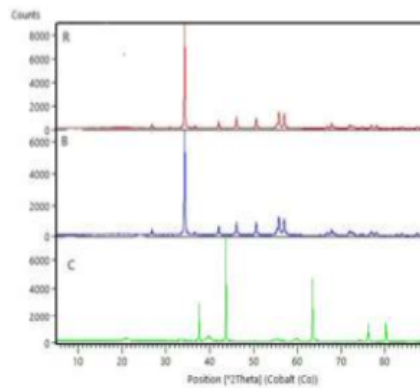
Figure 5.StackedXRD spectrometry of raw (R), boiled (B) and calcined (C) chicken eggshells

Table 1.Compound composition of raw, boiled and calcined chicken eggshells

Compound name	Chemical formula	Concentration (%)		
		Raw sample	Boiled sample	Calcined sample
Lime	CaO	-	-	63.8
Portlandite	$Ca(OH)_2$	-	-	24.9
Calcite	$CaCO_3$	79.3	99.2	0.4
Calcium oxalate	$C_2H_2CaO_5$		0.8	10.9
Calcite magnesium	$CaCO_3 Mg$	20.2	-	-
Graphite	C	0.5	-	-

3.2. SEM analysis

Scanning electron microscope (SEM) analysis was carried out to compare the surface morphology of raw chickeneggshell, boiled chicken eggshell and calcined eggshell to determine the effect of boiling and calcination on the eggshell at magnification of 2000X. Figure 6 compares the surface morphology of the raw, boiled and calcined eggshells. While the surface of the raw chicken eggshell is more settled, boiling appears to have slightly scattered or unsettled the particles of the sample. The calcined chicken eggshell presents a honeycomb-like structure [30, 52]. As shown in Table 2 and Figure 7, the boiled sample has the least calcium concentration and the highest oxygen concentration compared to the raw and the calcined chicken eggshells. The effect of the high calcination temperature may account for

this result. The low calcium concentrationmay be dueto the decomposition of calcium carbonate $CaCO_3$ to calcium oxide CaO and carbon dioxide CO_2after the calcination process as reported by Onwubu et al.[43].The high oxygen concentration may be due to formation of calcium hydroxide ($Ca(OH)_2$) as a result of the reactive moisture adsorption occasioned by high calcination temperature and time as corroborated by Tangboriboon et al.[53].
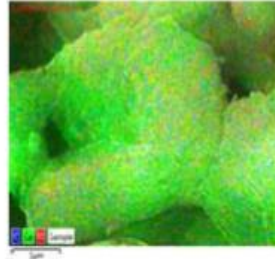
Table 2. Elemental composition of raw, boiled and calcined chicken eggshells

Element	Chicken eggshell weight (%)		
	Raw sample	Boiled sample	Calcined sample
Calcium (Ca)	41.31	21.91	46.08
Carbon (C)	14.93	26.40	6.22
Oxygen (O)	43.76	51.68	47.70
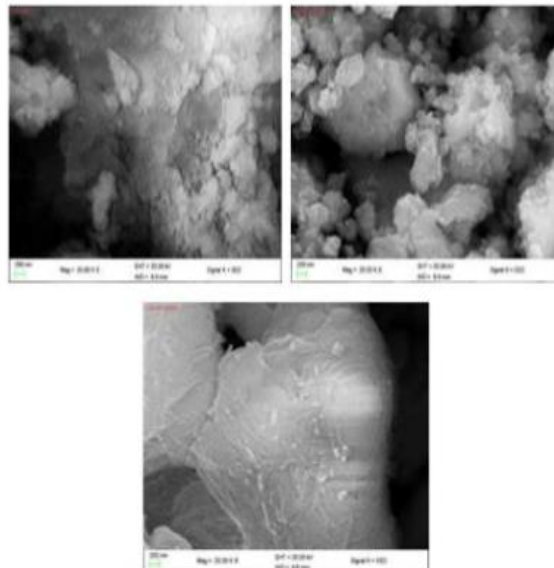
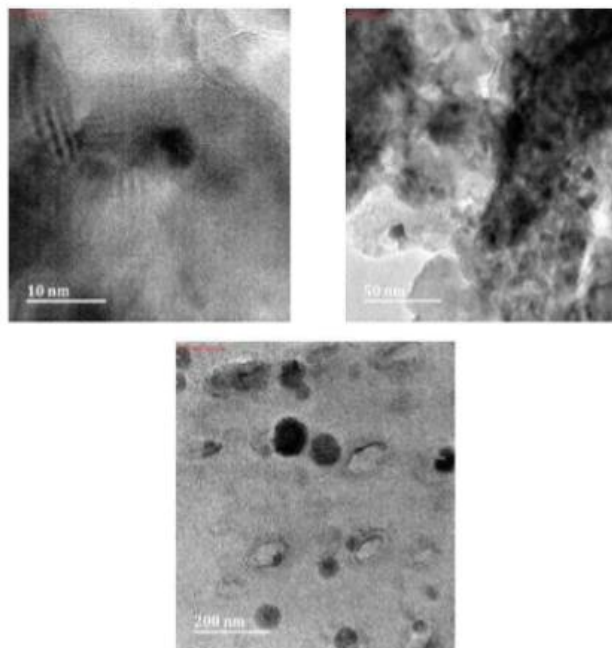Figure 6.SEMimage of raw, boiled and calcined chicken eggshells
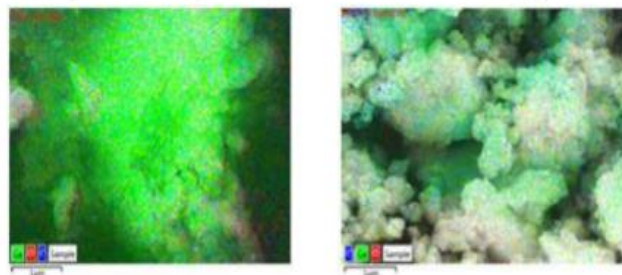
Figure 7. Elementalmapping of raw, boiled and calcined chicken eggshells showing the concentration of calcium (green), carbon (blue) and oxygen (red)

3.3. TEM analysis

The transmissionelectron microscopy micrographs of the surface of the raw, boiled and calcined waste chicken eggshells are shown in Figure 8.The calcined chicken eggshells have more pores when compared with the raw eggshell sample. This might be due to the effects of calcination. The boiled sample, on the other hand, appears blurred and irregularly shaped. The raw sample has less pores and more regular surface structure which is a reflection of the calcium carbonate in the sample. The TEM analysis confirms the result of the XRD analysis that the calcined eggshell sample has the potential to be an effective catalyst in the conversion of waste cooking oil into FAME by transesterification as reported by Pandit and Fulekar[54], Navajas [35] andTan et al.[55].

Figure 8.TEM micrographsof raw, boiled and calcined chicken eggshells3.4 Image analysis

184

Figure 9 shows the pores observable on the raw, boiled and calcined chicken eggshell samples. It was observed that the three samples presented varying surface configurations. As shown in Table 3, the boiled sample presented the least perimeter, area and diameter followed by the raw sample and the calcined sample. Previous studies by Salaudeen et al.[47], Tsai et al.[56] and Thommes et al.[57] have shown that pore diameter, perimeter and area increase with calcination. This may be attributed to the merging of smaller pores and the growth of CaO grain size due to sintering at high calcination temperatures as reported by Zhu et al.[58]. The increased pore size may provide space for moisture and accumulation of impurities. The reduced pore perimeter, diameter and area of the boiled chicken eggshell sample compared with the raw chicken eggshell sample might be due to deposit of salts on the pores during boiling. The calcined sample with 200 nmparticle size and aggregate resulted in the highest surface area. Calcined chicken eggshell is predicted to lead to enhanced reaction and consequently the highest FAME yield when compared with the other samples. This is in agreement with the work of Win, and Khine[59], and Piker et al. [49].
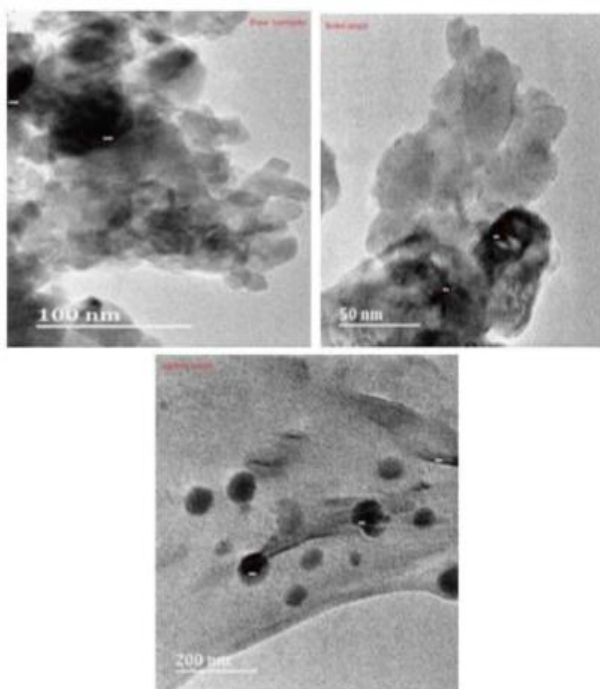
Figure 9. TEM micrograph for image analysis

Table 3. Details of pores of the raw, boiled, and calcined chicken eggshell

Chicken eggshell sample	Perimeter (nm)	Area (nm^2)	Diameter (nm)
Raw	75.73 – 90.79	210.75 – 343.14	28.33 – 30.55
Boiled	24.93 – 62.80	32.87 – 112.38	8.90 – 20.76
Calcined	129.02 – 184.41	192.60 – 1917.78	37.65 – 58.51

185

3.5. TGA analysis

The results of thermogravimetric analysis (TGA) of 14.278mg, 37.067mg and 6.663mg samples of raw chicken eggshell powder, boiled chicken eggshell power and calcined chicken eggshell powder respectively, is shown in Figure 10. TGA results show the temperature at which various samples of waste chicken eggshell powder decompose when heated in a controlled environment. Raw and boiled chicken eggshell samples followed the same pattern of decomposition,i.e. one-step weight loss. The weight loss occurred for both raw and boiled samples between 700°C and 900°C. The raw eggshell sample experienced 42% weight loss while the boiled eggshell sample experienced 44.5% weight loss. This confirmed the XRD result that indicated that boiling has no significant effect on eggshells because the boiling temperature is too low to cause decomposition of $CaCO_3$ to CaO, since decomposition depends on temperature according to Salaudeen et al.[47] and Fernando et al.[60].The calcined sample experienced 5.5% weight loss at 450°C with no further weight loss noticed. This confirmed that the calcination temperature of 900°C adopted for this work is sufficient for complete decomposition of $CaCO_3$. Above 500°C, the weight of the calcined eggshell sample became almost constant. This shows that a calcination temperature greater than 500°C is required to transform $CaCO_3$ to CaO. Similar observations were reported by Joshi et al.[52], Wei et al.[61], and Sharma et al.[62], though at different decomposition temperatures.
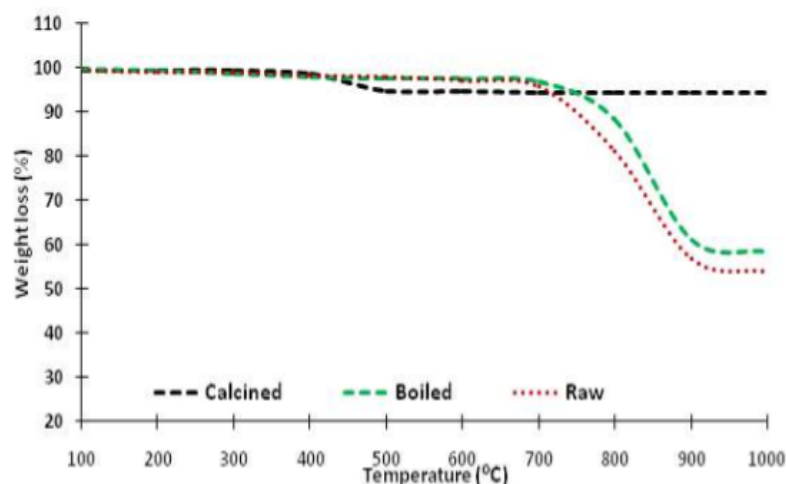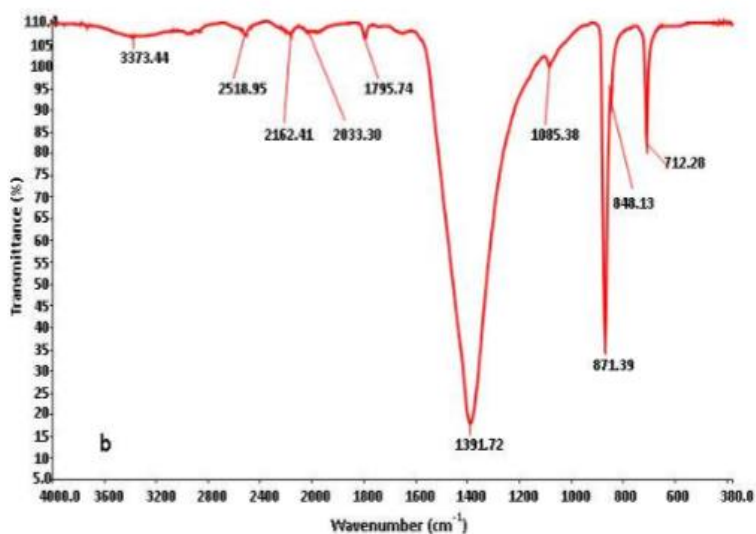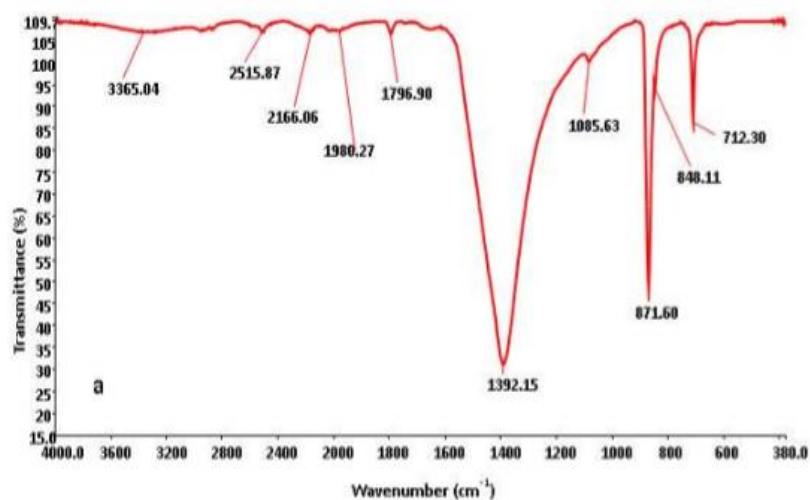

Figure 10.TGA curves of chicken eggshell powder

3.6. FTIR analysis

The FTIR analysis of raw, boiled and calcined chicken eggshells was performed and compared as shown in Figure 11. The FTIR spectra of raw and boiled chicken eggshells look similar with the major absorption band occurring at 1392 cm^{-1} followed by 872 cm^{-1} in both samples. This is an indication that boiling made little or no difference to the samples since the temperature of the boiling was not high enough to affect them. This is confirmed by the result of the XRD analysis which showed that both samples contained more CO^{-2} than the calcined sample. The medium broadband at712.3 cm^{-1} indicates the presence of HCO^3 for the two samples that were not calcined. Both raw and boiled samples have common peaks as shown in Figure 11 (a) and (b). This is in agreement with previous results from Goli and Sahu[48], Mosaddegh[63], Yusuff et al.[64] and Tsai et al.[56]. After calcination, there is decomposition of $CaCO_3$ into CaO which causes adecrease of the reduced mass of the functional group

attached to the CO_2^{-3} ions, and, as a result, a decrease in the intensity of the $CaCO_3$ peak. The calcined sample has a peak of $3641 cm^{-1}$ at around 88% transmittance which can be ascribed to the presence of theOH group in the calcium hydroxide. This result agrees with Tan et al.[19], Margaretha et al.[65], Roschat et al.[66] and Andherson et al.[67].
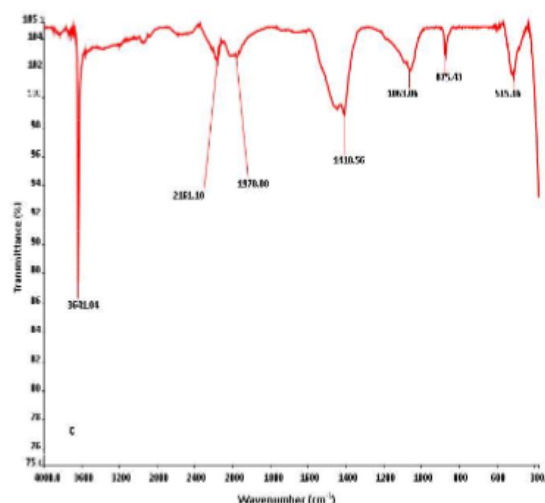
187

Omojola Awogbemi, Freddie L. Inambao, and Emmanuel I. Onuh

Figure 11. FITR of (a) Raw, (b) Boiled, and (c) Calcined chicken eggshell powder

4. CONCLUSION

The preparation, development and characterization of chicken eggshell waste has been presented. Chicken eggshell waste was collected from bakeries and prepared accordingly into raw, boiled and calcined 75 μm powder and stored in closed glass vials and characterized. The results of the XRD showed that while raw and boiled chicken eggshells consisted mainly of calcite ($CaCO_3$), calcined chicken eggshells were mainly lime (CaO). This is due to the thermal decomposition of $CaCO_3$ to CaO and portlandite ($Ca(OH)_2$) during calcination. TGA analysis also showed no significant difference in the thermal decomposition pattern in the raw and boiled chicken eggshells; there was a 44.5% and 42% weight loss for the boiled and raw eggshell samples respectively, while the calcined sample only witnessed a 5.5% weight loss at a lower temperature compared with the raw and boiled samples. SEM analysis showed that raw, boiled, and calcined eggshell powders contained 41.31%, 21.91%, and 46.08% of calcium, 14.93%, 26.40% and 6.22% of carbon, and 43.76%, 51.68%, and 47.70% of oxygen respectively. The high oxygen content can be attributed to exposure to the atmosphere during preparation and analysis. The import of this is that in the calcination process, most $CaCO_3$ in the chicken eggshell powder was transformed to CaO, confirming that a calcination temperature of 900°C is sufficient to convert $CaCO_3$ to CaO. The results of the various characterization processes show that there are no significant differences between raw and boiled eggshells in terms of composition, pore size, thermal decomposition and microstructural image. Thus, calcination at high temperature is needed to decompose the $CaCO_3$ in chicken eggshell waste into CaO which is more useful. This work is in agreement with the works of Navajas et al.[35], Tan et al.[55] and Mansir [68]that calcined chicken eggshell waste has great potential as a low cost and effective heterogeneous catalyst for the transesterification of waste cooking oil into FAME. Chicken eggshell waste calcined at not less than 900°C for 3 h with small particle size is suitable as a catalyst for the transesterification of waste cooking oil into FAME with high yield and reusability [34, 49, 59, 67].

REFERENCES

[1]   B. Sajjadi, A. A. A. Raman, and H. Arandiyan, "A comprehensive review on properties of edible and non-edible vegetable oil-based biodiesel: Composition, specifications and prediction models," Renewable and Sustainable Energy Reviews, vol. 63, pp. 62-92, 2016/09/01/ 2016.

[2]   "International Energy Outlook. A publication of US Energy International Administration (EIA). Available on https://www.eia.gov/outlooks/ieo/."

[3]   "Primary energy consumption worldwide by region 2010-2017. Available on https://www.statista.com/statistics/263457/primary-energy-consumption-by-region/. Released June, 2018."

[4]   "Global CO2 emissions related to energy 2010-2017. Available on https://www.statista.com/statistics/526002/energy-related-carbon-dioxide-emissions-worldwide/. March, 2018."

[5]   F. Ouanji, M. Kacimi, M. Ziyad, F. Puleo, and L. F. Liotta, "Production of biodiesel at small-scale (10 L) for local power generation," International Journal of Hydrogen Energy, vol. 42, no. 13, pp. 8914-8921, 2017.

[6]   R. A. M. Boloy, S. J. R. Ferrán, D. d. C. L. e Penalva, C. Corrêa, J. A. P. Angulo, and R. de Castro Pereira Filho, "Exergetic evaluation of incorporation of hydrogen production in a biodiesel plant," international journal of hydrogen energy, vol. 40, no. 29, pp. 8797-8805, 2015.

[7]   W. Roschat, T. Siritanon, B. Yoosuk, T. Sudyoadsuk, and V. Promarak, "Rubber seed oil as potential non-edible feedstock for biodiesel production using heterogeneous catalyst in Thailand," Renewable Energy, vol. 101, pp. 937-944, 2017.

[8]   B. R. Moser, "Fuel property enhancement of biodiesel fuels from common and alternative feedstocks via complementary blending," Renewable Energy, vol. 85, pp. 819-825, 2016.

[9]   W. Roschat, T. Siritanon, B. Yoosuk, and V. Promarak, "Biodiesel production from palm oil using hydrated lime-derived CaO as a low-cost basic heterogeneous catalyst," Energy conversion and management, vol. 108, pp. 459-467, 2016.

[10]   F. Ouanji, M. Khachani, M. Boualag, M. Kacimi, and M. Ziyad, "Large-scale biodiesel production from Moroccan used frying oil," International Journal of Hydrogen Energy, vol. 41, no. 45, pp. 21022-21029, 2016.

[11]   H. Hamze, M. Akia, and F. Yazdani, "Optimization of biodiesel production from the waste cooking oil using response surface methodology," Process Safety and Environmental Protection, vol. 94, pp. 1-10, 2015.

[12]   A. S. Roy, A. Chingkheihunba, and K. Pakshirajan, "An Overview of Production, Properties, and Uses of Biodiesel from Vegetable Oil," in Green Fuels Technology: Biofuels, C. R. Soccol, S. K. Brar, C. Faulds, and L. P. Ramos, Eds. Cham: Springer International Publishing, 2016, pp. 83-105.

[13]   S. H. Y. S. Abdullah et al., "A review of biomass-derived heterogeneous catalyst for a sustainable biodiesel production," Renewable and Sustainable Energy Reviews, vol. 70, pp. 1040-1051, 2017/04/01/ 2017.

[14]   S. N. Gebremariam and J. M. Marchetti, "Economics of biodiesel production: Review," Energy Conversion and Management, vol. 168, pp. 74-84, 2018/07/15/ 2018.

[15] S. E. Mahesh, A. Ramanathan, K. M. S. Begum, and A. Narayanan, "Biodiesel production from waste cooking oil using KBr impregnated CaO as catalyst," Energy Conversion and Management, vol. 91, pp. 442-450, 2015.

[16] R. Shan, C. Zhao, P. Lv, H. Yuan, and J. Yao, "Catalytic applications of calcium rich waste materials for biodiesel: current state and perspectives," Energy Conversion and Management, vol. 127, pp. 273-283, 2016.

[17] H. Jaliliannosrati, N. A. S. Amin, A. Talebian-Kiakalaieh, and I. Noshadi, "Microwave assisted biodiesel production from Jatropha curcas L. seed by two-step in situ process: optimization using response surface methodology," Bioresource technology, vol. 136, pp. 565-573, 2013.

[18] D. M. Marinković et al., "Calcium oxide as a promising heterogeneous catalyst for biodiesel production: Current state and perspectives," Renewable and Sustainable Energy Reviews, vol. 56, pp. 1387-1408, 2016.

[19] Y. H. Tan, M. O. Abdullah, C. Nolasco-Hipolito, and Y. H. Taufiq-Yap, "Waste ostrich- and chicken-eggshells as heterogeneous base catalyst for biodiesel production from used cooking oil: Catalyst characterization and biodiesel yield performance," Applied Energy, vol. 160, pp. 58-70, 2015.

[20] A. Laca, A. Laca, and M. Díaz, "Eggshell waste as catalyst: A review," Journal of environmental management, vol. 197, pp. 351-359, 2017.

[21] H. Mazaheri et al., "Rice bran oil based biodiesel production using calcium oxide catalyst derived from Chicoreus brunneus shell," Energy, vol. 144, pp. 10-19, 2018.

[22] P.-L. Boey, G. P. Maniam, and S. A. Hamid, "Performance of calcium oxide as a heterogeneous catalyst in biodiesel production: a review," Chemical Engineering Journal, vol. 168, no. 1, pp. 15-22, 2011.

[23] A. Marwaha, P. Rosha, S. K. Mohapatra, S. K. Mahla, and A. Dhir, "Waste materials as potential catalysts for biodiesel production: Current state and future scope," Fuel Processing Technology, vol. 181, pp. 175-186, 2018/12/01/ 2018.

[24] E. Fayyazi et al., "Optimization of biodiesel production over chicken eggshell-derived CaO catalyst in a continuous centrifugal contactor separator," Industrial & engineering chemistry research, vol. 57, no. 38, pp. 12742-12755, 2018.

[25] I. Reyero, G. Arzamendi, and L. M. Gandía, "Heterogenization of the biodiesel synthesis catalysis: CaO and novel calcium compounds as transesterification catalysts," Chemical Engineering Research and Design, vol. 92, no. 8, pp. 1519-1530, 2014.

[26] A. S. Yusuff, O. D. Adeniyi, S. O. Azeez, M. A. Olutoye, and U. G. Akpan, "THE POTENTIAL OF COMPOSITE ANTHILL-WASTE CHICKEN EGGSHELL AS HETEROGENEOUS CATALYST IN BIODIESEL PRODUCTION," Petroleum & Coal, vol. 60, no. 1, 2018.

[27] R. Y. Wee, "Top Egg Producing Countries In The World. Available on https://www.worldatlas.com/articles/top-egg-producing-countries-in-the-world.html," 2017.

[28] "Egg Industry Production Report for March 2018 produced by South African Poultry Association. 2018. Available on https://www.sapoultry.co.za/pdf-statistics/egg-industry.pdf."

[29] T. Zaman, M. Mostari, M. A. A. Mahmood, and M. S. Rahman, "Evolution and characterization of eggshell as a potential candidate of raw material," Cerâmica, vol. 64, no. 370, pp. 236-241, 2018.

[30] S. Niju, K. M. Meera, S. Begum, and N. Anantharaman, "Modification of egg shell and its application in biodiesel production," Journal of Saudi Chemical Society, vol. 18, no. 5, pp. 702-706, 2014/11/01/ 2014.

190

[31]   S. Majhi and S. Ray, "A study on production of biodiesel using a novel solid oxide catalyst derived from waste," Environmental Science and Pollution Research, vol. 23, no. 10, pp. 9251-9259, 2016.

[32]   D. Sinha and S. Murugavelh, "Comparative studies on biodiesel production from Waste Cotton Cooking Oil using alkaline, calcined eggshell and pistachio shell catalyst," in Energy Efficient Technologies for Sustainability (ICEETS), 2016 International Conference on, 2016, pp. 130-133: IEEE.

[33]   S. B. Chavan, R. R. Kumbhar, D. Madhu, B. Singh, and Y. C. Sharma, "Synthesis of biodiesel from Jatropha curcas oil using waste eggshell and study of its fuel properties," RSC Advances, vol. 5, no. 78, pp. 63596-63604, 2015.

[34]   N. S. El-Gendy and S. Deriase, "Waste eggshells for production of biodiesel from different types of waste cooking oil as waste recycling and a renewable energy process," Energy Sources, Part A: Recovery, Utilization, and Environmental Effects, vol. 37, no. 10, pp. 1114-1124, 2015.

[35]   A. Navajas, T. Issariyakul, G. Arzamendi, L. Gandía, and A. Dalai, "Development of eggshell derived catalyst for transesterification of used cooking oil for biodiesel production," Asia-Pacific Journal of Chemical Engineering, vol. 8, no. 5, pp. 742-748, 2013.

[36]   D. Fecheyr-Lippens, A. Nallapaneni, and M. D. Shawkey, "Exploring the Use of Unprocessed Waste Chicken Eggshells for UV-Protective Applications," Sustainability, vol. 9, no. 2, p. 232, 2017.

[37]   S. Yoo, J. S. Hsieh, P. Zou, and J. Kokoszka, "Utilization of calcium carbonate particles from eggshell waste as coating pigments for ink-jet printing paper," Bioresource technology, vol. 100, no. 24, pp. 6416-6421, 2009.

[38]   F. S. Murakami, P. O. Rodrigues, C. M. T. d. Campos, and M. A. S. Silva, "Physicochemical study of CaCO3 from egg shells," Food Science and Technology, vol. 27, no. 3, pp. 658-662, 2007.

[39]   M. V. Iyer, S. Ramkumar, T. V. Haar, and L. Fan, "High temperature carbon dioxide capture and hydrogen production using engineered eggshells," in The 2006 Annual Meeting, 2006.

[40]   A. Mittal, M. Teotia, R. Soni, and J. Mittal, "Applications of egg shell and egg shell membrane as adsorbents: a review," Journal of Molecular Liquids, vol. 223, pp. 376-387, 2016.

[41]   M. Sarder, N. Hafiz, and M. Alamgir, "Study on the Effective Reuse of Eggshells as a Resource Recovery from Municipal Solid Waste," in Waste Management and Resource Efficiency: Springer, 2019, pp. 71-79.

[42]   M. T. Souza, B. G. Maia, L. B. Teixeira, K. G. de Oliveira, A. H. Teixeira, and A. P. N. de Oliveira, "Glass foams produced from glass bottles and eggshell wastes," Process Safety and Environmental Protection, vol. 111, pp. 60-64, 2017.

[43]   S. C. Onwubu, A. Vahed, S. Singh, and K. M. Kanny, "Reducing the surface roughness of dental acrylic resins by using an eggshell abrasive material," The Journal of prosthetic dentistry, vol. 117, no. 2, pp. 310-314, 2017.

[44]   A. S. Oladipo et al., "Magnetic recyclable eggshell-based mesoporous catalyst for biodiesel production from crude neem oil: Process optimization by central composite design and artificial neural network," Comptes Rendus Chimie, vol. 21, no. 7, pp. 684-695, 2018/07/01/ 2018.

[45]   N. Mansir, S. H. Teo, U. Rashid, and Y. H. Taufiq-Yap, "Efficient waste Gallus domesticus shell derived calcium-based catalyst for biodiesel production," Fuel, vol. 211, pp. 67-75, 2018/01/01/ 2018.

[46] D. Cree and A. Rutter, "Sustainable bio-inspired limestone eggshell powder for potential industrialized applications," ACS Sustainable Chemistry & Engineering, vol. 3, no. 5, pp. 941-949, 2015.

[47] S. A. Salaudeen, S. H. Tasnim, M. Heidari, B. Acharya, and A. Dutta, "Eggshell as a potential CO2 sorbent in the calcium looping gasification of biomass," Waste Management, vol. 80, pp. 274-284, 2018/10/01/ 2018.

[48] J. Goli and O. Sahu, "Development of heterogeneous alkali catalyst from waste chicken eggshell for biodiesel production," Renewable Energy, vol. 128, pp. 142-154, 2018.

[49] A. Piker, B. Tabah, N. Perkas, and A. Gedanken, "A green and low-cost room temperature biodiesel production method from waste oil using egg shells as catalyst," Fuel, vol. 182, pp. 34-41, 2016/10/15/ 2016.

[50] A. Lesbani, P. Tamba, R. Mohadi, and F. Fahmariyanti, "Preparation of calcium oxide from Achatina fulica as catalyst for production of biodiesel from waste cooking oil," Indonesian Journal of Chemistry, vol. 13, no. 2, pp. 176-180, 2013.

[51] A. A. Ayodeji, O. E. Modupe, B. Rasheed, and J. M. Ayodele, "Data on CaO and Eggshell Catalysts Used for Biodiesel Production," Data in Brief, 2018.

[52] G. Joshi et al., "Transesterification of Jatropha and Karanja oils by using waste egg shell derived calcium based mixed metal oxides," Energy Conversion and Management, vol. 96, pp. 258-267, 2015/05/15/ 2015.

[53] N. Tangboriboon, R. Kunanuruksapong, and A. Sirivat, "Preparation and properties of calcium oxide from eggshells via calcination," Materials Science-Poland, vol. 30, no. 4, pp. 313-322, 2012.

[54] P. R. Pandit and M. H. Fulekar, "Egg shell waste as heterogeneous nanocatalyst for biodiesel production: Optimized by response surface methodology," Journal of Environmental Management, vol. 198, pp. 319-329, 2017/08/01/ 2017.

[55] Y. H. Tan, M. O. Abdullah, and C. Nolasco-Hipolito, "The potential of waste cooking oil-based biodiesel using heterogeneous catalyst derived from various calcined eggshells coupled with an emulsification technique: A review on the emission reduction and engine performance," Renewable and Sustainable Energy Reviews, vol. 47, pp. 589-603, 2015/07/01/ 2015.

[56] W. Tsai, J. Yang, C. Lai, Y. Cheng, C. Lin, and C. Yeh, "Characterization and adsorption properties of eggshells and eggshell membrane," Bioresource technology, vol. 97, no. 3, pp. 488-493, 2006.

[57] M. Thommes et al., "Physisorption of gases, with special reference to the evaluation of surface area and pore size distribution (IUPAC Technical Report)," Pure and Applied Chemistry, vol. 87, no. 9-10, pp. 1051-1069, 2015.

[58] Y. Zhu, S. Wu, and X. Wang, "Nano CaO grain characteristics and growth model under calcination," Chemical engineering journal, vol. 175, pp. 512-518, 2011.

[59] T. T. Win and M. M. Khine, "Chicken Eggshell Waste as a Suitable Catalyst for Transesterification of Palm Oil, Optimization for Biodiesel Production," in 5th International Conference on Food, Agricultural and Biological Sciences (ICFABS-2016) Dec, 2016, pp. 25-26.

[60] F. Luna Vera, M. Guancha Chalapud, I. Castillo Viveros, and E. A. Vásquez Medina, "From Eggshells to Quicklime: Using Carbonate Cycle as an Integrating Concept To Introduce Students to Materials Analysis by TGA and FTIR," Journal of Chemical Education, vol. 95, no. 4, pp. 625-630, 2018.

[61] Z. Wei, C. Xu, and B. Li, "Application of waste eggshell as low-cost solid catalyst for biodiesel production," Bioresource technology, vol. 100, no. 11, pp. 2883-2885, 2009.

[62] Y. Sharma, B. Singh, and J. Korstad, "Application of an efficient nonconventional heterogeneous catalyst for biodiesel synthesis from Pongamia pinnata oil," Energy & Fuels, vol. 24, no. 5, pp. 3223-3231, 2010.

[63] E. Mosaddegh, "Ultrasonic-assisted preparation of nano eggshell powder: A novel catalyst in green and high efficient synthesis of 2-aminochromenes," Ultrasonics Sonochemistry, vol. 20, no. 6, pp. 1436-1441, 2013/11/01/ 2013.

[64] A. S. Yusuff, O. D. Adeniyi, M. A. Olutoye, and U. G. Akpan, "Development and Characterization of a Composite Anthill-chicken Eggshell Catalyst for Biodiesel Production from Waste Frying Oil," International Journal of Technology, vol. 9, no. 1, pp. 110-119, 2018.

[65] Y. Y. Margaretha, H. S. Prastyo, A. Ayucitra, and S. Ismadji, "Calcium oxide from Pomacea sp. shell as a catalyst for biodiesel production," International Journal of Energy and Environmental Engineering, vol. 3, no. 1, p. 33, 2012.

[66] W. Roschat, M. Kacha, B. Yoosuk, T. Sudyoadsuk, and V. Promarak, "Biodiesel production based on heterogeneous process catalyzed by solid waste coral fragment," Fuel, vol. 98, pp. 194-202, 2012.

[67] T. Andherson, D. Rachmat, and D. D. Risanti, "Potential use of chicken egg shells and cacao pod husk as catalyst for biodiesel production," in AIP Conference Proceedings, 2018, vol. 1945, no. 1, p. 020058: AIP Publishing.

[68] N. Mansir et al., "Modified waste egg shell derived bifunctional catalyst for biodiesel production from high FFA waste cooking oil. A review," Renewable and Sustainable Energy Reviews, vol. 82, pp. 3645-3655, 2018/02/01/ 2018.

CHAPTER 8: PROPERTIES AND FATTY ACID COMPOSITIONS OF FEEDSTOCK AND BIODIESEL

This chapter presents the properties and fatty acid compositions of feedstock and FAME. It consists of two articles.

Article 1 compares the properties and FA compositions of neat vegetable oils and used vegetable oils. The article compared the density, pH, congealing temperature, kinematic viscosity, acid value, iodine value, and FA composition of neat sunflower, palm, sunfoil, depot margarine and waste vegetable oil derived from these neat oils. The effects of usage on properties, FA compositions, human and aquatic health were emphasized. It was published in the *International Journal of Low-Carbon Technologies*.

> **Awogbemi, O,** Onuh E. I, Inambao F. (2019). "Comparative Study of Properties and Fatty Acid Composition of Some Neat Vegetable Oils and Waste Cooking Oils," International Journal of Low-Carbon Technologies, Volume 14, Number 3, ISSN 1748-1317. EISSN 1748-1325, pp 417-425. https://doi.org/10.1093/ijlct/ctz038 . Published by Oxford University Press. (Published)

Article 2 illustrates the influence of usage on the FA composition and properties of neat palm oil, waste palm oil, and waste palm oil methyl ester. The article examined the effects of usage on the properties and FA composition on WPO samples used by restaurants to fry different food items and the waste palm oil methyl ester derived from the WPO samples. This is to deduce their suitability as feedstock for transesterification. It has been peer-reviewed and accepted for publication by the *International Journal of Engineering and Technology*

> **Awogbemi, O.,** Inambao F., Onuh E. I. (2019). "Effect of Usage on the Fatty Acid Composition and Properties of Neat Palm Oil, Waste Palm Oil, and Waste Palm Oil Methyl Ester," International Journal of Engineering & Technology (IJET). Science Publishing Corporation. (Accepted for publication).

CHAPTER 8 ARTICLE 1: Comparative Study of Properties and Fatty Acid Composition of Some Neat Vegetable Oils and Waste Cooking Oils

Comparative study of properties and fatty acid composition of some neat vegetable oils and waste cooking oils

Omojola Awogbemi*,†, Emmanuel Idoko Onuh and Freddie L. Inambao

Green Energy Solutions Research Group, Discipline of Mechanical Engineering, Howard College, University of KwaZulu-Natal, Durban 4041, South Africa

Abstract

Vegetable oils have been used as a feedstock for fatty acid methyl ester (FAME) production. The high cost of neat vegetable oil and its impact on food security have necessitated its replacement as a feedstock for FAME by used vegetable oil, also known as waste cooking oil (WCO). This study compares the properties and fatty acid (FA) compositions of samples of neat vegetable oil with those of samples of WCO, collected from restaurants and takeaway outlets at the point of disposal. The samples were subjected to property determination and pyrolysis gas chromatography mass spectrometer (PYGCMS) analysis. Analysis showed that degree of usage and the type of food items originally fried in the oil substantially affected its properties and FA composition. Density of neat vegetable oil varied between 904.3 and 919.7 kg/m^3 and of WCO between 904.3 and 923.2 kg/m^3. The pH of neat vegetable oil varied between 7.38 and 8.63 and of WCO between 5.13 and 6.61. The PYGCMS analysis showed that neat palm oil contains 87.7% unsaturated FA and 12.3% saturated FA, whereas neat sunfoil contains 74.37% saturated FA and 25% polyunsaturated FA. Generally, neat vegetable oils consisted mainly of saturated FAs and polyunsaturated FAs, whereas the WCO contained mainly of saturated FAs and monounsaturated FAs. This research confirms the suitability of WCO as feedstock for FAME.

*Corresponding author:
217080448@stuukzn.ac.za

1 INTRODUCTION

Energy demand has continued to increase due to increased population and continued development of the industrial sector over the past few decades. With mounting evidence of the negative environmental effects of incessant combustion of fossil fuel, renewable or green energy sources are gaining wide acceptance globally [1–3]. Among the green energy alternatives, biodiesel has received substantial attention and research in recent years. Biodiesel fuel is sustainable and environmentally friendly, can be produced by households and is economically advantageous, especially considering the unpredictability of petroleum-based diesel fuel prices and the absence of strong policies to minimize the use of fossil fuels [4]. The increasing demand for sustainable and environmentally friendly alternatives to fossil sourced fuel has made the search for a readily available, economical and environmentally acceptable feedstock for sustainable biodiesel production inevitable [5, 6].

High cost and threat to food security have made the use of edible oil as biodiesel feedstock unrealistic and impractical. The huge amount of land required for cultivation, the high cost of farming, the long waiting period between planting and harvesting, as well as the threat of deforestation and to wildlife have made the use of inedible crops as feedstock unattractive [7, 8]. These challenges have shifted attention to the adaptation of used vegetable oil as feedstock. Used vegetable oil, also known as waste cooking oil (WCO), is produced when vegetable oil sourced from palm, soybean, sunflower, cottonseed, olive, palm kernel and rapeseed or animal fats like butter, fish oil and tallow are used to cook or fry food [9]. With feedstock accounting for between 70% and 75% of the production cost of biodiesel, the use of WCO has resulted in a substantial reduction in production costs, thereby significantly reducing the cost of biodiesel fuel, which makes WCO more viable as a substitute fuel for internal combustion engines particularly the unmodified compression ignition engines [10]. The adaptation of WCO as feedstock for biodiesel production
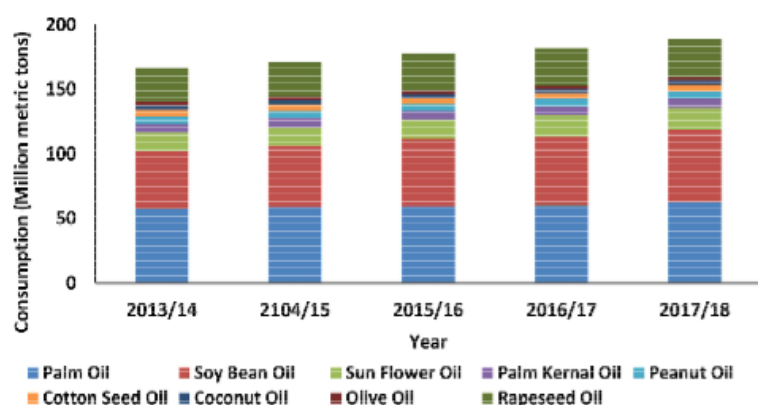
1

Figure 1. *Consumption of vegetable oils worldwide by oil type (million metric tonnes)* [13].

Table 1. *Estimated waste cooking oil collected in a year* [16, 18, 19].

Country	m³/year
The Netherlands	67 000
Italy	60 000
Portugal	28 000
Spain	270 000
Germany	250 000
Hungary	5500
Norway	1000

also helps in proper disposal of WCO; offers additional income to households, restaurants and fast-food outlets; prevents blockage of drains; minimizes water contamination; and preserves aquatic habitat [11]. The use of WCO as biodiesel feedstock also promotes employment generation and ensures social inclusion by engaging youths in the collection of WCO, thereby promoting community environmental education and campaigns [12].

Globally, consumption of vegetable oils has continued to increase, particularly in the last 5 years as shown in Fig. 1, with palm oil topping the list [13]. The largest percentage of these vegetable oils is used in households, restaurants and fast-food outlets for cooking and frying. Table 1 shows the estimated WCO collected by some countries. Canada is reported to generate between 120 000 and 135 000 tonnes of WCO per year [14, 15], while the USA produced 0.6 million tons of yellow grease in 2011. The UK and the European Union countries generated ~700 000–1 000 000 and 200 000 tonnes of WCO per year, respectively [16]. While 60 000 tonnes of WCO is collected yearly in South Africa, an estimated 200 000 tonnes of WCO is produced from households, bakeries, takeaway outlets and restaurants but uncollected annually [17, 18]. Japan, China and Malaysia generated 6000, 45 000 and 60 000 tonnes of WCO, respectively, annually. Of WCO generated globally, >60% is estimated to be disposed of inappropriately [18, 19].

It is evident that not all WCOs are used for biodiesel production or other fuel production processes. There are justifiable fears that some unscrupulous elements are filtering and rebottling the collected used vegetable oil for resale to unwary members of the public. Repeated consumption of food prepared with repack-aged WCO predisposes consumers to deleterious health consequences including diabetes, hypertension, vascular inflammation, and other pathologies [20–22]. Available statistics showed that WCO contributed 17% and 9% of the feedstock for the production of 11.92 million tons and 26.62 million tons of biodiesel by the European Union and globally, respectively, in 2015 [23]. Most people are not aware that WCO can be converted to fuel; hence, they dispose indiscriminately. A well-coordinated program of awareness for collection, transportation and conversion of WCO is required to motivate participants in the WCO chain.

The importance of utilizing WCO for biodiesel production has been well documented, but some knowledge gaps still exist with regard to the following: how local use of specific oil source alters their suitability for use as feedstock; how acid values and levels of saturation are altered by their primary applications; and what challenges these pose to the transesterification process at any given location [24, 25] The degree of usage of vegetable oil is believed to affect some of the properties, including the acid value and iodine value, which dictates the ease of conversion of the resulting WCO [26, 27]. Given the importance of WCO in the renewable fuel value chain, proper characterization of the feedstock is necessary to inform a research-based policy on how to unlock the actual economic value as well as combat the current recycling of WCO for human consumption, bearing in mind the attendant risks to public health.

Fatty acids (FAs) can be either saturated FAs (SFAs) or unsaturated FAs (USFAs) depending on the nature of carbon-to-carbon bonds. SFAs are carboxylic acids with between 12 and 24 single carbon-to-carbon bond and are chemically less reactive. They contain the maximum number of hydrogen atoms that a single

197

bond carbon atom can accommodate between the successive carbon atoms. The melting point of SFA has been found to increase with chain length, and those SFAs with 10 carbon atoms or more (capric, lauric, myristic, palmitic, margaric, stearic, arachidic and behenic acids) are solids at room temperature. Conversely, USFAs, unlike SFAs, have one or more carbon-to-carbon double bonds. USFAs can either be monounsaturated FAs (MUFAs) or polyunsaturated FAs (PUFAs) having one double bond or more than one double bond, respectively. Chemical reactivity increases with an increase in the number of double bonds. Oleic acid is the most naturally occurring MUFA. Other examples of MUFAs include caproleic, lauroleic, elaidic, myristoleic and palmitoleic acids. USFAs exist either in a cis-configuration or trans-configuration. Most cis-configurations are available in most of the naturally occurring USFAs, while the trans-configuration is precipitated due to hydrogenation and other technical processes. Notable examples of PUFAs with the number of double bonds include linoleic acids; two double bonds, linolenic acids; three double bonds, arachidic acids; four double bonds, eicosapentaenoic acids; five double bonds, docosahexaenoic acids; and six double bonds [28–30].

In one research, Vingering et al. [31] determined the FA composition of some commercial vegetable oil in the French market and reported that sunflower oil, for example, contains SFA, MUFA, and PUFA of 11.3%, 31.7% and 56.3%, respectively. Hellier et al. [32] experimentally carried out the FA compositions of seven vegetable oils, including palm oil and sunflower oil, and reported that while palm oil contains 40–47% palmitic acid and 36–44% oleic acid, sunflower oil is made up of 49–57% linoleic and 14–40% oleic acids. They also reported the density (at 20°C) and dynamic viscosity (at 59.7°C) of 910 kg/m³ and 19.4 mPa·s for palm oil and 916.9 kg/m³ and 17.2 mPa·s for sunflower oil, respectively. The FA composition of edible vegetable oil was determined after repeated cooking at elevated temperature by Banani et al. [33] using gas chromatography coupled to mass spectrometry (GCMS). It was reported that the oleic, linoleic, palmitic, stearic and linolenic acids contents were found to be 29.83%, 28.85%, 15.86%, 4.87% and 2.49%, respectively. The density at 15°C and viscosity at 40°C were found to be 910 kg/m³ and 23.12 mm²/s, respectively. Kumar and Negi [34] compared the FA composition of vegetable oil before and after repeated use and concluded that repeated use of vegetable oil alters the composition and induces various polymerized derivatives, hydrocarbons, and glyceride molecules, which make the oil unsafe for human consumption and disposal to the environment.

According to Panadare and Rathod [35], fresh vegetable oil undergoes lots of physio-chemical transformations during frying, which alters its properties, FA profiles and other fingerprints depending on factors like cooking duration, frying temperature and types of food items the oil was used for. In a research, Knothe and Steidley [36] analyzed the used and unused vegetable oil samples collected from 16 restaurants using FA profile, viscosity and acid value as a basis for comparison. They observed that WCO undergoes hydrogenation and oxidative degradation processes during high-temperature frying capable of altering its fingerprints. Owing to changes in FA profile of the oils during frying, the properties of the oil were altered by increasing in SFA and MUFA relative to PUFA. They attributed the changes in properties and FA composition to the effects of structural morphology of the fuel. Also, the palm oil used to fry the food items was reported to show an increased degree of saturation, higher viscosity, elevated cetane numbers, oxidative stability and other fingerprints of fatty acid methyl ester (FAME). The alteration in the fingerprint of the fuel as a result of the change of FA profile during frying was attributed to the known effects of compound structure on biodiesel properties. Due to the effect of high-temperature degradation during cooking, biodiesel derived from such feedstock is expected to exhibit a higher degree of saturation and greater oxidative stability. Also, the biodiesel is expected to possess elevated kinematic viscosity, higher cloud point and cetane number than does the biodiesel form of neat vegetable oil.

The objective of this research is to compare the properties and the FA composition of neat vegetable oil with WCO from such oils. The aim is to determine how the duration of usage and the type of food fried in the oil affect some properties and the FA composition of WCO compared with their neat vegetable oil source. The questions being investigated are as follows: How do duration of usage and the composition of food items fried by the neat vegetable oil influence the properties and FA composition of the WCO? How do the properties and FA composition of neat vegetable oil vary from those of WCO from the same source? What is the effect of consumption of these WCOs on human and the effect of their disposal on aquatic and terrestrial habitats? This current effort is limited to analysis of four samples of neat vegetable oil and six samples of WCO obtained from restaurants, bakeries, and takeaway outlets collected at the point of disposal. The degree of usage was not controlled, but the history of the samples was collected from the users.

2 MATERIALS AND METHOD

2.1 Material collection
Samples of neat vegetable oil and as-produced WCO were collected from restaurants, takeaway outlets and bakeries randomly from Durban, KwaZulu-Natal Province, South Africa. The degree and rate of usage of the oils were not monitored. The WCOs were collected as-produced and while awaiting disposal by the various outlets. The samples were collected for property determination and pyrolysis gas chromatography mass spectrometry (PYGCMS) analysis. Popular restaurants and fast-food outlets turned down requests for used oil samples and referred our requests to their regional offices. The samples used in the research were collected from small and owner-operated restaurants and takeaway outlets.

2.2 Treatment of WCO
The samples were poured into a beaker and heated at 110°C in an electric heater for 15 min to remove moisture. The WCO sample

Table 2. *Some properties and methods/instruments of determination* [37, 38]

Property	Unit	Method/instrument
Density at 20°C	kg/m³	ASTM D 1298
Kinematic viscosity at 40°C	mm²/s	ASTM D445
Acid value	—	AOCS Ca 4a-40
Iodine value	cg/g	AOCS Cd 1B-87
Molecular weight	g/mol	Calculated
pH	—	pH meter
Congealing temperature	°C	Digital thermometer

was allowed to cool to room temperature and subjected to vacuum filtration process to remove any food residue and other suspended solid matter in the sample. The clean WCO samples were stored in an airtight glass container.

2.3 Property determination of neat vegetable oil and WCO samples

The iodine value, pH, density, congealing temperature, acid value, viscosity, cetane index and an acid number of neat vegetable oil and clean WCO samples were determined using the appropriate methods [37] and equipment as shown in Table 2.

i. pH: The pH of the WCO was determined with the aid of a pH meter.
ii. Congealing temperature: The congealing temperature of the samples was determined by putting 20 ml of the sample of neat vegetable oil and WCO in a 100-ml beaker, inserting the probe of a digital thermocouple into the sample and putting it into deep freeze. The temperature of the neat and WCO samples was monitored through a thermometer. The congealing temperature is the mean of the temperatures at the commencement and completion of gelation of the oil samples.
iii. Density and kinematic viscosity: The density and kinematic viscosity of the neat vegetable oil and WCO samples were determined by a viscometer at 20°C using a DMA™ 4100 M density meter.
iv. Iodine value: The iodine value of the WCO samples was determined in accordance with the AOCS Cd 1b-87 method.
v. Acid number: The acid value of the WCO samples was determined in accordance with the AOCS Ca 5a-40 method.
vi. Molecular weight: Calculated from the molecular weight of the individual FAs in the neat vegetable oil and WCO samples.

2.4 Determination of FA composition of neat vegetable oil and WCO samples

The FA composition of the neat vegetable oil and WCO samples was determined by PYGCMS on Shimadzu gas chromatograph mass spectrometer using an ultra-alloy-5 capillary column and

GCMS-QP2010 Plus software. The choice of PYGCMS rather than the normal GCMS was due to the low volatility nature of the samples, which might clog the column of the GCMS machine. The selected carrier gas was helium, while 2 μl of sample was injected at column oven temperature and injection temperature of 40°C and 240°C, respectively. The total flow, column flow, linear velocity and purge flow were set and maintained at 58.2 ml/min, 1.78 ml/min, 48.1 cm/s and 3.0 ml/min, respectively, at a total time of 92.33 min. Split injection mode was adopted.

3 RESULT AND DISCUSSION

3.1 Effects of usage on properties and FA composition

Properties of samples of neat vegetable oil are shown in Table 3. The pH of the four neat vegetable oil samples varies between 6.34 and 8.63, while the congealing temperature varies between −10.25°C and 0.3°C. Though their density is almost the same, depot margarine presented the highest viscosity value when compared with other neat vegetable oil samples. Table 4 shows the sources, points of collection, usage, duration and properties of the WCO samples. Though the numbers of days of usage were known, the numbers of cycles of usage and frying temperature were not known.

The pH of WCO samples varies between 5.13 and 6.61, indicating a weak acid, which confirms its suitability as a biodiesel feedstock. It was observed that sausage triggered higher pH values than did fish. This might be a result of fats from fish being more acidic than those of beef [39]. WCO samples from bakeries were the most acidic samples. The reduction in the acidity of waste palm oil after repeated frying can be attributed to the effects of thermal degradation and contamination from the food items. Almost all the neat vegetable oil samples witnessed a reduction in pH as a result of usage. Samples D and F have the highest congealing temperature followed by sample B from depot margarine, while sample C has the least congealing temperature of −6.3°C (see Table 4). The change in the congealing temperature can be traced to the effects of contamination of the food items.

The results in Table 4 show that the subjection of vegetable oil to high temperature over a period of time has degraded and reduced its quality. Though the densities of neat vegetable oil are not remarkably different from each other, the densities of WCO vary with usage, generally. The density of the six WCO samples varied between 904 and 923 kg/m³. Sample E, which was used for 7 days, has a higher density than has sample C from the same source, used for the same purpose but for a longer duration. It can be deduced, therefore, that the density of WCO samples reduced with increased duration of usage. This thermal dissociation can be attributable to decomposition of the double chain in the carbon chain caused by pyrolysis. The viscosity of the WCO samples ranges between 33.46 mm²/s for sample A (used to fry fish and potatoes) and 48.32 mm²/s for sample B (taken from a bakery).

Table 5 shows that only nine FAs are present in the samples and in low percentages, with the highest being 45% linoleic acid in palm oil. Linoleic acid, capric acid and stearic acid are common in

Table 3. *Properties of neat vegetable oil samples*

Samples	pH	Congealing temperature (°C)	Density at 20°C (kg/m³)	Viscosity at 40°C (mm²/s)	Molecular weight (g/mol)
Sunflower	7.38	−8.65	919.21	28.744	670.82
Sunfoil	8.63	−9.8	919.6	28.224	119.71
Palm oil	6.34	−10.25	919.48	27.962	535.08
Depot margarine	6.39	0.3	919.72	29.334	563.87

Table 4. *Specifications and properties of the WCO samples*

Sample	Source oil	Outlet	Usage	Usage (days)	pH	Congealing temperature (°C)	Density at 20°C (kg/m³)	Viscosity at 40°C (mm²/s)	Iodine value (cg/g)	Acid value	Molecular weight (g/mol)
A	Sunflower oil	Restaurant	Fish and chips	14	5.34	−5.15	920.4	31.381	111.1	2.29	51.94
B	Depot margarine	Bakery	Doughnuts	14	5.13	4.9	917.18	40.927	54.9	2.87	534.01
C	Sunfoil	Takeaway	Chips	14	6.14	−6.3	919.8	43.521	116.7	0.72	55.18
D	Palm oil	Takeaway	Fish and chips	14	5.73	12.3	904.3	44.254	81.7	0.66	135.66
E	Sunfoil	Restaurant	Chips	7	6.61	−3.4	923.2	35.236	110.3	1.44	395.28
F	Palm oil	Takeaway	Chips and sausages	14	6.19	14.7	913.4	38.407	54.2	1.13	586.05

Table 5. *Fatty acid composition of neat vegetable oil samples*

Fatty acid				Neat vegetable oil samples			
Common name	Formula		Acronym	Sunflower oil	Sunfoil	Palm oil	Depot margarine
Palmitic acid	$CH_3(CH_2)_{14}COOH$		C16:0	32.21	—	—	8.07
Linoleic acid	$CH_3(CH_2)_4CH=CHCH_2CH=CH (CH_2)_7COOH$		C18:2	21.98	3.26	45.50	24.57
Erucid acid	$CH_3(CH_2)_7CH=CH (CH_2)_{11}COOH$		C22:1	—	—	6.83	—
Caprylic acid	$CH_3(CH_2)_6COOH$		C8:0	0.22	1.68	0.56	1.06
Enanthic acid	$CH_3(CH_2)_5COOH$		C7:0	0.51	—	0.82	—
Capric acid	$CH_3(CH_2)_8COOH$		C10:0	0.51	3.79	2.43	2.84
Stearic acid	$CH_3(CH_2)_{16}COOH$		C18:0	9.27	2.87	2.67	4.22
Arachidic acid	$CH_3(CH_2)_{18}COOH$		C20:0	12.36	—	—	—
Lauric acid	$CH_3(CH_2)_{10}COOH$		C12:0	—	1.12	0.86	0.83
Saturated fatty acid, SFA (%)				71.48	74.37	12.3	40.92
Monounsaturated fatty acid, MUFA (%)				—	—	11.45	—
Polyunsaturated fatty acid, PUFA (%)				28.52	25.63	76.25	59.08

all the samples, while arachidic acid only appeared in one sample. Sunflower oil and sunfoil contain mainly SFAs, while palm oil and depot margarine contain mainly PUFAs. However, only palm oil contains MUFAs as shown in Fig. 2.

As shown in Table 6, the WCO samples have a fewer number of FAs and in smaller quantities. This further confirms the samples' suitability as FAME feedstock [40]. Oleic acid is the most frequently occurring acid, appearing in all the samples. As shown in Table 6, samples B, C, D and F have more SFAs, while samples A and E have more MUFAs and PUFAs, respectively. For example, sample D (used to fry beef) is composed of SFA and MUFA, as confirmed by Abbas *et al.* [41].

The mainly SFAs in neat sunflower oil were converted to mostly MUFAs in WCO sample A, while the SFAs in neat sunfoil oil were also converted to PUFAs in WCO sample E.

Conversely, the neat palm oil and depot margarine, which were mostly made up of PUFAs, were converted into SFAs in samples B, D and E after repeated high-temperature cooking. These may be attributed to the effect of prolonged exposure to high temperature.

The variation in the FA compositions of samples C and E, despite being from the same sunfoil and used to fry potato chips, shows that the SFA in sunfoil is converted into the PFAs in sample E and SFAs in sample C. This may be attributed to the greater duration of usage of sample C compared with sample E. Food items, especially fish and beef, greatly affect the FA composition of WCO from those sources [39]. As shown in Table 6, the observed difference in the level of saturation between sample D and F was due to the fact that fish contains more unsaturated oil than does sausage. So even though both samples are from the same primary oil source, what they were used for altered the FA composition.

Generally, due to repeated and high cooking temperature, the PYGCMS showed the presence of hydrocarbons and polymerized derivative of glyceride. The transformation and the mechanism for generation of cyclic and noncyclic hydrocarbon in vegetable oil during high-temperature repeated cooking can be difficult to predict as a result of the myriads of reactions that produce many unstable intermediate hydrocarbons, including the weak C–H bond. Also, a persistent increase of peroxide value during multiple

200
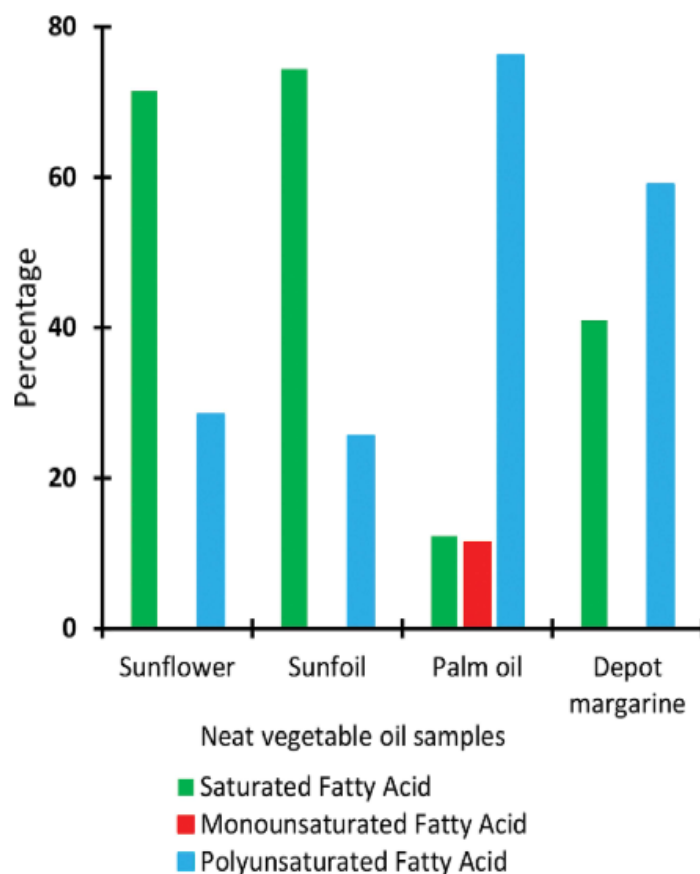
Figure 2. *SFA, MUFA and PUFA compositions of neat vegetable oil samples.*

Table 6. *Fatty acid composition of WCO samples*

Fatty acid			Waste cooking oil samples					
Common name	Formula	Acronym	A	B	C	D	E	F
Oleic acid	$CH_3(CH_2)_7CH=CH\ (CH_2)_{11}COOH$	C18:1	0.8	18.02	0.59	0.72	2.74	14.39
Palmitic acid	$CH_3(CH_2)_{14}COOH$	C16:0	0.36	43.2	—	—	5.98	40.21
Linoleic acid	$CH_3(CH_2)_4CH=CHCH_2CH=CH\ (CH_2)_7COOH$	C18:2	0.10	—	—	—	33.89	—
Erucid acid	$CH_3(CH_2)_7CH=CH\ (CH_2)_{11}COOH$	C22:1	0.26	—	—	—	—	—
Caprylic acid	$CH_3(CH_2)_6COOH$	C8:0	0.20	0.15	—	—	—	—
Undecylic acid	$CH_3(CH_2)_9COOH$	C11:0	—	1.85	0.43	—	0.52	—
Stearic acid	$CH_3(CH_2)_{16}COOH$	C18:0	—	—	1.14	—	—	—
Myristic acid	$CH_3(CH_2)_{12}COOH$	C14:0	—	—	—	—	—	17.04
Nonadecylic acid	$CH_3(CH_2)_{17}COOH$	C19:0	—	—	—	9.76	—	—
Saturated fatty acid, SFA (%)			32	71	73	93	15	80
Monounsaturated fatty acid, MUFA (%)			62	29	27	7	6	20
Polyunsaturated fatty acid, PUFA (%)			6	—	—	—	79	—

201

Table 7. *Some harmful chemicals in WCO and their effects*

Chemical		Effects	Reference
2,3-Dihydroxypropyl elaidate	$C_{21}H_{40}O_4$	• Harmful if ingested • Causes severe eye irritation	[47]
1-Hexanol	$C_6H_{14}O$	• Harmful if consumed or touches the skin • Causes severe eye irritation	[48]
Palmitic acid	$C_{16}H_{32}O_2$	• Causes acute skin, eye and respiratory irritations • Harmful to aquatic life with long-lasting effects	[49]
Linoleic acid	$C_{18}H_{32}O_2$	• Triggers skin, eye and respiratory irritations • The possibility of causing long-lasting damaging effects on aquatic life	[50]
i-Propyl 14-methyl-pentadecanoate	$C_{16}H_{32}O_2$	• Toxic to aquatic animals and wildlife habitat • Causes eye and skin irritations and lung injury • Long-term destructive health effects • Acute mammalian inhalation toxicity	[51]
1-Heptene	C_7H_{14}	• Highly combustible liquid and vapor • Maybe dangerous if swallowed and enters airways • Poisonous to aquatic life with long grave consequence	[52]
cis-9-Hexadecenal	$C_{16}H_{30}O$	• Causes skin, acute eye and respiratory irritations • Harmful if inhaled • Extremely poisonous to aquatic life	[52]

high temperatures energized water to act as a weak nucleophile for ester linkage, while heat mass transfer and induced oxygen aggravated thermal oxidation [34, 42].

3.2 Effects of usage of vegetable oil on health and aquatic habitat

Human consumption of used vegetable oil has undesirable effects on human health. Available facts reveal that consumption of SFA such as palmitic acid is injurious to cardiovascular health [43]. As shown in Table 6, most WCO samples consist mainly of SFAs and MUFAs and less of PUFAs. According to the Food and Agriculture Organization report of an expert consultation on fats and FAs in human nutrition, the SFAs and MUFAs in the WCO samples are higher than those recommended for human consumption. Intake of major SFAs including lauric, myristic and palmitic acids not only increases low-density lipoprotein (LDL) cholesterol but also increases the risk of diabetes. Replacing SFA with PUFA decreases the risk of coronary heart disease (CHD). Recommended human consumption of SFAs is less than 10%. Also, consumption of MUFAs is capable of increasing high-density lipoprotein (HDL) cholesterol concentrations, while consumption of oleic acid may aggravate insulin resistance, unlike the PUFAs. The effects of consumption of PUFAs on human health have been traced to the prevention of cardiovascular disease (DVD), coronary heart disease (CDH), cancer, diabetes, renal diseases, inflammatory, thrombotic and autoimmune disease, hypertension as well as renal diseases and rheumatoid arthritis [44–46]. The PUFAs in the neat vegetable oil samples have been converted to SFAs and MUFAs as a result of the thermal degradation occasioned by repeated subjection of the oil to high temperature during cooking and frying. This has made the WCO injurious for human consumption.

Contamination of aquatic habitat by WCO as a result of improper disposal has negative effects on aquatic animals. Apart

from the FA composition in WCO, the PYGCMS also revealed other components of the oil. Table 7 shows other components of WCO and their effects on human, wildlife and aquatic habitats. Inappropriate disposal and consumption of WCO should be discouraged by enforcing relevant regulations. Apart from the use of WCO as feedstock for FAME, WCO has been found to have household, personal and industrial applications. Hexanol is useful as a fuel, a fuel additive and a flavoring agent. 2,3-Dihydroxypropyl elaidate and 1-hexanol, which are present in some of the WCO samples, can be used in plastic and rubber products, lubricants and lubricant additives, greases, paint and coating additives, pigment solvents, cleaning and furniture care products, food packaging and personal care products, among other industrial and household applications [47, 48].

4 CONCLUSION

The application of WCO, in contrast to neat edible oil and inedible oil, as feedstock for FAME has been found to be economically beneficial. The use of WCO reduces the high production cost of biodiesel; solves problems associated with the disposal of WCO; eliminates problems associated with contamination of aquatic and terrestrial habitats, and blocking of drains and pipelines as a result of inappropriate disposal methodologies; and generates additional income for households and small-scale businesses. This research has shown that the properties and FA composition of neat vegetable oil can be modified by the degree of usage and food items. The exposure to high temperature during cooking, duration of usage, and what oil was used to fry have been found to substantially affect the properties and FA compositions of the oils. More importantly, this research has proved that the duration of usage and the variety of food have considerable influence on the properties and FA composition of used vegetable oil. To a very large extent, neat vegetable oil is made up mostly of SFA

202

and PUFA; WCO, on the other hand, consists mainly of SFA and MUFA. Human consumption and inappropriate disposal of WCO result in serious health challenges and negatively affect terrestrial and aquatic animals.

During the course of collecting these samples, it was discovered that all the outlets were not willing to give out their used oil because they had signed agreements with some companies that buy the used oils from them. Unconfirmed reports indicate that a large percentage of these oils are filtered and sold to unsuspecting consumers, with attendant health implications. Appropriate policies should be introduced not only to discourage human consumption of WCO but to also ensure all WCOs are channeled towards industrial and energy applications, most especially fuel. In order for the country to meet its share of renewable fuel quota, especially for transport vehicles, tax holidays and other incentives should be granted to small-scale fuel refiners to convert WCO to biodiesel, hydrogenated green diesel and other forms of fuel for internal combustion engines. Strict penalties against inappropriate disposal and consumption of WCOs should be enforced by relevant government agencies.

REFERENCES

[1] L. Fereidooni, K. Tahvildari, and M. Mehrpooya, "Trans-esterification of waste cooking oil with methanol by electrolysis process using KOH," *Renewable Energy*, vol. 116, pp. 183–193, 2018/02/01/2018.

[2] Grönman K *et al.* Carbon handprint—an approach to assess the positive climate impacts of products demonstrated via renewable diesel case. *Journal of Cleaner Production* 206;1059–72 2019/01/01/2019.

[3] Kalghatgi G. Development of fuel/engine systems—the way forward to sustainable transport. *Engineering* 2019/03/28/2019.

[4] Katre G, Raskar S, Zinjarde S et al. Optimization of the in situ transesterification step for biodiesel production using biomass of *Yarrowia lipolytica* NCIM 3589 grown on waste cooking oil. *Energy* 142;944–52 2018/01/01/2018.

[5] L. Fereidooni, K. Tahvildari, P. Maghsoodi, and M. Mehrpooya, "Removal of methyl *tert*-butyl ether from contaminated water using ZnO and CuO nanocatalyst and investigation of effect of nanoparticle structure in removal efficiency," *Nature Environment and Pollution Technology*, vol. 16, no. 1, p. 301, 2017.

[6] Aghaie M, Mehrpooya M, Pourfayaz F. Introducing an integrated chemical looping hydrogen production, inherent carbon capture and solid oxide fuel cell biomass fueled power plant process configuration. *Energy Conversion and Management* 2016;124:141–54.

[7] Saba T et al. Biodiesel production from refined sunflower vegetable oil over KOH/ZSM5 catalysts. *Renewable Energy* 2016;90:301–6.

[8] O. Awogbemi, F. Inambao, and E. Onuh, "A review of the performance and emissions of compression ignition engine fuelled with waste cooking oil methyl ester," in 2018 *International Conference on the Domestic Use of Energy (DUE)*, 2018, pp. 1–9: IEEE.

[9] N. Said, F. Ani, and M. Said, "Review of the production of biodiesel from waste cooking oil using solid catalysts," *Journal of Mechanical Engineering and Sciences*, vol. 8, no. unknown, pp. 1302–1311, 2015.

[10] A. N. Phan and T. M. Phan. Biodiesel production from waste cooking oils," *Fuel*, vol. 87, no. 17, pp. 3490–3496, 2008/12/01/2008.

[11] P. D. Patil, V. G. Gude, H. K. Reddy, T. Muppaneni, and S. Deng, "Biodiesel production from waste cooking oil using sulfuric acid and microwave irradiation processes," *Journal of Environmental Protection*, vol. 3, no. 1, p. 107, 2012.

[12] Moecke EHS *et al.* Biodiesel production from waste cooking oil for use as fuel in artisanal fishing boats: integrating environmental, economic and social aspects. *Journal of Cleaner Production* 2016;135: 679–88.

[13] Statista. "Vegetable Oils: Global Consumption by Oil Type 2013/14 to 2017/2018." Available: https: //www.statista.com/statistics/263937/vegetable-oils-global-consumption/ [Online].

[14] Canada S. Canada's population clock. *Statistics Canada, Demography Division.* 2006;2006.

[15] T. Issariyakul, M. G. Kulkarni, A. K. Dalai, and N. N. Bakhshi, "Production of biodiesel from waste fryer grease using mixed methanol/ethanol system," *Fuel Processing Technology*, vol. 88, no. 5, pp. 429–436, 2007.

[16] E. Martinez-Guerra and V. G. Gude, "Transesterification of waste vegetable oil under pulse sonication using ethanol, methanol and ethanol–methanol mixtures," *Waste Management*, vol. 34, no. 12, pp. 2611–2620, 2014/12/01/2014.

[17] Mbohwa C, Mudiwakure A. 2013. The status of used vegetable oil (UVO) biodiesel production in South Africa. In *Proceedings of the World Congress on Engineering.*

[18] Hamze H, Akia M, Yazdani F. Optimization of biodiesel production from the waste cooking oil using response surface methodology. *Process Safety and Environmental Protection* 2015;94:1–10.

[19] ETA-Florence Renewable Energies. 2013 "Guidelines for UCO Collection, Transport and Promotion Campaigns Based on Previous Experiences. [Online]. Available: https://ec.europa.eu/energy/intelligent/projects/sites/iee-projects/files/projects/documents/deliverable_d2.3-guidelines_for_uco_collection.pdf

[20] A. O. Falade, G. Oboh, and A. I. Okoh, "Potential health implications of the consumption of thermally-oxidized cooking oils—a review," *Polish Journal of Food and Nutrition Sciences*, vol. 67, no. 2, pp. 95–106, 2017.

[21] Venkata RP, Subramanyam R. Evaluation of the deleterious health effects of consumption of repeatedly heated vegetable oil. *Toxicology reports* 2016;3:636–43.

[22] A. K. S. Chandel. (2018) *Harmful Effect of Reusing of Cooking Oils on Health. Scientific India.* Available on http://www.scind.org.

[23] Union zur Förderung von Oel- und Proteinpflanzen (UFOP). "UFOP Supply Report 2016/2017". 2017. Available: https://www.ufop.de/

[24] J.-M. Park and J.-M. Kim, "Monitoring of used frying oils and frying times for frying chicken nuggets using peroxide value and acid value," *Korean journal for food science of animal resources*, vol. 36, no. 5, p. 612, 2016.

[25] Waghmare A, Patil S, LeBlanc JG et al. Comparative assessment of algal oil with other vegetable oils for deep frying. *Algal research* 2018;31:99–106.

[26] T. Maneerung, S. Kawi, Y. Dai, and C.-H. Wang, "Sustainable biodiesel production via transesterification of waste cooking oil by using CaO catalysts prepared from chicken manure," *Energy Conversion and Management*, vol. 123, pp. 487–497, 2016/09/01/2016.

[27] Kadapure, S.A. et al., Studies on process optimization of biodiesel production from waste cooking and palm oil, *International Journal of Sustainable Engineering* vol. 11, no. 3, pp. 167–172, 2018.

[28] T. Selvan and G. Nagarajan, "Combustion and emission characteristics of a diesel engine fuelled with biodiesel having varying saturated fatty acid composition," *International journal of green energy*, vol. 10, no. 9, pp. 952–965, 2013.

[29] D. Strayer, *Food Fats and Oils*, 9th Edition ed. 175 New York Avenue, NW, Suite 120, Washington, DC: Publication by Institute of Shortening and Edible Oil, 2006.

[30] Johnson S, Saikia N, Mathur H, Agarwal H. Fatty acids profile of edible oils and fats in India. *Centre for Science and Environment, New Delhi* 2009; 3–31.

[31] N. Vingering, M. Oseredczuk, L. du Chaffaut, J. Ireland, and M. Ledoux, "Fatty acid composition of commercial vegetable oils from the French market analysed using a long highly polar column," *Oléagineux, Corps gras, Lipides*, vol. 17, no. 3, pp. 185–192, 2010.

[32] P. Hellier, N. Ladommatos, and T. Yusaf, "The influence of straight vegetable oil fatty acid composition on compression ignition combustion and emissions," *Fuel*, vol. 143, pp. 131–143, 2015/03/01/2015.

203

[33] R. Banani, S. Youssef, M. Bezzarga, and M. Abderrabba, "Waste frying oil with high levels of free fatty acids as one of the prominent sources of biodiesel production," *J. Mater. Environ. Sci,* vol. 6, no. 4, pp. 1178–1185, 2015.

[34] S. Kumar and S. Negi, "Transformation of waste cooking oil into C-18 fatty acids using a novel lipase produced by *Penicillium chrysogenum* through solid state fermentation," *3 Biotech,* vol. 5, no. 5, pp. 847–851, 2015.

[35] D. Panadare and V. Rathod, "Applications of waste cooking oil other than biodiesel: a review," *Iranian Journal of Chemical Engineering,* vol. 12, no. 3, 2015.

[36] G. Knothe and K. R. Steidley, "A comparison of used cooking oils: a very heterogeneous feedstock for biodiesel," *Bioresource Technology,* vol. 100, no. 23, pp. 5796–5801, 2009/12/01/2009.

[37] AOAC (2019). *Official Methods of Analysis. 21st Edition. Association of Official Analytical Chemist,* Washington, DC, USA.

[38] Bockisch M. 2015. *Fats and Oils Handbook (Nahrungsfette und Öle).* Elsevier.

[39] R. Capita, S. Llorente-Marigomez, M. Prieto, and C. Alonso-Calleja, "Microbiological profiles, pH, and titratable acidity of chorizo and salchichón (two Spanish dry fermented sausages) manufactured with ostrich, deer, or pork meat," *Journal of food protection,* vol. 69, no. 5, pp. 1183–1189, 2006.

[40] L. F. Chuah, J. J. Klemeš, S. Yusup, A. Bokhari, and M. M. Akbar, "Influence of fatty acids in waste cooking oil for cleaner biodiesel," *Clean Technologies and Environmental Policy,* vol. 19, no. 3, pp. 859–868, 2017.

[41] K. Abbas, A. Mohamed, and B. Jamilah, "Fatty acids in fish and beef and their nutritional values: a review," *Journal of food, agriculture & environment,* vol. 7, no. 3&4, pp. 37–42, 2009.

[42] N. Susheelamma, M. Asha, R. Ravi, and A. V. Kumar, "Comparative studies on physical properties of vegetable oils and their blends after frying," *Journal of Food Lipids,* vol. 9, no. 4, pp. 259–276, 2002.

[43] R. H.-C. Lee *et al.,* "Fatty acid methyl esters as a potential therapy against cerebral ischemia," *OCL,* vol. 23, no. 1, p. D108, 2016.

[44] J. Orsavova, L. Misurcova, J. Ambrozova, R. Vicha, and J. Mlcek, "Fatty acids composition of vegetable oils and its contribution to dietary energy intake and dependence of cardiovascular mortality on dietary intake of fatty acids," *International journal of molecular sciences,* vol. 16, no. 6, pp. 12871–12890, 2015.

[45] Food and A. O. o. t. U. Nations. Fats and fatty acids in human nutrition: report of an expert consultation. *FAO Food Nutr Pap* 2010;91:1–166.

[46] R. K. Harika, A. Eilander, M. Alssema, S. J. Osendarp, and P. L. Zock, "Intake of fatty acids in general populations worldwide does not meet dietary recommendations to prevent coronary heart disease: a systematic review of data from 40 countries," *Annals of Nutrition and Metabolism,* vol. 63, no. 3, pp. 229–238, 2013.

[47] National Center for Biotechnology Information. 2018a. "2,3-Dihydroxypropyl elaidate." *PubChem Compound Database; CID=5364833,* https://pubchem.ncbi.nlm.nih.gov/compound/5364833.

[48] National Center for Biotechnology Information. 2018b. "1-Hexanol." *PubChem Compound Database; CID=8103,* https://pubchem.ncbi.nlm.nih.gov/compound/8103.

[49] National Center for Biotechnology Information. 2018c. "Palmitic acid." *PubChem Compound Database; CID=985,* https://pubchem.ncbi.nlm.nih.gov/compound/985

[50] National Center for Biotechnology Information. 2018d. "Linoleic acid." *PubChem Compound Database; CID=5280450,* https://pubchem.ncbi.nlm.nih.gov/compound/5280450

[51] SANTA CRUZ Biotechnology. 2009. *Material Safety Data Sheet. Methyl Pentadecanoate.* Available: http://datasheets.scbt.com/sc-215365.pdf.

[52] National Center for Biotechnology Information. 2018e. *"1-Heptene."* *PubChem Compound Database; CID=5364643,* https://pubchem.ncbi.nlm.nih.gov/compound/5364643 *(accessed Oct. 14, 2018).*

204

CHAPTER 8 ARTICLE 2: Effect of Usage on the Fatty Acid Composition and Properties of Neat Palm Oil, Waste Palm Oil, and Waste Palm Oil Methyl Ester

Effect of Usage on the Fatty Acid Composition and Properties of Neat Palm Oil, Waste Palm Oil, and Waste Palm Oil Methyl Ester

Awogbemi Omojola*, Inambao Freddie and Onuh Emmanuel Idoko

Green Energy Solutions Research Group, Discipline of Mechanical Engineering,
Howard College, University of KwaZulu-Natal, Durban 4041, South Africa
*Corresponding author E-mail: jolawogbemi2015@gmail.com

Abstract: *The need to find an environmentally friendly, renewable, and biodegradable fuel to reduce the growing dependence on fossil fuels and its attendant performance and emission inadequacies has increased research in biodiesel. Due to its low cost, availability, and a veritable means of waste disposal, waste vegetable oil from restaurants, waste fats from slaughterhouses, grease from wastewater treatment plants has gained prominence as biodiesel feedstock. This present effort compares the properties and fatty acid (FA) composition of neat palm oil (NPO), waste palm oil (WPO), and waste palm oil methyl ester (WPOME). WPO used to fry fish and chips (WPO$_{FC}$), and waste palm oil used to fry sausage and chips (WPO$_{SC}$) were collected at the point of disposal. The WPO$_{FC}$ and WPO$_{SC}$ were converted to WPOME$_{FC}$ and WPOME$_{SC}$, respectively, by transesterification and subjected to property determination and gas chromatography-mass spectrometer analysis. The characterization showed that the ratio of saturated FA to unsaturated FA changed from 19.64 %:80.36 % for NPO, to 37.67 %:62.33 % for WPO$_{FC}$, 54.75 %:45.25 % for WPO$_{SC}$, 30.43 %:69.58 % for WPOME$_{FC}$ and 16.2 %:83.8 % for WPOME$_{SC}$. These outcomes can be attributed to the effect of repeated heating and cooling during frying, contamination from moisture, food fried, and the transesterification reaction.*

Keywords— Characterization, FAME, fatty acid, feedstock, waste palm oil

1. Introduction

The increase in population, urbanization, and industrialization has an ongoing effect on energy demand putting enormous pressures on finite energy sources [1, 2]. Compression ignition (CI) engines have both on-road and off-road applications. The use of petroleum-based diesel fuel (PBDF) to power CI engines has attendant cost, performance, and environmental challenges. Unmodified CI engines fuelled with PBDF have been found to present lower engine power, lower thermal efficiency, lower combustion efficiency, and lower brake specific fuel consumption when compared with CI engines powered by biodiesel or its blends. In addition, compared with CI engines fuelled with biodiesel, PBDF triggers higher emissions of carbon monoxide, smoke opacity, and unburnt hydrocarbon in an unmodified engine under varying loads and engine speeds [3-5]. Despite some shortcomings, including the high cost of feedstock, low energy conversion, and degradation during transportation and storage, biofuel offers obvious advantages in the world's quest to meet its energy needs [6, 7]. Biodiesel, also commonly referred to as fatty acid methyl ester (FAME), is an important member of the biofuel family.

According to the European Biofuels Technology platform [8], FAMEs are fatty acid (FA) esters that are generated from the transesterification of feedstock, mainly vegetable oils (edible or inedible), and animal fats, using methanol in the presence or absence of a catalyst. Despite its renewability, low sulfur content, safer handling, higher cetane number, etc., large-scale production and application of FAME has been hampered by the high cost of feedstock, the food vs fuel debate, and the long time required to cultivate inedible vegetable feedstocks e.g. 3 to 4 years for a palm tree to bear fruit [9], and 2 to 3 years for a moringa tree to bear fruit [10]. Economically, it costs about US$0.35 to produce a litre of PBDF from fossil fuel compared to about US$0.5 to produce a litre of FAME, with raw materials accounting for most of the cost [11]. The feedstock is believed to account for between 70 % and 95 % of the cost of FAME production [12, 13]. One of the strategies to make the commercial production of FAME attainable and affordable is the adoption of waste cooking oil (WCO) as a feedstock. The initial hurdles in collection logistics and infrastructure pointed out by Janauna and Ellis [14] and Atadashi et al. [15] are being overcome by partnering with operators of fast food outlets, takeaways, and restaurants. The use of WCO as a feedstock will prevent its disposal to drainage and rivers thereby endangering aquatic habitats. A further advantage is that households and restaurant operators can make extra income by selling their used vegetable oils, including waste palm oil (WPO), to biodiesel producers.

Palm oil, one of the most widely used vegetable oils, is produced from palm fruit and the extracted red liquid has a range of industrial and domestic applications. The

global production and consumption of palm oil have continued to increase as shown in Fig. 1 [16]. According to Barrientos [17], Malaysia is the largest global producer and exporter of palm oil, exporting 16 469 thousand metric tonnes in 2017, contributing about 8 % gross national income per capita and creating thousands of jobs [18, 19]. In most Africa countries, smallholders account for between 70 % and 90 % of oil palm growers. Growing oil palm is credited with contributing to deforestation with damaging effects on wildlife and forests. Domestic palm oil consumption production has continued to marginally increase in most African countries in the last five years (Fig. 2) [17].

Many chemical reactions take place in palm oil during frying resulting in the generation of many chemical compounds. During frying, the oil is heated repeatedly to between 170 °C and 220 °C in the presence of oxygen, and sometimes moisture, which causes the palm oil to be exposed to physical, thermal and chemical degradation. This degradation affects the properties, fatty acid composition and the degree of saturation of the oil thereby lowering the quality of the oil.
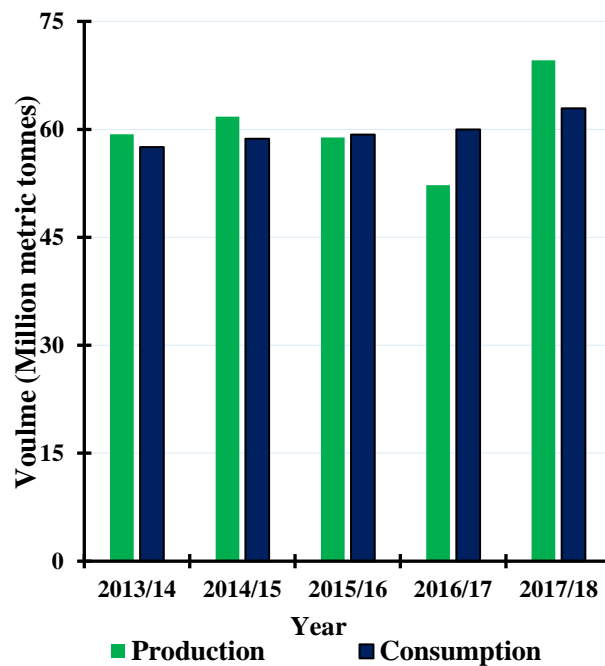

Fig. 1: Global palm oil production and consumption (million metric tonnes).
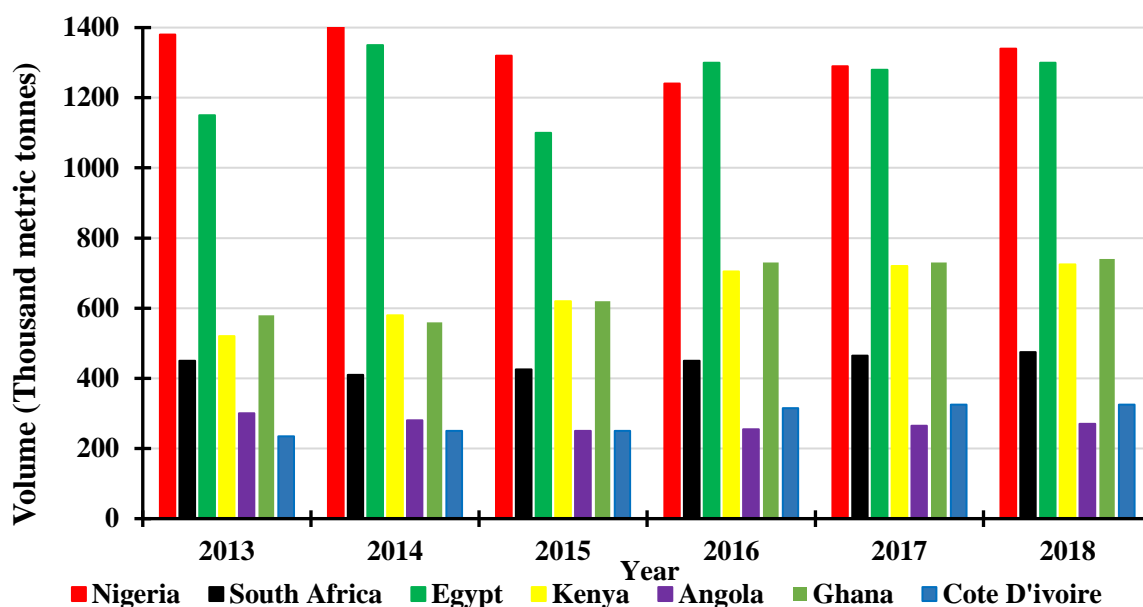
Fig. 2: Domestic consumption of palm oil in some African countries (thousand metric tonnes).

Repeated heating of palm oil at elevated temperatures for prolonged periods has been found to render the oil harmful for human consumption [20-23]. The process of transesterification is known to be a simple and low-cost conversion technique resulting in high conversion efficiency and better combustion in CI engines [24, 25].

Research on the utilization of WPO as an affordable and readily available feedstock for biodiesel production has been conducted in recent years with encouraging outcomes. Thushari et al. [26] employed esterification and transesterification to convert WPO into FAME and carried out investigations of the physicochemical properties and FA composition. Tran et al. [27] compared the chemical composition and physicochemical properties of both the WCO and the FAME derived from it and confirmed the viability of WPO for biodiesel production with 89.6 % yield. Similarly, Vargas et al. [28], Thushari and Babel [29], and Harahap et al. [30] confirmed that WPO is a readily available and cost-effective feedstock for biodiesel production with appreciable production and conversion

efficiency. Ullah et al. [31] determined and compared the physiochemical properties of unused palm oil, used palm oil and waste palm cooking oil biodiesel. The waste palm cooking oil biodiesel was produced in a two-step process using an acidic ionic liquid as a catalyst and reported obvious differences in the values of the properties.

It has been established that WPO can be converted to FAME, but the question remains as to whether the food items fried in the oil affect its properties, FA composition and degree of saturation of the waste palm oil methyl ester (WPOME) derived therefrom. This present research effort, therefore, aimed to (i) investigate the food items fried in the palm oil affect its properties and FA composition; (ii) compare the properties, FA composition and degree of saturation of neat palm oil (NPO), WPO and WPOME samples; (iii) evaluate and compare the properties and FA composition of FAME produced from WPO used to fry two different types of food. The motivation for this research was to carry out a comparative study of the properties and FA compositions of NPO, WPO, and WPOME with a view to ascertaining

the effect of food items on the feedstock and FAME. This current effort is limited to determining and comparing the properties and FA compositions of NPO, WPO, and WPOME with a view to determining their suitability as FAME feedstock.

2. Materials and Methods

2.1. Material collection and treatment

Three palm oil samples were collected from a local takeaway restaurant in Central Durban, KwaZulu-Natal province, Republic of South Africa. The palm oil samples were an NPO sample, a WPO sample used to fry fish and chips (WPO$_{FC}$) and a WPO sample used to fry sausage and chips (WPO$_{SC}$). Other details of the samples are as shown in Table 1. The samples are treated according to Sahar et al. [32].

Waste chicken eggshells were collected from restaurants at the Howard College cafeteria, University of KwaZulu Natal, Durban, Republic of South Africa. The waste chicken eggshells were converted to calcium oxide (CaO) powder through high-temperature calcination as described by Awogbemi et al. [33]. The calcined eggshell powder was warehoused in an airtight glass vial in a desiccator to prevent contamination and oxidation. Methanol (99.5 %; Merck, South Africa, analytical grade, univAR) was used as alcohol. Activated magnesium silicate, also known by the tradename Magnesol® (analytical grade, 60-100 mesh, the molar weight of 100.39 g/mol, Sigma-Aldrich, Germany), was used as an adsorbent. Magnesol® is hygroscopic once the package is opened, so care was taken to re-seal as tightly as possible and contact with eyes was avoided.

Table 1: Details of the oil samples.

Sample	Sample name	Food fried	Usage (Days)
NPO	Neat palm oil	-	-
WPO$_{FC}$	Waste palm oil	Fish and chips	14
WPO$_{SC}$	Waste palm oil	Sausage and chips	14

2.2. Transesterification of waste palm oil

The acid value of WPO$_{FC}$ and WPO$_{SC}$ were determined to ensure that a one stage transesterification process would convert the samples to WPOME$_{FC}$ and WPOME$_{SC}$ respectively. The clean WPO$_{FC}$ and WPO$_{SC}$, methanol and calcined calcium oxide (CaO) derived from waste chicken eggshell powder were mixed in a flat bottom flask in the required quantity and heated to 60 ℃. A digital thermocouple was utilized to verify the temperature of the reacting mixture throughout the 90 mins duration of the experiment. Methanol to oil ratio of 6:1, the catalyst particle size of 75 µm and 1 %w/w catalyst:oil ratio was the parametric process conditions for the transesterification reaction. Mixing was maintained by a magnetic stirrer at 1200 rpm to ensure homogeneous mixing of the reacting solution throughout the process. The resulting mixture was thereafter filtered in a vacuum filtration set up to recover the catalyst. The filtered mixture was transmitted to a separating funnel and permitted to settle for 12 hours and the glycerol coagulated at the bottom of the separating funnel. The glycerol was drained out from the bottom of the separating funnel followed by the draining of the crude biodiesel. Magnesol at 1 %w/w Magnesol:WPOME was added to the crude biodiesel and maintained at 60 °C for 30 min and mixed at 600 rpm by a magnetic stirrer. The resulting solution was filtered using vacuum filtration, heated to 110

°C to remove excess moisture and methanol trapped in the biodiesel, then further polished by using a 0.45 µm PTFE membrane syringe filter. The purified WPOME$_{FC}$ and WPOME$_{SC}$ were transferred into glass containers for further analysis and characterization.

2.3. Properties and FA determination of samples

The NPO, WPO$_{FC}$, WPO$_{SC}$, and WPOME were subjected to property determination. Table 2 shows the list and method adopted for the property determination and characterization of the samples.

The concentration of FAME composition of the waste oil samples was determined by pyrolysis Gas Chromatograph Mass Spectrometer (PyGCMS) using a Shimadzu Gas Chromatograph Mass Spectrometer using an ultra-alloy-5 capillary column and GCMS-QP2010 Plus software. The choice of PYGCMS for the WPO$_{FC}$ and WPO$_{SC}$ samples as against the normal GCMS was to prevent clogging of the column of the GCMS machine due to the low volatility nature of the samples. Table 3 shows the PyGCMS configuration used for the analysis of neat and WPO samples. The concentration of FAMEs was determined using a Shimadzu gas chromatography-mass spectrometer (GCMS) with an ultra-alloy-5 capillary column and GCMS-QP2010 Plus software. Table 4 shows the GCMS configuration used for the analysis of WPOME samples.

Table 2: Method/instrument of analysis.

Property	Unit	Method/Instrument	Ref.
Density @ 20 °C	Kg/m^3	ASTM D 1298	[34]
Kinematic viscosity @ 40 °C	mm^2/s	ASTM D445	[34]
Acid value	mgKOH/g	AOCS Ca 4a-40	[35]
Iodine value	Cg/g	AOCS Cd 1B-87	[35]
pH	-	pH meter	[36]
Congealing temperature	°C	Thermometer	[37]
FA composition (NPO, WPO$_{FC}$, and WPO$_{SC}$)	-	PYGCMS	[38]
FA composition (WPOME)	-	GCMS	[38]

Table 3: PyGCMS configuration.

Injector	
Inlet temperature	240 °C
Carrier gas	Helium
Sample size	2 µL
Injection mode	Split
Split ratio	30
Column temperature	40 °C
Detector	
Type	PyGCMS
Interface temperature	250 °C
Detector gain	1.22 kV + 0.00 kV
Oven temperature program	

Rate	Temperature (°C)	Holding time (min)
-	40	5
5.00	125	0
3.00	285	0
5.00	320	10

Column	
Type	Ultra alloy -5(MS/HT)
Specification	30 m, 0.25 mm ID, 0.25 µm
Flow rate	3.0 mL/min
Total flow	34 mL/min
Colum flow	1.00 mL/min

Table 4: GCMS configuration

Injector	
Inlet temperature	250 °C
Carrier gas	Helium
Sample size	2 µL
Injection mode	splitless
Column temperature	50 °C
Detector	
Type	GCMS
Interface temperature	280 °C
Detector gain	1.08 kV + 0.00 kV
Oven temperature program	

Rate	Temperature (°C)	Holding time (min)

-	50	1
15.00	180	1
7.00	230	1
5.00	350	5
Column		
Type	Ultra alloy - 5(MS/HT)	
Specification	30 m, 0.25 mm ID, 0.25 μm	
Flow rate	3.0 mL/min	
Total flow	4.9 mL/min	
Column flow	0.95 mL/min	

3. Result and Discussion

3.1. Effect of usage on properties

The result of property determination of NPO, WPO_{FC}, WPO_{SC}, $WPOME_{FC}$, and $WPOME_{SC}$ samples are shown in Table 5. The density of NPO is higher than that of the WPO_{FC}, and WPO_{SC} samples. This can be attributed to the effect of repeated pyrolysis leading to the production of a lighter hydrocarbon fraction resulting in a lower density. The pH of NPO was higher than that of waste oil samples with WPO_{FC} being the most acidic of the three samples. This might be due to the effect of the fish oil that has adulterated the oil during frying [39]. This result was also confirmed by the acid value of the waste oil samples where the WPO_{FC} presented an acid value of 0.66 mgKOH/g compared to the acid value of 1.13 mg/KOH/g of WPO_{SC}. The lower acid value of WPO_{FC} compared to WPO_{SC} can be attributed to the effect of the fish and sausage respectively on the palm oil during frying. In terms of kinematic viscosity, usage makes oil more viscous; WPO_{FC} was found to be more viscous than WPO_{SC} as a result of the effect of the fish oil on the NPO. The kinematic viscosity at 40 °C of the WPO samples was higher than that of NPO. This is in agreement with earlier results reported by Chuah et al. [40].

Transesterification altered the density and kinematic viscosity of the samples. As shown in Table 5, the density and kinematic viscosity of the WPO samples were higher than those of the FAME derived from the WPO samples. This was due to the effect of the production processes involved in the conversion of the waste palm oil into methyl esters. The transesterification reaction caused the $WPOME_{FC}$ and $WPOME_{SC}$ to be less dense and less viscous than WPO_{FC} and WPO_{SC}. Kinematic viscosity of WPO samples are higher than that of NPO due to the formation.

Table 5: Properties of neat and waste oil samples.

Properties	NPO	WPO_{FC}	WPO_{SC}	$WPOME_{FC}$	$WPOME_{SC}$	ASTM D6751	EN 14214
pH	6.34	5.73	6.19	-	-	-	-
Congealing temperature (°C)	-10.25	12.3	14.7	-	-	-	-
Density @ 20 °C (kg/m^3)	919.48	904.3	913.4	860	870	-	860 - 900
Kinematic Viscosity @ 40 °C (mm^2/s)	27.96	44.25	38.41	4.5	3.8	1.9 – 6	3.5 - 5
Iodine value (cg/g)	-	81.7	54.2	72.5	52.3	-	120 max
Acid value (mg KOH/g)	-	0.66	1.13	0.28	0.42	0.05 max	0.5 max

of dimeric and polymeric acids and glycerides during usage, and normally higher than the viscosity of FAME while lowering the density [41, 42]. These trends agree with similar work by Uddin et al. [43], and Thushari et al. [26].

The iodine values of the WPOME samples were lower than those of the WPO samples. A higher iodine value was recorded for the WPO_{FC} sample compared to the WPO_{SC} sample, and for the $WPOME_{FC}$ sample compared to the

WPOME$_{SC}$ sample. The difference in the lower iodine values of WPO samples can be traced to the effect of food fried, heating time, and probably the storage condition before analysis. The lower iodine value of WPOME samples compared with WPO samples can be adduced to the effect of heating during the transesterification process [44, 45]. High degree of unsaturation of WPO results in polymerization of FAME as a result of the formation of epoxide due to the addition of oxygen in double bonds [32]. This agrees with the outcome of previous research by Chuah et al. [46].

Considering the fingerprint of both WPO$_{FC}$ and WPO$_{SC}$, particularly the density and viscosity, it can be seen that a lower density and higher viscosity trigger a lower saturated fatty acid (SFA) and a higher monounsaturated fatty acid (MUFA), as shown in Fig. 4. This is unlike the case of NPO where a higher density and a lower viscosity resulted in a predominantly polyunsaturated fatty acid (PUFA). The pH of the samples showed that NPO presented with the highest pH followed by WPO$_{SC}$ and WPO$_{FC}$. The NPO had a higher acid value when compared with the WPO$_{FC}$ and WPO$_{SC}$ samples. The pH trend also followed the acid value trend of WPO$_{FC}$ and WPO$_{SC}$ and enhanced the transesterification process.

The viscosity of NPO in this research as shown in Table 5 was 27.96 mm^2/s which falls in the range of the 25.6 mm^2/s reported by Maneerung et al. [47] and 31.78 mm^2/s reported by Zein et al. [48] though the density of both WPO$_{FC}$ and WPO$_{SC}$ were found to be higher than the 902 kg/m^3 reported by Maneerung et al. [47]. These properties affect the FA compositions and the degree of saturation, and therefore their tendency to be converted to FAME.

3.2. Effect of usage on FA composition

The result of FA composition of the NPO, WPO$_{FC}$, and WPO$_{SC}$ as determined by the PYGCMS and that of WPOME$_{FC}$ and WPOME$_{SC}$ as determined by GCMS are shown in Table 6. NPO was found to contain linoleic acid, and brassidic acid, WPO$_{FC}$ consisted of mainly oleic and palmitic acids, while WPO$_{SC}$ was made up of mainly palmitic and linoleic acids. However, WPOME$_{FC}$ and WPOME$_{SC}$ were made up of oleic and palmitic acids and linoleic and caproleic acid respectively. Unlike NPO, oleic and palmitic acids were present in the WPO samples, while the brassidic acid present in the NPO was absent in the WPO samples. This may be due to high-temperature degradation, oxidation as a result of moisture addition, and contamination occasioned by the food items. The effect of fish oil contamination triggered the presence of stearic acid only in WPO$_{FC}$. However, these results did not wholly agree with those reported by Kadapure et al. [49]. This may be due to the difference in the types and species of palm oil used as well as the method of determining the FA composition. It should be noted that Kadapure et al. [49] obtained their palm oil samples and carried out their research in Belgium and the samples were analyzed by means of a gas chromatographic method. Also, the food items fried in the palm oil and the duration of usage were not disclosed. There was no guarantee that WPO was obtained from the same source as the neat oil. Chuah et al. [40] reported the same FA composition for neat cooking oil and waste cooking oil which is not different from the outcome of this research as it relates to NPO and the WPO samples. Also the presence of some transition metals in the

food items, for example, iron is present in meat, increased the rates of degradation and thermal degradation of the oil [50].

Oleic and palmitic acids were observed to be the most dominant FA in both WPO_{FC} and $WPOME_{FC}$ while the stearic and linoleic acids in WPO_{FC} were converted to brassidic acid, pelargonic acid, lauric acid, behenic acid, and caproleic acid in $WPOME_{FC}$ as a result of the transesterification process. Apart from the contamination of the oil by the food, moisture is also added to the oil during frying. Addition of salt, sauces, intermittent heating and cooling during repeated frying results into the deterioration of the oil and the change in its degree of saturation. The effect of hydrogenation which occurs during frying can also contribute to the conversion [51]. The process of conversion of WPO_{SC} to $WPOME_{SC}$ by transesterification introduced caproleic acid into FAME. Oleic, palmitic and caproleic acids are the common FA in both $WPOME_{FC}$ and $WPOME_{SC}$ which can be traced to the properties of the WPO sample, notwithstanding the type of food which they fried.

The NPO used in this research consisted of 52.55 % PUFA which was reduced to 37.35 % in WPO_{SC} and 3.76 % in WPO_{FC} as shown in Figure 3. The low percentage of SFA in NPO was increased in the WPO samples due to usage which confirmed the outcome of similar research by Kadapure et al. [49]. The effect of the food items the oil fried greatly influenced the degree of saturation of both the WPO_{FC} and WPO_{SC}. The 54.75 % SFA in WPO_{SC} was reduced to 37.67 % in WPO_{FC} while the 7.9 % MUFA and 37.37 % PUFA in WPO_{SC} became 58.57 % MUFA and 3.78 % PUFA in WPO_{FC}. The FA composition for the WPO_{FC} and WPO_{SC}

were similar to the outcome of FA analysis of WPO by Kadapure et al. [49]. However, the high percentage of PUFA in NPO differed greatly from the result of similar research by Maneerung et al. [47]. No explanation was found for the differences in the FA compositions other than the different geographical sources and species of the palm oil samples.

The process of transesterification not only triggered the increase of the 58.57 % MUFA and 37.67 % SFA in WPO_{FC} to 69.58 % MUFA and 30.43 % SFA in $WPOME_{FC}$ but also caused the 3.76 % PUFA in WPO_{FC} to completely disappear. The percentage of PUFA in WPO_{SC} and $WPOME_{SC}$ remained almost the same while there was a drastic increment in MUFA from 7.9 % to 46.05 % as a result of the transesterification process. The influence of food items was noticeable in the FA composition and degree of saturation of both $WPOME_{FC}$ and $WPOME_{SC}$. Fig. 4 compares the FA composition of WPO_{FC} and WPO_{SC} in this research to the outcomes of similar research obtained from the literature. Maneerung et al. [47], Zein et al. [48] and Nguyen et al. [52] reported almost the same value for MUFA for waste oil samples. Maneerung et al. [47] and Nayak et al. [53] reported close values of PUFA though lower than that reported by Rahmanlar et al. [54]. From the eight samples of WPO shown in Fig. 4, it can be deduced that there is no consensus on the degree of saturation and type of chain in all the WPO samples. Degradation temperature, usage, duration and degree of usage, type food items that were fried, among other elements, dictates the FA composition and degree of saturation of the WPO samples.

Table 6: Fatty acid composition of NPO, WPO, and WPOME.

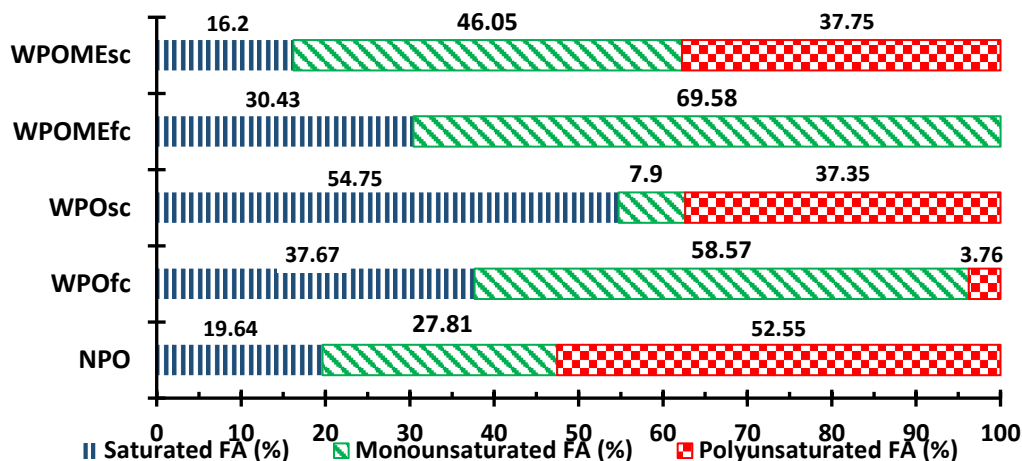| Common name	Structure	NPO	WPO$_{FC}$	WPO$_{SC}$	WPOME$_{FC}$	WPOME$_{SC}$
Oleic acid	C18:1	-	58.57	7.9	63.96	20.35
Palmitic acid	C16:0	-	36.13	54.75	23.72	16.2
Capric acid	C10:0	5.92	-	-	-	-
Stearic acid	C18:0	13.72	1.54	-	-	-
Linoleic acid	C18:2	52.55	3.76	37.35	-	37.75
Brassidic acid	C22:1	27.81	-	-	-	-
Pelargonic acid	C9:0	-	-	-	1.1	-
Lauric acid	C12:0	-	-	-	3.47	-
Behenic acid	C22:0	-	-	-	2.14	-
Caproleic acid	C10:1	-	-	-	5.62	25.7

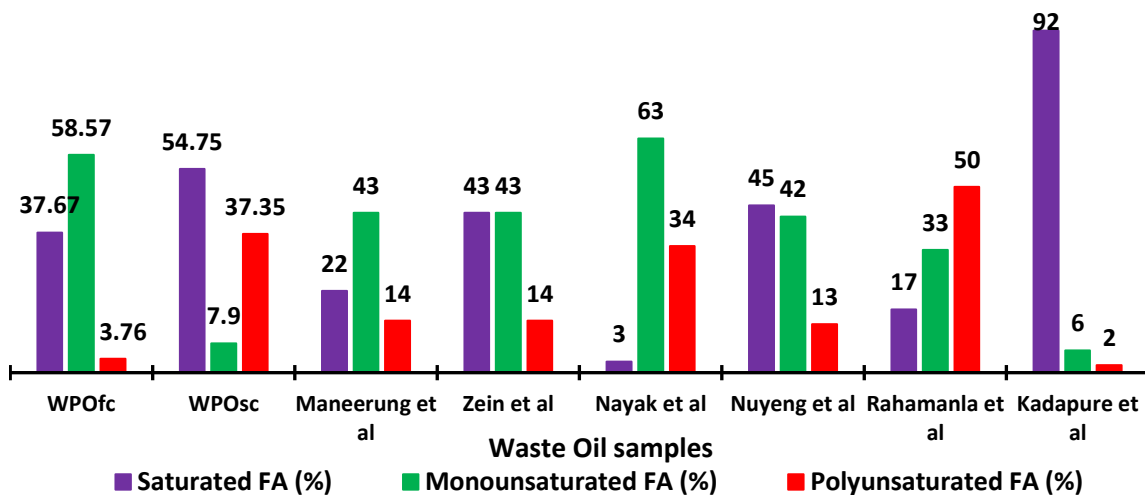
Fig. 3: Degree of saturation of NPO, WPO$_{FC}$, WPO$_{SC}$, WPOME$_{FC}$, and WPOME$_{SC}$.

Fig. 4: SFA, MUFA and PUFA compositions of WPO samples.

215

4. Conclusion

The application of otherwise known waste raw materials such as used vegetable oil from restaurants, households and canteens and takeaway outlets, waste animal (beef, chicken, pig, etc) fats from slaughterhouses and abattoirs, rendered fats, and grease recovered from wastewater treatment plants have gained acceptance as biodiesel feedstock. Though they are low-grade feedstocks, appropriate selection of production and refining techniques ensure derivation of the benefits in their usage. They are cheaper than other forms of feedstock and help in solving problems waste oil and fats disposal challenges. The properties and the FA composition of NPO, WPO samples and WPOME were investigated with a view to determining the effects of usage and food items on the samples. The trajectory from NPO through WPO used to fry particular food items and the WPOME derived from the transesterification of the WPO samples were reported. The following inferences can be drawn:

- The pH and density of WPO samples were found to be lower than those of NPO while the congealing temperature and viscosity of NPO were found to be lower than that of the WPO sample.

- The pH, congealing temperature, density and acid value of WPO_{FC} were found to be lower than those of WPO_{SC} but WPO_{FC} had higher iodine and viscosity values.

- The degree of usage, the food fried, the effect of repeated heating and cooling, storage environment, the type of oil, the source of the NPO, and transesterification process have been found to affect the concentration of the FAME composition, and degree of saturation.

- NPO was found to consist of 52.55 % PUFA and 27.81 % MUFA.

- The composition of saturated fatty acid and unsaturated fatty acid were found to be affected by the degree of usage, the degradation temperature, species of palm oil and the food items the oil fried.

- The degree of saturation of WPO_{FC} and WPO_{SC} was less than that of NPO, in most cases, and agrees with some of the results reported in the literature.

- The low acid value of the WPO samples signifies their suitability for FAME production by transesterification.

- The density of $WPOME_{FC}$ was found to be higher than that of $WPOME_{SC}$; on the other hand, the kinematic viscosity of $WPOME_{FC}$ was higher than that of $WPOME_{SC}$.

- The 52.55 % PUFA in NPO was converted to 3.76 % in WPO_{FC} and completely disappeared in $WPOME_{FC}$ while the MUFA was found to increase from 27.81 % in NPO to 58.57 % in WPO_{FC} and 69.58 % in $WPOME_{FC}$.

- The 19.64 % SFA in NPO increased to 54.75 % in WPO_{SC} but reduced to 16.2 % in $WPOME_{SC}$ while the MUFA which was 27.81 % in NPO reduced to 7.9 % in WPO_{SC} but increased to 46.05 % in $WPOME_{SC}$.

The significance of this investigation is that the type of food that NPO fries affects the FA composition, properties, and degree of saturation of palm oil and consequently influences the FA composition and properties of the resulting FAME. The FA composition and properties of FAME will, in turn, have considerable influence on the engine

performance and emission characteristics of a CI engine fuelled by FAME as well as the stability of the FAME. In conclusion, when selecting WCO as a feedstock for transesterification, consideration should be paid to these three factors: the degree of usage, the type of food fried by the palm oil, and the NPO source.

Going forward, considerable research opportunities exist regarding the effect of frying temperature and time on NPO, the cycle of frying, palm oil species, etc. Such research will contribute towards establishing the optimal conditions to obtain feedstock for FAME production from palm oil.

Acknowledgement

References

[1] P. Sadorsky, "Shifts in energy consumption driven by urbanization. In: Davidson," *The Oxford Handbook of Energy and Society,* p. 179, 2018.

[2] UN. W o r l d U r b a n i z a t i o n P r o s p e c t s :The 2018 Revision. Available on https://esa.un.org/unpd/wup/Publications/Files/WUP2018-KeyFacts.pdf. Accessed 18 June 2019 [Online].

[3] Worldometers. Current World Population. Available on https://www.worldometers.info/world-population/. Accessed 18 June 2019 [Online].

[4] BP. Statistical review of world energy, 67th edition, June 2018. Available on https://www.bp.com/content/dam/bp/business-sites/en/global/corporate/pdfs/energy-economics/statistical-review/bp-stats-review-2018-full-report.pdf. Accessed 18th June 2019 [Online].

[5] IEA. Key World Energy Statistics 2018. Availabel on https://webstore.iea.org/key-world-energy-statistics-2018 [Online].

[6] TERM, "Transport Indicators Tracking Progress towards Environmental Targets in Europe; No 7/2015; European Environment Agency: Copenhagen, Denmark," 2015.

[7] (2017). *Energy Information Administration, International Energy Outlook 2017. Available on https://www.eia.gov/outlooks/ieo/.*

[8] I. Staffell *et al.*, "The role of hydrogen and fuel cells in the global energy system," *Energy & Environmental Science,* vol. 12, no. 2, pp. 463-491, 2019.

[9] G. Dwivedi and M. Sharma, "Potential and limitation of straight vegetable oils as engine fuel–An Indian perspective," *Renewable and Sustainable Energy Reviews,* vol. 33, pp. 316-322, 2014.

[10] Q. Li, F. Backes, and G. Wachtmeister, "Application of canola oil operation in a diesel engine with common rail system," *Fuel,* vol. 159, pp. 141-149, 2015.

[11] S. Sidibé, J. Blin, G. Vaitilingom, and Y. Azoumah, "Use of crude filtered vegetable oil as a fuel in diesel engines state of the art: Literature review," *Renewable and Sustainable Energy Reviews,* vol. 14, no. 9, pp. 2748-2759, 2010.

[12] S. Che Mat, M. Y. Idroas, M. F. Hamid, and Z. A. Zainal, "Performance and emissions of straight vegetable oils and its blends as a fuel in diesel engine: A review," *Renewable and Sustainable Energy Reviews,* vol. 82, pp. 808-823, 2018/02/01/ 2018.

[13] F. Aydın and H. Öğüt, "Effects of using ethanol-biodiesel-diesel fuel in single cylinder diesel engine to engine performance and emissions," *Renewable Energy,* vol. 103, pp. 688-694, 2017/04/01/ 2017.

[14] S. Jain, "The current and future perspectives of biofuels," in

Biomass, Biopolymer-Based Materials, and Bioenergy: Elsevier, 2019, pp. 495-517.

[15] D. Dias, A. P. Antunes, and O. Tchepel, "Modelling of Emissions and Energy Use from Biofuel Fuelled Vehicles at Urban Scale," *Sustainability,* vol. 11, no. 10, p. 2902, 2019.

[16] H. Jääskeläinen. Biodiesel Standards & Properties 2009. Available : https://www.dieselnet.com/tech/fuel_biodiesel_std.php [Online].

[17] R. Goosen, K. Vora, and C. Vona, "Establishment of the Guidelines for the Development of Biodiesel Standards in the APEC Region," ed: April, 2009.

[18] J.-H. Ng, H. K. Ng, and S. Gan, "Advances in biodiesel fuel for application in compression ignition engines," *Clean Technologies and Environmental Policy,* journal article vol. 12, no. 5, pp. 459-493, November 01 2010.

[19] R. R. Shahruzzaman, A. Salmiaton, R. Yunus, and Y. Taufiq-Yap, "Modified local carbonate mineral as deoxygenated catalyst for biofuel production via catalytic pyrolysis of waste cooking oil," in *AIP Conference Proceedings*, 2018, vol. 2030, no. 1, p. 020006: AIP Publishing.

[20] K. Dhanasekaran and M. Dharmendirakumar, "Biodiesel characterization and optimization study of used frying palm oil," *International journal of current research and academic review,* vol. 2, pp. 105-120, 2014.

[21] D. F. Correa *et al.*, "Towards the implementation of sustainable biofuel production systems," *Renewable and Sustainable Energy Reviews,* vol. 107, pp. 250-263, 2019/06/01/ 2019.

[22] L. P. Chrysikou, V. Dagonikou, A. Dimitriadis, and S. Bezergianni, "Waste cooking oils exploitation targeting EU 2020 diesel fuel production: Environmental and economic benefits," *Journal of Cleaner Production,* vol. 219, pp. 566-575, 2019/05/10/ 2019.

[23] J. Hill, E. Nelson, D. Tilman, S. Polasky, and D. Tiffany, "Environmental, economic, and energetic costs and benefits of biodiesel and ethanol biofuels," *Proceedings of the National Academy of sciences,* vol. 103, no. 30, pp. 11206-11210, 2006.

[24] G. Knothe, "Biodiesel and renewable diesel: a comparison," *Progress in energy and combustion science,* vol. 36, no. 3, pp. 364-373, 2010.

[25] C. M. Noor, M. Noor, and R. Mamat, "Biodiesel as alternative fuel for marine diesel engine applications: A review," *Renewable and Sustainable Energy Reviews,* vol. 94, pp. 127-142, 2018.

[26] S. Zailani, M. Iranmanesh, S. Sean Hyun, and M. H. Ali, "Barriers of Biodiesel Adoption by Transportation Companies: A Case of Malaysian Transportation Industry," *Sustainability,* vol. 11, no. 3, p. 931, 2019.

[27] C. Stead, Z. Wadud, C. Nash, and H. Li, "Introduction of Biodiesel to Rail Transport: Lessons from the Road Sector," *Sustainability,* vol. 11, no. 3, p. 904, 2019.

[28] S. Raj and M. Bhandari, "Comparison of Methods of Production of Biodiesel from Jatropha Curcas," *Journal of Biofuels,* vol. 8, no. 2, pp. 58-80, 2017.

[29] H. Ibifubara, N. I. Obot, and M. A. Chendo, "Comparative Studies on Some Edible Oils for Biodiesel Production in Nigeria," *Energy,* vol. 9, no. 10, p. 11, 2014.

[30] A. Atabani, M. El-Sheekh, G. Kumar, and S. Shobana, "Edible and nonedible biodiesel feedstocks: microalgae and future of biodiesel," in *Clean Energy for Sustainable Development*: Elsevier, 2017, pp. 507-556.

[31] A. E. Atabani *et al.*, "Non-edible vegetable oils: A critical evaluation of oil extraction, fatty acid compositions, biodiesel production,

characteristics, engine performance and emissions production," *Renewable and Sustainable Energy Reviews,* vol. 18, pp. 211-245, 2013/02/01/ 2013.

[32] W. A. Kawentar and A. Budiman, "Synthesis of Biodiesel from Second-Used Cooking Oil," *Energy Procedia,* vol. 32, pp. 190-199, 2013/01/01/ 2013.

[33] K.-C. Ho, C.-L. Chen, P.-X. Hsiao, M.-S. Wu, C.-C. Huang, and J.-S. Chang, "Biodiesel Production from Waste Cooking Oil by Two-step Catalytic Conversion," *Energy Procedia,* vol. 61, pp. 1302-1305, 2014/01/01/ 2014.

[34] K. Dutta, A. Daverey, and J.-G. Lin, "Evolution retrospective for alternative fuels: First to fourth generation," *Renewable Energy,* vol. 69, pp. 114-122, 2014/09/01/ 2014.

[35] B. Abdullah *et al.*, "Fourth generation biofuel: A review on risks and mitigation strategies," *Renewable and Sustainable Energy Reviews,* vol. 107, pp. 37-50, 2019.

[36] A. Martínez, G. E. Mijangos, I. C. Romero-Ibarra, R. Hernández-Altamirano, and V. Y. Mena-Cervantes, "In-situ transesterification of Jatropha curcas L. seeds using homogeneous and heterogeneous basic catalysts," *Fuel,* vol. 235, pp. 277-287, 2019/01/01/ 2019.

[37] M. B. Navas, I. D. Lick, P. A. Bolla, M. L. Casella, and J. F. Ruggera, "Transesterification of soybean and castor oil with methanol and butanol using heterogeneous basic catalysts to obtain biodiesel," *Chemical Engineering Science,* vol. 187, pp. 444-454, 2018/09/21/ 2018.

[38] A. B. Avagyan and B. Singh, "Biodiesel from Plant Oil and Waste Cooking Oil," in *Biodiesel: Feedstocks, Technologies, Economics and Barriers*: Springer, 2019, pp. 15-75.

[39] J. Borton, F. D. N. Lopez, L. Doan, W. E. Holmes, and T. J. Benson, "Conversion of High Free Fatty Acid Lipid Feedstocks to Biofuel Using Triazabicyclodecene Catalyst (Homogeneous and Heterogeneous)," *Energy & Fuels,* 2019.

[40] O. S. Valente, V. M. D. Pasa, C. R. P. Belchior, and J. R. Sodré, "Physical–chemical properties of waste cooking oil biodiesel and castor oil biodiesel blends," *Fuel,* vol. 90, no. 4, pp. 1700-1702, 2011/04/01/ 2011.

[41] E. Zahir, R. Saeed, M. A. Hameed, and A. Yousuf, "Study of physicochemical properties of edible oil and evaluation of frying oil quality by Fourier Transform-Infrared (FT-IR) Spectroscopy," *Arabian Journal of Chemistry,* vol. 10, pp. S3870-S3876, 2017/05/01/ 2017.

[42] X. Yin, H. Ma, Q. You, Z. Wang, and J. Chang, "Comparison of four different enhancing methods for preparing biodiesel through transesterification of sunflower oil," *Applied Energy,* vol. 91, no. 1, pp. 320-325, 2012.

[43] N. Mansir *et al.*, "Modified waste egg shell derived bifunctional catalyst for biodiesel production from high FFA waste cooking oil. A review," *Renewable and Sustainable Energy Reviews,* vol. 82, pp. 3645-3655, 2018/02/01/ 2018.

[44] P. Verma and M. P. Sharma, "Review of process parameters for biodiesel production from different feedstocks," *Renewable and Sustainable Energy Reviews,* vol. 62, pp. 1063-1071, 2016/09/01/ 2016.

[45] G. Baskar and R. Aiswarya, "Trends in catalytic production of biodiesel from various feedstocks," *Renewable and Sustainable Energy Reviews,* vol. 57, pp. 496-504, 2016.

[46] I. Ambat, V. Srivastava, and M. Sillanpää, "Recent advancement in biodiesel production methodologies using various feedstock: A review," *Renewable and Sustainable Energy Reviews,* vol. 90, pp. 356-369, 2018/07/01/ 2018.

[47] S. H. Shuit, K. F. Yee, K. T. Lee, B. Subhash, and S. H. Tan, "Evolution towards the utilisation of

functionalised carbon nanotubes as a new generation catalyst support in biodiesel production: an overview," *RSC Advances,* vol. 3, no. 24, pp. 9070-9094, 2013.

[48]   M. K. Lam, K. T. Lee, and A. R. Mohamed, "Homogeneous, heterogeneous and enzymatic catalysis for transesterification of high free fatty acid oil (waste cooking oil) to biodiesel: a review," *Biotechnology advances,* vol. 28, no. 4, pp. 500-518, 2010.

[49]   V. G. Tacias-Pascacio *et al.,* "Comparison of acid, basic and enzymatic catalysis on the production of biodiesel after RSM optimization," *Renewable Energy,* vol. 135, pp. 1-9, 2019.

[50]   V. B. Veljković, I. B. Banković-Ilić, and O. S. Stamenković, "Purification of crude biodiesel obtained by heterogeneously-catalyzed transesterification," *Renewable and Sustainable Energy Reviews,* vol. 49, pp. 500-516, 2015/09/01/ 2015.

[51]   D. Vujicic, D. Comic, A. Zarubica, R. Micic, and G. Boskovic, "Kinetics of biodiesel synthesis from sunflower oil over CaO heterogeneous catalyst," *Fuel,* vol. 89, no. 8, pp. 2054-2061, 2010.

[52]   T. Maneerung, S. Kawi, and C. Wang, "Gasification bottom ash as a CaO catalyst source for biodiesel production from transesterification of palm oil," *Energy Convers. Manage.,* vol. 112, pp. 199-207, 2016.

[53]   W. W. S. Ho, H. K. Ng, S. Gan, and S. H. Tan, "Evaluation of palm oil mill fly ash supported calcium oxide as a heterogeneous base catalyst in biodiesel synthesis from crude palm oil," *Energy Conversion and Management,* vol. 88, pp. 1167-1178, 2014.

[54]   A. Inayat, A. M. Nassef, H. Rezk, E. T. Sayed, M. A. Abdelkareem, and A. G. Olabi, "Fuzzy modeling and parameters optimization for the enhancement of biodiesel production from waste frying oil over montmorillonite clay K-30,"

Science of The Total Environment, vol. 666, pp. 821-827, 2019/05/20/ 2019.

[55]   M. Ayoub, S. Ullah, A. Inayat, A. H. Bhat, and S. M. Hailegiorgis, "Process Optimization for Biodiesel Production from Waste Frying Oil over Montmorillonite Clay K-30," *Procedia Engineering,* vol. 148, pp. 742-749, 2016/01/01/ 2016.

[56]   N. Banerjee, S. Barman, G. Saha, and T. Jash, "Optimization of process parameters of biodiesel production from different kinds of feedstock," *Materials Today: Proceedings,* vol. 5, no. 11, Part 2, pp. 23043-23050, 2018/01/01/ 2018.

[57]   R. E. Gumba, S. Saallah, M. Misson, C. M. Ongkudon, and A. Anton, "Green biodiesel production: a review on feedstock, catalyst, monolithic reactor, and supercritical fluid technology," *Biofuel Research Journal,* vol. 3, no. 3, pp. 431-447, 2016.

[58]   Y. M. Sani, W. M. A. W. Daud, and A. R. Abdul Aziz, "Solid acid-catalyzed biodiesel production from microalgal oil—The dual advantage," *Journal of Environmental Chemical Engineering,* vol. 1, no. 3, pp. 113-121, 2013/09/01/ 2013.

[59]   I. J. Stojković, O. S. Stamenković, D. S. Povrenović, and V. B. Veljković, "Purification technologies for crude biodiesel obtained by alkali-catalyzed transesterification," *Renewable and Sustainable Energy Reviews,* vol. 32, pp. 1-15, 2014/04/01/ 2014.

[60]   H. Taher, S. Al-Zuhair, A. H. Al-Marzouqi, Y. Haik, and M. M. Farid, "A review of enzymatic transesterification of microalgal oil-based biodiesel using supercritical technology," *Enzyme research,* vol. 2011, 2011.

[61]   A. K. Agarwal, "Biofuels (alcohols and biodiesel) applications as fuels for internal combustion engines," *Progress in energy and combustion science,* vol. 33, no. 3, pp. 233-271, 2007.

220

[62] I. Atadashi, M. Aroua, A. A. Aziz, and N. Sulaiman, "Refining technologies for the purification of crude biodiesel," *Applied energy,* vol. 88, no. 12, pp. 4239-4251, 2011.

[63] H. Bateni, A. Saraeian, and C. Able, "A comprehensive review on biodiesel purification and upgrading," *Biofuel Research Journal,* vol. 4, no. 3, pp. 668-690, 2017.

[64] J. M. Fonseca, J. G. Teleken, V. de Cinque Almeida, and C. da Silva, "Biodiesel from waste frying oils: Methods of production and purification," *Energy conversion and management,* vol. 184, pp. 205-218, 2019.

[65] S. Živković and M. Veljković, "Environmental impacts the of production and use of biodiesel," *Environmental Science and Pollution Research,* vol. 25, no. 1, pp. 191-199, 2018.

[66] C. J. Mota, B. P. Pinto, and A. L. De Lima, *Glycerol: A Versatile Renewable Feedstock for the Chemical Industry*. Springer, 2017.

[67] M. R. Monteiro, C. L. Kugelmeier, R. S. Pinheiro, M. O. Batalha, and A. da Silva César, "Glycerol from biodiesel production: Technological paths for sustainability," *Renewable and Sustainable Energy Reviews,* vol. 88, pp. 109-122, 2018/05/01/ 2018.

[68] M. Berrios and R. L. Skelton, "Comparison of purification methods for biodiesel," *Chemical Engineering Journal,* vol. 144, no. 3, pp. 459-465, 2008/11/01/ 2008.

[69] R. S. Malani, V. Shinde, S. Ayachit, A. Goyal, and V. S. Moholkar, "Ultrasound–assisted biodiesel production using heterogeneous base catalyst and mixed non–edible oils," *Ultrasonics Sonochemistry,* vol. 52, pp. 232-243, 2019/04/01/ 2019.

[70] J. Gardy *et al.*, "A magnetically separable SO4/Fe-Al-TiO2 solid acid catalyst for biodiesel production from waste cooking oil," *Applied Catalysis B: Environmental,* vol. 234, pp. 268-278, 2018/10/15/ 2018.

[71] Z. Ma and F. Zaera, "Characterization of heterogeneous catalysts," *Surface and Nanomolecular Catalysis,* pp. 1-37, 2006.

[72] T. T. V. Tran *et al.*, "Green biodiesel production from waste cooking oil using an environmentally benign acid catalyst," *Waste management,* vol. 52, pp. 367-374, 2016.

[73] M. Farooq, A. Ramli, and D. Subbarao, "Biodiesel production from waste cooking oil using bifunctional heterogeneous solid catalysts," *Journal of Cleaner Production,* vol. 59, pp. 131-140, 2013.

[74] M. Chai, Q. Tu, M. Lu, and Y. J. Yang, "Esterification pretreatment of free fatty acid in biodiesel production, from laboratory to industry," *Fuel processing technology,* vol. 125, pp. 106-113, 2014.

[75] *Standard specification for biodiesel fuel blend stock (B100) for middle distillate fuels. Report no. D6751-08. ASTM; 2008.*

[76] G. Knothe, "The Biodiesel Handbook. 1-302. Knothe, G., Van Gerpen, J., and Krahl, J," ed: AOCS Press, Urbana, IL, 2005.

[77] *European Committee for Standardization. EN 14214: automotive fuels – fatty acid methyl esters (FAME) for diesel engines – requirements and test methods. Report no. EN 14214:2008. Management Centre; 2008.*

[78] *Worldwide Fuel Charter. Available on* http://www.oica.net/wp-content/uploads//WWFC5-2013-Final-single-page-correction2.pdf*,* 2013.

[79] *South African National Standard (SANS 1935:2011) for Automotive biodiesel — Fatty Acid Methyl Esters (FAME) for diesel engines — Requirements and test methods. available on* www.sabs.co.za*.*

[80] L. F. Ramírez-Verduzco, J. E. Rodríguez-Rodríguez, and A. del Rayo Jaramillo-Jacob, "Predicting

cetane number, kinematic viscosity, density and higher heating value of biodiesel from its fatty acid methyl ester composition," *Fuel,* vol. 91, no. 1, pp. 102-111, 2012.

[81] C. Patel *et al.*, "Comparative compression ignition engine performance, combustion, and emission characteristics, and trace metals in particulates from Waste cooking oil, Jatropha and Karanja oil derived biodiesels," *Fuel,* vol. 236, pp. 1366-1376, 2019/01/15/ 2019.

[82] O. Özener, L. Yüksek, A. T. Ergenç, and M. Özkan, "Effects of soybean biodiesel on a DI diesel engine performance, emission and combustion characteristics," *Fuel,* vol. 115, pp. 875-883, 2014.

[83] M. Suresh, C. P. Jawahar, and A. Richard, "A review on biodiesel production, combustion, performance, and emission characteristics of non-edible oils in variable compression ratio diesel engine using biodiesel and its blends," *Renewable and Sustainable Energy Reviews,* vol. 92, pp. 38-49, 2018/09/01/ 2018.

[84] U. Rajak, P. Nashine, T. S. Singh, and T. N. Verma, "Numerical investigation of performance, combustion and emission characteristics of various biofuels," *Energy Conversion and Management,* vol. 156, pp. 235-252, 2018.

[85] S. Salam and T. N. Verma, "Appending empirical modelling to numerical solution for behaviour characterisation of microalgae biodiesel," *Energy conversion and management,* vol. 180, pp. 496-510, 2019.

[86] Y. H. Tan, M. O. Abdullah, C. Nolasco-Hipolito, and N. S. A. Zauzi, "Application of RSM and Taguchi methods for optimizing the transesterification of waste cooking oil catalyzed by solid ostrich and chicken-eggshell derived CaO," *Renewable energy,* vol. 114, pp. 437-447, 2017.

[87] A. Sarve, S. S. Sonawane, and M. N. Varma, "Ultrasound assisted biodiesel production from sesame (Sesamum indicum L.) oil using barium hydroxide as a heterogeneous catalyst: comparative assessment of prediction abilities between response surface methodology (RSM) and artificial neural network (ANN)," *Ultrasonics sonochemistry,* vol. 26, pp. 218-228, 2015.

[88] M. Mostafaei, H. Javadikia, and L. Naderloo, "Modeling the effects of ultrasound power and reactor dimension on the biodiesel production yield: Comparison of prediction abilities between response surface methodology (RSM) and adaptive neuro-fuzzy inference system (ANFIS)," *Energy,* vol. 115, pp. 626-636, 2016.

[89] V. B. Veljković, A. V. Veličković, J. M. Avramović, and O. S. Stamenković, "Modeling of biodiesel production: Performance comparison of Box–Behnken, face central composite and full factorial design," *Chinese Journal of Chemical Engineering,* 2018.

[90] M. Corral Bobadilla, R. Fernández Martínez, R. Lostado Lorza, F. Somovilla Gómez, and E. Vergara González, "Optimizing Biodiesel Production from Waste Cooking Oil Using Genetic Algorithm-Based Support Vector Machines," *Energies,* vol. 11, no. 11, p. 2995, 2018.

[91] A. P. Tchameni, L. Zhao, J. X. Ribeiro, and T. Li, "Predicting the rheological properties of waste vegetable oil biodiesel-modified water-based mud using artificial neural network," *Geosystem Engineering,* vol. 22, no. 2, pp. 101-111, 2019.

[92] E. G. Giakoumis and C. K. Sarakatsanis, "Estimation of biodiesel cetane number, density, kinematic viscosity and heating values from its fatty acid weight composition," *Fuel,* vol. 222, pp. 574-585, 2018.

[93] O. D. Samuel and M. O. Okwu, "Comparison of Response Surface Methodology (RSM) and Artificial

Neural Network (ANN) in modelling of waste coconut oil ethyl esters production," *Energy Sources, Part A: Recovery, Utilization, and Environmental Effects,* vol. 41, no. 9, pp. 1049-1061, 2019.

[94] A. Datta and B. K. Mandal, "Numerical prediction of the performance, combustion and emission characteristics of a CI engine using different biodiesels," *Clean Technologies and Environmental Policy,* vol. 20, no. 8, pp. 1773-1790, 2018.

[95] G. R. Stansell, V. M. Gray, and S. D. Sym, "Microalgal fatty acid composition: implications for biodiesel quality," *Journal of Applied Phycology,* journal article vol. 24, no. 4, pp. 791-801, August 01 2012.

[96] N. Cotabarren, P. Hegel, and S. Pereda, "Thermodynamic model for process design, simulation and optimization in the production of biodiesel," *Fluid Phase Equilibria,* vol. 362, pp. 108-112, 2014.

[97] S. Pinzi, P. Rounce, J. M. Herreros, A. Tsolakis, and M. Pilar Dorado, "The effect of biodiesel fatty acid composition on combustion and diesel engine exhaust emissions," *Fuel,* vol. 104, pp. 170-182, 2013/02/01/ 2013.

[98] P. R. Menon and A. Krishnasamy, "A Composition-Based Model to Predict and Optimize Biodiesel-Fuelled Engine Characteristics Using Artificial Neural Networks and Genetic Algorithms," *Energy & fuels,* vol. 32, no. 11, pp. 11607-11618, 2018.

[99] S. M. Krishna, P. A. Salam, M. Tongroon, and N. Chollacoop, "Performance and emission assessment of optimally blended biodiesel-diesel-ethanol in diesel engine generator," *Applied Thermal Engineering,* vol. 155, pp. 525-533, 2019.

[100] R. Piloto-Rodríguez *et al.*, "Conversion of fatty acid distillates into biodiesel: engine performance and environmental effects," *Energy Sources, Part A: Recovery,*

Utilization, and Environmental Effects, pp. 1-12, 2019.

[101] H. Hosseinzadeh-Bandbafha, M. Tabatabaei, M. Aghbashlo, M. Khanali, and A. Demirbas, "A comprehensive review on the environmental impacts of diesel/biodiesel additives," *Energy conversion and management,* vol. 174, pp. 579-614, 2018.

[102] B. Ashok and K. Nanthagopal, "Eco friendly biofuels for CI engine applications," in *Advances in Eco-Fuels for a Sustainable Environment*: Elsevier, 2019, pp. 407-440.

[103] International, Energy, and Agency. Renewable 2018. Market analysis and forecast from 2018 to 2023. Available on https://www.iea.org/renewables2018/ [Online].

CHAPTER 9: CONCLUSION AND RECOMMENDATIONS FOR FUTURE WORK

9.1 Conclusion

The quest for an alternative and sustainable fuel to replace PDB fuel to power CI engines has been engaging the attention of researchers over the past decades. Though a lot has been achieved, obvious research gaps are still visible and require conscious efforts. The utilization of WCO for the synthesis of FAME by transesterification has been escalated by this research due to its obvious advantages over other feedstocks. Experimental and numerical techniques have been employed for the property's determination and prediction, optimization, engine performance and emission characteristics of CI engine fuelled by FAME. The following conclusions can be drawn from the research.

1. It is possible to synthesize FAME with the requisite properties and capacity for improved engine performance and mitigated emission of regulated gases in a conventional CI engine. This has been demonstrated in this research.

2. FAMEs were produced through a simple conversion process of transesterification using waste vegetable oil collected from restaurants, take away outlets and households. The produced FAMEs meet the ASTM and EN standards.

3. The optimal FAME candidate determined by mathematical and numerical tools was synthesized by transesterification of WCO and defined in terms of two FA compositions. The new FAME contains palmitic acid (C16:0) of 36.4 % and oleic acid (C18:1) of 59.8 %.

4. The new FAME candidate exhibited better engine performance when compared with PBD fuel and biodiesel from other sources when tested on a conventional and unmodified CI engine. The constituents of the exhaust gases emanating from the application of the new fuel in a conventional CI engine was more tolerable than that from PBD fuel, though the NOx emission was still relatively high.

5. Application of property prediction techniques guarantees the conversion of WCO to high-quality FAME thereby eliminating the cumbersome, and costly experimental process. Five FA compositions were used as inputs and the outcome were within acceptable error limits.

6. Application of modelling and optimization techniques allows for the synthesis of FAME using the minimum quantity of materials, less energy consumption, and in less time for optimal FAME production. This prevents time and material wastage, and ensures that FAME is generated from available feedstocks.

7. Chicken eggshell waste calcined at high temperature contained CaO capable of being and suitable as a heterogeneous catalyst for conversion of WCO to FAME. The CaO from chicken eggshell waste is advantageous based on its recoverability and reusability.

8. Further analysis of the WCO feedstock revealed that the degree of usage and type of food items that the oil was used to fry affect the FA composition and properties of the WCO and the resulting FAME.

9. The selected feedstock and conversion technique allow for sustainable, easy to use, and environmentally friendly production of FAME.

10. This study has further revealed the applicability of FAME as a sustainable remedy to the unpleasant effects of the use of PBD fuel to power CI engines. The determination of an optimal FAME candidate has created a viable pathway for improvement of the quality of biodiesel and make its use as CI engine fuel more efficient and environmentally acceptable in line with international protocols and standards.

9.2   Recommendation for future work

Internal combustion engines, particularly CI engines, will continue to find applications in diverse capacities for decades to come. The persistent demand by customers for more efficient CI engines with minimum fuel consumption, and the ever-increasing stringent emission requirements by various environmental standards organizations, will increase demand cost-effective, combustion efficient, readily available, and environmentally sustainable fuel alternatives for CI engines. Biodiesel is one of those alternatives, and more targeted research studies are still needed to improve every stage of the trajectory from feedstock through to FAME quality to performance evaluation, in terms of combustion, performance and emission characteristics, of a FAME candidate fuel in a CI engine.

9.2.1   Experimental

Huge and potential research opportunities exist in widening the scope, definition, and characterization of the FAME candidate with a view to improving and streamlining its production and application. Specifically, more parameters that can further define and characterize the optimal FAME should be investigated. More optimization techniques should be employed to determine more robust parametric parameters for the efficient and cost-effective synthesis of biodiesel irrespective of the source, degree of usage, frying temperature, and cycle, food items fried, as well as the level of contamination and thermal degradation of the WCO. Also, more targeted real-time engine tests under varying conditions of load and speeds are needed to get more data sets to further consolidate the advantages of the new fuel.

9.2.2 Numerical

The use of CFD, FORTE, ANSYS FLUENT, and combustion software for the prediction of fingerprints, performance parameters and emission characteristics of the optimal FAME mix should be investigated. The application of research engines fixed with high-speed digital cameras and other techniques should be exploited to ensure a better understanding of the activities of the fuel inside the combustion chambers with a view to improving the performance and emission characteristics of the engine in line with established protocols and standards.

APPENDICES

APPENDIX I: CALCULATION OF MOLAR RATIO OF METHANOL TO OIL

The molar ratio (methanol to oil) for the transesterification process is calculated by following the following steps.

Step1: Calculation of molecular weight of pure fatty acids

The molecular weight of pure fatty acids is calculated using Equation App. A1

Molecular weight of fatty acids $MW_{FA} = N_C \times MW_C + N_H \times MW_H + N_O \times MW_O$ (App. A1)

Where, N_C, N_H, and N_O are the number of carbon, hydrogen, and oxygen atoms in the fatty acid (FA) chain, respectively. MW_C, MW_H, and MW_O are the molecular weight of carbon, hydrogen, and oxygen, which are 12.0107, 1.00794, and 15.9994 grams per mole, respectively.

Step 2: Calculation of molecular weight of vegetable oils

Molecular weight of vegetable oil is calculated from the molecular weight of individual fatty acids and fatty acid composition using

Molecular weight of vegetable oil = $\sum_{i=1}^{n} W_i \times MW_i$ (App. A2).

Table App. A1. Molecular weight of pure fatty acids

Fatty Acid	Chemical formula	Molecular weight of FA (g/mol)
Erucic	$C_{22}H_{42}O_2$	338.58
Oleic	$C_{18}H_{34}O_2$	282.46
Linoleic	$C_{18}H_{32}O_2$	280.45
Caprylic	$C_8H_{16}O_2$	144.21
Palmitic	$C_{16}H_{32}O_2$	256.42
Stearic	$C_{18}H_{36}O_2$	284.48
Undeclyic	$C_{11}H_{22}O_2$	186.29
Nonadecylic	$C_{19}H_{38}O_2$	312.54
Myristic	$C_{14}H_{28}O_2$	228.37
Capric	$C_{10}H_{20}O_2$	144.21
Arachidic	$C_{20}H_{40}O_2$	312.53
Enanthic	$C_7H_{14}O_2$	130.19
Lauric	$C_{12}H_{24}O_2$	178.14

Sample Molecular weight calculation (for Sample A):

The fatty acid composition (in weight %) of neat sunflower oil is 32.21% of palmitic acid, 21.98% of Linoleic acid, 0.22% of Caprylic acid, 0.51% of Enanthic acid, 0.51% of Capric acid, (.21% of Stearic acid and 12.38% of Arachidic acid.

Substituting the weight percentage of fatty acids and their molecular weight (from Table App. A1) into Equation (A2), the molecular weight of Sunflower vegetable oil is calculated thus,

$$\frac{(32.21 \times 256.42) + (21.98 \times 280.45) + (0.02 \times 144.21) + (0.51 \times 130.187) + (0.51 \times 172.26) + (9.21 \times 284.48) + (12.36 \times 312.53)}{100}$$

= 210.92 g/mol

Similarly, the molecular weight of other neat vegetable oils and WCO samples are calculated and tabulated below

Table App. A2: Molecular weight of vegetable oil

Vegetable oil	Molecular weight (g/mol)
Sunflower	210.92
Sunfoil	27.22
Palm oil (B)	165.91
Red Palm oil	74.81
Moringa oil	109.50
Depot Margarine	109.50
Used sunflower	4.63
Used Depot margarine	165.32
Used sunfoil	5.71
Used palm oil (FC)	32.53
Used Sunfoil 2	119.07
Used palm oil (SC)	182.66

Step 3: Calculation of molecular weight of Triglyceride

The structure of any vegetable oil is a triglyceride, i.e. a glycerol molecule attached with three fatty acids. In Step 2, the molecular weight of vegetable oil does not include the molecular weight of glycerol. The calculation of the molecular weight of triglyceride is as follows.

The molecular weight of a triglyceride ($MW_{triglyceride}$) is given by the Equation (App. A4).

$$MW_{Triglyceride} = (3 \times AverageMW_{oil}) + MW_{glycerol} - 3MW_{water} \qquad \text{(App. A4)}$$

Where, $MW_{glycerol}$ and MW_{water} are the molecular weight of glycerol and water, which are 92.0938 and 18.0153 grams per mole, respectively.

Using Equation (App. A4), the molecular weight of the triglyceride of the vegetable oils are calculated and tabulated

Table App. A3. Molecular weight of triglyceride of vegetable oils

Vegetable oil	Molecular weight (g/mol)
Sunflower	670.82
Sunfoil	119.71
Palm oil (B)	535.08
Red Palm oil	262.51
Moringa oil	563.87
Depot Margarine	366.56
Used sunflower	51.94
Used Depot margarine	534.01
Used sunfoil	55.18
Used palm oil (FC)	135.66
Used Sunfoil 2	395.28
Used palm oil (SC)	586.05

SAMPLE CALCULATIONS ON METHANOL TO OIL RATIO

1. Mass of methanol required at a 6:1 methanol to oil molar ratio

mm_{so} = 359.28 g/mol

Basis: mass of feed oil, M = 400g

$$n_{feed} = \frac{M}{mm}$$

Where

n_{feed} = the number of moles in the source oil

M = mass of oil (g)   mm = molar mass

Therefore, $n = \frac{400}{359.28} = 1.0119 \; mol$

Molar ratio = 6:1 therefore

$$n_{methanol} = 6 \times 1.1133 = 6.0714 \; mol$$
$$mm_{methanol} = 32.04 \; g/mol$$

Mass of methanol required, $M = n \times mm$

$$M = 6.0714 \times 32.04$$
$$M = 194.54 \; g$$

% yield of biodiesel produced

Feed oil mass = 400 g

Mass of biodiesel produced = 376.8 g

$$Yield \; \% = \frac{Mass_{Biodiesel}}{Mass_{Oil}} \times 100\%$$

$$= \frac{376.8}{400} \times 100$$

$$= 94 \; \%$$

APPENDIX II: CODE TO COMPUTE OPTIMAL FAME

```
clc;close all; clear all;

format
count=0;
for p1=0:.1:100
    for p2=0:.1:100
        for p3=0:.1:100
            for p4=0:.1:100
                for p5=0:.1:100

                CN=56.16 + (0.15*p1) + (0.23*p2)  -(0.03*p3)    -(0.19*p4)    -(0.31*p5);
                    if ((CNN>=100)&&(CNN<=100))

                CV=32629.061 + (71.795*p1)+   (16.913*p2) + (66.268*p3)+(70.501*p4)+(387.989*p5);
                        if ((CV>=34400)&&(CV<=45200))


                CP=-40.278 + (0.514*p1)+   (0.6364*p2) + (0.38363*p3)+(0.35362*p4)+(0.26341*p5);
                           if ((CP>=-25)&& (CP<=26))

                DN=2204.5  -  (13.2*p1)-(16*p2)-(13.8*p3)-(13.3*p4)-(3.717*p5);
                                if ((DN>=860)&& (DN<=900))

                KV=337.4774  -  (3.7096*p1)-  (3.812*p2) - (3.743*p3)-(3.6808*p4)-(3.717*p5);
                                   if (KV <=4.5)

                CFPP=-16.447+(0.3141*p1)+ (1.57085*p2);
                                      if (CFPP<=-5)&&(CFPP>=-15)
                                        count=count+1;

                                        CN(count)=CNN;
                                        A(count,:)=[p1 p2 CFPP];
                                        C(count,:)=[CP DN KV CV CFPP];
                                      end
                                   end
                                end
                             end
                          end
                       end
                    end


              end
           end
        end
end
VALUE1=A(opt2,:)
VALUE2=C(opt2,:)
```

APPENDIX III: PICTURES

Plate 1: Chicken eggshell waste

Plate 2: Chicken eggshell waste powder

Plate 3: Weighing the chicken eggshell waste powder

Plate 4: Weighing the waste cooking oil

Plate 5: Weighing the Methanol

Plate 6: Methanol, catalyst and waste cooking oil

Plate 7: Separation of glycerol and crude biodiesel in a separating funnel

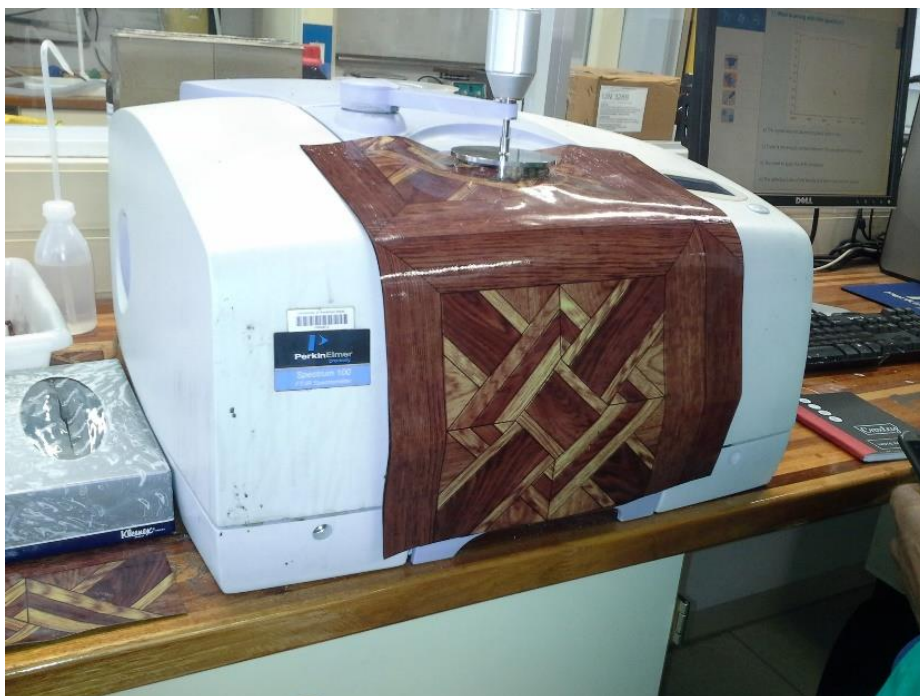**Plate 8: Ovens for chicken eggshell waste calcination**

Plate 9: Viscometer

Plate 10: PyGCMS/GC-MS machine
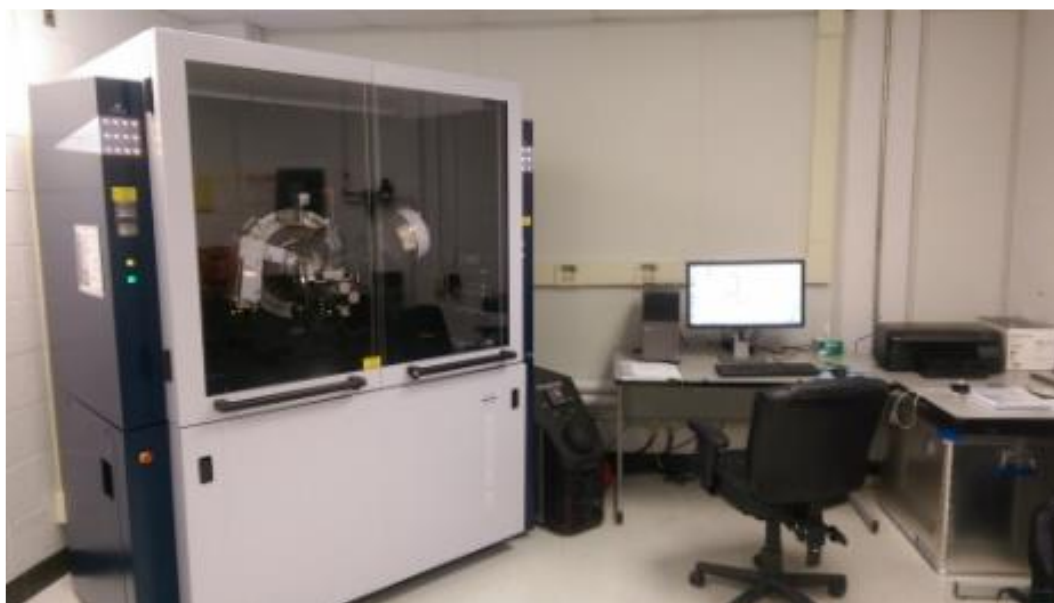

Plate 11: Simultaneous Thermal Analyser

Plate 12: FT-IR Spectrometer

Plate 13: Spottering machine

Plate 14: FEG-SEM

Plate 15: X-Ray Diffractometer